

JANNE RÄSÄNEN

# Novel Methods for the Treatment and Diagnosis of Skin Cancers and their Precursors



JANNE RÄSÄNEN

Novel Methods for the Treatment  
and Diagnosis of Skin Cancers  
and their Precursors

ACADEMIC DISSERTATION

To be presented, with the permission of  
the Faculty Council of the Faculty of Medicine and Health Technology  
of Tampere University,  
for public discussion in the Lecture room F115  
of the Arvo building, Arvo Ylpön katu 34, Tampere,  
on 3 September 2021, at 12 o'clock.

## ACADEMIC DISSERTATION

Tampere University, Faculty of Medicine and Health Technology  
Tampere University Hospital, Department of Dermatology and Veneorology  
Päijät-Häme Joint Authority for Health and Wellbeing  
Finland

<i>Responsible supervisor</i>	Docent Mari Grönroos Tampere University Finland	
<i>Supervisor</i>	Docent Noora Neittaanmäki University of Gothenburg Sweden	
<i>Pre-examiners</i>	Docent Johanna Höök-Nikanne University of Helsinki Finland	Docent Laura Huilaja University of Oulu Finland
<i>Opponent</i>	Professor Veli-Matti Kähäri University of Turku Finland	
<i>Custos</i>	Professor Teea Salmi Tampere University Finland	

The originality of this thesis has been checked using the Turnitin OriginalityCheck service.

Copyright ©2021 author

Cover design: Roihu Inc.

ISBN 978-952-03-2049-2 (print)  
ISBN 978-952-03-2050-8 (pdf)  
ISSN 2489-9860 (print)  
ISSN 2490-0028 (pdf)  
<http://urn.fi/URN:ISBN:978-952-03-2050-8>

PunaMusta Oy – Yliopistopaino  
Joensuu 2021



To Maaria, Vilja and Touko



# ACKNOWLEDGEMENTS

There has been a lot of water under the bridge of Tammerkoski since the start of this thesis. To be precise, 11 billion m<sup>3</sup> from September 2016 to September 2021, calculated using a mean streamflow of 70 m<sup>3</sup>/s. A lot of other things have happened as well. Me and my spouse have bought a house from Tampere, a daughter and son were born for us, I have finished my residency in dermatology, bicycled several thousand kilometers and my left patella tendon has been operated three times. This thesis has intertwined with my life all along, at times being in the main focus and stealing most of my time, and at times more or less being dragged behind. There has been ups and downs, triumphs and defeats, you know how it is. But like all good things in life, this too has come to an end. And what a journey it has been!

I could never have accomplished this project without the help of many others. I want to express my deepest gratitude to my supervisors Professor Emerita Erna Snellman, Docent Mari Grönroos and Docent Noora Neittaanmäki for supplying me with the Newcomer's Guide to the Clinical Research. Erna was the person who aided me to start my residency in dermatology in the first place and couraged me into research. Mari was the main organizer, co-investigator and my boss in Päijät-Häme Central Hospital, and she has taught me plenty on diagnosing and treating skin tumours. Noora was the brain behind this thesis, coming up with all the study designs and checking and correcting my manuscripts for the most part. I want to thank you all for the ideas, advice and enthusiasm during these years! I have always felt welcomed to your research group since the first research meeting which I attended in December 2014 in Erna's room.

My very special thanks to the research nurse Ulla Oesch-Lääveri for scheduling and arranging virtually all practical aspects of the clinical studies. If Noora was the brain, then Ulla was the brawn behind this thesis. Thank you for all the hard work, cheerful spirit and discount coupons for the superb outdoor jackets!

I want to thank all the co-authors of the original articles: M.D. P.h.D. Leea Ylitalo and M.D. P.h.D. Johanna Hagman for their particpance in the actinic keratosis study, Professor Pekka Rissanen for conducting the cost-effectiveness analysis, Senior Scientist Lasse Ylianttila for his expertise in light dosimetry, and dermatopathologist Leila Jeskanen for the histopathological analyses. My special

thanks to the co-researchers P.h.D. Ilkka Pölönen for the mathematical analyses of hyperspectral images, and to M.D. P.h.D. Mari Salmivuori for assisting in my studies, being a colleague, and a friend. I also want to thank study coordinator Marjo Soini for her effort in the study set up, research nurse Tiina Mäki for her assistance in the actinic keratosis study, and statistician Mika Helminen for his expertise in statistical analysis.

I sincerely thank the pre-examiners Docent Laura Huilaja and Docent Johanna Höök-Nikanne for their thorough review and valuable comments to improve this dissertation. I also warmly thank Mr. Malcolm Higgs for proofreading the article manuscripts, and Ms. Virginia Mattila, M.A., for revising the English language of the dissertation.

I would also like to thank the members of my dissertation advisory committee Professor Emerita Erna Snellman, Docent Annikki Vaalasti and M.D. P.h.D. Lea Ylitalo for their comments and support along the way. I am particularly grateful to Docent Annikki Vaalasti and Docent Maria Lönnrot, the previous and current Heads of the Department of Dermatology at Tampere University Hospital, for their support for clinical research and flexibility in allowing research leaves from hospital duties when needed.

My warm thanks to my colleagues and other employees in Päijät-Häme Central Hospital and Tampere University Hospital. Special acknowledgement goes to dermatologists Kari Saarinen, Sari Itälina and Ulla Tuovinen for assisting in recruiting patients and sharing their vast clinical experience with me. I am also thankful for my brothers in arms, i.e. peers and fellow dermatology residents with whom I have had a pleasure to work with and learn dermatology. Thank you Mari Salmivuori, Toni Karppinen, Veera Nikkola, Maria Lagerstedt, Niina Korhonen, Heli Joronen and many others. My deepest thanks and salute also to my friends outside work for offering the counterbalance for work and research. Bruno and Hanna, it is invaluable to have friends like you with whom to celebrate the Christmas Eve during the COVID-19 pandemic. Thank you Toni and Salla for dinners and play dates with our kids, Atte and Maija for long-distance peer-support in family life, Tatu and Janita for five-star bed & breakfast in Kuopio and Iisalmi, Lauri and Salla for good ol' chats by the beer glass, Sofia and Henkka for the Saturday night game riots, and Semitekninen mountain bike gang for all the bruises, cramps and over-the-bars. Your friendship means a lot to me.

Lastly, and paramountly, I want to thank my family. I am most grateful to my parents Tuula and Raimo, who have raised me, loved me and supported me through all my endeavours in life. I truly appreciate everything you have done for me. I am

thankful for my brothers Markus and Tuomas for all the fun moments we have had together, for all our common bro-trips, bro-cations and bro-Xmases. Thank you Vilja and Touko, our two most amazing children, who have shown me what true love and happiness are. Kaija and Mikko, thank you for the child care help and for borrowing the textile washer to clean our white sofa time and again. I want to give my most important thanks to my wife-to-be Maaria, who has supported me the most during the hardship. Thank you for loving me the way I am, for being the dear mother to our children, and for letting me go bicycle from time to time. I love you.

This study received financial support from the Finnish Dermatological Society, the University of Tampere, the Competitive Research Financing of Tampere University Hospital, the Cancer Foundation of Finland, the Foundation for Clinical Chemistry Research, and the State Research Funding. I want to acknowledge all of these organizations. Finally, I also wish to offer my thanks to all the patients who participated in this study and thus supported the science. Cheers and remember to wear the sunscreen!

Tampere 2021

Janne Räsänen



# ABSTRACT

Actinic keratosis (AK) is a common premalignant skin lesion carrying a risk of progression into invasive cutaneous squamous cell carcinoma (cSCC). Many international guidelines recommend field-directed therapy for multiple AKs and for field-cancerized skin.

Lentigo maligna (LM) is an *in situ* form of melanoma that grows very slowly radially and eventually can progress into invasive lentigo maligna melanoma (LMM). The gold standard treatment for LM is wide local excision but surgery is not always feasible due to elderly age of the patients and location on cosmetically sensitive head and neck area. Alternative, non-surgical therapies have been investigated with varying results.

Basal cell carcinoma (BCC) is the most common skin cancer among whites in Western countries and approximately 7% of all BCCs contain melanin, being clinically pigmented. Pigmented BCCs may be difficult to distinguish from melanoma and other melanocytic tumours even for an experienced dermatologist.

The dissertation consists of three separate studies. Study **I** was a randomized double-blind trial intended to compare clinical efficacy, tolerability and cost-effectiveness of two photosensitizers, 5-aminolaevulinic acid nanoemulsion (BF-200 ALA) and methyl-5-aminolaevulinate (MAL) in daylight photodynamic therapy (DL-PDT) for AKs. Altogether 69 patients with 767 mild to moderate AKs were given a single DL-PDT treatment in a randomized split-face setting. In a follow-up of 12 months, BF-200 ALA was more effective than MAL, clearing 79.7% vs. 73.5% of all AKs. The tolerability of both treatments was very good, with no difference in pain, cosmetic outcome or patient preference, but BF-200 ALA caused more intense local skin reactions.

Study **II** was a prospective study intended to investigate the efficacy of ablative fractional laser (AFL)-assisted PDT in the treatment of LM. BF-200 ALA was used as a photosensitizer. Ten biopsy-verified LM lesions were treated with AFL-assisted PDT three times at two-week intervals. Four weeks after the last PDT treatment all LM lesions were surgically excised for histopathological evaluation. The complete histopathological clearance rate was seven out of ten lesions (70%). Some severe and unanticipated skin reactions occurred after PDT sessions.

Study **III** was a prospective diagnostic study piloting hyperspectral imaging (HSI) and convolutional neural network (CNN) for differential diagnosis of pigmented skin lesions. A total of 26 pigmented lesions were imaged with HSI *in vivo* and then surgically excised for histopathological evaluation. HSI images were divided into two halves, one of which was used for the training of the CNN and the other for the classification task. For two-class classifier (melanocytic tumours vs. pigmented BCCs) using majority of the pixels to predict the class of the lesion, we obtained high sensitivity of 100%, specificity of 90% and positive predictive value (PPV) of 94% for diagnosis of melanocytic tumours.

The results of this thesis permit the following conclusions: 1) BF-200 ALA is more effective than MAL in DL-PDT for mild to moderate AKs and is slightly more cost-effective than MAL. BF-200 ALA caused more intense local skin reactions, which could affect the tolerability of the treatment. 2) AFL-assisted PDT showed good efficacy of 70% for lentigo maligna in terms of histopathological clearance. It could be considered a minimally invasive alternative treatment for LM in cases where surgery is not an option. 3) a CNN classifier can accurately and pixel-wise differentiate melanocytic tumours from pigmented BCCs in hyperspectral images. A larger sample dataset with multiple tumour types and a separate training dataset is warranted in the future to confirm these preliminary results.



# TIIVISTELMÄ

Aktiinikeratoosi (AK) on yleinen ihosyövän esiastemuutos, johon liittyy riski invasiivisen okasolusyövän (cSCC) kehittymiselle. Monet kansainväliset hoitosuositukset suosittavat kenttähoitoa, mikäli iholla on useita AK-leesioita tai kenttäkarsinogeneesiä.

Lentigo maligna (LM) on melanooman esiastemuutos, joka kasvaa ensin hitaasti kokoa ja voi lopulta kehittyä invasiiviseksi lentigo maligna -melanoomaksi (LMM). LM:n vakiintunut hoitokäytäntö on leikkaus laajalla marginaalilla. Aina kirurgia ei kuitenkaan onnistu potilaan korkean iän tai leesioita esteettisesti haastavan sijainnin vuoksi. LM:n hoidossa on tutkittu myös vaihtoehtoisia ei-kirurgisia menetelmiä, mutta niiden tulokset vaihtelevat.

Tyvisolusyöpä (BCC) on vaaleaihoisten yleisin ihosyöpä, ja noin 7% kaikista tyvisolusyövästä on pigmentoituneita eli ne sisältävät melaniinipigmenttiä. Jopa kokeneen ihotautilääkärin voi olla vaikea erottaa pigmentoitunut tyvisolusyöpä melanoomasta tai muista melanosyyttikasvaimista.

Väitöskirja koostuu kolmesta erillisestä osatyöstä. Osatyö I oli satunnaistettu ja kaksoissokkoutettu tutkimus, jossa verrattiin kahden valoherkistäjävoiteen, aminolevulinahappo-nanoemulsion (BF-200 ALA) ja metyyliaminolevulinahappoa (MAL) tehoa, siedettävyyttä ja kustannustehokkuutta AK:ien päivänvalo-fotodynaamisessa hoidossa (DL-PDT). Tutkimukseen osallistui 69 potilasta, joilla oli yhteensä 767 lievää tai keskivaikeaa AK:ia. Potilaat hoidettiin DL-PDT:llä kertahoitona käyttäen eri kasvopuoliskoille eri voiteita satunnaistamisen mukaan. Vuoden kuluttua hoidosta BF-200 ALA oli tehokkaampi kuin MAL, parantaen 79,7% kaikista AK-leesioista, kun MAL paransi 73,5%. Molemmat hoidot olivat hyvin siedettyjä. Kivun, kosmeettisen lopputuloksen tai potilaiden hoitomieltymyksen välillä ei ollut merkitsevää eroa, mutta BF-200 ALA aiheutti voimakkaampia paikallisia ihoreaktioita.

Osatyö II oli prospektiivinen tutkimus, jossa selvitettiin fotodynaamisen hoidon (PDT) tehoa LM:n hoidossa käyttäen valoherkistäjänä BF-200 ALA:a. Kymmenen biopsiavarmennettua LM:a hoidettiin AFL-avusteisella (ablatiivinen fraktionaalinen laser) PDT-hoidolla kolme kertaa kahden viikon välein. Neljä viikkoa viimeisen PDT-hoidon jälkeen LM-leesiot leikattiin kirurgisesti, ja kudospalat analysoitiin

histopatologisesti. Seitsemän kymmenestä (70%) LM:sta parani kokonaan histopatologisesti. PDT-hoitojen jälkeen kuitenkin ilmeni muutamia vaikeita ja odottamattomia ihoreaktioita.

Osatyö **III** oli prospektiivinen diagnostinen pilottitutkimus, jossa käytettiin tekoälyä (syväoppiva neuroverkko) ihokasvainten hyperspektrikuvien automaattiseen luokitteluun. Yhteensä 26 pigmentoitunutta ihokasvainta kuvattiin ensin hyperspektrikameralla ja sitten leikattiin kirurgisesti histopatologista diagnoosia varten. Hyperspektrikuvat jaettiin kahteen osaan, joista toista käytettiin neuroverkon koulutukseen ja toista luokittelutehtävään. Neuroverkon herkkyys erottaa melanosyyttikasvaimet pigmentoituneista tyvisolusyöivistä oli 100%, tarkkuus 90% ja positiivinen ennustearvo 94%, kun käytettiin kuvan pikselienemmistöä ennustamaan koko kasvaimen diagnoosi.

Tämän väitöskirjan tulosten perusteella voidaan tehdä seuraavat johtopäätökset: 1) BF-200 ALA on tehokkaampi kuin MAL lievien ja keskivaikeiden AK:ien päivänvalo-PDT-hoidossa, ja se on lisäksi hieman kustannustehokkaampi. BF-200 ALA aiheuttaa voimakkaampia paikallisia ihoreaktioita, millä voi olla vaikutusta hoidon siedettävyyteen. 2) AFL-avusteinen PDT-hoito on kohtalaisen tehokas LM:n hoidossa, parantaen 70% leesioista histopatologisesti. Sitä voidaan pitää vaihtoehtona LM:n hoidossa silloin, kun kirurgia ei tule kyseeseen. 3) Syväoppiva neuroverkko pystyy erottamaan melanosyyttikasvaimet ja pigmentoituneet basaliomat hyperspektrikuvissa tarkasti ja pikselikohtaisesti. Jatkossa tarvitaan suurempi otos hyperspektrikuvia useista erilaisista kasvaimista näiden alustavien tulosten varmistamiseksi.

# CONTENTS

1	INTRODUCTION .....	19
2	REVIEW OF THE LITERATURE .....	21
2.1	Actinic keratosis .....	21
2.1.1	Clinical characteristics .....	21
2.1.2	Diagnosis and histopathology .....	23
2.1.3	Pathophysiology .....	24
2.1.4	Risk factors.....	25
2.1.5	Epidemiology.....	25
2.1.6	Prognosis .....	26
2.1.7	Should actinic keratosis be treated? .....	27
2.1.8	Treatment .....	28
2.1.8.1	Lesion-directed therapies .....	28
2.1.8.2	Field-directed therapies .....	29
2.1.8.3	Comparison of efficacy for actinic keratosis therapies	32
2.1.9	Prevention .....	32
2.2	Lentigo maligna and lentigo maligna melanoma .....	33
2.2.1	Clinical characteristics .....	34
2.2.2	Diagnosis and histopathology .....	35
2.2.3	Risk factors and pathophysiology.....	37
2.2.4	Epidemiology.....	38
2.2.5	Prognosis .....	39
2.2.6	Treatment .....	39
2.2.6.1	Surgical treatment.....	40
2.2.6.2	Non-surgical treatment.....	41
2.3	Photodynamic therapy .....	44
2.3.1	History and principle .....	44
2.3.2	Photosensitizers.....	46
2.3.3	Light sources.....	47
2.3.4	Clinical procedure .....	49
2.3.4.1	Pretreatment .....	49
2.3.4.2	Laser-assisted photodynamic therapy .....	49
2.3.5	Efficacy .....	50
2.3.6	Tolerability and side-effects.....	52
2.4	Non-invasive skin imaging methods .....	56
2.4.1	Dermoscopy.....	57
2.4.2	Reflectance confocal microscopy .....	58
2.4.3	Optical coherence tomography.....	59
2.4.4	Multispectral imaging.....	60

2.4.5	Raman spectroscopy .....	62
2.4.6	Hyperspectral imaging.....	63
2.4.6.1	Hyperspectral camera medical prototype .....	64
2.5	Convolutional neural networks.....	66
3	AIMS OF THE STUDY.....	68
4	MATERIALS AND METHODS.....	69
4.1	Patients.....	69
4.1.1	Inclusion and exclusion criteria.....	69
4.2	Methods.....	70
4.2.1	Clinical evaluation .....	70
4.2.2	Hyperspectral image acquisition (II and III) .....	71
4.2.3	Photodynamic therapy procedures (I and II) .....	72
4.2.4	Surgery (II and III).....	75
4.2.5	Histopathological evaluation (II and III) .....	75
4.2.6	Tolerability assessment (I and II) .....	75
4.2.7	Statistical analyses.....	76
4.2.8	Cost-effectiveness analysis (I) .....	76
4.2.9	Convolutional neural network (III).....	77
5	RESULTS .....	79
5.1	The efficacy of photodynamic therapy.....	79
5.1.1	Clinical clearance of actinic keratoses (I).....	79
5.1.2	Histological clearance of lentigo malignas (II) .....	80
5.2	Safety and tolerability of photodynamic therapy (I and II).....	82
5.3	Cost-effectiveness analysis (I) .....	83
5.4	Hyperspectral analyses and convolutional neural network classification (III) .....	83
6	DISCUSSION .....	86
6.1	The efficacy of photodynamic therapy for premalignant skin lesions (I & II).....	86
6.2	Tolerability of photodynamic therapy (I & II).....	89
6.3	Hyperspectral imaging and diagnostic accuracy of convolutional neural network (III) .....	91
6.4	Strengths and limitations.....	92
7	CONCLUSION AND FUTURE ASPECTS.....	93
8	REFERENCES .....	95

# ABBREVIATIONS

1D	One-dimensional
2D	Two-dimensional
3D	Three-dimensional
AFL	Ablative Fractional Laser
AI	Artificial Intelligence
AK	Actinic Keratosis
ALA	5-Aminolaevulinic Acid
AUC	Area Under Curve
BCC	Basal Cell Carcinoma
BRAF	V-Raf Murine Sarcoma Viral Oncogene Homolog B1
CEA	Cost-Effectiveness Analysis
CI	Confidence Interval
CNN	Convolutional Neural Network
CO <sub>2</sub>	Carbon Dioxide
COX-2	Cyclo-Oxygenase 2
CSD	Chronically Sun-Damaged
cPDT	Conventional Photodynamic Therapy
cSCC	Cutaneous Squamous Cell Carcinoma
DNA	Deoxyribonucleic Acid
DL-PDT	Daylight Photodynamic Therapy
FPI	Fabry-Perot Interferometer
FWHM	Full Width of Half Maximum
HAL	Hexylaminolaevulinate
HPV	Human Papillomavirus
HSI	Hyperspectral Imaging
ICER	Incremental Cost-Effectiveness Ratio
IHC	Immunohistochemical
KIN	Keratinocytic Intraepithelial Neoplasia
LED	Light-emitting Diode
MAL	Methyl-5-Aminolaevulinate

MIS	Melanoma In Situ
MM	Malignant Melanoma
MMS	Mohs Micrographic Surgery
MSI	Multispectral Imaging
NMSC	Non-Melanoma Skin Cancer
NSAID	Non-Steroidal Anti-Inflammatory Drug
OR	Odds Ratio
OTR	Organ Transplant Recipient
PDT	Photodynamic Therapy
PpIX	Protoporphyrin IX
PPV	Positive Predictive Value
QoL	Quality of Life
RCM	Reflectance Confocal Microscopy
RCT	Randomized Clinical Trial
RNA	Ribonucleic Acid
ROC	Receiving Operating Characteristics
ROS	Reactive Oxygen Species
RS	Raman Spectroscopy
SPF	Sun Protection Factor
SSE	Staged Surgical Excision
UV	Ultraviolet
WLE	Wide Local Excision
YAG	Yttrium Aluminum Garnet

# ORIGINAL PUBLICATIONS

This thesis is based on the following original publications, which are referred to in the text by their Roman numerals (I–III):

- I Räsänen JE, Neittaanmäki N, Ylitalo L, Hagman J, Rissanen P, Ylianttila L, Salmivuori M, Snellman E, Grönroos M. 5-aminolaevulinic acid nanoemulsion is more effective than methyl-5-aminolaevulinate in daylight photodynamic therapy for actinic keratosis: a nonsponsored randomized double-blind multicentre trial. *Br J Dermatol*. 2019 Aug;181(2):265-274.
- II Räsänen JE, Neittaanmäki N, Jeskanen L, Pölönen I, Snellman E, Grönroos M. Ablative fractional laser-assisted photodynamic therapy for lentigo maligna: a prospective pilot study. *J Eur Acad Dermatol Venereol*. 2020 Mar;34(3):510-517.
- III Räsänen J, Salmivuori M, Pölönen I, Grönroos M, Neittaanmäki N. Hyperspectral imaging reveals spectral differences and can distinguish malignant melanoma from pigmented basal cell carcinomas: a pilot study. *Acta Derm Venereol*. 2021 Feb 19;101(2):adv00405.





# 1 INTRODUCTION

Actinic keratosis (AK) is a common premalignant skin lesion arising on chronically sun-exposed skin of elderly patients. For example, in Dutch population aged 50 years or older the estimated prevalence of at least one AK is 23.5%, and this increases with age (Flohil et al., 2013). AKs are considered to be early precursors of cutaneous squamous cell carcinoma (cSCC), for which the incidence has doubled in a decade due to ageing population and increased exposure to ultraviolet radiation (Goon et al., 2016). The individual risk of malignant progression for a single AK is low (less than 1/1000 per year) (Marks et al., 1988), but increases with multiple lesions and field-cancerization, i.e. chronically sun-damaged skin with recurrent AKs surrounded by subclinical lesions harbouring neoplastic alterations. Thus, many international guidelines recommend early field-directed therapy for AKs. Photodynamic therapy (PDT) allows treatment of large fields at one time, but a major drawback with conventional PDT using a LED lamp is intense pain during illumination. Daylight photodynamic therapy (DL-PDT) using methyl-5-aminolaevulinate (MAL) as a photosensitizer has proved to be as effective as conventional PDT for thin and moderate AKs, but provides practically painless illumination leading to high patient satisfaction. Aminolaevulinic acid nanoemulsion gel (BF-200 ALA) is a promising novel photosensitizer, but data on its efficacy is limited.

Lentigo maligna (LM) is an in-situ form of melanoma occurring on chronically sun-exposed skin of elderly patients, most often in the head or neck region. LM grows slowly over the years and may eventually progress to invasive lentigo maligna melanoma (LMM), with an estimated lifetime risk of 5–50% (Stevenson & Ahmed, 2005; Weinstock & Sober, 1987). As with cSCC, the incidence of LM and LMM has increased considerably in recent decades due to ageing population and high UV exposure (Greveling et al., 2016; Mirzoyev et al., 2014; Swetter et al., 2005; Toender et al., 2014; Youl et al., 2013). LMM accounts for 4–15% of all invasive melanomas (McKenna et al., 2006). The gold standard treatment for LM is wide local excision with 5–10 mm margins, but in some instances the patient may be unfit or unwilling to undergo surgery. Alternative non-invasive treatment modalities have been investigated with varying recurrence rates, including cryotherapy, laser therapy

radiotherapy, topical imiquimod and PDT. There is only one retrospective study reporting the efficacy of PDT for LM with promising results, but prospective trials are lacking (Karam et al., 2013).

Basal cell carcinoma (BCC) is the most common skin cancer in fair-skinned individuals with an estimated lifetime risk of over 30% (Cameron et al., 2019). Approximately 7% of superficial and nodular BCCs are clinically pigmented, which may be difficult to distinguish from melanocytic tumours even to experienced dermatologists (Menzies, 2002). Pigmented BCCs frequently have clinical features that mimic melanoma. Hyperspectral imaging (HSI) is a non-invasive imaging method that measures the reflectance spectra of the skin *in vivo* to identify and delineate different biological tissues, and may aid in differential diagnosis of skin lesions. Convolutional neural networks (CNN) represent a form of artificial intelligence in decision-making and have many applications in diagnostic medicine, including skin-cancer classification from clinical and dermoscopic images.

This dissertation consists of three original communications, two of which are clinical intervention studies focusing on PDT, and the third is a diagnostic pilot study utilizing HSI and deep-learning CNN as an automatic tumour classifier.

## 2 REVIEW OF THE LITERATURE

### 2.1 Actinic keratosis

Actinic keratosis (AK), synonymous with solar keratosis, is a common keratotic lesion arising on chronically sun-exposed skin of fair-skinned individuals (Moy, 2000; Salasche, 2000). It was first described by the French dermatologist Dubreuilh in 1896, who used the term ‘keratosis senilis’ (Heaphy & Ackerman, 2000). Dubreuilh recognized that this lesion had a natural tendency to develop into invasive cutaneous squamous cell carcinoma (cSCC) and thus introduced the concept of precancerosis (Ackerman & Mones, 2006). Since then, despite the numerous scientific publications on AK, there remains some uncertainty regarding the precise nature of AK (Calzavara-Pinton et al., 2017). Some scientists consider AKs to be premalignant skin lesions representing keratinocytic intraepithelial dysplasia, while others classify them as malignant lesions representing an early stage of in situ cSCC (Röwert-Huber et al., 2007; Werner et al., 2013). The number of AKs is exponential compared to cSCCs, thus not all AKs develop into invasive carcinoma. However, it is not possible to predict which individual AKs will progress to SCC (Arenberger & Arenbergerova, 2017; Salasche, 2000). AKs are the earliest clinically perceptible signs of keratinocytic dysplasia and thus serve as a marker of chronic ultraviolet (UV) radiation damage to skin (Berman & Cockerell, 2013). In the entire area of photodamaged skin visible AKs are surrounded by clinically undetectable but neoplastically altered cells with the potential to transform into AKs, resulting in skin field cancerization (Braakhuis et al., 2003). Skin field cancerization accounts for the chronic appearance of novel AKs and relapses (Figueras Nart et al., 2018).

#### 2.1.1 Clinical characteristics

Clinically AKs present as red, scaling papules or plaques on chronically sun-exposed areas of middle-aged and elderly patients (de Berker et al., 2017). They have a gritty, sandpaper-like texture that is often more easily felt than seen (Moy, 2000). The diameter of AKs ranges from a few millimetres to several centimetres and they

usually occur as multiple lesions located in sun-exposed areas on a bald scalp, face, or dorsum of the hands (Moy, 2000). Usually AKs are asymptomatic but may sometimes be tender or itch (T. Rosen & Lebwohl, 2013). The clinical grading system by Olsen et al. can be used to assess the severity of single AK lesions based on their thickness on a three-point scale I–III (Figure 1 and Table 1) (E. A. Olsen et al., 1991). Olsen grading has been widely used in clinical trials, but it is worth noting that clinical thickness does not correlate with the histopathological severity of AK lesions (Schmitz, Kahl, et al., 2016). Recently, two novel clinical classification systems called AKASI (Actinic Keratosis Area and Severity Index) and AK-FAS (Actinic Keratosis Field Assessment Scale), intended to assess the photodamage and field cancerization of the entire affected skin area, have been proposed (Dirschka, Pellacani, et al., 2017; Dréno et al., 2017).

**Table 1.** Olsen grading of actinic keratosis (E. A. Olsen et al., 1991)

Grade I	mild (pink or grey marks with slight scale or gritty to touch, easier felt than seen)
Grade II	moderate (moderately thick actinic keratoses that are easily seen and felt)
Grade III	severe (very thick, hyperkeratotic actinic keratoses)
Field change	Confluent areas of several centimetres or more with a range of features matching any or all of the grades of AK

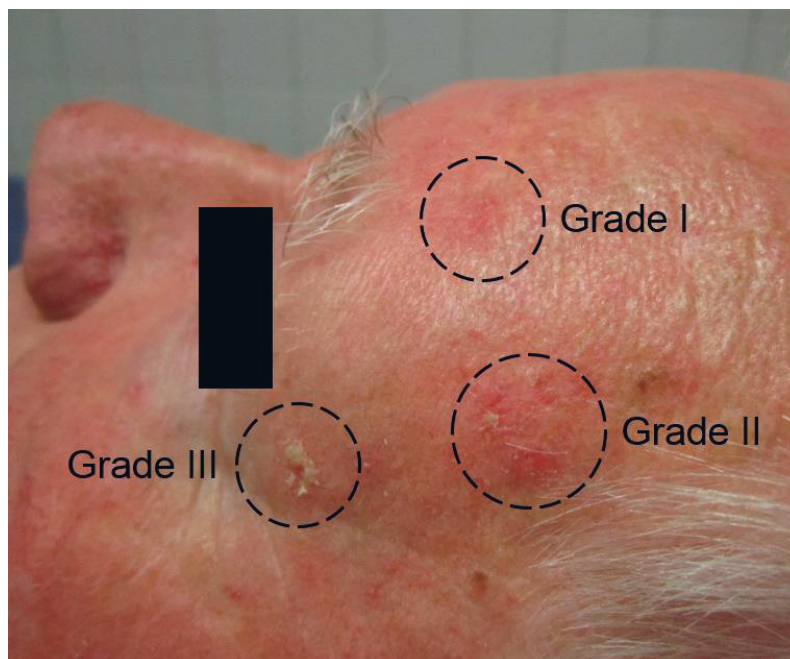


**Figure 1.** Actinic keratosis clinical grades I–III. With permission from the patient.

## 2.1.2 Diagnosis and histopathology

Most AKs are diagnosed by a dermatologist based solely on clinical characteristics and history of risk factors (Dirschka, Gupta, et al., 2017). Dermoscopy (see Chapter 2.4.1) improves the clinical diagnosis of AK, with reported sensitivity and specificity of 98.7% and 95.0% respectively (Huerta-Brogeras et al., 2012). In dermoscopy, three prevalent patterns have been associated with non-pigmented AK (Figure 2) (Zalaudek & Argenziano, 2015).

Usually a biopsy is taken to exclude the possibility of SCC, especially when a given lesion is large, bleeds, is ulcerated or indurated (Rossi et al., 2007). Histologically, AK is characterized by the presence of atypical and pleomorphic keratinocytes at the basal layer of the epidermis, which in advanced lesions may extend to involve the entire epidermis (Cockerell, 2000). The disturbed maturation of keratinocytes results in parakeratosis alternating with hyperkeratosis (Röwert-Huber et al., 2007). Seven major histologic variants of AK have been described: hypertrophic, atrophic, Bowenoid, acantholytic, epidermolytic, lichenoid and pigmented (Rossi et al., 2007). The histopathological severity of AK lesion can be presented on a three-point classification scale KIN (Keratinocytic Intraepithelial Neoplasia) I–III corresponding the degree of dysplasia and extension of the atypical keratinocytes in the epidermis (Figure 3) (Cockerell, 2000).



**Figure 2.** Dermoscopy patterns of nonpigmented AK. (a) first degree, a red pseudonetwork pattern and discrete white scales; (b) second degree, erythematous background, the so-called “strawberry pattern”; (c) third degree, enlarged follicular openings with keratotic plugs over a scaly and white to yellow-appearing background. From *Dianzani et al., 2020*, with permission from Wiley.

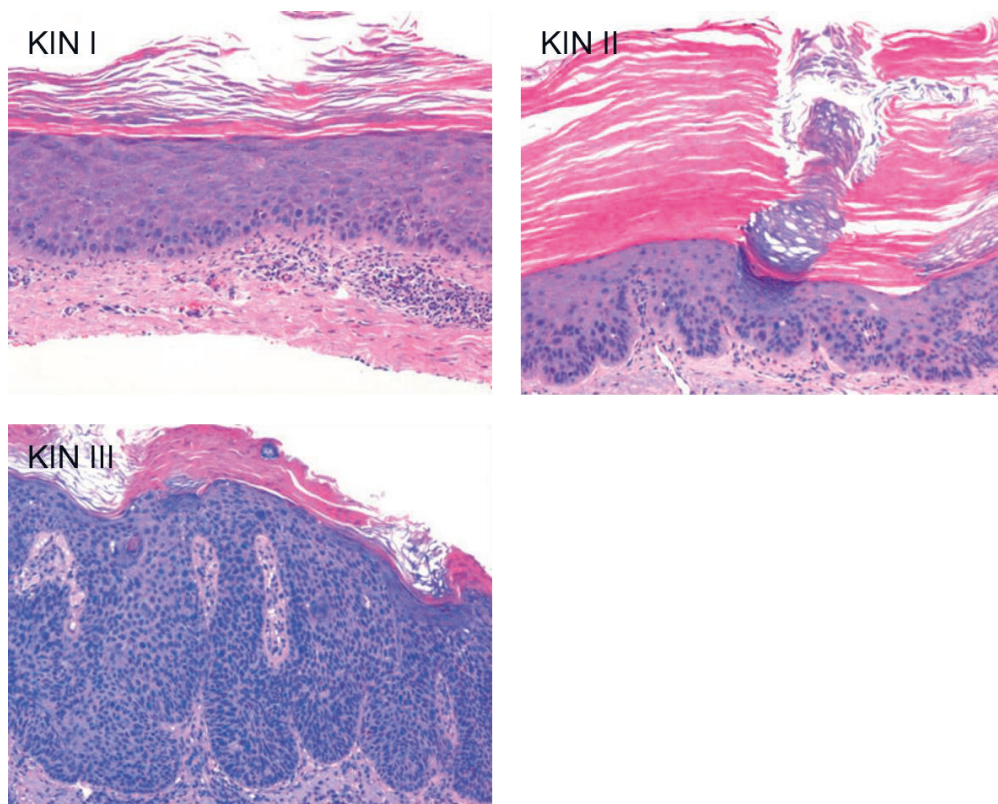


**Figure 3.** Histopathological severity of actinic keratosis on a scale of KIN I–III (keratinocytic intraepithelial neoplasia). KIN I: atypical keratinocytes are limited to the lower one third of the epidermis. KIN II: Crowded atypical keratinocytes are situated in the lower two thirds of the epidermis with loss of orderly keratinocytes maturation, hyperchromatism and pleomorphism. There is also overlying alternating orthokeratosis and parakeratosis. KIN III: Mild epidermal hyperplasia and atypical keratinocytes with a complete loss of maturation involve the entire epidermis. Figures adapted from *Röwert-Huber et al., 2007*, with permission from Wiley.

### 2.1.3 Pathophysiology

The most important risk factor for AK development is chronic UVB exposure (wavelength 290–320 nm) from sunlight (Cockerell, 2003). UVB radiation causes thymidine dimer formation in DNA and RNA of keratinocytes and may lead to mutations in tumour suppressor genes such as p53 (Röwert-Huber et al., 2007). The suppression of p53 function plays a crucial role in the clonal expansion of keratinocytes into AK and further in the development of SCC (Werner et al., 2015). The mutations of gene p53, which normally allows for repair in damaged DNA, are

present in >90% of the neoplastically altered cells in invasive cSCC but are frequently also present in AK lesions (Leffell, 2000). An important event in the development of AK is mutation and inactivation of both p53 alleles which renders keratinocytes resistant to UV-induced apoptosis (Nissinen et al., 2016). It has also been suggested that human papillomaviruses (HPV), especially HPV-3 subtypes, may serve as a cocarcinogen with UV and increase the severity of AK lesions (Lebwohl et al., 2010). The progression of AK into invasive and metastatic cSCC requires further accumulation of UV-induced mutations in driver genes including NOTCH1, NOTCH2, HRAS, EGFR and PIK3CA (Nissinen et al., 2016).

#### 2.1.4 Risk factors

According to epidemiological studies, the known risk factors for AK development include fair skin (Fitzpatrick phototypes I–II), older age, male gender, cumulative UV exposure, proximity to the equator and immunosuppression (Costa et al., 2015). In German population, significantly associated risk factors for AK were skin phototype I, sunburns in childhood and solar lentigines (Schaefer et al., 2014). In an Italian prevalence study light hair and eye colour, facial solar lentigos, history of other NMSC, working outdoors >6 hours/day, prolonged outdoor recreational activities and alcohol consumption were independent risk factors (Fargnoli et al., 2017). In a Rotterdam prevalence study male gender, older age, light pigmentation, severe baldness, skin wrinkling and high tendency for sunburn were significantly associated with extensive actinic damage ( $\geq 10$  AKs) (Flohil et al., 2013). Other reported risk factors are use of thiazide diuretics and cardiac drugs (Traianou et al., 2012).

Organ transplant recipients (OTR) with chronic systemic immunosuppression are at a higher risk of developing AKs, SCC and other skin malignancies (Heppt et al., 2019). Approximately 40% of OTR patients develop AKs within 5 years and they have a 40–250 fold increase in appearance of cSCC (Braathen et al., 2012).

#### 2.1.5 Epidemiology

AK is one of the most commonly seen and treated skin lesion by dermatologists, and it has been estimated that 60% of predisposed individuals aged over 40 years have at least one AK (Lanoue et al., 2015). In the United States actinic keratoses were diagnosed at >10% of dermatology visits and altogether almost 40 million people were affected by AK in 2004 (Bickers et al., 2006). In Austria >30% of

patients attending a dermatology clinic (mean age 61 years) had AK, and by the age of 70 years >70% of those attending had an AK (Eder et al., 2014). In the northern hemisphere, the reported prevalence rates of AK range from 11 to 25%, and among Australian adults the range is higher, from 40 to 60% (Frost & Green, 1994). In South Wales (UK) the estimated incidence rate of AK for 60-year-old subjects was 149 per 1000 person-years (Harvey et al., 1996).

In Europe only few epidemiological studies have been conducted with the estimated point prevalence of AK highly varying from 1 to 38% (Eder et al., 2014; Flohil et al., 2013; Memon et al., 2000; Naldi et al., 2006; Schaefer et al., 2014). In a Rotterdam prevalence study of over 2000 Dutch men and women (mean age 72 years), 21% had 1–3, 9% had 4–9 and 8% had  $\geq 10$  AKs, overall AK prevalence being 49% for men and 28% for women. In a German cohort of over 90,000 employees the standardized prevalence of AK was 2.7% (3.9% for men and 1.5% for women) and the rate increased with age (11.5% in the age group 60–70 years). In Italy the point prevalence in adult population was only 1.4%, however, this number is believed to be biased due to underreporting (Naldi et al., 2006). In a more recent Italian study the prevalence of AK was 27.4% (34.3% in men and 20.0% in women) among outpatients aged  $\geq 30$  years attending dermatology clinics (Fagnoli et al., 2017). In a Northern Finland birth cohort study, the prevalence of AKs in 46-year-olds was 0.6% and in 70- to 93-year-olds 22.3% (Sinikumpu et al., 2014, 2020).

AKs are very prevalent in fair-skinned elderly individuals, commonly treated and thus cause enormous costs for the healthcare system (Siegel et al., 2017). In the USA in 2004 the direct costs of AK management were estimated at \$1.2 billion per year, with indirect costs totalling \$295 million USD (Neidecker et al., 2009). In Sweden the annual direct cost of outpatient treatment for AK was 18 million euros in 2011 (Eriksson & Tinghög, 2015). The incidence of AKs and other skin cancers related to chronic UV exposure is expected to further increase as life expectancy rises in western countries (Siegel et al., 2017).

### 2.1.6 Prognosis

The course of a single AK will follow one of three paths: spontaneous regression, stable existence or malignant transformation into invasive cSCC (Siegel et al., 2017). Spontaneous regression of AKs is common, the regression rates of single AK lesions ranging between 21 and 70% over a period of 1–4 years (Criscione et al., 2009; Harvey et al., 1996; Marks et al., 1986). In prospective evaluation the malignant



transformation rate of a single AK into invasive cSCC has been less than 1/1000 per year (Marks et al., 1988). A mathematical model derived from the study by Marks et al. predicts that for a person with an average of 7.7 AKs, the probability of developing one cSCC is around 10% within 10 years (Dodson et al., 1991). In a systematic review the reported malignant progression rates of AK to cSCC ranged 0–0.075 % per lesion-year, with a risk of up to 0.53% in patients with earlier history of NMSC (Werner et al., 2013). However, the authors concluded that the data currently available is limited and no reliable estimate concerning the progression rate of single AKs to cSCC can be given (Werner et al., 2013). For the sake of comparison, the risk of progression of Bowen’s disease to invasive cSCC appears to be between 3% and 5% per year (Bonarandi et al., 2011).

The presence of AKs has been shown to increase the risk for any skin cancer (both NMSC and melanoma) more than sixfold (G. J. Chen et al., 2005). In another study conducted in Australia the presence of more than 20 AKs increased the risk of cSCC by 11-fold, and of BCC by 10-fold compared to the risk in the absence of AKs (Green & Battistutta, 1990). Thus AKs can be considered to be epiphenomena of chronically photodamaged skin and serve as a marker of increased risk for NMSC (Siegel et al., 2017).

### 2.1.7 Should actinic keratosis be treated?

The reasons for treating AKs may be multiple. AK is not a fatal condition, but as discussed above, may constitute a risk of developing into invasive carcinoma. Furthermore, it has a negative effect on cosmesis and reduces the patient’s quality of life (QoL) (Lanoue et al., 2015; Siegel et al., 2017). Higher number of AK lesions is associated with poorer QoL in patients with previous history of keratinocyte cancer (Weinstock et al., 2009). AKs may impair cosmetic appearance because >80% of AKs occur on highly visible areas such as the head, neck, back of the hands, and forearms (Lanoue et al., 2015). Regarding the risk of AKs progressing to cSCC, there is so far not enough scientific evidence to justify treatment of all AKs in order to prevent malignant transformation (de Berker et al., 2017). A Cochrane review on AK treatments found no data to suggest that treatment of AKs would lead to a possible reduction in cSCC (Gupta et al., 2012). However, one double-blind RCT of topical 5% fluorouracil cream demonstrated a 75% risk reduction for the development of cSCC during the first year after treatment (Weinstock et al., 2018). Many international guidelines recommend the treatment of AKs on the basis of

inherent risk of developing a cSCC and due to the inability to determine which lesions are at higher risk (Braathen et al., 2012; Calzavara-Pinton et al., 2017; Werner et al., 2015). An indirect benefit of the treatment is also to indicate lesions unresponsive to usual therapy and likely to represent higher malignant potential (de Berker et al., 2017).

## 2.1.8 Treatment

A wide range of treatment modalities is available for AK. The choice of the most suitable treatment modality by a clinician depends on several factors: the site and number of AKs, the need for field therapy, availability, cosmetic outcome, patient preference, tolerance for adverse effects and the cost of treatment (de Berker et al., 2017; Lanoue et al., 2015).

### 2.1.8.1 Lesion-directed therapies

Lesion-directed therapies include focal ablative techniques effective for single lesions but unable to address field cancerization (Costa et al., 2015).

#### *Cryotherapy*

Cryotherapy with liquid nitrogen spray ( $-196\text{ C}^\circ$ ) is widely available and a commonly used method in office-based dermatology for the destruction of single AKs (Dirschka, Gupta, et al., 2017). It is a first-line approach for patients with only a few or isolated lesions, or for patients unable to tolerate topical agents (Dianzani et al., 2020). Complete lesion response rates vary from 75% to 98% and recurrence rates have been estimated from 1.2% to 12% in one-year follow-up (Krawtchenko et al., 2007). The cure rate and potential side-effects of cryotherapy are user-dependent and depend on the duration of freeze and number of freeze-thaw cycles. In a prospective study the complete response at 3 months was 39% for freeze time  $<5\text{ s}$ , 69% for freeze time  $>5\text{ s}$ , and 83% for freeze time  $>20\text{ s}$  (Thai et al., 2004). Side effects of cryotherapy include pain, redness, edema, blistering and permanent hypopigmentation (Chetty et al., 2015). Extensive cryotherapy used over large areas is called cryopeeling and can be used to treat fields of AK with widespread photodamage (Chiarello, 2000). The British, German and international AK treatment guidelines strongly recommend cryotherapy for single or few isolated AK

lesions per field or affected body region (de Berker et al., 2017; Heppt et al., 2020; Werner et al., 2015).

### *Laser therapy*

Laser therapy with carbon dioxide (CO<sub>2</sub>) or erbium-YAG (yttrium aluminum garnet) laser is another option for local ablation of AKs, but it is more expensive than cryotherapy and requires specialized training (Chetty et al., 2015). The AK treatment guidelines agree that dermabrasion by ablative CO<sub>2</sub> or Er:YAG laser may be offered for single or multiple grade I–III AKs or field cancerization (Heppt et al., 2020; Werner et al., 2015).

### *Surgical excision*

Surgical excision is not routinely used to treat AK but may be considered in case of hyperkeratotic, horny lesions and when there is a strong suspicion of cSCC (Rossi et al., 2007). Curettage can be used for hyperkeratotic lesions or those refractory to other local treatments, and it allows obtaining a skin sample for histopathological examination (Dianzani et al., 2020). There is less evidence supporting the use of other ablative therapies than cryotherapy in the treatment of AK and they may result in poor outcome or scarring (Dirschka, Gupta, et al., 2017). There are no trials of surgery for AK, but AK treatment guidelines state that surgical removal by curettage, shave biopsy or excision should be considered especially in case of thick grade III AKs which do not respond to other therapies (de Berker et al., 2017; Heppt et al., 2020).

#### 2.1.8.2 Field-directed therapies

With field-directed therapies it is possible to treat multiple AKs and field-cancerization with extensive actinic damage and subclinical lesions (Dianzani et al., 2020). The field-directed therapies approved in Finland and their application schemes for AK are shown in Table 2. Photodynamic therapy is also regarded as a field-directed therapy, but is addressed separately in Chapter 2.3.

**Table 2.** Field-directed therapies for AK available on prescription in Finland, excluding PDT and DL-PDT. †) European Medicines Agency suspended the licence for Picato in January 2020.

Therapy	Trade name	Indication	Application for AK
5-fluorouracil (5-FU) 5%	Efudix® 5% cream	AK, sBCC, genital warts	1–2x/day for 3–4 weeks
5-FU 0.5% in 10% salicylic acid	Actikerall® 5/100mg/g solution	grade I–II AK	1x/day for 12 weeks
Imiquimod 5%	Aldara® 5% cream	grade I–II AK, sBCC, genital warts	3x/week for 4 weeks, can be repeated
Imiquimod 3.75%	Zyclara® 3.75% cream	grade I–II AK	1x/day for 2 weeks on, 2 weeks off, 2 weeks on
Diclofenac 3%	Solaraze 3% gel	AK	2x/day for 3 months
Ingenol mebutate 0.015%†	Picato 0.015% gel	grade I–II AK on face or scalp	1x/day for 3 days
Ingenol mebutate 0.05%†	Picato 0.05% gel	grade I–II AK on body	1x/day for 2 days

### *5-fluorouracil*

5-fluorouracil (5-FU) is a pyrimidine analogue and a chemotherapeutic anticancer agent. It inhibits thymidylate synthetase, disrupting DNA and RNA synthesis, thereby inducing cell cycle arrest and apoptosis (Costa et al., 2015). The mechanism of 5-FU is not specific and the application may cause as an adverse effect severe dermatitis with acute infections, itching, pain and ulceration with scarring (Krawtchenko et al., 2007). 5% 5-FU has relatively good efficacy on AKs, with lesion clearance in clinical trials being approximately 70% (Kurwa et al., 1999; Lawrence et al., 1995). The AK treatment guidelines strongly recommend the use of 5-FU especially for multiple grade I–II AKs and field cancerization, but also for single lesions on the back of the hands and forearms as well (de Berker et al., 2017; Werner et al., 2015).

### *Imiquimod*

Imiquimod, an imidazoquinoline amine, is a toll-like-receptor-7 (TLR-7) agonist that stimulates both innate and adaptive arms of the immune system and has antiviral and anticancer properties (Sauder, 2003). In a controlled clinical study the clearance of AKs was 85% after two 4-week courses with 5% imiquimod cream (Stockfleth et al., 2007). In a systematic meta-analysis complete clearance of AKs was 50% after 12–16 weeks' course with 5% imiquimod (Hadley et al., 2006). Imiquimod 3.75% has comparable efficacy with 5% cream but causes fewer local adverse effects (Swanson et al., 2014). The side-effects are similar to those of 5-FU, including severe erythema (30%), scabbing and crusting (30%) and erosions and ulceration (10%) (de

Berker et al., 2017). There are also rare reports of fatigue, flu-like symptoms and angioedema associated with application of imiquimod (Samrao & Cockerell, 2013). The AK treatment guidelines strongly recommend imiquimod for field treatment of multiple grade I–II AKs and field cancerization (de Berker et al., 2017; Heppt et al., 2020; Werner et al., 2015).

### *Diclofenac*

Diclofenac is a non-steroidal anti-inflammatory drug (NSAID) which inhibits cyclooxygenase-2 (COX-2) resulting in lower levels of prostaglandin E2 (de Berker et al., 2017). Diclofenac has been shown to inhibit tumour cell proliferation and angiogenesis and to induce matrix metalloproteinases resulting in increased keratolysis and collagen degradation (Samrao & Cockerell, 2013). The treatment with diclofenac gel lasts for 3 months and for many patients may be difficult to comply with (Dirschka, Gupta, et al., 2017). Diclofenac has modest efficacy on mild AKs with reported complete clearance of 58% 30 days after treatment (G. M. Martin & Stockfleth, 2012). Diclofenac gel is better tolerated than 5-FU and imiquimod, but local adverse effects are possible, including mild erythema, pruritus and xerosis (Samrao & Cockerell, 2013). The AK treatment guidelines recommend the use of diclofenac for single or multiple grade I–II AKs and field cancerization (de Berker et al., 2017; Heppt et al., 2020; Werner et al., 2015).

### *Ingenol mebutate*

Ingenol mebutate is a diterpene ester extracted from the plant *Euphorbia peplus* (milkweed) and it was licensed in 2012 by the European Medicines Agency (EMA) for topical treatment of non-hypertrophic, non-hyperkeratotic AKs (grade I–II) (de Berker et al., 2017). It has a dual action mechanism: 1) rapid lesion necrosis by disruption of mitochondrial membranes and 2) specific, neutrophil-mediated, antibody-dependent cellular cytotoxicity that targets any residual dysplastic epidermal cells (R. H. Rosen et al., 2012). In a pooled analysis of trials on the face and scalp, the complete clearance rate of AKs was 42% and median reduction of AK lesions 83% 57 days after short-course treatment (Lebwohl et al., 2012). In long-term follow-up of 12 months, a sustained complete clearance rate of 46.1% and a lesion reduction rate of 87.2% have been reported (Lebwohl et al., 2013). The adverse reactions include erythema, scabbing and scaling which peaks on days 3–8 and resolves within 2–4 weeks (Samrao & Cockerell, 2013). The short course of treatment leads to good patient adherence and ingenol mebutate may be a useful

option for AKs, especially in primary care. However, in January 2020 EMA suspended the licence for Picato due to suspicion that it may increase the risk for skin cancers, especially for cSCC. Therefore, the current German AK treatment guideline no longer recommends the use of ingenol mebutate for AKs (Heppt et al., 2020).

### 2.1.8.3 Comparison of efficacy for actinic keratosis therapies

In a RCT comparing four field-directed treatments for multiple AKs (5% 5-FU, 5% imiquimod, cPDT with MAL and 0.015% ingenol mebutate), at 12 months 5-FU was the most effective treatment (Jansen et al., 2019). A Cochrane review with network meta-analysis based on participant complete clearance ranked 5-FU as the most efficient of the main topical treatments (Gupta & Paquet, 2013). The other interventions were ranked as follows: 5-FU > cPDT with ALA  $\approx$  imiquimod  $\approx$  ingenol mebutate  $\approx$  cPDT with MAL > cryotherapy > diclofenac > placebo (Gupta & Paquet, 2013).

Imiquimod has shown good long term-efficacy for AKs. In a three-arm RCT between cryotherapy, 5-FU and 5% imiquimod, the sustained clearance rate of individual AK lesions at 12 months was 28%, 54% and 73%; and sustained clearance of total treatment field was 4%, 33% and 73%, respectively (Krawtchenko et al., 2007).

A systematic review of AK interventions from post-marketing surveillance trials outlined the following participant complete clearances in descending order of efficacy: 0.05% ingenol mebutate 88.9%, 0.015% ingenol mebutate 45.1–76.6%, imiquimod 52.1%, cPDT with ALA 33.6%, diclofenac 23.1–48.7%, cryotherapy + diclofenac 42.4% and cryotherapy 25.7% (Steeb et al., 2020). In another systematic review comparing five AK treatment modalities (cryotherapy, PDT, 5-FU, ingenol mebutate and colchicine cream) in non-face and non-scalp locations, cryotherapy showed the highest participant and lesion complete clearance rates (Steeb et al., 2021).

## 2.1.9 Prevention

In the prevention of AKs the key elements are regular use of high sun protection factor (SPF  $\geq$  50) sunscreen, avoidance of midday sun exposure between 11 a.m. and 3 p.m. and protection of the skin and scalp during outdoor activities by wearing

sunglasses, brimmed hat and loose protective clothing (Dirschka, Gupta, et al., 2017). In an Australian community-based RCT of over 1,300 immunocompetent participants (mean age 48 years) followed up for 4.5 years, the regular use of sunscreen significantly reduced the risk of cSCC but not of BCC (Green et al., 1999). In immunosuppressed OTR patients the daily use of broad-spectrum sunscreen (SPF >50, high UVA-absorption) for 2 years significantly reduced the incidence of AKs and invasive cSCC and also significantly reduced the number of existing AKs at baseline (C. Ulrich et al., 2009). In addition to sun protection measures, oral nicotinamide (vitamin B3) has recently shown promising results in chemoprevention of NMSC and AK in high-risk population (patients with  $\geq 2$  NMSC in the last 5 years). Oral nicotinamide 500 mg b.i.d. for 12 months reduced the rate of new BCCs by 20%, of cSCCs by 30% and of AKs by 11% in comparison to placebo (A. C. Chen et al., 2015).

## 2.2 Lentigo maligna and lentigo maligna melanoma

Lentigo maligna (LM), also referred to as ‘Hutchinson’s melanotic freckle’, is a subtype of melanoma in situ (MIS) which occurs on chronically sun-exposed skin (DeWane et al., 2019). It was first described by the British dermatologist Hutchinson in 1892, and four years later Dubreuilh reported four cases of “lentigo maligna of the elderly” (van Ruth & Toonstra, 2008). LM is the most common MIS subtype accounting for 79–83% of all MIS cases (Swetter et al., 2005). It occurs on the chronically sun-damaged skin of elderly patients, typically on the head or neck, but is also occasionally found in the trunk and extremities (Kasprzak & Xu, 2015; Robinson et al., 2019). LM can be considered a precursor of melanoma and, if left untreated, it can progress to invasive lentigo maligna melanoma (LMM) with an estimated lifetime risk varying from as low as 5% to as high as 30–50% (Stevenson & Ahmed, 2005; Weinstock & Sober, 1987). However, it has been suggested that most patients with LM will eventually develop a LMM if they live long enough (L. M. Cohen, 1995). LMM accounts for 4–15% of all invasive melanomas that also include superficial spreading (70%), nodular (10–15%) and oral-acral subtypes (McKenna et al., 2006). Once LMM develops, it has a prognosis similar to that of other invasive melanomas correlating with Breslow thickness of the lesion (L. M. Cohen, 1995).

## 2.2.1 Clinical characteristics

LM and LMM have similar clinical appearance (Figure 4). LM/LMM typically presents as an asymmetric pigmented patch or macule with ill-defined borders and wide variation in size, shape and shade (from tan to black to the rare amelanotic) (Juhász & Marmur, 2015). These lesions are slowly enlarging, change in appearance over time and there may be partial regression within the lesion (Reed & Shea, 2011). The surrounding skin may exhibit signs of chronic solar damage such as solar elastosis, solar lentigines and AKs (Juhász & Marmur, 2015). LM can develop de novo or within a pre-existing solar lentigo (Kasprzak & Xu, 2015). Clinically, it is difficult to distinguish between LM and LMM (McKenna et al., 2006). Typically, LM lesions are slowly radially growing before entering an invasive vertical growth phase (McGuire et al., 2012). The risk for LMM may increase with the size of the lesion, and large lesions often contain small foci of invasion (L. M. Cohen, 1995). Several histologic studies have suggested that 16–50% of LM lesions already have an invasive component when only the in situ type is clinically suspected (McLeod et al., 2011). The development of dark pigmentation, sharp borders or elevated areas within a LM lesion may indicate progression to LMM (Juhász & Marmur, 2015). The differential diagnoses of LM/LMM include dysplastic nevus, pigmented BCC, SCC, seborrheic keratosis, pigmented AK and solar lentigo (Bosbous et al., 2010).

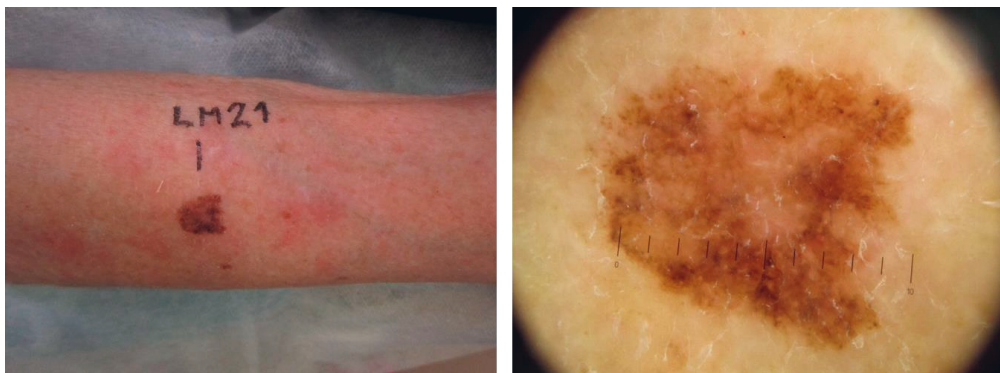


**Figure 4.** A clinical and dermoscopic photograph of a lentigo maligna on forearm. This lesion was treated in Study III with photodynamic therapy but was a non-responder. With permission from the patient.



## 2.2.2 Diagnosis and histopathology

The suspicion of LM/LMM is based on clinical and dermoscopic features, but diagnosis is confirmed by biopsy and histopathological examination (Robinson et al., 2019). The clinical diagnosis is challenging as the lesions may be subtle and vary in appearance (Kasprzak & Xu, 2015). Early diagnosis relies on a high clinical suspicion and low threshold for biopsy (McGuire et al., 2012). It is worth noting that earlier treatments may alter the appearance of the lesion. Cryotherapy or other ablative therapies used for a suspected solar lentigo may cause partial depigmentation and thus complicate the clinical examination of LM (McKenna et al., 2006). The delay in the diagnosis of LMM may be up to four times longer than for the other forms of cutaneous melanoma (Bosbous et al., 2010).

Several non-invasive methods have been developed to facilitate the early diagnosis of LM/LMM, including dermoscopy and reflectance confocal microscopy (Kasprzak & Xu, 2015), which are further discussed in Chapter 2.4. Wood's light improves the contrast between a pigmented lesion containing epidermal melanin and the surrounding normal tissue and may be useful in delineating the margin of an LM lesion (Paraskevas et al., 2005). The four most important dermoscopic features of LM or LMM are asymmetrically pigmented follicular openings, dark rhomboidal structures, slate-grey dots and slate-grey globules with a diagnostic sensitivity of 89% and a specificity of 96% (Schiffner et al., 2000). Additional criteria described more recently include increased vascular density, red rhomboidal structures and target patterns (Pralong et al., 2012). Of note, pigmented AK bears clinical and dermoscopic features strikingly similar to those of LM/LMM and represents a diagnostic challenge (Akay et al., 2010). In a recent meta-analysis dermoscopy showed good accuracy in the diagnosis of LM/LMM with reported mean sensitivity of 82.4% and specificity of 83.5%, the most frequent dermoscopic features associated with LM/LMM being rhomboid structures, pseudonetwork and homogenic areas (Carapeba et al., 2019).

The gold standard for the confirmation of LM/LMM diagnosis is skin biopsy and histopathological evaluation (McKenna et al., 2006). Excisional biopsy is the optimal method, although is not often feasible in the case of LM because of its ill-defined borders, large size or location in cosmetically sensitive areas e.g. on the eyelid. An incisional excision or diagnostic punch biopsy should be taken from the darkest or most concerning part of the lesion to avoid sampling error (Kasprzak & Xu, 2015).

Histologically, LM is characterized by atypical junctional melanocytic hyperplasia combined with underlying photodamage. The lesions typically demonstrate a

proliferation of atypical melanocytes at the dermo-epidermal junction, confluence of atypical melanocytes and angulated nuclei replacing the basal layer and nesting of atypical melanocytes with occasional pagetoid spread (Kasprzak & Xu, 2015). Adnexal and follicular involvement of atypical melanocytes is typically seen (Figure 5) (Kraft & Granter, 2014). Because LM occurs almost exclusively on chronically sun-damaged skin, the histologic features related to actinic damage, such as epidermal atrophy, increased pigmentation in basal keratinocytes and prominent solar elastosis are consistently present (Reed & Shea, 2011). Since actinically damaged skin also tends to exhibit some degree of melanocyte hyperplasia, diagnostically it is not always easy to distinguish LM from background sun damage. In addition, early lesions may yield quite subtle histologic findings (Connolly et al., 2015). The histologic diagnosis of LM/LMM is difficult and the degree of diagnostic concordance among dermatopathologists is not very high (Florell et al., 2003). Immunohistochemical (IHC) stains may be used to assist in the histological diagnosis of unclear cases. The melanocytic markers used in the diagnosis of LM include S100 protein, HMB45 (*Human Melanoma Black*), MITF (*Microphthalmia Transcription Factor*), SOX10 (*SRY-related HMG-box 10 protein*) and Melan A/MART-1 (*Melanoma Antigen Recognized by T-cells*) (Connolly et al., 2015). A newer marker R21, a monoclonal antibody against soluble adenylyl cyclase (sAC), has recently been utilized in the diagnosis of LM/LMM. The sensitivity of pan-nuclear staining with R21 in LM was 88%, whereas nuclear expression was observed in 40% of other melanomas and only 2.3% of benign nevi (Magro et al., 2012).

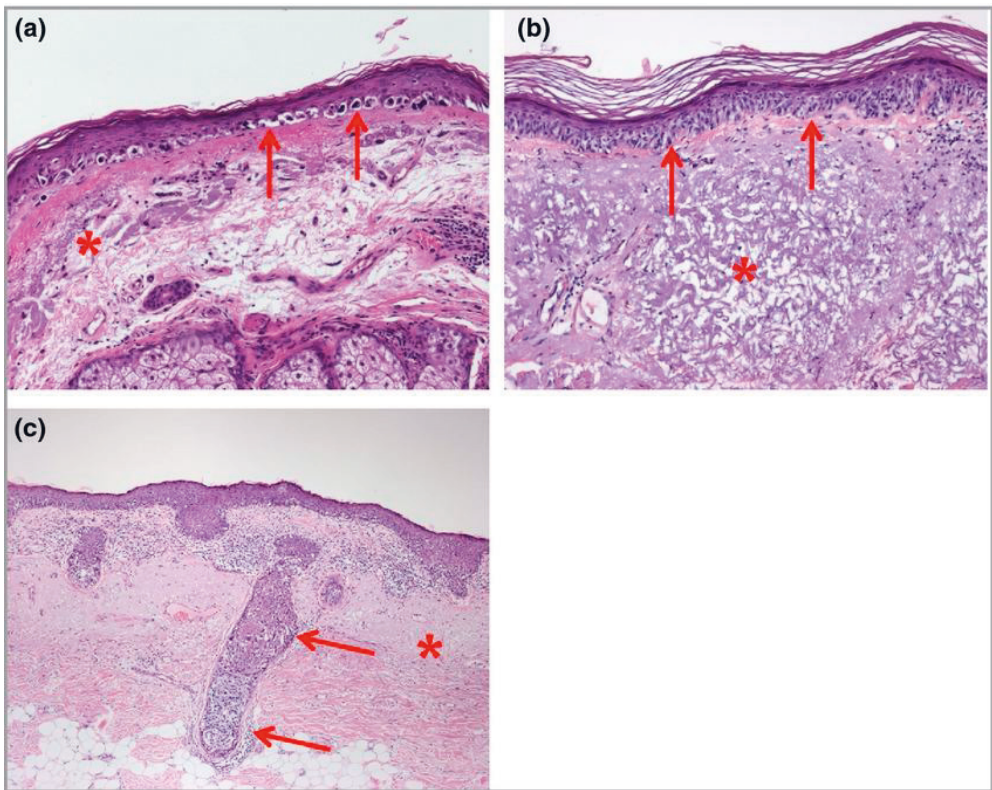


**Figure 5.** Histopathological features of lentigo maligna (LM). (\* indicates solar elastosis) (a) In the earliest stages LM is characterized by scattered atypical melanocytic cells (arrows) along the basal epidermis. Note the associated epidermal atrophy with loss of rete ridges and the thick zone of severe solar elastosis in the superficial dermis. (b) A more advanced LM with greater density and degree of cytological atypia of the melanocytes (arrows). (c) Advanced LM (arrows) with a confluent proliferation of atypical melanocytes and flord extension down a pilosebaceous unit (arrows) the dermosubcutaneous junction. From *Fogarty et al., 2014*, with permission from Wiley.

### 2.2.3 Risk factors and pathophysiology

In the latest WHO classification of melanoma from 2018, LM/LMM is categorized into chronically sun-damaged (CSD) melanomas by its evolutionary pathway (Elder et al., 2020). CSD and non-CSD melanomas differ in their site of anatomical location, degree of cumulative UV exposure, patient age, mutation burden and types of genetic alteration (Shain & Bastian, 2016). LM is a melanocytic malignancy occurring by definition on chronically sun-damaged skin. Chronic UV exposure is the most widely accepted risk factor for the development of LM (L. M. Cohen, 1995).

UV radiation seems to play a different role in pathogenesis than in other subtypes of melanoma in that chronic rather than intermittent UV exposure appears to increase the risk of LM (Swetter et al., 2005). However, no dose-effect relationship with cumulative sun-exposure has been found (Gaudy-Marqueste et al., 2009). Other risk factors for the development of LM include a history of NMSC, older age, light skin phototype and tendency to form solar lentigines. Unlike superficial spreading melanoma, LM is not associated with the number of nevi nor with the genetic propensity to develop nevi (Gaudy-Marqueste et al., 2009; Kvaskoff et al., 2012). It has been suggested that stem cells in hair follicles mutated from UV radiation may be responsible for the development of LM (Bongiorno et al., 2008).

LM has a different genetic composition than other types of melanoma. BRAF (*V-Raf Murine Sarcoma Viral Oncogene Homolog B1*) mutations may not play as significant a role in LM as they do in other types of melanoma (Kasprzak & Xu, 2015). Unlike in superficial spreading melanoma, there is a low incidence of BRAF mutations in LM (Lee et al., 2011). When present, BRAF<sup>V600K</sup> mutations are more frequently seen than BRAF<sup>V600E</sup> mutations, which is in line with the observation that BRAF<sup>V600K</sup> mutations are increased in melanomas arising from chronically sun-damaged skin (Stadelmeyer et al., 2014). P53 mutations are more commonly seen in LM along with other melanomas occurring in sun-damaged skin (Kraft & Granter, 2014). CSD melanomas, including LMM, have a very high mutational burden and are associated with mutations in NF1 (*neurofibromin 1*), NRAS (*neuroblastoma RAS viral oncogene homolog*), BRAF<sup>nonV600E</sup> or KIT (*Tyrosine-Protein Kinase Kit*). By contrast, non-CSD melanomas have a moderate mutational burden and a predominance of BRAF<sup>V600E</sup> mutations (Bastian, 2014). Melanoma in situ lesions such as LM also demonstrate a high frequency of TERT (*telomerase reverse transcriptase*) promoter mutations, which seem to emerge at a very early stage of neoplastic progress (Shain et al., 2015).

## 2.2.4 Epidemiology

The peak incidence of LM occurs between 65 and 80 years, but it has also been reported in 20- and 30-year-olds (Stevenson & Ahmed, 2005). Due to population ageing and high cumulated UV exposure, the incidence of LM and LMM has increased markedly in recent decades in Denmark, the Netherlands, the USA and Australia (Greveling et al., 2016; Mirzoyev et al., 2014; Swetter et al., 2005; Toender et al., 2014; Youl et al., 2013). For example, in Olmsted County, Minnesota, USA,

the overall age- and sex-adjusted incidence of LM increased from 2.2 to 13.7 per 100,000 person-years between 1970–1989 and 2004–2007 (Mirzoyev et al., 2014). The mean age at diagnosis was 70 years (Mirzoyev et al., 2014). In the Netherlands the age-standardized incidence rate for LM increased from 0.72 to 3.84 per 100,000 person-years, and for LMM from 0.24 to 1.19 between 1989 and 2013 (Greveling et al., 2016).

### 2.2.5 Prognosis

The annual and lifetime risk of progression of LM to LMM has been estimated in only two epidemiological studies. In a study by Weinstock et al. utilizing epidemiological data from the 1970s in the USA, the annual progression rate of LM to LMM ranged from 0.03% in <45 year-olds to 0.14% in 65–74 year-olds, corresponding to a lifetime risk of 2.2–4.7% for developing LMM (Weinstock & Sober, 1987). In a recent Australian prospective population-based survey the estimated annual rate of progression of LM to LMM was 3.5% per year. This corresponds to an average time of 28.3 years for an LM to undergo malignant progression to LMM (Menzies et al., 2020). The 5-year survival rate of LMM in whites is among the highest of all melanoma subtypes, estimated at 97.2% (Wu et al., 2011). This emphasizes the slow-growing and indolent nature of LM/LMM even when an invasive component has developed.

### 2.2.6 Treatment

There are a variety of treatment options for LM which can be divided into surgical and non-surgical methods. The gold standard treatment is complete surgical excision, which is also recommended by the current treatment consensus. However, in some instances the patient may be unfit or unwilling to undergo surgery, and in these cases alternative therapies may be considered (Bichakjian et al., 2011). LM lesions are frequently located in the cosmetically sensitive head and neck area, which poses an aesthetic challenge for the surgeon. In addition, LM patients are often elderly and may have contraindications to surgical treatment (Erickson & Miller, 2010). Surgical methods have an average recurrence rate of 6.8% at 5 years, while non-surgical methods have shown recurrence rates of 20–100%, depending on the method (Juhász & Marmur, 2015). When surgery is not an option, even observation

may be accepted considering the relatively benign and slow-growing nature of LM (Bichakjian et al., 2011).

### 2.2.6.1 Surgical treatment

The most common surgical methods are wide local excision (WLE), Mohs micrographic surgery (MMS) and staged surgical excision (SSE).

#### *Wide local excision*

WLE is the standard, one-stage elliptical excision. Surgical margins of 5–10 mm are recommended by multiple guidelines to ensure complete resection of LM and to reduce the likelihood of recurrence (Juhász & Marmur, 2015). Hazan et al. reported that the mean total surgical margin required to clear LM was 7.1 mm and to clear LMM it was 10.3 mm (Hazan et al., 2008). In another study, 6 mm margins successfully excised 86% and 9 mm margins 98.9% of LMs (Kunishige et al., 2012). Furthermore, larger lesions tend to have greater subclinical spread and require larger surgical margins for clearance (Bub et al., 2004). Excised tissue is processed with permanent sections using bread-loaf technique and vertical sections at 2–4 mm intervals (McGuire et al., 2012). A limitation of WLE and conventional bread-loafing during pathological sectioning is that only 5% of the peripheral margin is examined histologically, which may not sample the surgical margin adequately in case of LM (Connolly et al., 2015). It has been estimated that in order to detect 100% of positive margins for LM, bread-loafing with 0.1 mm intervals would be necessary (Kimyai-Asadi et al., 2007). Recurrence rates from 6% to 20% have been reported after standard excision with 5 mm margins (Erickson & Miller, 2010). Thus, alternative surgical techniques have been proposed in order to enhance detection and mapping of tumour at peripheral margins.

#### *Mohs micrographic surgery*

MMS is a tissue-conserving excision technique that uses vertical sectioning of a frozen excision specimen during the surgical procedure which can be completed in a single patient visit. The margins are excised with the scalpel angled at 45° degrees to the skin surface and processed with *en face* frozen sections, enabling the examination of 100% of the peripheral margin (McGuire et al., 2012). However, the identification of malignant melanocytes from frozen sections is more difficult than

in permanent sections. Vacuolar keratinocytes may mimic melanocytes, processing artefact may complicate reading the specimen and dermal inflammatory cells may obscure the melanocytes in frozen sections (Stevenson & Ahmed, 2005). Thus conventional MMS is not the optimal method for excising LM, and variations of the technique have been developed, including ‘slow Mohs’ using rush permanent sections and MMS utilizing IHC stains on frozen sections (McGuire et al., 2012). The recurrence rates for MMS have been reported to be 0–33%, with the majority of studies reporting rates less than 3% (Bosbous et al., 2010).

### *Staged surgical excision*

SSE is any excision technique incorporating more than one stage, usually with the next stage determined by the histologic findings of the previous stage (McLeod et al., 2011). SSE allows for surgical margin control as comprehensive as MMS but relies on horizontal rush permanent sections at the peripheral margin. Various SSE techniques have been developed, including ‘square method’, ‘perimeter technique’ or ‘spaghetti technique’, staged radial sections and staged ‘mapped’ excisions but the principle in all these remains the same (Kasprzak & Xu, 2015). The results with SSE have been excellent with local recurrence rates ranging from 0 to 7.3%, making it a preferred treatment for LM and LMM (Bosbous et al., 2010). The disadvantages with staged methods is the necessity for patients to undergo multiple procedures and delayed wound closure (Connolly et al., 2015). Regardless of method, the centre of the tumour should be always be assessed in permanent sectioning to rule out the invasive component (Erickson & Miller, 2010).

#### 2.2.6.2 Non-surgical treatment

Non-surgical treatment methods used for LM include radiotherapy, topical imiquimod, laser therapy, cryotherapy and photodynamic therapy (Juhász & Marmur, 2015).

##### *Radiotherapy*

Radiotherapy is considered to be a superior non-invasive treatment because it may eradicate the potentially invasive components of LM (Juhász & Marmur, 2015). In the setting of LM/LMM, soft X-rays (20–50 kV) or ultrasoft X-rays i.e. Grenz rays (12 kV) have been employed (Hedblad & Mallbris, 2012). These low-voltage

regimens deliver X-rays at around 1 mm depth and are intended to target epidermal lesions more specifically with fewer adverse effects than high-voltage regimens (Bosbous et al., 2010). One fractionated treatment with Grenz rays for LM or early LMM showed a complete clearance of 83% when used as a primary therapy, and 90% when combined with partial excision (Hedblad & Mallbris, 2012). In a retrospective analysis of all studies from 1941 to 2009 with a mean follow-up of 3 years, the recurrence rate with radiotherapy was 5% (Fogarty et al., 2014). Radiation therapy may be considered as a primary therapy in selected patients for whom surgery is not a reasonable option (Bichakjian et al., 2011).

In Finland, radiotherapy is very rarely used as a primary treatment for LM but is occasionally used as an adjuvant therapy if surgical margins have been left positive after primary excision and patient cannot withstand general anaesthesia (radiation oncologist Tanja Skyttä, personal communication, April 19, 2021).

### *Imiquimod*

Imiquimod, a topical immune response modulator with antitumour properties, has been evaluated for the treatment of LM in limited, uncontrolled studies, case series and case reports with a relatively short follow-up of less than 5 years (Kasprzak & Xu, 2015). In a systematic review of 5% imiquimod cream used for LM, complete clinical clearance was seen in 78.3% and histological clearance in 77% of patients, with 6–7 applications per week and a total of >60 applications showing the greatest odds for complete clinical and histological response (Tio et al., 2017). In nine cases LM progressed to LMM shortly after treatment, but the authors hypothesized that LMM may already have been present before treatment initiation. Imiquimod has also been investigated as a neoadjuvant therapy before staged excision but it does not improve the recurrence rate compared to standard staged excision by MMS or *en face* permanent sections (Donigan et al., 2018). In rare instances imiquimod may remove the pigment of LM without affecting the histologic findings (Fleming et al., 2004).

### *Laser therapy*

Various forms of laser therapy have been investigated for the management of LM, including carbon dioxide, argon, Q-switched ruby, neodymium-doped yttrium aluminium garnet (nd-YAG), alexandrite or combinations of the above. However, the recurrence rates with laser therapy have been as high as 40% to 50% and thus laser therapy is not recommended for LM (Bosbous et al., 2010). The current laser therapies may not penetrate to a sufficient depth to destroy atypical melanocytes



extending deep into the adnexal structures, or atypical melanocytes may be resistant to laser destruction (McLeod et al., 2011).

In a recent review of non-surgical treatments available for LM, the recurrence rates were 0–31% (mean 11.5%) for radiotherapy, 4–50% (mean 24.5%) for imiquimod and 0–100% (mean 34.4%) for laser therapy, which are all inferior to those achieved with surgical methods (Read et al., 2016).

### *Cryotherapy*

Cryotherapy has also been used in the treatment of LM. Melanocytes are more sensitive to freezing than keratinocytes and fibroblasts, but it is not known whether this applies to atypical melanocytes associated with LM (McLeod et al., 2011). Several protocols with different freezing times and freeze-thaw cycles have been studied with varying recurrence rates from 0 to 34%. Because of the lack of consistency and definitive controlled studies, cryotherapy is not recommended for LM (Bosbous et al., 2010). A drawback in cryotherapy is the lack of microscopic margin control and the lack of histologic evaluation of the destroyed lesion. As a result of the latter, microscopic invasive foci of LMM or an aggressive form of melanoma may go unnoticed (Tzellos et al., 2014). This shortcoming also applies to all other non-invasive treatment modalities for LM.

### *Photodynamic therapy*

The use of PDT in the treatment of LM has been evaluated in only one retrospective study. Karam et al. treated 15 histologically confirmed LM lesions using 3–9 PDT sessions with light dose ranging from 40 to 90 J/cm<sup>2</sup> per session, resulting in a cure rate of 12/15 lesions (80%) (Karam et al., 2013). However, the clearance of lesions was assessed by clinical follow-up (range 18–50 months) and by using multiple biopsies representing only parts of the lesions.

## 2.3 Photodynamic therapy

### 2.3.1 History and principle

The principle of photodynamic reaction (PDT) was invented over 100 years ago when acridine orange was shown to be lethal for *Paramecium* cells in the presence of daylight (Babilas et al., 2010). An important milestone in the history of PDT as cancer therapy was reached in 1978, when Dougherty et al. successfully treated cutaneous and subcutaneous cancers with intravenous injection of a hematoporphyrin derivative followed by local exposure to red light (Dougherty et al., 1978). Over the next two decades PDT gained popularity as a primary or adjuvant cancer therapy. Porfimer sodium (Photofrin®) was the first systemic photosensitizer approved by the FDA (US Food and Drug Association) to treat oesophageal and early stage lung cancer (Zeitouni et al., 2003). However, the intravenous administration of photosensitizers is severely limited by prolonged general photosensitivity, which lasts for several weeks (Marmur et al., 2004).

The birth of modern topical PDT occurred in 1990, when Kennedy et al. utilized topical 5-aminolaevulinic acid (ALA) in the treatment of superficial skin cancers, mainly BCCs, with a high response rate of 90% (Kennedy et al., 1990). Since then, topical PDT has given rise to numerous scientific studies in the field of dermatology and it has become a well-established treatment for NMSC, including AK, Bowen's disease and BCC (Braathen et al., 2012; Morton et al., 2013a). PDT may also be effective in some non-neoplastic dermatologic conditions like acne vulgaris, photoaging, plantar and genital warts, cutaneous leishmaniasis, morphea and lichen sclerosus (Babilas et al., 2010; Morton et al., 2013b; Wiegell & Wulf, 2006). Outside dermatology, PDT with systemic photosensitizers is used for the treatment of bronchial and oesophageal cancer, aggressive head and neck tumours, maculopathies and eye cancers (Blasi et al., 2018; M. Chen et al., 2006; Schweitzer, 2001). 5-ALA mediated PDT is also utilized in the diagnosis and treatment of bladder cancer (Inoue, 2017).

PDT requires three essential components: a photosensitizer, oxygen and light of appropriate wavelength (D. K. Cohen & Lee, 2016). The most commonly used photosensitizers in topical PDT are ALA and its methyl ester MAL (methyl-5-aminolaevulinate) (Szeimies et al., 2005). These both have a small molecular weight and easily penetrate stratum corneum, after which they are selectively taken up by malignant cells (Griffin & Lear, 2016). ALA and MAL are precursors of

protoporphyrin IX (PpIX), a compound in the heme synthesis pathway which is present to some degree in all tissues of the body (Thunshelle et al., 2016). ALA formation occurs early in the pathway and is the rate-limiting step. The administration of exogenous ALA leads to selective ALA uptake and accumulation of PpIX in epithelial tumour cells due to their altered stratum corneum and differences in heme synthesis pathway (D. K. Cohen & Lee, 2016). After exposure of PpIX to light containing wavelength in its activation spectrum, a phototoxic reaction occurs and releases highly reactive oxygen species (ROS), mainly cytotoxic singlet oxygen (Ozog et al., 2016). The ROS cause intracellular damage in proteins and DNA leading to tissue necrosis and apoptosis (Babilas et al., 2010). Secondary to PDT occurs an inflammatory reaction causing neutrophil migration to the treated malignant cells (Gollnick et al., 2003). The mechanism of PDT is presented in Figure 6.

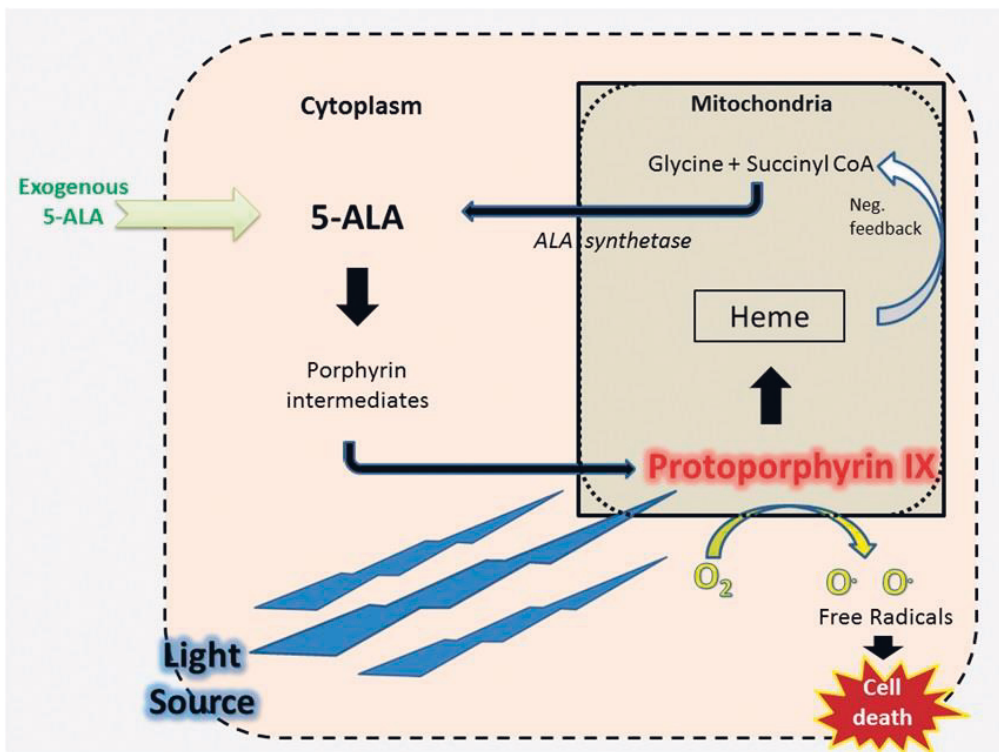


**Figure 6.** Mechanism of PDT. Exogenous 5-aminolaevulinic acid (ALA) enters the porphyrin-heme pathway and is converted endogenously into PpIX. Once PpIX is activated by the proper wavelength of light, it produces singlet oxygen free radicals, which destroy the target cell. From Ozog et al., 2016, with permission from Wolters Kluwer.

## 2.3.2 Photosensitizers

For dermatological purposes, there are currently three licensed photosensitizers available for PDT in Europe (Table 3) (Morton et al., 2013a). In North America there is also available ALA hydrochloride approved for AKs in a protocol that uses blue light (Babilas et al., 2010).

**Table 3.** The photosensitizers licensed in Europe and USA for topical photodynamic therapy. †) Levulan Kerastick® is only approved in USA, Canada and Japan. BD = Bowen's disease, nBCC = nodular BCC, sBCC = superficial BCC.

Photosensitizer	Trade name	Formulation	Manufacturer	Light source	Indication
Methyl-5-aminolaevulinate (MAL)	Metvix®	16% cream	Galderma (Lausanne, Switzerland)	Red LED, daylight	LED: non-hyperkeratotic AK, sBCC, nBCC, BD Daylight: grade I-II AK
5-aminolaevulinic acid nanoemulsion (BF-200 ALA)	Ameluz®	7.8% gel	Biofrontera (Leverkusen, Germany)	Red LED	Grade I-II AK, sBCC, nBCC
5-aminolaevulinic acid (ALA)	Alacare®	8mg patch	Photonamic (Pinneberg, Germany)	Red LED	Grade I AK
5-aminolaevulinic acid hydrochloride (ALA HCL)†	Levulan Kerastick®	20% solution	DUSA, Wilmington, MA, USA	Blue LED	Grade I-II AK

ALA is a hydrophilic molecule with modest tissue penetration and its uptake in tissue requires active transport via the GABA transporters (D. K. Cohen & Lee, 2016). Methyl-5-aminolaevulinate (MAL), a methyl ester of ALA, is a lipophilic molecule with better penetration and higher intracellular accumulation of PpIX than ALA (Gaulhier et al., 1997). MAL uptake in cells is thought to occur by passive diffusion and non-polar amino acid transport, in contrast to ALA (D. K. Cohen & Lee, 2016). After topical application, both ALA and MAL are selectively taken up by malignant cells of epithelial origin and converted into PpIX (Fritsch et al., 1998). MAL has shown a high selectivity for neoplastic cells, with a 10-fold difference between lesional skin of BCCs or AKs and healthy skin (Angell-Petersen et al., 2006). A nanoemulsion of ALA (BF-200 ALA) has been developed in order to improve penetration and PpIX accumulation (Maisch et al., 2010). In *ex vivo* human skin, 78mg/g BF-200 ALA gel has been shown to induce more than 3-fold higher PpIX concentration than 20% ALA cream after an incubation time of 3 hours (Schmitz, Novak, et al., 2016). When ALA or MAL is applied topically, it penetrates the epidermis and dermis in sufficient amounts, but the dermal cells do not develop significant PpIX levels to become photosensitized. This makes it possible to treat

epidermal cancers without damaging the dermis, which may explain why scarring is unusual in topical PDT (Ericson et al., 2008)

In addition to ALA and MAL, a more lipophilic hexyl ester of ALA called hexylaminolaevulinate (HAL) has been investigated in the treatment of NMSC with promising results but there is no commercial product available for dermatological indications (Neittaanmäki-Perttu, Grönroos, Karppinen, Tani, et al., 2016; Salmivuori et al., 2020; Togsverd-Bo et al., 2010).

### 2.3.3 Light sources

Over the years, several light sources emitting coherent and incoherent light have been used in PDT (Ozog et al., 2016). A proper light source should meet two criteria: it has to match the absorption spectrum of PpIX to induce the photochemical reaction and it has to be able to penetrate the tissue deep enough to reach the target cells (Ericson et al., 2008). PpIX has its maximum absorption peak at 410 nm followed by several smaller peaks at 505, 540, 580 and 630 nm (Morton et al., 2013a). In Europe, the most commonly used light sources for conventional PDT (cPDT) are narrowband red LED lights matching the absorption peak of 630 nm for PpIX. The light dose in the red LED devices is set at 37 J/cm<sup>2</sup> and corresponds to a PpIX-weighted light dose of approximately 1 J<sub>eff</sub>/cm<sup>2</sup> (Wiegell, Wulf, et al., 2012). In clinical studies, narrow-spectrum light sources have shown relatively higher response rates for AKs in PDT when compared to broad-spectrum devices (Dirschka et al., 2012; Szeimies et al., 2010). The use of red light (630 nm) is preferred over blue light (410 nm) because of better tissue penetration (>2 mm), even though the absorption maximum of PpIX is in the blue region (Ozog et al., 2016). However, in the USA a blue fluorescent lamp (peak emission at 417 nm) is approved for PDT along with Levulan Kerastick® to treat non-hyperkeratotic AKs (Piacquadio et al., 2004). There is also a range of other light sources that can be used in topical PDT, including lasers, metal halide lamps, fluorescent lamps and filtered xenon lamp arcs (Morton et al., 2013a).

Daylight can also be used as a light source in PDT. In 2008 Wiegell et al. reported for the first time that the continuous activation of PpIX using daylight is as effective as cPDT for the treatment of AKs (Wiegell et al., 2008). Since then, daylight photodynamic therapy (DL-PDT) has attracted a lot of scientific attention and established a firm status in the treatment guidelines for AKs (Calzavara-Pinton et al., 2017; Ibbotson et al., 2017; Wiegell, Wulf, et al., 2012). Visible daylight contains all the peaks in the absorption spectrum of the PpIX. If the tissue penetration is disregarded, an estimated 87% of the daylight activation is caused by the violet-blue-cyan light (380–495 nm) but only 10% and 3% by the green-yellow (495–590 nm) and orange-red (590–750 nm) light respectively. During 2-hour daylight exposure, the minimum mean illuminance should be 100000 lux in order to achieve the same effective red light dose as from cPDT, but because the other wavelengths also activate PpIX, as low as 2300 lux has been estimated to be efficient (Wiegell, Wulf, et al., 2012). Wiegell et al. have suggested that the PpIX-weighted light dose in DL-PDT should be  $>3.5$  or  $8 J_{\text{eff}}/\text{cm}^2$  and the ambient temperature  $>10$  °C, which at higher latitudes imposes a seasonal limitation for executing DL-PDT (Wiegell, Fabricius, et al., 2012; Wiegell, Wulf, et al., 2012). For example, in Helsinki (60°N), the effective light dose for 2 hours of clear sky daylight exposure would be  $> 8 J_{\text{eff}}/\text{cm}^2$  from February to October, but the ambient temperature limits the applicability of DL-PDT probably from May to September (Wiegell, Wulf, et al., 2012).

To overcome the seasonal limitation in the Nordic countries and to standardize the light dose and ambient temperature, a simulated DL-PDT with artificial lamps mimicking daylight has also been developed (Kellner et al., 2015). There are also other alternative light sources for “indoor DL-PDT” such as halogen lamps (overhead and slide projector), white LED lamps, or red LED lamps used in cPDT. Also, a glass greenhouse could be used when the weather is cold, windy or wet outside (Lerche et al., 2016).

## 2.3.4 Clinical procedure

### 2.3.4.1 Pretreatment

In cPDT, first a gentle curettage of crusts and hyperkeratosis of the target lesions should be performed, then topical photosensitizing agent is applied topically on the skin and left under occlusion for 3 hours. After incubation time the treated area is irradiated with visible light activating accumulated PpIX at once (Szeimies et al., 2005). After treatment the patient must avoid direct sunlight for 48 hours as PpIX is still formed (Petersen et al., 2014).

In DL-PDT procedure, first a pretreatment (e.g. curettage or sand paper abrasion) is given and an organic sunscreen spread over the whole treatment area, followed by application of photosensitizing agent to the skin. Occlusion is not needed. After an incubation time of 30 minutes the patient is exposed to daylight for 2 hours, during which PpIX is formed and activated continuously in contrast to cPDT (Philipp-Dormston et al., 2016; Wiegell et al., 2008).

### 2.3.4.2 Laser-assisted photodynamic therapy

The concept of fractional photothermolysis was first introduced by Manstein in 2004, and since then has revolutionized dermatological laser therapies (Manstein et al., 2004). In fractional photothermolysis focused laser beams are used to create arrays of microscopic thermal injuries to the skin, while leaving intermediate skin intact (Hædersdal et al., 2016).

In ablative fractional laser (AFL) therapy an ablative laser, usually carbon dioxide (CO<sub>2</sub>) or erbium-doped yttrium-aluminium-garnet (Er:YAG) generates microscopical ablative channels into the skin, which provide an alternative pathway for cutaneous drug delivery (Hædersdal et al., 2016).

In vivo studies with porcine skin models have shown that AFL pretreatment before topical application of MAL significantly enhances PpIX fluorescence from the skin surface to the reticular dermis (hair follicles, dermis) down to 1.8 mm (Hædersdal et al., 2010, 2011). The AFL laser channel depth (300–1200 µm) does not affect MAL-induced PpIX fluorescence intensities at the skin surface and in deep skin layers as long as the epidermis is penetrated (Haak et al., 2012). In a comparative study between ALA and MAL along with AFL CO<sub>2</sub> laser pretreatment, fluorescence

microscopy expressed higher fluorescence in hair follicle epithelium for ALA than for MAL (180-minute incubation) (Hædersdal et al., 2014).

### 2.3.5 Efficacy

#### *Conventional photodynamic therapy*

The cPDT with ALA or MAL using a LED light source is an effective treatment for AKs, Bowen's disease and superficial and nodular BCC (Morton et al., 2013a). However, it is not indicated for invasive SCC nor for more aggressive forms of BCC such as infiltrating or morphoic subtypes which express high recurrence rates after treatment (Fiechter et al., 2012).

In MAL cPDT for mild to moderate AKs, the lesion response rate at 3 months after one or two PDT sessions was 86–93%, but for thick AKs only 70% (Lacour et al., 2015; Morton et al., 2006; Pariser et al., 2008). In ALA-PDT using blue light for AKs (1 or 2 treatment sessions) the lesion response rate at 3 months was 91% (for the vehicle 25%) and patient complete response rate (i.e. patient 100% clear of AKs) 73% (for the vehicle 8%) (Piacquadio et al., 2004). A 12-month sustained lesion clearance rate of 78% has been reported after 1-2 treatment sessions with ALA-PDT using blue light (Tschen et al., 2006). In an intraindividual, split-scalp study comparing ALA and MAL, there was no significant difference in the efficacy of the treatments but ALA-PDT was more painful (Moloney & Collins, 2007).

cPDT with BF-200 ALA for mild to moderate AKs achieved lesion clearance rates of 81–94% and patient complete clearance rates of 64–91% after two PDT sessions (Reinhold et al., 2016; Szeimies et al., 2010). In a randomized interindividual trial the lesion response rates were 90% and 83%, and patient complete response rates 78% and 64% for BF-200 ALA and MAL respectively, demonstrating the superior efficacy of BF-200 ALA over MAL (Dirschka et al., 2012). Long-term patient complete clearance rates at 12 months were 47% for BF-200 ALA and 36% for MAL (Dirschka et al., 2013). AK treatment guidelines highly recommend cPDT with ALA or MAL for multiple AKs and field cancerization (de Berker et al., 2017; Werner et al., 2015). It is especially useful for confluent and recalcitrant AKs failing other treatments (de Berker et al., 2017).



### *Daylight photodynamic therapy*

The reported efficacies of DL-PDT for AK in several prospective RCTs are presented in Table 4. Most earlier studies on DL-PDT have focused on short-term efficacy (follow-up of 3 months), with reported lesion clearance rates after a single treatment with MAL-PDT of 74–79% in the Nordic countries (Neittaanmäki-Perttu et al., 2014; Neittaanmäki-Perttu, Grönroos, Karppinen, Tani, et al., 2016; Wiegell et al., 2008, 2011; Wiegell, Fabricius, et al., 2012; Wiegell, Hædersdal, Eriksen, et al., 2009), 70–90% in central and southern Europe (Assikar et al., 2020; Lacour et al., 2015; Moggio et al., 2016; Sotiriou et al., 2018), and 89% in Australia (Rubel et al., 2014). Most of the DL-PDT studies have used 16% MAL as a photosensitizing agent, but in a pilot study BF-200 ALA seemed more effective than MAL in a follow-up of 3 and 12 months (Neittaanmäki-Perttu et al., 2014; Neittaanmäki-Perttu, Grönroos, Tani, et al., 2016). In a recent company-sponsored trial of 49 patients, BF-200 was non-inferior to MAL in DL-PDT for mild to moderate AKs (Dirschka et al., 2019).

DL-PDT using MAL for mild to moderate AKs has been shown to be as effective as cPDT but more easily tolerated, being almost painless and associated with fewer and milder skin reactions (Lacour et al., 2015; Rubel et al., 2014; Wiegell et al., 2008, 2011; Wiegell, Hædersdal, Eriksen, et al., 2009). The German AK treatment guideline recommends DL-PDT for single and multiple AKs and field cancerization (Heppt et al., 2020). Recently, two international expert groups have positioned DL-PDT as a first-line treatment for patients with multiple AKs and field cancerization (Calzavara-Pinton et al., 2017; Philipp-Dormston et al., 2016).

### *Laser-assisted photodynamic therapy*

The efficacy of AFL-assisted PDT for the treatment of keratinocyte cancer (AK, BCC and Mb Bowen) has been investigated in several clinical studies. AFL-assisted PDT has shown significantly better efficacy for grade I–III facial and scalp AKs (clinical clearance of 87–92%) than LED-PDT as monotherapy (61–67% clearance) at 3 months after treatment, but with no significant difference in tolerability or cosmesis (S. H. Choi et al., 2015b; Ko, Jeon, et al., 2014; Togsverd-Bo et al., 2012). The AFL-assisted PDT for AKs has demonstrated superior long-term efficacy compared to LED-PDT (complete response rates at 12 months 79–85% vs. 45–51%), and leads to lower recurrence rates in a follow-up of 12 months (8–10% vs.

22–27%) (S. H. Choi et al., 2015b; Ko, Jeon, et al., 2014). In addition, AFL-assisted DL-PDT has been performed to treat AKs and field-cancerized skin in OTR patients, showing complete response rates of 74–75.5% at 3–4 months after treatment thereby outperforming DL-PDT, conventional PDT or AFL treatment alone (Rizvi et al., 2019; Togsverd-Bo et al., 2015). A recent intraindividual trial compared AFL pretreatment and microabrasion in DL-PDT for cancerized skin fields (>50 cm<sup>2</sup>), AFL-assisted PDT leading to significantly higher AK clearance rate (81% vs. 60%), lower recurrence rate and superior improvement in dyspigmentation and skin texture at 3 months, although AFL-fortified DL-PDT induced more intense local skin responses than microneedling (Wenande et al., 2019).

AFL-assisted PDT has moreover been investigated in the treatment of actinic cheilitis (S. H. Choi et al., 2015a), nodular and superficial BCC (Ferrara et al., 2019; Haak et al., 2015; Lippert et al., 2013) and Bowen's disease (Genouw et al., 2018; Kim & Song, 2018; Ko, Kim, et al., 2014), leading to significantly improved clinical and histological efficacy compared to MAL-PDT alone.

### 2.3.6 Tolerability and side-effects

The most severe acute side-effect in cPDT is the pain during the LED illumination, which may be an intense prickling, burning or stinging sensation, but is usually restricted to the illumination phase and a few hours thereafter (Ibbotson et al., 2019). Cold air, water sprays or nerve blocks can be used for pain management and to make the treatment more tolerable for the patient (Klein et al., 2015; Wiegell, Hædersdal, & Wulf, 2009). It has been shown that ALA-PDT causes more pain than MAL, which may be explained by the non-selective GABA transport of ALA into nerve cells (Wiegell et al., 2003). However, in a large multicentre study by Dirschka et al. comparing BF-200 ALA and MAL, no difference in pain or other adverse effects was seen between treatment arms (Dirschka et al., 2012). After light exposure, significant inflammation with erythema and crusting often occur, which can be reduced by the use of superpotent corticosteroid cream without impairing efficacy (Wiegell et al., 2014). PDT has an excellent cosmetic outcome and can be even used to alleviate signs of photoaging (Basset-Seguín et al., 2008; Kohl et al., 2010).

In comparison to cPDT, DL-PDT is almost painless and well-tolerated and yields high patient satisfaction (Lacour et al., 2015; Rubel et al., 2014; See et al., 2017). DL-PDT could also be conducted at home with patients self-applying the

photosensitizing agent before sunlight exposure, saving both patients' and physicians' time (Karrer et al., 2019).

**Table 4.** Reported efficacy of DL-PDT for AK in prospective randomized and controlled studies. AFL = ablative fractional laser, AWL = artificial white light, BF-200 ALA = 5-aminolaevulinic acid nanoemulsion gel, HAL = hexylaminolaevulinate, IMB = ingenol mebutate gel, MAL = methyl-5-aminolaevulinate, NS = non-significant, OTR = organ transplant recipient, VAS = visual assessment scale, Tx = treatment.

Study	Treatment protocol	Study design	Sub- jects, n	Lesions, n	Follow- up time	Lesion complete response (CR)	Patient complete response	Pain VAS during illumination	Conclusion
Wiegell 2008 (Denmark)	16% MAL DL-PDT vs. LED-PDT, single Tx	randomized inpatient (split-face)	29	634, most gr I	3 mo	79% vs. 71% (p=0.13)	-	2.0 vs. 6.7 (p<0.0001)	DL-PDT as effective as LED-PDT.
Wiegell 2009 (Denmark)	16% MAL vs. 8% MAL DL-PDT, single Tx	randomized inpatient (split-face), double-blinded	30	1107, most gr I	3 mo	76.9 vs. 79.5% (p=0.37)	-	3.7 vs. 3.6 (p=0.74)	16% and 8% MAL as effective
Wiegell 2011 (Denmark, Norway, Sweden)	16% MAL DL-PDT 1.5h vs. 2.5h illumination, single Tx	randomized inpatient, multicentre	120	1572, gr I	3 mo	77% vs 75% (p=0.57)	-	1.3 vs. 1.3 (p=0.94)	2 h daylight exposure effective
Wiegell 2012 (Denmark, Norway, Sweden)	16% MAL DL-PDT 1.5h vs. 2.5h illumination, single Tx	randomized inpatient, multicentre	145	2768, gr I-III	3 mo	75.9% (gr I), 61.2% (gr II), 49.1% (gr III) (p<0.0001)	-	-	DL-PDT less effective for thick AKs
Rubel 2014 (Australia)	16% MAL DL-PDT vs. LED-PDT, single Tx	randomized intraindividual, multicentre	100	2751, gr I 97%, gr II 3%	3 and 6 mo	3 mo: 89.2 vs. 92.8% (gr I), 85.3 vs. 88.9% (all grades) 6 mo: 96% vs. 96.6% of gr I maintained healed	-	0.8 vs. 5.7 (p<0.001)	DL-PDT non-inferior to LED-PDT for mild AKs
Neittaanmäki- Perttu 2014 (Finland)	BF-200 ALA vs. MAL DL-PDT, gr I one Tx, gr II-III two Tx	randomized, intraindividual (split-face)	13	177, gr I 76%, gr II 22%, gr III 2%	3 mo	clinical: 84.5% vs. 74.2% (p=0.099) histological: 61.5 vs. 38.5% (p=0.375)	-	1st Tx: 1.7 vs. 1.9 (p=0.722) 2nd Tx: 2.4 vs. 2.1 (p= 0.463)	A trend of BF-200 ALA being more effective than MAL
Neittaanmäki- Perttu 2016 (Finland)	BF-200 ALA vs. MAL DL-PDT, gr I one Tx, gr II-III two Tx	randomized, intraindividual (split-face)	13	177, gr I 76%, gr II 22%, gr III 2%	12 mo	clinical: 87% vs. 62% (p=0.007) histological: 50% vs. 41.6% (p=0.417)	69.2% vs. 23.1% (p=0.07)	1st Tx: 1.7 vs. 1.9 (p=0.722) 2nd Tx: 2.4 vs. 2.1 (p= 0.463)	BF-200 ALA more effective than MAL in long-term follow- up
Neittaanmäki- Perttu 2016 (Finland)	16% MAL DL-PDT vs. LED-PDT, gr I one Tx, gr II-III two Tx	randomized, inter-individual cost-effective- ness study	70	210, gr I 88%, gr II-III 12%	6 mo	72.4% vs. 89.2% (p=0.0025)	42.9% vs. 68.8% (p=0.030)	1.53 vs. 4.36 (p<0.001)	DL-PDT less effective and less costly than LED- PDT

Neitaaanmäki-Perttu 2016 (Finland)	HAL 0.2% vs. 16% MAL DL-PDT, gr I one Tx, gr II-III two Tx	randomized, intraindividual (split-face)	14	201, gr I 81%, gr II-III 19%	3 mo	clinical: 73.4% vs. 77.8% (p=0.754) histological: 38.5 vs. 69.2% (p=0.289)	-	≤1 in both groups (p=NS)	HAL is promising photosensitizer for DL-PDT
Neitaaanmäki-Perttu 2017 (Finland)	HAL 0.2% vs. 16% MAL DL-PDT, gr I one Tx, gr II-III two Tx	randomized, intraindividual (split-face)	13	201, gr I 81%, gr II-III 19%	12 mo	clinical: 67% vs 66% (p=1.00) histological: 42% vs. 50% (p=0.688)	-	≤1 in both groups (p=NS)	HAL and MAL have similar long-term efficacy
Togsverd-Bo 2015 (Denmark)	AFL-assisted DL-PDT vs. DL-PDT vs. LED-PDT vs. AFL, single Tx	randomized, intra-individual (four treatment areas)	16, OTR patients	542, gr I-III	3 mo	74% vs. 46% vs. 50% vs. 5% (p<0.001)	-	median 0 vs. 0 vs. 5.5 (p<0.001)	AFL-assisted DL-PDT enhances CR in OTR patients
Lacour 2015 (Sweden, Germany, Netherlands, France, Spain)	16% MAL DL-PDT vs. LED-PDT, single Tx	randomized, intra-individual (split-face), multicentre	108	1917, gr I 58%, gr II 42%	3 mo	70% vs. 74%	-	0.7 vs. 4.4 (p<0.001)	DL-PDT as effective as LED-PDT and better-tolerated
Moggio 2016 (Italy)	IMB for 3 days vs. 16% MAL DL-PDT, single Tx	randomized, intra-individual (split-face)	22	311, gr I 37%, gr II 63%	3 mo	75.8% vs. 77.9%	36.4% vs. 31.8% (p=NS)	3.55 vs. 2.05 (p<0.01)	3 days' IMB and MAL DL-PDT as effective
O'Gorman 2016 (Ireland)	16% MAL DL-PDT vs. AWL-PDT	randomized, intra-individual (split-scalp)	22	965, palpable AKs	1, 3, 6 and 9 mo	3 mo: 52.3% vs. 58.0% (p=0.29) 9 mo: 48.4% vs. 64.4% (p=0.05)	-	4/100 vs. 6/100 (p=0.51)	AWL-PDT as effective as DL-PDT
Sotiropoulos 2018 (Greece)	16% MAL DL-PDT vs. LED PDT, single Tx	randomized, intra-individual (split-face), multicentre	46	453, gr I 49%, gr II 51%	3 and 12 mo	3 mo: 77.9% vs. 80.6% (p=0.307) 12 mo: 71.2% vs. 73.7% (p=0.729)	-	1.14 vs. 6.06 (p=0)	DL-PDT and LED-PDT similar in long-term efficacy
Zhu 2018 (China)	10% ALA DL-PDT vs. LED-PDT, three Tx with 2 wk intervals	randomized, inter-individual	55	249, gr I-III	1 mo after 3 Tx	95.5% vs. 96.8% (p=0.856)	-	1.7 vs. 5.2 (p<0.05)	DL-PDT as effective as LED-PDT
Dirschka 2019 (Germany, Spain)	7.8% BF-200 ALA vs. 16% MAL, single Tx	randomized, intra-individual (split-face), multicentre	49	628, gr I 49%, gr II 51%	3 and 12 mo	3 mo: clinical 79.8 vs. 76.5%, histological 75.5 vs. 69.4% 12 mo: recurrence rate 19.9% vs. 31.6% (p=0.01)	42.9% vs. 38.8%	1.2 vs. 1.1, face: 1.5 vs. 1.5, scalp: 0.8 vs. 0.7	DL-PDT with BF-200 ALA is well-tolerated and non-inferior to MAL
Assikar 2020 (France)	16% MAL DL-PDT vs. blue-light LED-PDT	randomized, intra-individual (split-face)	26	1119, gr I-II	3 and 6 mo	3 mo: 90.5% vs 94.2% (p=0.846) 6 mo: 90.0% vs. 94.6%	-	1.2 vs. 5.1 (p<0.0001)	DL-PDT seems as effective as blue-light LED-PDT

## 2.4 Non-invasive skin imaging methods

Given the constantly increasing incidence of melanoma and NMSC, in the clinical setting there is demand for fast, non-invasive and accurate techniques to facilitate early diagnosis of a suspected skin malignancy. There is a plethora of emerging non-invasive imaging methods which allow the visualization of skin with no need for excisional biopsy (Table 5). They offer features which are not available through routine histology, such as examination of the whole lesion rather than a section of it, ability to visualize skin in real time and ability to track temporal changes in lesion growth and cellular structure over time (Wassef & Rao, 2013). Each of these non-invasive imaging tools of the skin varies in terms of resolution depth, clarity of image, applicability in a clinical setting, accuracy, sensitivity and specificity (M. Ulrich, Stockfleth, et al., 2007).

**Table 5.** Comparison of non-invasive skin imaging methods available for skin cancer diagnosis.

Method	Example of commercial device	Image plane	Light source	Field of view	Resolution	Imaging depth	Imaging time
Dermoscopy	Dermlite®	Horizontal	Cross-polarized light	Several cm <sup>2</sup>	Cellular aggregates	Papillary dermis (≈100 μm)	Few seconds
Reflectance confocal microscopy (RCM)	Vivascope 1500® and 3000®	Horizontal	830 nm laser	0.5 x 0.5 mm <sup>2</sup> or 0.75 x 0.75 mm <sup>2</sup>	Subcellular structures (0.5–1 μm lateral, 3–5 μm axial)	250 μm	Several minutes
Optical coherence tomography (OCT)	VivoSight®	Cross-sectional	1305 nm laser	6 x 6 mm <sup>2</sup>	Cellular (< 7.5 μm lateral, < 5 μm axial)	1 mm	1 minute or less
Multispectral imaging (MSI)	Melafind®	Horizontal	10 narrow wavebands (430–950 nm)	2.5 x 2.0 cm <sup>2</sup>	Cellular aggregates (20 μm per pixel)	2.5 mm	Few seconds
	SIAscope®	Horizontal	8 narrow wavebands (400–1000 nm)	2.4 x 2.4 cm <sup>2</sup>	Cellular aggregates (40 μm per pixel)	2 mm	15 s
Raman spectroscopy (RS)	Verisante Aura®	Single-point measurement	785 nm laser	3.5 mm diameter area	-	200 μm	Less than 1 second
Hyperspectral imaging (HSI)	Prototype used in this study	Horizontal	70 narrow wavebands (500–850 nm)	12 cm <sup>2</sup>	Cellular aggregates (125 μm per pixel)	2 mm	Few seconds

## 2.4.1 Dermoscopy

In addition to mere visual inspection, a rapid, inexpensive and easily available diagnostic method for skin cancer screening is dermoscopy (also called epiluminescence microscopy). A dermoscope is a hand-held tool with high-quality magnifying lens and a polarized light that aids in visualizing the skin at microscopic level. The magnification in dermoscopy varies from 6 to 100-fold depending on the device, and penetration depth reaches the level of the papillary dermis (M. Ulrich, Stockfleth, et al., 2007). Dermoscopy uses mainly horizontal pattern analysis for diagnosis, and diagnosis or risk of possible malignancy is assessed based on certain architectural characteristics of the lesions, such as globules and nests, and the presence of different blood vessel configurations (Wassef & Rao, 2013). Dermoscopy can be used to aid the clinician in the differential diagnosis of LM from other pigmented lesions, especially from pigmented AK, solar lentigo and flat seborrheic keratosis. Dermoscopy has achieved sensitivity and specificity of 88% and 86% for the diagnosis of melanoma (Rajpara et al., 2009), and of 81.9% and 81.8% for the diagnosis of superficial BCC (Lallas, Tzello, et al., 2014). It has been demonstrated to increase the rate of detection of pigmented BCC from 60% to 90% (Demirtasoglu et al., 2006). Furthermore, dermoscopy may be a useful aid in the diagnosis of several inflammatory and infectious dermatoses, such as scabies, human papillomavirus (HPV) infections, psoriasis, lichen planus, urticarial vasculitis, Grover's disease and many more (Lallas, Giacomel, et al., 2014).

A limitation of dermoscopy is that the diagnostic reliability depends heavily on clinical experience. In one study, the sensitivity and specificity in melanoma diagnoses were 69% and 94% for inexperienced dermatologists (residents with 6 months' experience) compared to 92% and 99% for dermatologists experienced with dermoscopy (5 years' experience) (Piccolo et al., 2002). Another limitation is that dermoscopy increases the time required for skin examination. Zalaudek et al. compared the complete skin examination times with and without dermoscope in 2008, reporting that median time for complete skin examination was increased from 70 to 142 seconds with the use of dermoscope, and that the time increase was directly proportional to the patient's total lesion count (Zalaudek et al., 2008).

For digital dermoscopic images, several automated algorithms based on artificial intelligence have been developed, and these have demonstrated diagnostic performance similar to that of as manual dermoscopy using diagnostic algorithms (e.g. ABCD rule, seven-point checklist and pattern analysis) (Rajpara et al., 2009).

## 2.4.2 Reflectance confocal microscopy

Reflectance confocal microscopy (RCM) is a technology that allows imaging of the skin *in vivo*, in real time and at a nearly histological level resolution (Fink & Haenssle, 2017). In a RCM device a point laser source illuminates the skin, from which light is refracted, directed through a small pinhole and arrives at the detector, where an image is formed of optically sectioned layers of the skin (Malvey & Pellacani, 2017; Shahriari et al., 2021). The horizontal (*en face*) images are produced in black and white (Figure 7) representing the different refractive indices of the various intracellular structures, of which melanin provides the strongest contrast (Fink & Haenssle, 2017; Wassef & Rao, 2013). The RCM images provide lateral resolution of 0.5–1  $\mu\text{m}$  and axial resolution (section thickness) of 3–5  $\mu\text{m}$ , which is comparable to routine histopathology (M. Ulrich, Stockfleth, et al., 2007). Sections for diagnostic purposes can be taken up to a depth of 200  $\mu\text{m}$ , which corresponds to the superficial dermis (Malvey & Pellacani, 2017). RCM also permits imaging of vertical stacks, which can be combined with the horizontal sections for 3-dimensional visualization of skin section (M. Ulrich, Stockfleth, et al., 2007).

There are several studies assessing the diagnostic accuracy of RCM and it is reportedly especially useful in diagnosing difficult BCC (Guitera et al., 2016; Nori et al., 2004), distinguishing BCC subtypes (Longo et al., 2014), differentiating benign nevi from melanoma (Gerger et al., 2005; Pellacani et al., 2007), diagnosing LM (Guitera et al., 2010) and diagnosing AK and field cancerization and monitoring their treatment response (M. Ulrich et al., 2018; M. Ulrich, Maltusch, et al., 2007). RCM can detect histological features typical of LM and aid in differential diagnosis between benign pigmented macules (Guitera et al., 2010). In meta-analysis RCM has been shown to outperform dermoscopy in diagnostic accuracy with reported sensitivity and specificity of 92.7% and 78.3% for detecting melanoma, and of 91.7% and 91.3% for detecting BCC respectively (Xiong et al., 2016). The utility of RCM has also been investigated in several inflammatory dermatoses, such as contact dermatitis, psoriasis, discoid lupus erythematosus, lichen planus and seborrheic dermatitis (Ardigo et al., 2016).

The major limitation of RCM is the depth of laser penetration being restricted to the superficial dermis, which makes it unsuitable for visualizing the depth of invasion in skin tumours such as SCC or mycosis fungoides. Also, hyperkeratosis and lesions with scales are not well visualized with RCM due to its depth limitations (Wassef & Rao, 2013). The RCM device is expensive, the interpretation of images requires



extensive training and the results are user-dependent; i.e. they vary with the experience of the physician (Fink & Haenssle, 2017).

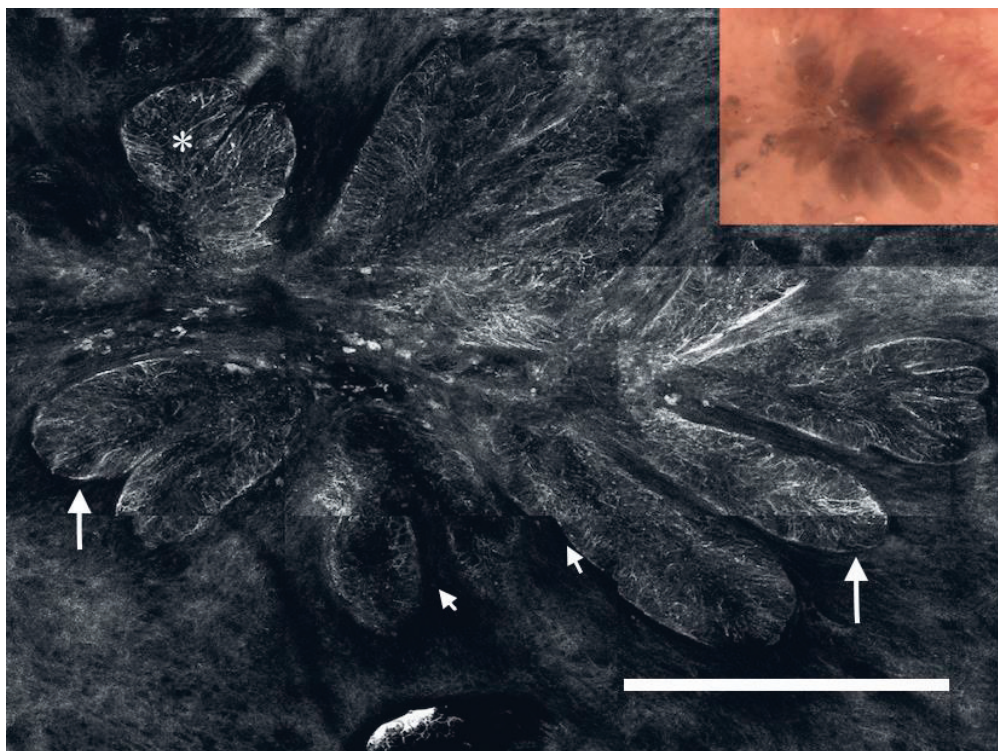


**Figure 7.** Reflectance confocal microscope (RCM) image of a pigmented BCC. Vivablock of the tumour shows nests of basaloid cells (asterisk), palisading (arrows) and clefting (arrowheads). Scale bar corresponds to 1 mm. From *Malveyh & Pellacani, 2017*, with permission from ActaDV.

### 2.4.3 Optical coherence tomography

Optical coherence tomography (OCT) is an emerging non-invasive and real-time imaging technique based on interferometry. The principle is similar to that of ultrasound, but instead of longitudinal ultrasound waves, OCT uses infrared light and interferometric methods to sense reflected light from the tissue (Wassef & Rao, 2013). The OCT images are 2-dimensional cross-sections of the skin with lateral dimension of 4 to 6 mm, axial, lateral resolution between 3 to 15  $\mu\text{m}$  and imaging depth of up to 1–2 mm, depending on the system (Malveyh & Pellacani, 2017; M. Ulrich, Stockfleth, et al., 2007). This technique can reliably visualize subsurface

structures of normal skin, including epidermis, dermoepidermal junction, dermis, hair follicles, sweat ducts and blood vessels (Gambichler et al., 2011). However, no cellular or subcellular structures may be seen (M. Ulrich, Stockfleth, et al., 2007). OCT is rapid; it takes about four seconds to generate a 4-mm scan using a scan frequency of 100 Hz (Wassef & Rao, 2013). Images are represented in grey scale or false colour. A novel algorithm of high-definition OCT was recently presented using a combination of *en face* and cross-sectional images for 3-dimensional real-time imaging (Boone et al., 2015).

In the field of dermatology, OCT has been widely investigated in the diagnosis of NMSC (AK, SCC and BCC) (Boone et al., 2012, 2013, 2015; Maier et al., 2013; J. Olsen et al., 2016). OCT has clinical value in providing a precise classification of BCC subtypes (superficial, nodular and infiltrative) and it can aid in delineating tumour margins in BCC before excision (Alawi et al., 2013; Boone et al., 2012). High-definition OCT can reliably distinguish SCC from AK by detecting evidence of invasive growth at the dermoepidermal junction (Marneffe et al., 2016). However, OCT has its limitations in the diagnosis of melanocytic lesions and detecting early melanoma, which is due to light scattering and absorption by melanin and less resolution than RCM (J. Olsen et al., 2018). In a recent meta-analysis, the pooled sensitivities of OCT for detecting BCC, SCC, AK and MM were 92.4%, 92.3%, 73.8% and 81.0% respectively. The pooled specificities were 86.9%, 99.5%, 91.5% and 93.8 respectively (Xiong et al., 2018). OCT may also be a useful diagnostic aid in some infectious and inflammatory dermatoses, including onychomycosis, scabies, psoriasis, contact dermatitis, blistering diseases and vascular skin lesions (Gambichler et al., 2011).

#### 2.4.4 Multispectral imaging

Multispectral imaging (MSI) is a non-invasive technique in which image data is captured within multiple specific wavelengths across a spectral range. Two commercial diagnostic devices for skin cancer screening have utilized MSI. One is MelaFind® (MELA Sciences, NY, USA), a computer-assisted multispectral digital dermoscope to aid in the clinical diagnosis of melanoma (Wassef & Rao, 2013). The device illuminates the skin with 10 narrow wavebands in both infrared and visible spectra (range 430–950 nm), capturing 10 images and uses automated mathematical algorithms on them, based on linear classifiers, for pattern recognition and generating a diagnostic score for melanoma (Elbaum et al., 2001). Melafind produces

high-resolution images with minimal distortion and low noise of images over the field of view of approximately 2.5 x 2.0 cm (Gutkowicz-Krusin et al., 2000). In clinical studies MelaFind has demonstrated very high sensitivity of 96–100% but low specificity of 5–10% in identifying melanomas, whereas the biopsy sensitivity and specificity achieved by dermatologists were 78–80% and 4–43% respectively (Fink et al., 2017; Monheit et al., 2011; Wells et al., 2012). It has been shown that MelaFind reduces the number of biopsies necessary for clinically ambiguous lesions, but MelaFind scores do not correlate with histologic degree of cytologic atypia (Shrivastava et al., 2019).

Although MelaFind is a highly sensitive tool to assist in the evaluation of pigmented lesions, there are some drawbacks. Its average specificity in clinical studies has been lower than that of dermatologists, which has raised some concerns (MelaFind almost always suggests biopsy) (Cukras, 2013). MelaFind's diagnostic algorithm and parameter database were generated for melanoma screening, which makes its use very limited and it cannot be used to identify NMSC or other lesions (Wassef & Rao, 2013). MelaFind may misclassify NMSC lesions such as BCCs because the technology is designed to assess overall structural disorganization of lesions rather than atypical cellular features (March et al., 2015). The system itself is very sensitive for imaging artefacts, and if an image fails to meet a particular image quality, MelaFind does not provide a diagnostic result (Wassef & Rao, 2013).

Another MSI device for the evaluation of pigmented skin lesions and detecting melanoma is SIAscope® (spectrophotometric intracutaneous analysis), initially a trademark of Astron Clinica, Cambridge, UK, but from 2011 owned by MedX Health Corp., Ontario, Canada (Walter et al., 2012). A handheld SIAscope scanner captures 8 narrowband spectral images in the range of 400–1000 nm and produces SIAgraph images that visualize the quantity and microscopic architecture of skin chromophores (melanin, blood and collagen) over an area of 24 x 24 mm (Moncrieff et al., 2002). Newer versions of SIAscope are also able to capture dermoscopic images (March et al., 2015). In one study, a significant correlation between SIAscope-derived eumelanin values and actual eumelanin content in the skin was found across all Fitzpatrick skin types I–IV (Matts et al., 2007). However, in another topographic comparative study of 60 suspicious pigmented lesions, the SIAscopic features of dermal melanin, blood displacement and dermal melanin did not correlate with the histopathological results (Terstappen et al., 2013). In several clinical studies, SIAscopy did not improve diagnostic accuracy over dermoscopy in the diagnosis of melanoma, NMSC or pigmented BCC (Glud et al., 2009; Hacıoglu et al., 2013; Haniffa et al., 2007; Sgouros et al., 2014; Terstappen et al., 2007). An improved and

validated diagnostic algorithm for SIAscope has been developed to improve diagnostic accuracy for pigmented lesions in primary care settings (Emery et al., 2010). This algorithm was later commercialized in a computer-linked hand-held device named MoleMate® (MedX Health Corp., Ontario, Canada) (March et al., 2015). One large randomized study of 1,580 pigmented lesions compared the performance of MoleMate® with best clinical practice of primary care clinicians, resulting in no significant difference in appropriateness of referral between groups. There were 18/18 correctly diagnosed melanomas with MoleMate and 17/18 in the control group, but for benign lesions the MoleMate was inferior to best practice in recommending a significantly higher proportion of lesions for biopsy (90.6% vs. 84.4%) (Walter et al., 2012).

For multispectral imaging data, other diagnostic algorithms based on neural networks have been investigated. Tomatis et al. developed an artificial neural network classifier for 1,391 pigmented lesions imaged with MSI, which was able to distinguish melanoma from other lesions with a sensitivity of 80% and specificity of 76% (Tomatis et al., 2005). In another study, Carrara et al. developed a neural network classifier for MSI data to differentiate between excision-needing and reassuring lesions using a data set of 1966 excised and 1940 non-excised and clinically non-suspicious lesions, resulting in a sensitivity of 88% and specificity of 80% (Carrara et al., 2007).

## 2.4.5 Raman spectroscopy

Raman spectroscopy (RS) is a non-invasive optical method that uses 785-nm laser light to change the vibration state of tissue biomolecules. Most of the photons scatter elastically from a molecule (i.e. they have the same energy and wavelength as the incident photon), whereas a minor fraction of photons scatter inelastically (Raman scattering), causing a shift in the wavelength of the light that is reflected back to a sensor (Fink & Haenssle, 2017). The resultant spectrum of light transitions represents the molecular composition of the cells (“molecular fingerprint”), mainly protein and lipid conformations, and may be used to identify cancerous tissue (Lui et al., 2012). A limitation of the method is that RS is mainly used for single-point measurement on the skin and, unlike other non-invasive imaging methods, it does not produce an image (Tkaczyk, 2017).

A commercial device utilizing RS has been developed for real-time *in vivo* skin cancer diagnosis, designated Verisante Aura™ (Verisante Technology Inc.,

Vancouver, Canada). The hand-held Raman probe of Verisante Aura™ collects the raw signal from a 3.5 mm diameter area of the skin and the attached spectrometer performs spectral analysis in less than 1 second (Lui et al., 2012). In a proof-of-concept clinical study by Lui et al., RS showed sensitivities of 95–99% and specificities of 15–54% in distinguishing MM from benign pigmented lesions (Lui et al., 2012). In other studies the sensitivities for melanoma detection have ranged from 85% to 100%, and specificities from 94% to 100% (Gniadecka et al., 2004; Lim et al., 2014; Schleusener et al., 2015). However, in a recent prospective clinical accuracy study comparing three commercial non-invasive diagnostic devices (Melafind®, Verisante Aura™ and Fotofinder® Moleanalyzer Pro), Verisante Aura™ demonstrated the lowest sensitivity of 21.4% in melanoma detection (MacLellan et al., 2020). RS has also been used to recognize NMSC, mainly BCC, SCC and AK, from normal skin with reported sensitivities ranging from 92% to 100% (Lieber et al., 2008; Lim et al., 2014; Silveira et al., 2015). The diagnosis of MM and BCC based on their Raman spectra is not influenced by the extent of skin or lesion pigmentation (Philipsen et al., 2013).

Due to the single-point measurement, it is not possible to use conventional RS for mapping tumour margins or to detect possible invasive foci within a lesion. Confocal Raman microscopy is a novel modality combining RS and confocal microscopy, and allows the acquisition of spatially resolved Raman information, with state-of-the-art devices capable of a lateral resolution of 500 nm, axial resolution of 200 nm and imaging depth of 40  $\mu\text{m}$  into the skin (Franzen & Windbergs, 2015).

## 2.4.6 Hyperspectral imaging

Hyperspectral imaging (HSI) is a non-invasive optical imaging technique that combines reflectance spectroscopy with plane imaging. HSI technique originated from remote sensing applications by NASA, and has been applied in numerous areas since then, including biomedicine and cancer detection (Lu & Fei, 2014). Conventional spectroscopy records the signal at every wavelength within a spectral range, but only for a single point of interest (M. E. Martin et al., 2006). With HSI it is possible to collect spectral information at each pixel of a two-dimensional (2D) detector array, producing a three-dimensional (3D) dataset known as hypercube (Figure 8), which contains both spatial and spectral information (Lu & Fei, 2014). In comparison to the regular camera, which captures images in three broad wavebands of visible light (red, green and blue), HSI captures images in up to tens or hundreds

of consecutive narrow wavebands within a selected spectral range that can cover UV, visible, near-infrared or mid-infrared light. As a result, HSI has the potential to capture subtle spectral differences under different pathological conditions, while multispectral imaging may miss significant spectral information (Lu & Fei, 2014). Every pixel in a hyperspectral image has its own unique reflectance spectrum, which can be used to identify different biological tissues with mathematical algorithms based on the spectral characteristics of different tissues (M. E. Martin et al., 2006; Neittaanmäki-Perttu et al., 2013; Panasyuk et al., 2007; Siddiqi et al., 2008).

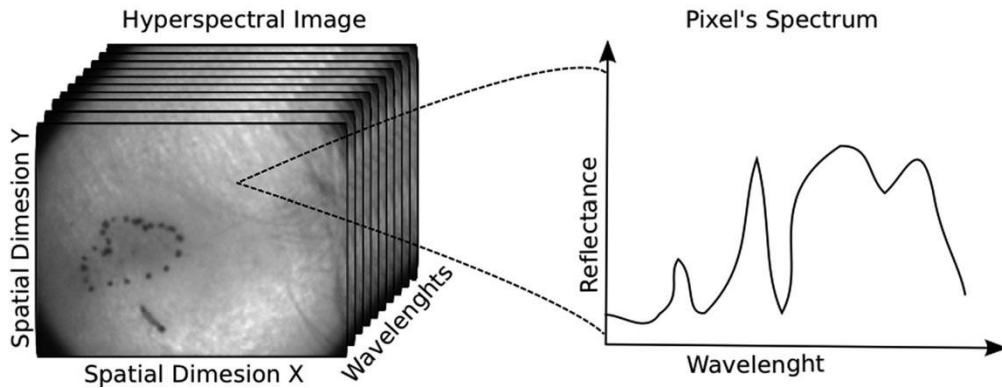


**Figure 8.** A schematic illustration of the hypercube containing spatial information (x and y dimensions on the skin plane) and spectral information (z intensity). Every pixel of the image has its own spectral signature. From Noora Neittaanmäki-Perttu et al., 2013, with permission from Wiley.

#### 2.4.6.1 Hyperspectral camera medical prototype

The imaging system consists of a hand-held hyperspectral camera (weight 1.2 kg), a visible light source (a broadband halogen lamp connected to a ring-shaped diffusor via optic fibre), and a laptop computer with data acquisition and analysis software (Figure 11). Spectral separation of the imager is based on Fabry-Perot interferometer (FPI), a piezo-actuated interferometer, which enables imaging of the entire spectral range by quickly changing wavebands. The spectral waveband widths are 5–10 nm and each spectral layer is captured within 100 ms. Within a few seconds, the camera acquires 70 wavebands between 500 and 850 nm with a 12 cm<sup>2</sup> field of view, spatial resolution 6400 pixels/cm<sup>2</sup> (pixel = 125 x 125 μm) and imaging depth of approximately 2 mm (Neittaanmäki et al., 2017). After imaging, the resulting hypercube requires mathematical analysis to extract clinically relevant information

and to visualize the data meaningfully for the clinician. In our earlier HSI studies we have used the technique of linear signal unmixing for data processing (Neittaanmäki-Perttu et al., 2013, 2015; Neittaanmäki et al., 2017; Salmivuori et al., 2019a). This method is based on the assumption that each pixel's unique reflectance spectra is formed from a linear mixture of some pure spectra (i.e. endmember spectra) which represents the reflectance of distinct tissue types in the image. The endmember spectra are obtained from the raw data cube by using mathematical methods of vertex component analysis (VCA) and a filter vector algorithm (FVA). The result is represented in abundance maps, which show the locations of different endmembers in the area imaged and can be used for visualizing tumour margins, different lesion types, or possible invasive foci within lesion (Figure 9).

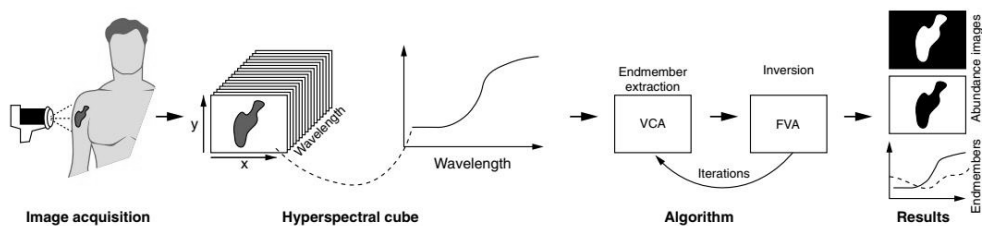


**Figure 9.** Hyperspectral image processing. From Salmivuori et al., 2019b, with permission from Wiley.

The hyperspectral camera has proven to be useful in many ways for the detection of skin cancer and delineation of tumour margins. HSI was able to detect clinically visible and subclinical AKs from the surrounding photodamaged skin (Neittaanmäki-Perttu et al., 2013). HSI was shown delineate the margins of LM and LMM more accurately than clinical examination, and HSI analysis matched the histopathological analysis in all cases except one (Neittaanmäki-Perttu et al., 2015). In a subsequent study HSI could identify the dermal invasion of LMM lesions with 90% sensitivity, 86% specificity and 75% positive predictive value (PPV) (Neittaanmäki et al., 2017). HSI was also investigated for delineating 16 ill-defined BCCs (10 of aggressive subtype and 6 of nodular or superficial subtype) and could define the lesion margin more accurately than clinical evaluation in 12/16 BCCs (Salmivuori et al., 2019b).

HSI has also been investigated for automated skin cancer diagnosis. Hosking et al. developed an automated hyperspectral dermoscope (21 wavelengths between 350 and 950 nm) combined with artificial intelligence algorithms, demonstrating overall sensitivity of 100% and specificity of 36% in detecting melanoma (Hosking et al.,

2019). In another study, a HSI system (125 spectral bands between 450 and 950 nm) was combined with automatic identification and classification algorithms, reaching 87.5% sensitivity and 100% specificity in the discrimination of malignant and benign pigmented skin lesions (Leon et al., 2020).

## 2.5 Convolutional neural networks

Convolutional neural networks (CNN) represent a form of artificial intelligence (AI) in decision-making and are a strongly emerging concept in many fields of medicine, including dermatological diagnostics. The name comes from the mathematical operation of convolution, in which linear filters are swept across, or integrated, over an image (Mieloszyk & Bhargava, 2018). The resulting convoluted images can be aggregated in pooling operations, subjected to repeated convolutions and finally mapped to a vector of probabilities corresponding to likelihoods that the image or part of it belongs to a certain class. A major strength of the CNN architecture is that there is no need to predefine specific features for image classification, but CNN learns to recognize them from the annotated training images, thus mimicking the human brain (Mieloszyk & Bhargava, 2018).

Deep learning neural networks have been shown to perform skin cancer classification with an accuracy similar to that achieved by expert-level dermatologists, with the area under curve (AUC) for receiver operating characteristics (ROC) curve ranging from 0.74 to 0.96 (Esteva et al., 2017; Haenssle et al., 2018; Tschandl et al., 2019). In one meta-analysis, the pooled sensitivity of artificial intelligence used for dermoscopic images was slightly higher than expert-level dermoscopy (91% vs. 88%), whereas the pooled specificity for artificial intelligence was significantly lower (86% vs. 79%) (Rajpara et al., 2009)

FotoFinder® (Bad Birnbach, Bayern, Germany) has recently developed Moleanalyzer Pro which is the first commercial and validated deep learning CNN for skin cancer diagnosis in digital dermoscopy images (Fink et al., 2020; Winkler et al., 2020). Moleanalyzer Pro demonstrated a sensitivity of 97.1% and specificity of 78.8% in the classification of melanoma from combined nevi, outperforming a group of 11 trained dermatologists with different levels of experience (Fink et al., 2020). A recent prospective diagnostic accuracy study compared three non-invasive imaging techniques (Melafind®, Verisante Aura™ and Fotofinder® Moleanalyzer Pro), dermatologist's clinical examination and teledermatology in the detection of melanoma (MacLellan et al., 2020). The CNN-based diagnostics appeared superior



to the others as Moleanalyzer Pro achieved the highest sensitivity and specificity (88.1% and 78.8%), followed by Melafind® (82.5% and 52.4%) and Verisante Aura™ (21.4% and 86.2%). The sensitivity and specificity of a teledermoscopist were 84.5% and 82.6% and of a local dermatologist 96.6% and 32.2% (MacLellan et al., 2020).

In addition to 2D skin images, a deep learning neural network has also been investigated for hyperspectral images. Halicek et al. developed a CNN tissue classifier for HSI data in order to detect cancer-normal margins in gross *ex vivo* specimens of head and neck tumours (SCC of oral cavity and thyroid carcinoma) (Halicek et al., 2018, 2019). Using leave-one-patient-out cross-validation, their CNN could classify cancer-normal margins with AUC of 0.82, 81% sensitivity and 80% specificity for SCC patients, and with AUC of 0.95, 92% sensitivity and 92% specificity for thyroid carcinoma patients (Halicek et al., 2019).

The use of AI-based support in clinical decision-making has been shown to increase diagnostic accuracy compared to either AI or physicians alone, with the highest gain for the least experienced clinicians (Fink et al., 2020; Tschandl et al., 2020). Thus, the CNN algorithms may prove a valuable aid for dermatologists, probably not replacing clinical decision-making, but their ultimate benefit is in primary health care, enabling more efficient and timelier skin cancer screening.

### 3 AIMS OF THE STUDY

The specific aims of the present study were:

1. To investigate the efficacy and tolerability of aminolaevulinic nanoemulsion gel in daylight photodynamic therapy for mild to moderate actinic keratoses. To compare the cost-efficacy of aminolaevulinic nanoemulsion gel and methylaminolaevulinate in daylight photodynamic therapy for mild to moderate AKs **(I)**.
2. To investigate the efficacy of ablative fractional laser-assisted photodynamic therapy using aminolaevulinic nanoemulsion gel as a photosensitizer in the treatment of lentigo maligna **(II)**.
3. To utilize an automated 3-dimensional convolutional neural network as a tumour classifier in hyperspectral images and to test its applicability in differential diagnosis between pigmented basal cell carcinomas and melanoma **(III)**.

## 4 MATERIALS AND METHODS

### 4.1 Patients

All Studies **I–III** were conducted in accordance with the Declaration of Helsinki, and the study protocols were approved by the local ethics committee of Tampere University Hospital. Being medical intervention studies, the protocols for Studies **I** and **II** were also approved by the Finnish Medicines Agency (Fimea). Written informed consent was obtained from all participants. Voluntary patients were recruited from among those referred for suspected skin malignancies to the Department of Dermatology in Lahti Central Hospital (61°N) (Studies **I–III**), Tampere University Hospital (61°N) (Study **I**) and Vaasa Central Hospital (63°N) (Study **I**). The complete study population consisted of patients with AK (Study **I**), LM (Studies **II** and **III**), pigmented BCC (Study **III**) and invasive MM (Study **III**) lesions. The patient characteristics of Studies **I–III** are presented in Table 6.

**Table 6.** Patient characteristics in Studies I–III. †) One patient had two lentigo maligna lesions. ‡) One patient participated in all Studies I–III.

Study	Time period	Patients enrolled / completed	Total lesions treated	Mean AKs (range)	Female / Male	Mean age (range)	Photo-type (I–VI)	Previous treatments				
								AK	BD	SCC	BCC	MIS / MM
I	2015-2017	73 / 69	767 AKs	11.1 (4-32)	F = 26 M = 43	74.8 (49-92)	I = 12 II = 41 III = 16	40	8	4	25	4
II	2016-2017	24 / 9†	10 LM†	-	F = 2 M = 7	73.8 (62-83)	I = 1 II = 7 III = 1	4	1	2	3	2
III	2014-2017	31 / 24	10 BCC 12 MIS 4 MM	-	F = 9 M = 15	73.1 (53-91)	II = 13 III = 8 NA = 3	8	4	3	9	4
Total		126 / 100‡										

#### 4.1.1 Inclusion and exclusion criteria

The inclusion criteria were age over 18 years and the presence of grade I–II AKs on the face or scalp located symmetrically (Study **I**), a biopsy-confirmed LM located on

the face, neck or upper body (Study **II**), and histologically confirmed pigmented BCC, MIS, or invasive MM (Study **III**).

The exclusion criteria were as follows: grade III AKs, diffuse field-cancerization where the AK count could not be assessed, or earlier treatment of the same area for AKs within the last 6 months (Study **I**); a histologically verified invasive LMM (Study **II**); and porphyria or photosensitivity, allergy to either photosensitizer, or pregnancy or breastfeeding (Studies **I** and **II**).

## 4.2 Methods

### 4.2.1 Clinical evaluation

In Study **I** the baseline AK count and grades, and the clearance of AKs at 12 months after a single DL-PDT treatment were assessed clinically. During the treatment visit the AKs were first outlined in two symmetrical and equal-sized treatment fields on both sides of the face or scalp. AK lesions within the fields were counted and graded clinically to Olsen grades I–II (E. A. Olsen et al., 1991). The borders of the treatment fields and AK lesions were marked on the skin, copied on transparent plastic sheet and photographed.

At the 12-month control visit the original treatment field borders were marked on the skin by reference to the transparent plastic sheets and the clinical photographs from the treatment visit (Figure 10). In most cases some anatomical landmarks (e.g. the contour of the nose, an ear or an eyebrow) were drawn on the plastic sheets to assist in finding exactly the right position on the skin. A lesion was regarded as cleared by disappearance of the lesion visually and upon palpation. All residual AKs inside the treatment fields were counted and clinically graded as I–III, and they were marked on the original plastic sheets using a different colour. If a residual lesion was clearly located separately from the baseline lesions marked on the plastic sheet, it was regarded as a new lesion.

In Studies **II** and **III**, all included lesions were examined clinically with a dermoscope (Dermlite® DL3, 3Gen, California, U.S.A.) and photographed. In Study **II**, the LM lesions were also inspected under Wood's light (Burton Div.-Cavitron Corp; Model 9312, Van Nuys, CA, USA) to aid in delineating the clinical borders which were marked on a transparent plastic sheet.

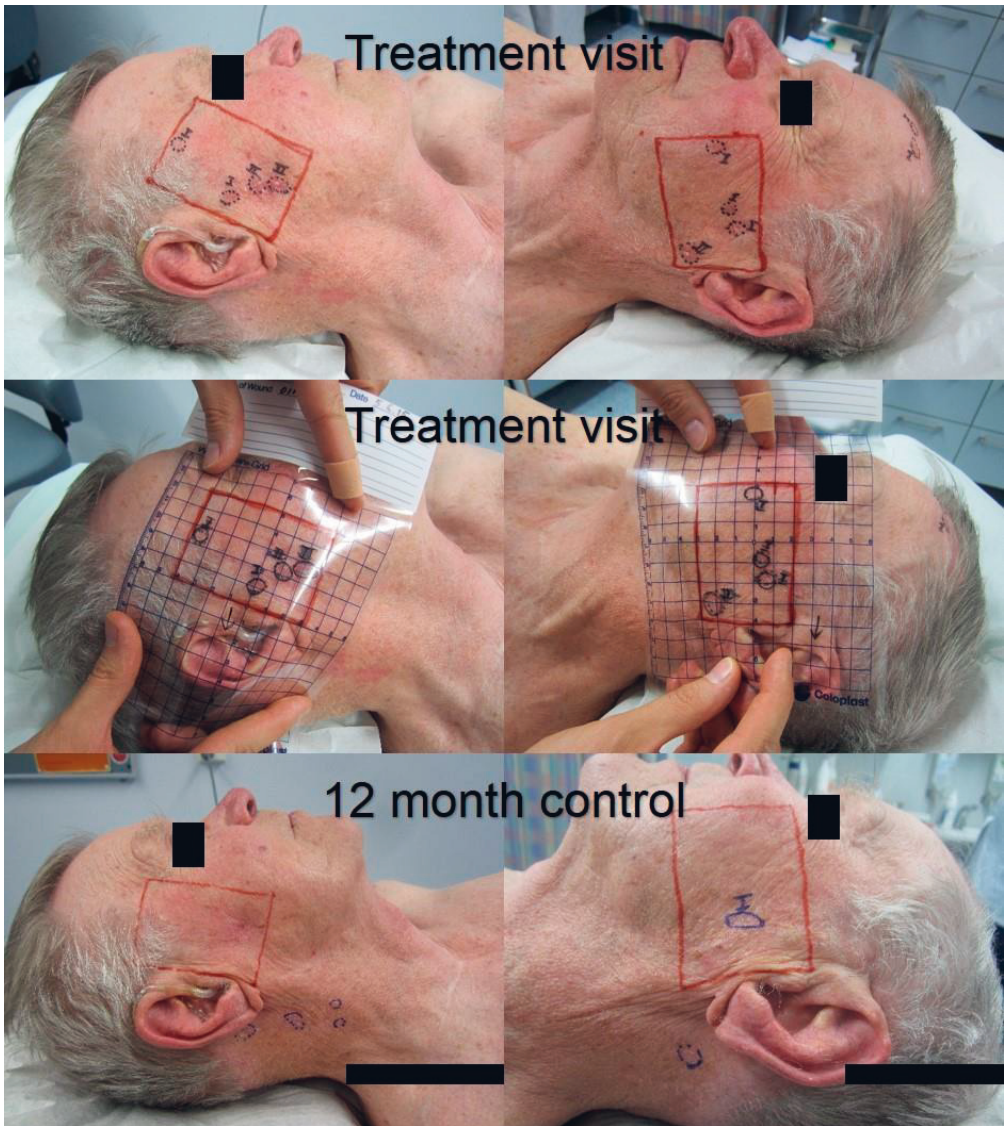


**Figure 10.** The treatment fields and AK lesions were marked on the skin and copied onto transparent plastic film at baseline to help mapping of the lesions at the control visit (Study I). With permission from the patient.

#### 4.2.2 Hyperspectral image acquisition (II and III)

In Studies **II** and **III**, all included skin lesions were imaged *in vivo* with a hyperspectral camera prototype before biopsy or excision, using either HSCP2 (Revenio Group,

Vantaa, Finland) (Study **II**) or VTT FPI VIS-VNIR Spectral Camera (VTT Technical Research Centre of Finland, Espoo, Finland) (Study **III**). VTT's prototype is shown in Figure 11. Before image acquisition, a small line was drawn on the skin beside the lesion with a black marker pen in order to retain orientation information later on. In Study **II**, the purpose of HSI was to reveal possible site of invasion within LM lesion and to determine the most suspicious site for biopsy. All melanocytic lesions imaged in Study **II** (ten LM and two LMM) were also included in the analysis of Study **III**. The main principles of hyperspectral imaging are explained in Chapter 2.4.6.



**Figure 11.** A handheld prototype of hyperspectral camera used in Study III. The camera is connected to a laptop with the image acquisition software. On the right side of the laptop is a broadband halogen light source which is connected to the camera via optical fibre. Photo by author.

### 4.2.3 Photodynamic therapy procedures (I and II)

In Studies **I** and **II**, PDT was used for the treatment of premalignant skin lesions. The DL-PDT procedure of Study **I** is presented in Figure 12. DL-PDT was not conducted in rainy weather. In one study centre (Päijät-Häme Central Hospital) the cumulative light dose during daylight illumination was measured with a light dosimeter (X9-7, Gigahertz-Optik, Türkenfeld, Germany) equipped with a blue light hazard sensor (UV-3709-4, Gigahertz-Optik, Türkenfeld, Germany) to mimic the absorption spectrum of PpIX. The meter and sensor were calibrated for the PpIX-

weighted light dose with a spectroradiometer (S2000, Ocean Optics, Florida, USA) by the Radiation and Nuclear Safety Authority of Finland (STUK). The uncertainty of the calibration coefficient was  $\pm 14\%$  using a confidence interval of 95%.

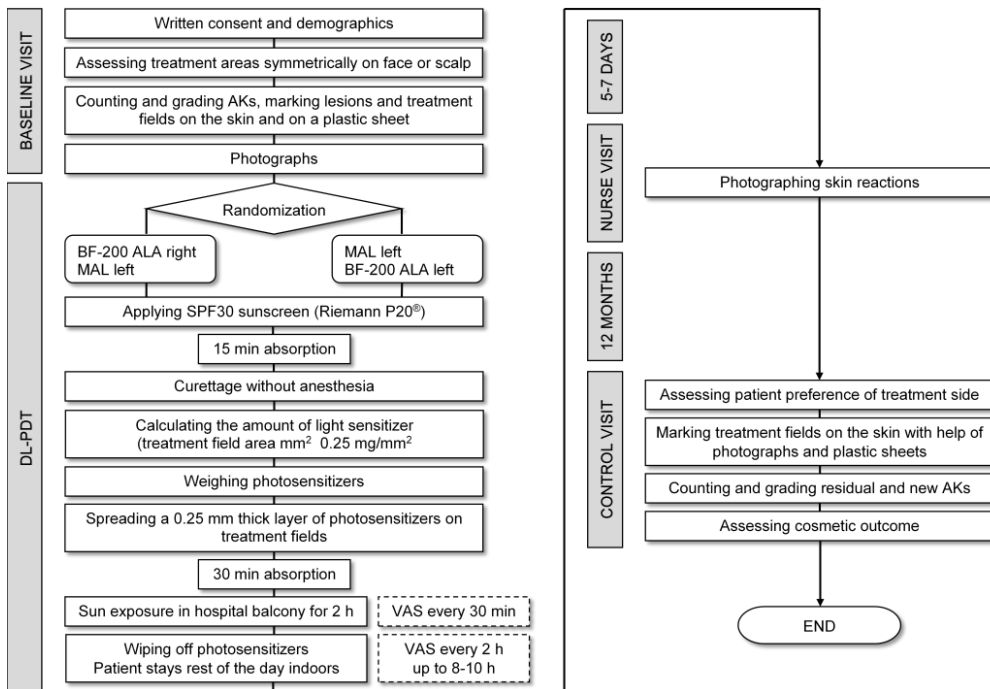


**Figure 12.** Flowchart of Study I.

A flowchart of treatment protocol in Study II is presented in Figure 13. In study II, LM lesions were treated with AFL-assisted PDT. The laser settings used were: Density level = 5, Depth level = 7 and Pulse duration = 700ms, which correspond to a distance of 0.8 mm between the laser channels on the grid and a calculated pulse energy of 84 mJ per channel. A photograph of AFL pretreatment is presented in Figure 14.



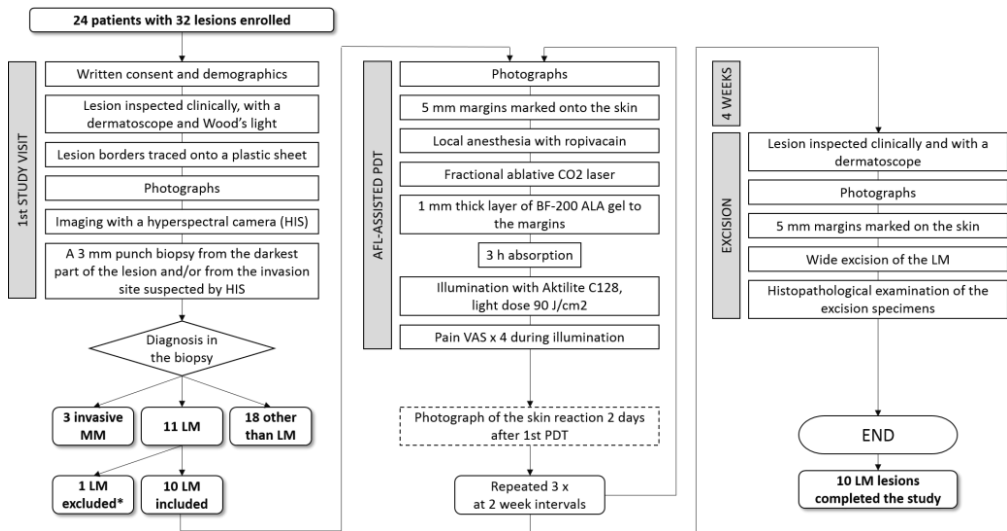


Figure 13. Flowchart of Study II.



Figure 14. Ablative fractional laser pretreatment (Study II). Photo by Ulla Oesch-Lääveri, with permission from the patient.



#### 4.2.4 Surgery (II and III)

In Study **II**, the treated LM lesions were surgically excised four weeks after the third PDT using a 5 mm peripheral margin. In Study **III**, all included lesions were first imaged with a hyperspectral camera *in vivo* and then surgically excised to achieve the true histopathological diagnosis. All surgical procedures were conducted by an experienced dermatosurgeon (Mari Grönroos).

#### 4.2.5 Histopathological evaluation (II and III)

All biopsies and excised tissue specimens were fixed in 4% formalin, embedded in paraffin, sectioned using the vertical bread-loaf technique and stained with haematoxylin-eosin (H&E) (Studies **II** and **III**).

At the screening visit of Study **II** a standard 3 mm punch biopsy was taken from the darkest part and/or from the most suspicious area of the lesion pointed out by HSI to verify the histological diagnosis and to exclude the invasive component before PDT treatment. The biopsies and final excision specimens were evaluated by an experienced dermatopathologist in a blinded manner, i.e. without any clinical information other than the location of the lesion. Immunohistochemistry stains (MART1/Melan A) were used to aid diagnosis when necessary. LM lesion was regarded as histologically cleared if no sign or suspicion of atypical melanocytes could be seen, and uncured if the histological criteria for LM were still fulfilled or if there was any suspicion of atypical melanocyte proliferation.

#### 4.2.6 Tolerability assessment (I and II)

The patient-reported pain during and after PDT was assessed with pain visual analogue scales (VAS, 0–10) (Hawker et al., 2011). In Study **I**, the patients were asked to fill in pain VAS scales separately for each treatment side at 30-minute intervals during the daylight exposure, and at 2-hour intervals for up to 8–10 hours after exposure. In Study **II**, patients filled in VAS scales i) before the LED illumination, ii) one minute after the start of the illumination, ii) in the middle, and iv) at the end.

The skin reactions were photographed by a nurse 5–7 days after DL-PDT treatment (Study **I**) or two days after the first PDT session (Study **II**) and later assessed from the photographs by a blinded investigator (the present author) on a scale of 1–4 (1 negligible; 2 mild; 3 moderate; 4 severe). In Study **II**, the delayed

skin reactions 2 weeks after PDT were also photographed during the following PDT session, and patients were also asked to report any intense or unexpected adverse reactions after any PDT session.

The cosmetic outcome (Study I) was assessed at the 12-month control visit by a blinded investigator separately for both sides (1 excellent; 2 good; 3 moderate; 4 poor), and the patient was also asked about the preference between the two treatments (right side, left side, or no preference).

#### 4.2.7 Statistical analyses

In Study I, Fisher's exact test was used for testing statistical differences in baseline lesion distribution, complete lesion clearance, the partial response in clinical grading, the count of new lesions and the differences in lesion clearance between the weather groups. Wilcoxon's signed-rank test was used for per patient (half-face) differences in the baseline lesion count, lesion clearance, cosmetic outcome, local skin reaction severity and VAS pain score. Kruskal-Wallis test was used to test for correlation between lesion response and weather conditions, temperature and light dose. Individually, temperatures and light doses were tested using Mann-Whitney test to ascertain whether they introduced an added variance component into the lesion clearance data. P-values <0.05 were considered statically significant.

The confidence intervals were calculated by the aid of VassarStats: Website for Statistical Computation (<http://vassarstats.net/prop1.html>) (Studies I–III).

#### 4.2.8 Cost-effectiveness analysis (I)

To assess the cost-effectiveness, the prices obtained from the Swedish drug database (FASS, Farmaceutiska Specialiteter i Sverige, <https://www.fass.se/LIF/startpage>) were used because BF-200 ALA gel is not currently imported to Finland. The Swedish prices for both photosensitizers were almost identical (Ameluz 201 € / 2 g tube, Metvix 205 € / 2 g tube). The other costs of DL-PDT treatment were estimated to be equal to those in an earlier cost-effectiveness study by our group, with the exception of the local anaesthetic, which was not used in this study (Neittaanmäki-Perttu, Grönroos, Karppinen, Snellman, et al., 2016). In the cost-effectiveness analysis (CEA), BF-200 ALA was considered as the intervention and MAL as the control treatment. The total cost of treatment (C) was defined as the photosensitizer cost for each patient with the mean societal and patients' costs for DL-PDT

treatment derived from our earlier study (Neittaanmäki-Perttu, Grönroos, Karppinen, Snellman, et al., 2016). Effectiveness (E) was defined as field lesion clearance at 12 months for each patient's treatment field (ranging between 0–1). CEA was performed to generate incremental cost-effectiveness ratio (ICER) which is calculated by the formula  $(C_1 - C_2) / (E_1 - E_2)$ , where 1 denotes the intervention and 2 the control treatment. Uncertainty of CEA was assessed using 10,000 bootstrapping iterations and the results were presented in the cost-effectiveness (CE) plane. The CEA was conducted by Pekka Rissanen (professor of Health economics, Tampere University).

#### 4.2.9 Convolutional neural network (III)

In Study **III**, a convolutional neural network (CNN) was trained and utilized as a tumour classifier in hyperspectral images pixel-wise to acquire a predicted diagnosis for each lesion. A combination of 3D, 2D and 1D CNN was used for classifying the lesions (Pölonen et al., 2019). Hyperspectral image data is three-dimensional in nature, and 3D CNN was utilized because it operates simultaneously in both spatial and spectral domains. The CNN used in the study consisted of two parts. Briefly, the first part executes feature learning by using the convolutional operator and the second part executes the actual classification with a deep-forward neural network (Pölonen et al., 2019). A schematic presentation of CNN is shown in Figure 15.

Labelled data from captured hyperspectral images was used for the training of the CNN. For each image, a clinical investigator (the present author) manually annotated areas of histologically confirmed tumour, healthy surrounding skin, and black marker pen. From the annotated areas of each image 1000 data sets containing the annotated pixel and its 5x5-pixel neighbourhoods were selected for training purposes. The actual training data was randomly sampled from annotated points to contain approx. 27,000 data points from each class. For annotated points, data augmentation was used to artificially create new training data and increase the diversity of the data for training. This was done by mirroring and flipping the training data cube horizontally and vertically. By these operations the number of inputs in the training phase was quadrupled and resulted in the final training set of approx. 655,000 data points.

Because the number of imaged lesions was limited (26 lesions), the hyperspectral images were divided into two halves in the middle of the annotated lesion. One half served as a training image and the other half was used separately for the classifying

task. This ensured that the training set did not contain data points from the image currently under classification and that the training set contained a sufficient variety of different lesion types.

Keras library, Tensorflow backend and Python 3.6 were used in the implementation of CNN. All calculations were executed on IBM PowerAI Platform, which includes two Nvidia Tesla V100-SXM2 16 GB GPU units. The hyperspectral analyses and lesion classification with CNN were conducted by a trained mathematician (Ilkka Pölonen).

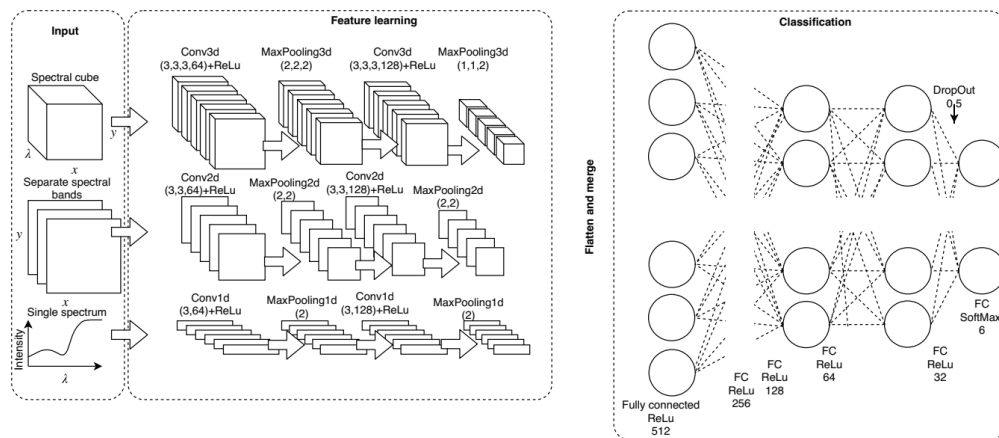


**Figure 15.** A schematic structure of 1D, 2D and 3D convolutional neural networks used in the Study III. Conv, MaxPooling, Fully connected (FC), ReLU, Dropout and Softmax are names of layers and functions in the implementation of CNN. From *Pölonen et al., 2019*, with permission from SPIE.

## 5 RESULTS

### 5.1 The efficacy of photodynamic therapy

#### 5.1.1 Clinical clearance of actinic keratoses (I)

Altogether 69 patients with 767 grade I–II AKs symmetrically on face or scalp completed the Study I. The distribution of AK grades at baseline was similar in both treatment groups. The half-face analysis showed no statistically significant difference in the baseline lesion count for all, grade I or grade II lesions.

The clinical lesion response rates at 12 months are presented in Table 7. In residual lesions, which were initially grade II AKs, the grade decreased in 17/97 for BF-200 ALA and 31/93 for MAL ( $p = 0.019$ ). The grade was unchanged in 13/97 and 11/93 and the grade increased in 0/97 and 1/93 for BF-200 ALA and MAL, respectively. Residual lesions located clearly separate from the baseline lesions marked on the plastic sheet were classified as new lesions ( $n = 36$ ; 32 grade I and 4 grade II for BF-200 ALA, and  $n = 30$ ; 26 grade I and 4 grade II for MAL).

**Table 7.** Clinical lesion response rates of Study I.

		<b>BF-200 ALA</b>	<b>MAL</b>	<b>P-value</b>
Complete	<b>All AKs</b>	299 / 375 (79.7%)	288 / 392 (73.5%)	<b>0.041</b>
response rate	<b>Grade I</b>	232 / 278 (83.5%)	238 / 299 (79.6%)	0.241
at 12 months	<b>Grade II</b>	67 / 97 (69.1%)	50 / 93 (53.8%)	<b>0.037</b>

In per patient (half-face) analysis of Study I, a significant difference in clinical lesion clearance between the BF-200 ALA and MAL groups was found. In 33 patients more lesions were cleared on the BF-200 ALA treated sides than on the corresponding MAL sides; in 16 patients more lesions were cleared on the MAL sides than on the BF-200 ALA sides while in 20 patients no differences between the sides were seen ( $p = 0.008$ ). No significant difference was seen in clearance of grade I and grade II lesions separately. At 12 months, complete field clearance (the treatment field being completely clear of all AKs) was the same for both treatments: 19 out of 69 fields (27.5%).

The treatment months of the 69 patients in Study **I** were as follows: May  $n = 4$ ; June  $n = 34$ ; July  $n = 1$ , August  $n = 22$  and September  $n = 8$ . The daylight illumination was carried out between 9 a.m. and 5 p.m. and the weather was sunny for 45, half cloudy for 16 and cloudy for 8 patients. The mean temperature was  $+20.4$  °C (range 8.5–29 °C). For both photosensitizers the lesion clearance rate (all lesions) differed significantly between weather groups (BF-200 ALA: sunny 83.5%; half-cloudy 73.1%; cloudy 69.8%,  $p = 0.028$ ) (MAL: sunny 77.5%; half-cloudy 69.1%; cloudy 51.4%,  $p = 0.004$ ). The PpIX-weighted light dose was measured in Pääjät-Häme Central Hospital for 27 patients with a mean dose  $12.89 J_{\text{eff}}/\text{cm}^2$  (range 5.96–17.93), but no significant correlation between light-dose and lesion clearance, or cut-off light dose for lesion clearance was found for either photosensitizer.

### 5.1.2 Histological clearance of lentigo malignas (II)

A total of nine patients with ten LM lesions completed the Study **II** (one patient had two LM lesions, one on the right temple and one on the right side of the neck). None of the patients had received any previous treatment such as cryotherapy, surgery or PDT on the skin area where the LM lesion was situated. The mean  $\pm$  SD (standard deviation) area of the lesions was  $98 \pm 58 \text{ mm}^2$ .

As the primary outcome of Study **II**, seven out of ten lesions (70%) were histologically completely cleared in the wide excision specimens, whereas in three lesions the histology demonstrated a residual LM. In two out of three unhealed lesions there was some clinically detectable pigmentation left after the PDT treatments and thus a residual was suspected. In one unhealed lesion all visible pigmentation had vanished, causing the lesion to appear clinically cured (Figure 16). In the histologically cleared lesions there was either no visible pigmentation left (four lesions) or the pigmentation was almost invisible with only a small area of pigmentation left (three lesions). In dermoscopy the most prevalent findings were erythema (nine lesions) and white streaks (four lesions), the latter most likely representing dermal scarring due to AFL pretreatment and/or PDT treatment.

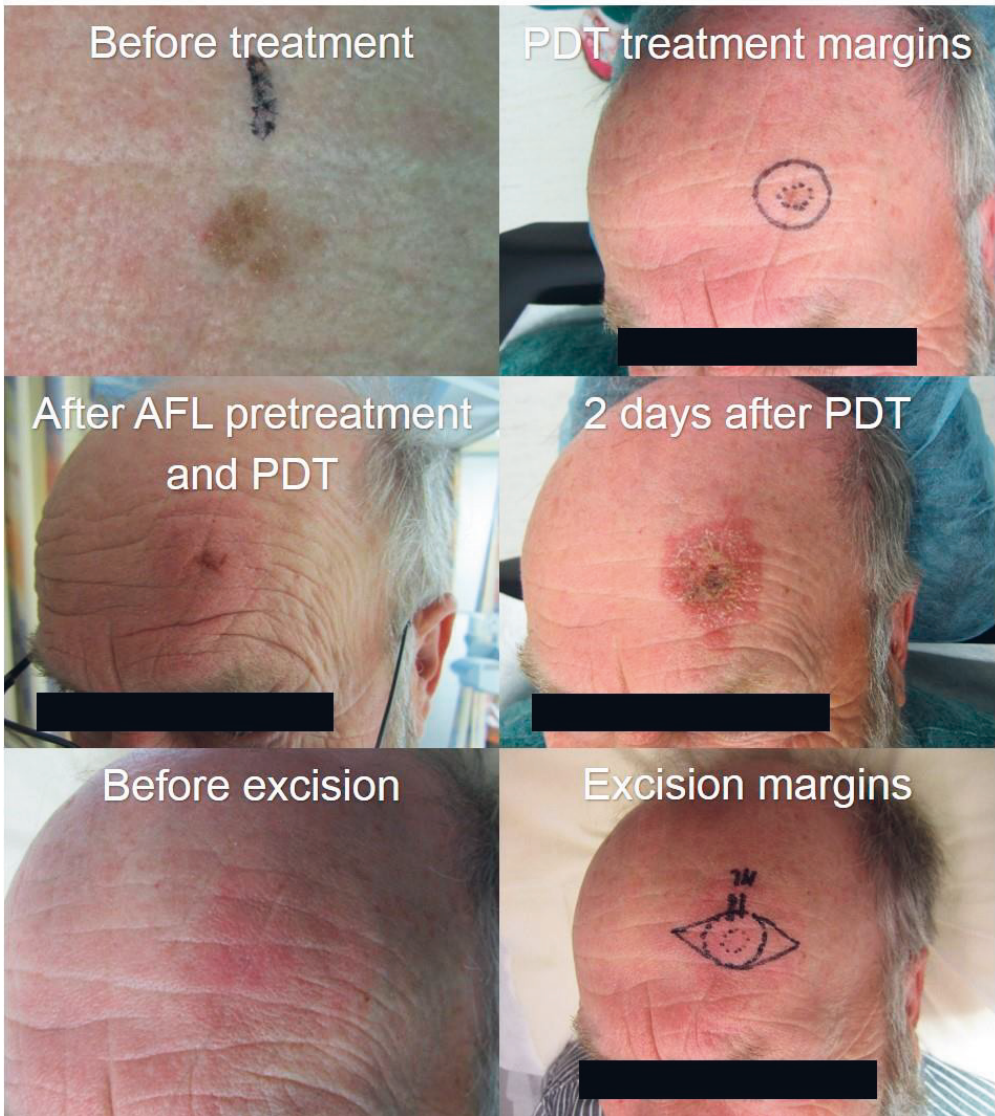


**Figure 16.** A lentigo maligna of the forehead included in Study II. The same lesion was photographed in different phases of the study protocol. Note the severe local skin reaction with pustules and intensive erythema two days after the first PDT session. After three PDT sessions there was no visible pigmentation left, only faint post-inflammatory erythema. However, in this particular case the final excision revealed an LM residual. With permission from the patient.

## 5.2 Safety and tolerability of photodynamic therapy (I and II)

The tolerability measures in Studies **I** and **II** are presented in Table 8.

In Study **I**, the pain scales were reported by 68 patients and the skin reactions (erythema, crusting) were assessed in 54 patients one week after DL-PDT. Overall, both photosensitizers were well tolerated and almost painless. When asked which of the two treatments the patient would prefer, 12 patients chose BF-200 ALA, 12 patient MAL and 56 expressed no preference.

In Study **II**, some unexpectedly severe adverse effects were seen. Two patients experienced moderate pain which continued for several hours after the second PDT session. One patient had a very intense skin reaction and one patient swelling of the eyelid and the neck after the second PDT. One patient with LM located on the cheek experienced intense swelling, erythema and burning pain leading to hospitalization on the day after the third PDT session. In one patient, after wide local excision a constant stinging pain occurred in the excision area for four weeks until a second excision was performed to increase the margins.

**Table 8.** Pain during illumination, severity of skin reactions and cosmetic outcome in Studies I and II. VAS = visual assessment scale (0–10).

		<b>BF-200 ALA</b>	<b>MAL</b>	<b>P-value</b>
<b>Study I</b>	Pain VAS, <i>mean ± SD (range)</i>	1.51 ± 1.61 (0 – 7.7)	1.35 ± 1.45 (0 – 7.7)	0.061
	Severity of skin reaction, <i>n (%)</i>			<b>0.001</b>
	1, negligible	14 (25%)	26 (46%)	
	2, mild	27 (48%)	23 (41%)	
	3, moderate	13 (23%)	6 (11%)	
	4, severe	2 (4%)	1 (2%)	
	Cosmetic outcome at 12 mo, <i>n (%)</i>			1.000
	1, excellent	38 (55%)	35 (51%)	
	2, good	25 (36%)	30 (43%)	
	3, moderate	6 (9%)	4 (6%)	
	4, poor	0 (0%)	0 (0%)	
		<b>1st PDT</b>	<b>2nd PDT</b>	<b>3rd PDT</b>
<b>Study II</b>	Pain VAS, <i>mean ± SD (range)</i>	3.1 ± 1.9 (0 – 5.4)	3.8 ± 2.1 (0.1 – 6.5)	2.9 ± 1.6 (1.2 – 5.5)
	Severity of skin reaction 2 days after 1st PDT, <i>mean ± SD (range)</i>	3.3 ± 0.7 (2 – 4)		



### 5.3 Cost-effectiveness analysis (I)

The mean total costs per patient were 176.4 € for BF-200 ALA and 178.0 € for MAL, which generated an incremental cost saving of -1.60 €. The mean field lesion clearances were 0.784 for BF-200 ALA and 0.701 for MAL, producing an increase of 0.083 in efficacy. The incremental cost-effectiveness ratio (ICER) yielded a monetary saving of -19.37 € per unit of effectiveness gained for BF-200 ALA in comparison to MAL. The simulated replica data of 10,000 bootstrapping iterations presented in the cost-effectiveness plane demonstrated that the costs of DL-PDT for the two photosensitizers were almost equal (in 58.7% of the simulations MAL was more costly) but the effectiveness was slightly greater for BF-200 ALA (in 96.4% of the simulations BF-200 ALA was more effective). Approximately 57% of the simulated replica data points were located on the southeastern quadrant of the plane, indicating that BF-200 ALA offers slightly better value for money than MAL.

### 5.4 Hyperspectral analyses and convolutional neural network classification (III)

A total of 26 pigmented lesions were included in the study **III**, with the following histopathological diagnoses: 10 BCCs (6 nodular, 2 superficial, 2 both superficial and nodular), 12 MIS (all LM subtype), and 4 invasive MM (3 LMM subtypes and one superficial spreading subtype, Breslow depths ranging from 0.3 to 1.4 mm). The mean  $\pm$  SD diameter of the lesions was  $9.8 \pm 2.9$  mm (range 5.3–19 mm) and the mean  $\pm$  SD area  $71.2 \pm 46.9$  mm<sup>2</sup> (range 11.0–247 mm<sup>2</sup>).

Because of limited sample size in Study **III**, the lesion classification was conducted first by combining all melanocytic tumours into a single group (MIS + MM) thus resulting in a two-class classification ('melanocytic tumours' vs. 'pigmented BCC'). After the training phase, 3D CNN classified every hyperspectral image pixel-wise in an automated manner and generated a classification map comprehending four classes ('pigmented BCC', 'melanocytic tumour', 'healthy skin' and 'marker pen') (Figure 17). The last layer of the classifier also produced likelihood maps indicating how certain the CNN is about the classification. The maximum likelihood (= the highest value of each pixel in likelihood maps) was used for selecting the predicted class for each pixel over the image.

The histological diagnoses of the excised lesions represented the true label, whereas the classification generated by the CNN represented the predicted label of

the lesions. We explored two different approaches for lesion classification: 1) majority of pixels classification and 2) pixelwise classification. In the majority of pixels method, the whole lesion was assigned to the same class as the majority of the pixels in lesional area. In pixelwise classification we compared the accuracy of CNN classification per individual pixel to manually annotated pixels in the images (the four pixel classes mentioned above). The pixelwise classification increased the number of classified objects from 26 lesions to 164,144 classified pixels.

In diagnosing melanocytic tumours from pigmented BCCs, for the majority of the pixels classification we achieved good accuracy with a calculated sensitivity of 100% (16/16) (95% confidence interval [CI] 81–100%), specificity of 90% (9/10) (95% CI 60–98%) and PPV of 94% (16/17) (95% CI 73–99%). Only one true pigmented BCC was erroneously classified as melanocytic tumour but all melanocytic tumours were classified correctly. For the pixelwise classification the diagnostic accuracy was also high, showing a sensitivity of 99.98% (95% CI 99.95–99.99%), specificity 93.2% (95% CI 92.6–93.7%) and PPV 97.8% (95% CI 97.6–98.0%).

In addition, a subgroup classification using three classes ('MIS', 'MM' and 'pigmented BCC'), was performed as above. In 3-class classification, for the majority of the pixels method the sensitivity was 100% (4/4) (95% CI 51–100%), specificity 100% (22/22) (95% CI 85–100%) and PPV 100% (4/4) (95% CI 51–100%) in diagnosing MM from other lesions (MIS and pigmented BCC). The pixelwise classification for the class "MM" yielded a sensitivity of 99.6% (95% CI 99.5–99.7%), specificity 98.6% (95% CI 98.5–98.8%) and PPV 97.3% (95% CI 97.0–97.6%).

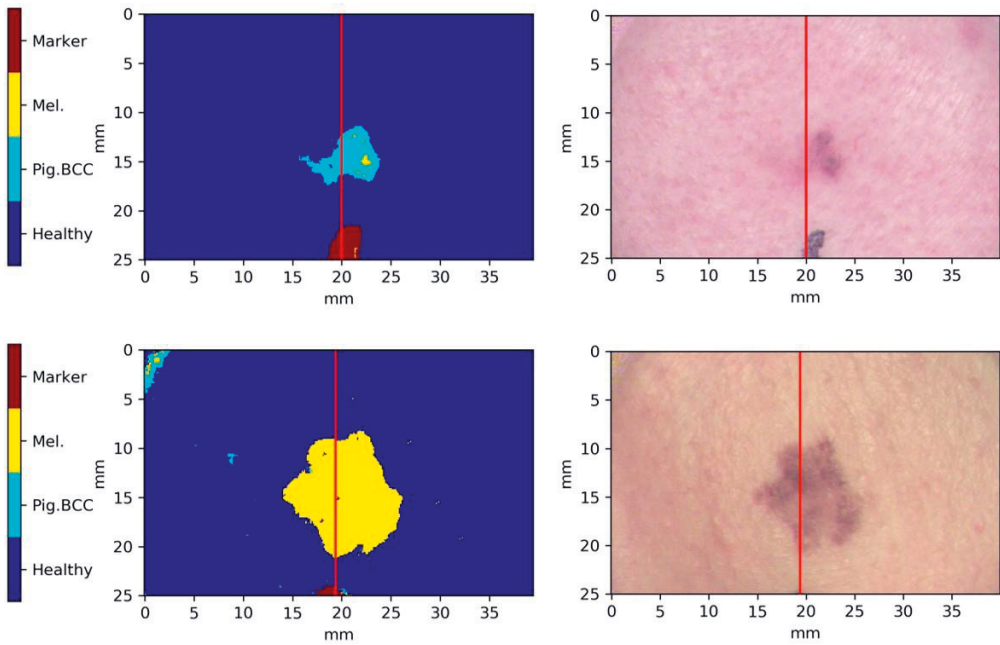


**Figure 17.** Two examples of pixel-wise classification maps generated by CNN in case of two classes ('melanocytic tumours' and 'pigmented BCC'). The histopathologically confirmed diagnosis for the lesion in the upper row was a nodular BCC, and for the lesion in the lower row LM. The image on the right side is a three-colour (RGB) visualization of the lesion's hyperspectral image.

## 6 DISCUSSION

### 6.1 The efficacy of photodynamic therapy for premalignant skin lesions (I & II)

The results of this study demonstrated that BF-200 ALA is more effective than MAL in DL-PDT for grade I–II AKs in a follow-up of 12 months. This confirmed the preliminary results of an earlier pilot study by our group, in which BF-200 ALA showed only a trend of improved efficacy (Neittaanmäki-Perttu et al., 2014; Neittaanmäki-Perttu, Grönroos, Tani, et al., 2016). This study was the first to investigate the efficacy of PDT for treating LM in a prospective trial, resulting in histopathological clearance rate of 70% (7 out of 10 LM lesions).

The majority of earlier DL-PDT studies have reported only short-term follow-up of 3 months, with AK clearance rates after a single MAL DL-PDT ranging between 70 and 89%, depending on the country and latitude (see Table 4). Because AK is a chronic condition with spontaneous recurrences and constant appearance of novel AKs (Werner et al., 2013), 12-month follow-up is more reliable in showing the long-term efficacy for field cancerization and the need for repeat treatments. However, only few studies have assessed the long-term efficacy of DL-PDT. In the 12-month follow-up of our earlier pilot study the mean complete clearance rates per patient (half-face) were 87% for BF-200 ALA and 62% for MAL, which is not directly comparable to lesion-based response rates (Neittaanmäki-Perttu, Grönroos, Tani, et al., 2016). In a recent Greek study the clearance rate for grade I–II AKs at 12 months in MAL DL-PDT was 71.8% compared to 73.7% in MAL LED-PDT, which concurs with our present results for MAL (Sotiriou et al., 2018). Interestingly, a company-sponsored non-inferiority study of BF-200 ALA compared to MAL in DL-PDT was published only a few months prior to Study I (Dirschka et al., 2019). In this multicentre, intraindividual study of 49 patients with 628 mild and moderate AKs, BF-200 ALA completely cleared 79.8% and MAL 76.5% of AKs at 3 months after single DL-PDT. The recurrence rates at 12 months were 19.9% and 31.6%, corresponding to estimated lesion-based clearance rates of 62.9% and 56.6% for BF-200 ALA and MAL respectively (Dirschka et al., 2019). The response rates at 3 months reported by Dirschka et al. are almost equal to those in Study I, but decline

in long-term follow-up of 12 months compared to our study. The complete field clearance in Study **I** was 27.5% for both treatments. In our earlier pilot study the complete field clearances were 69% for BF-200 ALA and 23% for MAL (Neittaanmäki-Perttu et al., 2014). This difference may be explained by the fact that in our pilot study grade II–III AKs were treated twice whereas in Study **I** only a single treatment was given, which may have led to an increase in residual lesions. In the non-inferiority study by Dirschka et al. complete field clearances at 3 months were 42.9% for BF-200 ALA and 38.8% for MAL, which is consistent with our results taking into account their shorter follow-up time.

Topical 5-ALA PDT is a well-established treatment for keratinocyte cancers and premalignant lesions, namely AK, Bowen's disease and BCC, but it has not proven effective in melanoma (Abels et al., 1997; Robertson & Abrahamse, 2010). In experimental melanoma models *in vivo*, PDT has seldom achieved complete remission but instead most of the reports have shown partial remission or recurrence of the melanoma (Baldea & Filip, 2012). One explanation for this may be that melanin restricts the penetration of red light through the skin and slows down the photobleaching (Robertson & Abrahamse, 2010). Another characteristic that may make melanoma cells more resistant to PDT is the ability of melanin to act as an intracellular antioxidant which neutralizes ROS and thus protects the cells from PDT-induced necrosis and apoptosis (Baldea & Filip, 2012).

In addition to Study **II**, there is only one retrospective case series investigating the efficacy of PDT for LM (Karam et al., 2013). Karam et al. treated 15 LM lesions with regular topical MAL LED-PDT resulting in a clinical cure rate of 80% (12/15 lesions) which is in accordance with our present results. Karam et al. used a varying light dose from 40 to 90 J/cm<sup>2</sup> and the number of PDT treatments ranged from 3 to 9 sessions depending on the clinical response. For lesions with partial depigmentation the number of PDT sessions was increased. In Karam's work lesion clearance was determined by clinical evaluation in a follow-up of 18–50 months and by using multiple biopsies 3 weeks after the last PDT session. This protocol may have caused some histological residuals to be missed as the pigment may also be bleached in non-responsive LM lesions, as was the case with one unhealed LM in our study. Also, LM is notorious for skipping areas in biopsy which may lead to false negative results (Juhász & Marmur, 2015). The clinical follow-up of 50 months at maximum can be regarded short on the scale of LM, for which the radial growth phase can last 10–50 years before developing into LMM (L. M. Cohen, 1995). For these reasons the lesion clearance in Karam's study may actually have been overestimated. In Study **II** the LM lesions were treated with wide local excision after

PDT for full histopathological examination, which is a more robust method for assessing treatment response than partial biopsies. There is still a possibility that the use of routine bread-loaf technique in the histological assessment could cause small foci of histological LM residuals to go unnoticed, which can be regarded as a limitation in our study. One way to minimize this risk would have been to use melanocyte-specific IHC stains such as Melan-A and gp100 routinely for all excision specimens as they can be of help particularly in the diagnosis of amelanotic lentigo maligna (Reed & Shea, 2011).

The failure rate i.e., the recurrence rate after AFL-assisted PDT in Study **II** was 30% (3 out of 10 LM lesions). The gold standard treatment for LM is surgical excision, and reported recurrence rates after wide local excision using 5 mm margins are approximately 7–20%, after staged excision 0–9.7% and after Mohs micrographic surgery 0–6.25% (McLeod et al., 2011). However, excision of LM is not always applicable given the large size of lesions, possible peripheral subclinical extension, location on cosmetically delicate areas and high age of the patients (Erickson & Miller, 2010; McLeod et al., 2011). Thus, LM poses a therapeutic challenge and reveals a need for alternative non-surgical therapies, many of which have been investigated with varying results. The reported recurrence rates with non-surgical modalities have ranged from 0 to 40% for cryotherapy (McLeod et al., 2011), from 0 to 100% (mean 34.4%) for laser therapy (Read et al., 2016), from 15.8 to 28% for topical imiquimod (Papanikolaou & Lawrence, 2019; Tio et al., 2017, 2019) and from 0 to 25% (mean 5%) for radiotherapy including Grenz rays (Fogarty et al., 2014; Hedblad & Mallbris, 2012) all of which are inferior to those achieved with surgery. The cure rate in Study **II** is superior to that with laser therapy or cryotherapy, at the same level as imiquimod but inferior to radiotherapy and Grenz rays. It appears that both imiquimod and PDT result in the healing of the LM in the majority of cases, but approximately 20–30% of lesions are non-responsive to treatment and lead to recurrences. One clinicopathologic study of imiquimod-treated LM lesions failed to find any histopathologic features of LM which would have prognostic significance for treatment response, but the ability to develop an inflammatory reaction to imiquimod predicted a good therapeutic effect (Powell et al., 2009). A high recurrence rate of LM with any treatment modality may stem from a deep follicular component, unsuspected invasive focus already present, or subclinical peripheral extension of the lesion (McGuire et al., 2012). The follicular extension of atypical melanocytes is very frequent in LM and can reach a depth of 1.1 mm (Connolly et al., 2019).

In Study **II** we opted to use the AFL pretreatment to enhance the penetration of photosensitizer through intact stratum corneum of LM and to increase its concentration in deeply situated follicular melanocytes. In the PDT protocol we used a standard incubation time of 3 hours, but higher light dose of 90 J/cm<sup>2</sup> for PpIX activation. This is more than double of the standard light dose 37 J/cm<sup>2</sup> for treating AK and BCC (Morton et al., 2013a). When treating non-melanocytic lesions the photobleaching of PpIX is very rapid in the initial phase of illumination (55% of PpIX is activated during the first 4.5 J/cm<sup>2</sup>, and over 70% during the first 10 J/cm<sup>2</sup>) but it continues gradually until the dose of 37 J/cm<sup>2</sup> is completed (Tyrrell et al., 2010). There is no published data on PpIX photobleaching in melanoma but we assumed that it occurs more slowly, especially in deep follicular extension of atypical cells because melanin markedly reduces the diffusion of red light through superficial layers of the skin (Robertson & Abrahamse, 2010). However, this is merely an assumption since we did not measure PpIX photobleaching during skin illumination. A further unknown quantity is the PpIX accumulation rate in atypical melanocytes. Too low PpIX accumulation in deep follicular atypical cells may be one explanation for treatment failure in the three uncured LM lesions of our study. To investigate these aspects further and to refine the PDT protocol for LM, measurements of ALA-induced PpIX photofluorescence in LM lesions would be required in future studies. The optimal PDT protocol for LM is not necessarily the same as for keratinocyte cancers and the clearance rate might be improved by changing the photosensitizer precursor to more lipophilic, extending the incubation time and possibly by fractionating skin illumination. Unfortunately, LM is not an easy target for clinical intervention studies due to its low incidence. In Study **II**, it took us almost two years to recruit over ten LM lesions in one central hospital in Finland.

## 6.2 Tolerability of photodynamic therapy (I & II)

In Study **I**, the mean pain VAS during daylight illumination was slightly lower with MAL (1.51 for BF-200 ALA and 1.35 for MAL,  $p = 0.061$ ) which is in accordance with earlier studies (Dirschka et al., 2019; Neittaanmäki-Perttu et al., 2014). In Study **II**, the mean patient-reported pain during LED illumination was low (2.9–3.8 on the VAS scale from 0 to 10). The highest pain level was reported during the second PDT session, with the highest pain VAS score being 6.5. Of note, a local anaesthetic (ropivacaine) was used 3 hours before illumination in Study **II**.

The tolerability of both photosensitizers in Study **I** was very good, with no significant difference in pain, cosmetic outcome or patient preference, but BF-200 ALA caused more intense local skin reactions. Another study comparing BF-200 ALA and MAL in LED-PDT also reported more intense local skin reactions caused by BF-200 ALA (Serra-Guillén et al., 2018). This is likely caused by increased penetration of BF-200 ALA into the skin resulting in higher PpIX accumulation, but also by less specificity for dysplastic cells than with MAL (Maisch et al., 2010; Reinhold, 2017; Serra-Guillén et al., 2018). There was no difference in patient preference or in the cosmetic outcome for one photosensitizer over another 12 months after treatment. Cosmetic outcome was excellent or good for both treatments in >90% of cases, which is consistent with earlier DL-PDT studies (Dirschka et al., 2019; Lacour et al., 2015; Moggio et al., 2016; Rubel et al., 2014).

The local skin reactions in Study **II** can be regarded definitely more severe than the ones occurring in cPDT when treating NMSC. The AFL pretreatment increases the unselective uptake of photosensitizer into non-malignant cells and the higher light dose increases the cumulative amount of phototoxic reactions inside cells. Presumably the combinatory effect of both the AFL pretreatment and the experimental light dose of 90 J/cm<sup>2</sup> explains the intense skin reactions.

Despite several studies having been conducted, the threshold light dose for sufficient daylight illumination in DL-PDT is not yet known (Fitzmaurice & Eisen, 2016). Wiegell et al. suggested a threshold of > 3.5 or 8 J<sub>eff</sub>/cm<sup>2</sup> for the PpIX-weighted light dose in DL-PDT (Wiegell, Fabricius, et al., 2012; Wiegell, Hædersdal, Eriksen, et al., 2009), but two other recent studies failed to find an association between light dose and AK reduction rate (Assikar et al., 2020; O’Gorman et al., 2016). In Study **I**, we measured the PpIX-weighted light dose for 27 patients in Lahti Central Hospital, but found no significant treatment effect between light dose and lesion clearance, nor a threshold level under which the clearance rate would be reduced. This may be due to the limited number of measurements or because the light dose for most or all patients did not fall below the true threshold level. Hence the threshold light dose in DL-PDT remains to be determined in future studies. However, the clearance rate in Study **I** was significantly associated with the weather conditions on the treatment day such that the highest lesion clearances were achieved on sunny days and lowest in overcast weather.



### 6.3 Hyperspectral imaging and diagnostic accuracy of convolutional neural network (III)

The CNN model used in Study **III** worked well and produced accurate classification maps containing only few and sporadic misclassified pixels. The inspection of lesion classification maps (an example shown in Figure 17) revealed that there were few misclassified pixels both within the lesion and in the surrounding healthy skin, but by far most pixels were classified correctly. Close to all included lesions demonstrated a very similar scenario, except for one pigmented BCC (Figure 4 in original publication) for which the CNN classifier erroneously showed multiple pixels representing a melanocytic tumour within the lesion area. This could be partly explained by some entrapped melanocytes within the pigmented BCC or pigment macrophages mistaken for melanocytes. Pigmented BCCs do not only contain more melanin, but also have more melanocytes than do non-pigmented lesions (Brankov et al., 2016). Another explanation for erroneous classification may be inherent error in the CNN model. In this particular case the hyperspectral image quality was low, resulting in misclassified pixels also in the surrounding healthy skin. It seems that the spectrum of normal skin in this image is very close to the trained spectrum of pigmented BCC, thereby creating difficulties for CNN to distinguish between normal and malignant tissue and to delineate the lesion correctly. Due to the hidden nature of the learning process in the CNN architecture, we do not exactly know which features the neural network actually used for selecting each class.

The few misclassified pixels in other images may be explained by imaging errors (local increased noise or other perturbation in the hyperspectral image) or by inaccuracy in the CNN model. However, by using the majority of the pixels to classify the entire lesion, the few misclassified pixels were averaged and our CNN achieved high sensitivity and specificity in both two-class (all melanocytic lesions vs. pigmented BCCs) and three-class classifications (MM vs. MIS vs. pigmented BCC). We also attempted lesion classification using leave-one-out cross-validation, but this did not yield the desired result (data not shown), which is due to the too small dataset. The accuracy of CNN classification per individual pixel (in comparison to manually annotated pixels) was also computed, resulting in high sensitivity and specificity of >90%, which reflects the robustness of the CNN model used. A limitation with CNN architecture is that the learning process is of a hidden nature.

## 6.4 Strengths and limitations

The strengths of Study **I** are the prospective split-face design, where the patients acted as their own controls, the large sample size and long follow-up of 12 months. The limitations are the lack of patient-oriented outcomes (such as cosmetic outcome from the patient perspective) and the lack of untreated control patients. Another limitation is that the complete field clearance and the costs of re-treatments were omitted from the CEA.

The main strength of Study **II** is that it is the first prospective study assessing the efficacy of AFL-assisted PDT for LM, thus serving as a basis for future trials. The limitations were the small sample size, due to the piloting nature of the study, and the use of the routine bread-loaf technique in the histopathological evaluation of the excised lesions which could have caused us to miss some small residual focus of a LM lesion.

Study **III** is the first to utilize a combination of HSI and a deep-learning CNN for skin lesion classification which makes it a pivotal study in this field. The results were promising and demonstrate that the CNN was able to distinguish malignant melanocytic tumours from pigmented BCCs with comparable or better results than achieved in current practice by a specialist dermatologist. The main limitation was the small and limited sample. Diagnostic studies using artificial intelligence classifiers usually include hundreds or thousands of images in their datasets. We compensated for this by using pixelwise analyses which increased the number of classified cases from 26 lesions to 164,144 classified pixels. This was also done with the training set, which included 655,000 data points. However, due to the limited number of cases our study sample may not be representative of all possible variability encountered in MM and pigmented BCC cases. Another limitation is that CNN was trained and tested on the same lesion images even though they were divided into two separate halves. However, this was also compensated for by the pixelwise analysis (not per lesion or image), where the pixels were analysed separately and could be counted as separate lesions. Thus, the training and classification sets can be regarded as independent. Ideally, the CNN training phase should be conducted with a separate dataset from that used for the classification task. With a larger sample a separate training dataset is warranted. One further limitation is that our sample did not include other melanocytic lesions such as benign or dysplastic nevi. Other pigmented lesions (benign nevi, dysplastic nevi, congenital nevi, seborrheic keratoses, pigmented AKs) were not included and warrant further studies in the future.

## 7 CONCLUSION AND FUTURE ASPECTS

The primary conclusions of the present study are the following:

1. BF-200 ALA (Ameluz®) was more effective than MAL (Metvix®) in DL-PDT for mild to moderate AKs in long-term follow-up of 12 months. BF-200 ALA was also slightly more cost-effective, which could lead to cost-savings in the implementation of DL-PDT. There was no difference in treatment-induced pain, cosmetic outcome or patient preference between photosensitizers, but BF-200 ALA caused more intense local skin reactions after treatment which may affect the tolerability of the treatment.
2. AFL-assisted PDT (three treatments with an experimental light dose of 90 J/cm<sup>2</sup>) in the treatment of in situ LM resulted in moderate histological clearance of 70% (7 out of 10 lesion). Thus, AFL-assisted PDT could constitute a minimally invasive alternative therapy for non-operable LM lesions. A clinical follow-up with repeated biopsies should always be arranged after PDT due to possible recurrency and the ability of PDT to destroy visible pigment, also in the case of histologically confirmed residual.
3. A deep learning CNN lesion classifier used in conjunction with HSI was able to distinguish malignant melanocytic tumours from pigmented BCCs in an automated and pixel-wise manner. The combination of 3D, 2D and 1D CNN classifier demonstrated high sensitivity and specificity using two different approaches: 1) using the majority of pixels to classify the entire lesion, and 2) in single pixel classification compared to manually annotated pixels. The implemented CNN classifier is generalizable and can be expanded for multiple lesion types. With a larger training dataset, the CNN classifier can be further developed to be more accurate and robust, but this will require more studies with considerably larger samples and multiple lesion types in the future. This study may

have an impact on melanoma diagnostics in near future when a hyperspectral camera for skin imaging will be commercially available.

## 8 REFERENCES

- Abels, C., Fritsch, C., Bolsen, K., Szeimies, R. M., Ruzicka, T., Goerz, G., & Goetz, A. E. (1997). Photodynamic therapy with 5-aminolaevulinic acid-induced porphyrins of an amelanotic melanoma in vivo. *Journal of Photochemistry and Photobiology B: Biology*, *40*(1), 76–83. [https://doi.org/10.1016/S1011-1344\(97\)00027-4](https://doi.org/10.1016/S1011-1344(97)00027-4)
- Ackerman, A. B., & Mones, J. M. (2006). Solar (actinic) keratosis is squamous cell carcinoma. *British Journal of Dermatology*, *155*(1), 9–22. <https://doi.org/10.1111/j.1365-2133.2005.07121.x>
- Akay, B. N., Kocyigit, P., Heper, A. O., & Erdem, C. (2010). Dermatoscopy of flat pigmented facial lesions: Diagnostic challenge between pigmented actinic keratosis and lentigo maligna. *British Journal of Dermatology*, *163*(6), 1212–1217. <https://doi.org/10.1111/j.1365-2133.2010.10025.x>
- Alawi, S. A., Kuck, M., Wahrlich, C., Batz, S., McKenzie, G., Fluhr, J. W., Lademann, J., & Ulrich, M. (2013). Optical coherence tomography for presurgical margin assessment of non-melanoma skin cancer - a practical approach. *Experimental Dermatology*, *22*(8), 547–551. <https://doi.org/10.1111/exd.12196>
- Angell-Petersen, E., Sørensen, R., Warloe, T., Soler, A. M., Moan, J., Peng, Q., & Giercksky, K. E. (2006). Porphyrin formation in actinic keratosis and basal cell carcinoma after topical application of methyl 5-aminolevulinic acid. *Journal of Investigative Dermatology*, *126*(2), 265–271. <https://doi.org/10.1038/sj.jid.5700048>
- Ardigo, M., Longo, C., Gonzalez, S., Agozzino, M., Debarbieux, S., Di Stefani, A., Gerittsen, M. J., Gill, M., Hofmann-Wellenhof, R., Kline, M., Malvey, J., Menezes, N., Moscarella, E., Pellacani, G., Puig, S., Rao, B., Rao, B., Segura, S., Soyer, P., ... Venturini, M. (2016). Multicentre study on inflammatory skin diseases from The International Confocal Working Group: specific confocal microscopy features and an algorithmic method of diagnosis. *British Journal of Dermatology*, *175*(2), 364–374. <https://doi.org/10.1111/bjd.14516>
- Arenberger, P., & Arenbergerova, M. (2017). New and current preventive treatment options in actinic keratosis. *Journal of the European Academy of Dermatology and Venereology*, *31*, 13–17. <https://doi.org/10.1111/jdv.14375>
- Assikar, S., Labrunie, A., Kerob, D., Couraud, A., & Bédane, C. (2020). Daylight photodynamic therapy with methyl aminolevulinic acid cream is as effective as conventional photodynamic therapy with blue light in the treatment of actinic keratosis: a controlled randomized intra-individual study. *Journal of the European Academy of Dermatology and Venereology*. <https://doi.org/10.1111/jdv.16208>
- Babilas, P., Schreml, S., Landthaler, M., & Szeimies, R. M. (2010). Photodynamic therapy in dermatology: State-of-the-art. In *Photodermatology Photoimmunology and Photomedicine* (Vol. 26, Issue 3, pp. 118–132). Blackwell Munksgaard. <https://doi.org/10.1111/j.1600-0781.2010.00507.x>
- Baldea, I., & Filip, A. G. (2012). Photodynamic therapy in melanoma - An update. *Journal of Physiology and Pharmacology*, *63*(2), 109–118.

- Basset-Seguín, N., Ibbotson, S. H., Emtestam, L., Tarstedt, M., Morton, C., Maroti, M., Calzavara-Pinton, P., Varma, S., Roelandts, R., & Wolf, P. (2008). Topical methyl aminolaevulinate photodynamic therapy versus cryotherapy for superficial basal cell carcinoma: a 5 year randomized trial. *European Journal of Dermatology : EJD*, *18*(5), 547–553. <https://doi.org/10.1684/ejd.2008.0472>
- Bastian, B. C. (2014). The molecular pathology of melanoma: An integrated taxonomy of melanocytic neoplasia. *Annual Review of Pathology: Mechanisms of Disease*, *9*, 239–271. <https://doi.org/10.1146/annurev-pathol-012513-104658>
- Berman, B., & Cockerell, C. J. (2013). Pathobiology of actinic keratosis: Ultraviolet-dependent keratinocyte proliferation. *Journal of the American Academy of Dermatology*, *68*(1 SUPPL.1), S10–S19. <https://doi.org/10.1016/j.jaad.2012.09.053>
- Bichakjian, C. K., Halpern, A. C., Johnson, T. M., Foote Hood, A., Grichnik, J. M., Swetter, S. M., Tsao, H., Barbosa, V. H., Chuang, T. Y., Duvic, M., Ho, V. C., Sober, A. J., Beutner, K. R., Bhushan, R., & Smith Begolka, W. (2011). Guidelines of care for the management of primary cutaneous melanoma. *Journal of the American Academy of Dermatology*, *65*(5), 1032–1047. <https://doi.org/10.1016/j.jaad.2011.04.031>
- Bickers, D. R., Lim, H. W., Margolis, D., Weinstock, M. A., Goodman, C., Faulkner, E., Gould, C., Gemmen, E., & Dall, T. (2006). The burden of skin diseases: 2004. A joint project of the American Academy of Dermatology Association and the Society for Investigative Dermatology. *Journal of the American Academy of Dermatology*, *55*(3), 490–500. <https://doi.org/10.1016/j.jaad.2006.05.048>
- Blasi, M. A., Pagliara, M. M., Lanza, A., Sammarco, M. G., Caputo, C. G., Grimaldi, G., & Scupola, A. (2018). Photodynamic therapy in ocular oncology. *Biomedicines*, *6*(1), 2–7. <https://doi.org/10.3390/biomedicines6010017>
- Bonerandi, J. J., Beauvillain, C., Caquant, L., Chassagne, J. F., Chaussade, V., Clavère, P., Desouches, C., Garnier, F., Grolleau, J. L., Grossin, M., Jourdain, A., Lemonnier, J. Y., Maillard, H., Ortonne, N., Rio, E., Simon, E., Sei, J. F., Grob, J. J., & Martin, L. (2011). Guidelines for the diagnosis and treatment of cutaneous squamous cell carcinoma and precursor lesions. *Journal of the European Academy of Dermatology and Venereology*, *25*(SUPPL. 5), 1–51. <https://doi.org/10.1111/j.1468-3083.2011.04296.x>
- Bongiorno, M. R., Doukaki, S., Malleo, F., & Aricò, M. (2008). Identification of progenitor cancer stem cell in lentigo maligna melanoma. *Dermatologic Therapy*, *21*(SUPPL. 1), 1–5. <https://doi.org/10.1111/j.1529-8019.2008.00193.x>
- Boone, M. A. L. M., Marneffe, A., Suppa, M., Miyamoto, M., Alarcon, I., Hofmann-Wellenhof, R., Malvehy, J., Pellacani, G., & Del Marmol, V. (2015). High-definition optical coherence tomography algorithm for the discrimination of actinic keratosis from normal skin and from squamous cell carcinoma. *Journal of the European Academy of Dermatology and Venereology*, *29*(8), 1606–1615. <https://doi.org/10.1111/jdv.12954>
- Boone, M. A. L. M., Norrenberg, S., Jemec, G. B. E., & Del Marmol, V. (2012). Imaging of basal cell carcinoma by high-definition optical coherence tomography: Histomorphological correlation. A pilot study. *British Journal of Dermatology*, *167*(4), 856–864. <https://doi.org/10.1111/j.1365-2133.2012.11194.x>
- Boone, M. A. L. M., Norrenberg, S., Jemec, G. B. E., & Del Marmol, V. (2013). Imaging actinic keratosis by high-definition optical coherence tomography. Histomorphologic correlation: A pilot study. *Experimental Dermatology*, *22*(2), 93–97. <https://doi.org/10.1111/exd.12074>

- Bosbous, M. W., Dzwierzynski, W. W., & Neuburg, M. (2010). Lentigo Maligna: Diagnosis and Treatment. *Clinics in Plastic Surgery*, 37(1), 35–46. <https://doi.org/10.1016/j.cps.2009.08.006>
- Braakhuis, B. J. M., Tabor, M. P., Kummer, J. A., Leemans, C. R., & Brakenhoff, R. H. (2003). A genetic explanation of slaughter's concept of field cancerization: Evidence and clinical implications. *Cancer Research*, 63(8), 1727–1730.
- Braathen, L. R., Morton, C. A., Basset-Seguín, N., Bissonnette, R., Gerritsen, M. J. P., Gilaberte, Y., Calzavara-Pinton, P., Sidoroff, A., Wulf, H. C., & Szeimies, R. M. (2012). Photodynamic therapy for skin field cancerization: An international consensus. International Society for Photodynamic Therapy in Dermatology. *Journal of the European Academy of Dermatology and Venereology*, 26(9), 1063–1066. <https://doi.org/10.1111/j.1468-3083.2011.04432.x>
- Brankov, N., Prodanovic, E. M., & Hurley, M. Y. (2016). Pigmented basal cell carcinoma: increased melanin or increased melanocytes? *Journal of Cutaneous Pathology*, 43(12), 1139–1142. <https://doi.org/10.1111/cup.12819>
- Bub, J. L., Berg, D., Slee, A., & Odland, P. B. (2004). Management of lentigo, maligna and lentigo maligna melanoma with staged excision: A 5-year follow-up. *Archives of Dermatology*, 140(5), 552–558. <https://doi.org/10.1001/archderm.140.5.552>
- Calzavara-Pinton, P., Hædersdal, M., Barber, K., Basset-Seguín, N., Del Pino Flores, M. E., Foley, P., Galimberti, G., Gerritsen, R., Gilaberte, Y., Ibbotson, S., Peris, K., Sapra, S., Sotiriou, E., Torezan, L., Ulrich, C., Guillemot, J., Hendrich, J., & Szeimies, R. M. (2017). Structured expert consensus on actinic keratosis: Treatment algorithm focusing on daylight PDT. *Journal of Cutaneous Medicine and Surgery*, 21, 3S-16S. <https://doi.org/10.1177/1203475417702994>
- Cameron, M. C., Lee, E., Hibler, B. P., Barker, C. A., Mori, S., Cordova, M., Nehal, K. S., & Rossi, A. M. (2019). Basal cell carcinoma: Epidemiology; pathophysiology; clinical and histological subtypes; and disease associations. *Journal of the American Academy of Dermatology*, 80(2), 303–317. <https://doi.org/10.1016/j.jaad.2018.03.060>
- Carapeba, M. de O. L., Pineze, M. A., & Nai, G. A. (2019). Is dermoscopy a good tool for the diagnosis of lentigo maligna and lentigo maligna melanoma? A meta-analysis. *Clinical, Cosmetic and Investigational Dermatology*, 12, 403–414. <https://doi.org/10.2147/CCID.S208717>
- Carrara, M., Colombo, A., Santinami, M., Carrara, M., Bono, A., Bartoli, C., Colombo, A., Lualdi, M., Moglia, D., Santoro, N., Tolomio, E., Tomatis, S., Tragni, G., Santinami, M., & Marchesini, R. (2007). Multispectral imaging and artificial neural network: Mimicking the management decision of the clinician facing pigmented skin lesions. *Article in Physics in Medicine and Biology*, 52, 2599–2613. <https://doi.org/10.1088/0031-9155/52/9/018>
- Chen, A. C., Martin, A. J., Choy, B., Fernandez-Penas, P., Dalziel, R. A., McKenzie, C. A., Scolyer, R. A., Dhillon, H. M., Vardy, J. L., Krickler, A., George, G. S., Chinniah, N., Halliday, G. M., & Damian, D. L. (2015). A phase 3 randomized trial of nicotinamide for skin-cancer chemoprevention. *New England Journal of Medicine*, 373(17), 1618–1626. <https://doi.org/10.1056/NEJMoa1506197>
- Chen, G. J., Feldman, S. R., Williford, P. M., Hester, E. J., Kiang, S. H., Gill, I., & Fleischer, A. B. (2005). Clinical diagnosis of actinic keratosis identifies an elderly population at high risk of developing skin cancer. *Dermatologic Surgery*, 31(1), 43–47. <https://doi.org/10.1097/00042728-200501000-00009>

- Chen, M., Pennathur, A., & Luketich, J. D. (2006). Role of photodynamic therapy in unresectable esophageal and lung cancer. *Lasers in Surgery and Medicine*, 38(5), 396–402. <https://doi.org/10.1002/lsm.20364>
- Chetty, P., Choi, F., & Mitchell, T. (2015). Primary Care Review of Actinic Keratosis and Its Therapeutic Options: A Global Perspective. *Dermatology and Therapy*, 5(1), 19–35. <https://doi.org/10.1007/s13555-015-0070-9>
- Chiarello, S. E. (2000). Cryopeeling (Extensive cryosurgery) for treatment of actinic keratoses: An update and comparison. *Dermatologic Surgery*, 26(8), 728–732. <https://doi.org/10.1046/j.1524-4725.2000.99197.x>
- Choi, S. H., Kim, K. H., & Song, K. H. (2015a). Efficacy of ablative fractional laser-assisted photodynamic therapy for the treatment of actinic cheilitis: 12-month follow-up results of a prospective, randomized, comparative trial. *British Journal of Dermatology*, 173(1), 184–191. <https://doi.org/10.1111/bjd.13542>
- Choi, S. H., Kim, K. H., & Song, K. H. (2015b). Efficacy of ablative fractional laser-assisted photodynamic therapy with short-incubation time for the treatment of facial and scalp actinic keratosis: 12-month follow-up results of a randomized, prospective, comparative trial. *Journal of the European Academy of Dermatology and Venerology*, 29(8), 1598–1605. <https://doi.org/10.1111/jdv.12953>
- Cockerell, C. J. (2000). Histopathology of incipient intraepidermal squamous cell carcinoma (“actinic keratosis”). *Journal of the American Academy of Dermatology*, 42(1 SUPPL. 1). <https://doi.org/10.1067/mjd.2000.103344>
- Cockerell, C. J. (2003). Pathology and pathobiology of the actinic (solar) keratosis. *British Journal of Dermatology, Supplement*, 149(66), 34–36. <https://doi.org/10.1046/j.0366-077x.2003.05625.x>
- Cohen, D. K., & Lee, P. K. (2016). Photodynamic therapy for non-melanoma skin cancers. *Cancers*, 8(10). <https://doi.org/10.3390/cancers8100090>
- Cohen, L. M. (1995). Lentigo maligna and lentigo maligna melanoma. *Journal of the American Academy of Dermatology*, 33(6), 923–936. [https://doi.org/10.1016/0190-9622\(95\)90282-1](https://doi.org/10.1016/0190-9622(95)90282-1)
- Connolly, K. L., Giordano, C., Dusza, S., Busam, K. J., & Nehal, K. (2019). Follicular involvement is frequent in lentigo maligna: Implications for treatment. *Journal of the American Academy of Dermatology*, 80(2), 532–537. <https://doi.org/10.1016/j.jaad.2018.07.071>
- Connolly, K. L., Nehal, K. S., & Busam, K. J. (2015). Lentigo maligna and lentigo maligna melanoma: contemporary issues in diagnosis and management. *Melanoma Management*, 2(2), 171–178. <https://doi.org/10.2217/mmt.15.3>
- Costa, C., Scalvenzi, M., Ayala, F., Fabbrocini, G., & Monfrecola, G. (2015). How to treat actinic keratosis? An update. *Journal of Dermatological Case Reports*, 9(2), 29–35. <https://doi.org/10.3315/jdcr.2015.1199>
- Criscione, V. D., Weinstock, M. A., Naylor, M. F., Luque, C., Eide, M. J., & Bingham, S. F. (2009). Actinic keratoses: Natural history and risk of malignant transformation in the veterans affairs topical tretinoin chemoprevention trial. *Cancer*, 115(11), 2523–2530. <https://doi.org/10.1002/cncr.24284>
- Cukras, A. R. (2013). On the comparison of diagnosis and management of melanoma between dermatologists and melafind. In *JAMA Dermatology* (Vol. 149, Issue 5, pp. 622–623). American Medical Association. <https://doi.org/10.1001/jamadermatol.2013.3405>



- de Berker, D., McGregor, J. M., Mohd Mustapa, M. F., Exton, L. S., & Hughes, B. R. (2017). British Association of Dermatologists' guidelines for the care of patients with actinic keratosis 2017. *British Journal of Dermatology*, 176(1), 20–43. <https://doi.org/10.1111/bjd.15107>
- Demirtasoglu, M., Ilknur, T., Lebe, B., Kuşku, E., Akarsu, S., & Özkan, Ş. (2006). Evaluation of dermoscopic and histopathologic features and their correlations in pigmented basal cell carcinomas. *Journal of the European Academy of Dermatology and Venerology*, 20(8), 916–920. <https://doi.org/10.1111/j.1468-3083.2006.01620.x>
- DeWane, M. E., Kelsey, A., Oliviero, M., Rabinovitz, H., & Grant-Kels, J. M. (2019). Melanoma on chronically sun-damaged skin: Lentigo maligna and desmoplastic melanoma. *Journal of the American Academy of Dermatology*, 81(3), 823–833. <https://doi.org/10.1016/j.jaad.2019.03.066>
- Dianzani, C., Conforti, C., Giuffrida, R., Corneli, P., di Meo, N., Farinazzo, E., Moret, A., Magaton Rizzi, G., & Zalaudek, I. (2020). Current therapies for actinic keratosis. *International Journal of Dermatology*, 1–8. <https://doi.org/10.1111/ijd.14767>
- Dirschka, T., Ekanayake-Bohlig, S., Dominicus, R., Aschoff, R., Herrera-Ceballos, E., Botella-Estrada, R., Hunfeld, A., Kremser, M., Schmitz, B., Lübbert, H., & Puig, S. (2019). A randomized, intraindividual, non-inferiority, Phase III study comparing daylight photodynamic therapy with BF-200 ALA gel and MAL cream for the treatment of actinic keratosis. *Journal of the European Academy of Dermatology and Venerology*, 33(2), 288–297. <https://doi.org/10.1111/jdv.15185>
- Dirschka, T., Gupta, G., Micali, G., Stockfleth, E., Basset-Séguin, N., Del Marmol, V., Dummer, R., Jemec, G. B. E., Malvehy, J., Peris, K., Puig, S., Stratigos, A. J., Zalaudek, I., & Pellacani, G. (2017). Real-world approach to actinic keratosis management: practical treatment algorithm for office-based dermatology. *Journal of Dermatological Treatment*, 28(5), 431–442. <https://doi.org/10.1080/09546634.2016.1254328>
- Dirschka, T., Pellacani, G., Micali, G., Malvehy, J., Stratigos, A. J., Casari, A., Schmitz, L., Gupta, G., Panagiotopoulos, A., Hasapi, V., Befon, A., Potouridou, I., Polydorou, D., Kousta, F., Polychronaki, E., Kyriazopoulou, M., Kosmadaki, M., Stefanaki, I., Soura, E., ... Chatzinasiou, F. (2017). A proposed scoring system for assessing the severity of actinic keratosis on the head: actinic keratosis area and severity index. *Journal of the European Academy of Dermatology and Venerology*, 31(8), 1295–1302. <https://doi.org/10.1111/jdv.14267>
- Dirschka, T., Radny, P., Dominicus, R., Mensing, H., Brüning, H., Jenne, L., Karl, L., Sebastian, M., Oster-Schmidt, C., Klövekorn, W., Reinhold, U., Tanner, M., Gröne, D., Deichmann, M., Simon, M., Hübinger, F., Hofbauer, G., Krähn-Senftleben, G., Borrosch, F., ... Szeimies, R. M. (2012). Photodynamic therapy with BF-200 ALA for the treatment of actinic keratosis: Results of a multicentre, randomized, observer-blind phase III study in comparison with a registered methyl-5-aminolaevulinate cream and placebo. *British Journal of Dermatology*, 166(1), 137–146. <https://doi.org/10.1111/j.1365-2133.2011.10613.x>
- Dirschka, T., Radny, P., Dominicus, R., Mensing, H., Brüning, H., Jenne, L., Karl, L., Sebastian, M., Oster-Schmidt, C., Klövekorn, W., Reinhold, U., Tanner, M., Gröne, D., Deichmann, M., Simon, M., Hübinger, F., Hofbauer, G., Krähn-Senftleben, G., Borrosch, F., ... Szeimies, R. M. (2013). Long-term (6 and 12 months) follow-up of two prospective, randomized, controlled phase III trials of photodynamic therapy with BF-200 ALA and methyl aminolaevulinate for the treatment of actinic keratosis. *British Journal of Dermatology*, 168(4), 825–836. <https://doi.org/10.1111/bjd.12158>

- Dodson, J. M., DeSpain, J., Hewett, J. E., & Clark, D. P. (1991). Malignant Potential of Actinic Keratoses and the Controversy Over Treatment: A Patient-Oriented Perspective. *Archives of Dermatology*, 127(7), 1029–1031. <https://doi.org/10.1001/archderm.1991.01680060103013>
- Donigan, J. M., Hyde, M. A., Goldgar, D. E., Hadley, M. L., Bowling, M., & Bowen, G. M. (2018). Rate of recurrence of lentigo maligna treated with off-label neoadjuvant topical imiquimod, 5%, cream prior to conservatively staged excision. *JAMA Dermatology*, 154(8), 885–889. <https://doi.org/10.1001/jamadermatol.2018.0530>
- Dougherty, T. J., Kaufman, J. E., Goldfarb, A., Weishaupt, K. R., Boyle, D., & Mittleman, A. (1978). Photoradiation Therapy for the Treatment of Malignant Tumors. *Cancer Research*, 38(8), 2628–2635.
- Dréno, B., Cerio, R., Dirschka, T., Figueras Nart, I., Lear, J. T., Peris, K., Ruiz de Casas, A., Kaleci, S., & Pellacani, G. (2017). A novel actinic keratosis field assessment scale for grading actinic keratosis disease severity. *Acta Dermato-Venereologica*, 97(9), 1108–1113. <https://doi.org/10.2340/00015555-2710>
- Eder, J., Prillinger, K., Korn, A., Geroldinger, A., & Trautinger, F. (2014). Prevalence of actinic keratosis among dermatology outpatients in Austria. *British Journal of Dermatology*, 171(6), 1415–1421. <https://doi.org/10.1111/bjd.13132>
- Elbaum, M., Kopf, A. W., Rabinovitz, H. S., Langley, R. G. B., Kamino, H., Mihm, M. C., Sober, A. J., Peck, G. L., Bogdan, A., Gutkowitz-Krusin, D., Greenebaum, M., Keem, S., Oliviero, M., & Wang, S. (2001). Automatic differentiation of melanoma from melanocytic nevi with multispectral digital dermoscopy: A feasibility study. *Journal of the American Academy of Dermatology*, 44(2), 207–218. <https://doi.org/10.1067/mjd.2001.110395>
- Elder, D. E., Bastian, B. C., Cree, I. A., Massi, D., & Scolyer, R. A. (2020). The 2018 World Health Organization classification of cutaneous, mucosal, and uveal melanoma detailed analysis of 9 distinct subtypes defined by their evolutionary pathway. In *Archives of Pathology and Laboratory Medicine* (Vol. 144, Issue 4, pp. 500–522). College of American Pathologists. <https://doi.org/10.5858/arpa.2019-0561-RA>
- Emery, J. D., Hunter, J., Hall, P. N., Watson, A. J., Moncrieff, M., & Walter, F. M. (2010). Accuracy of SIAscopy for pigmented skin lesions encountered in primary care: Development and validation of a new diagnostic algorithm. *BMC Dermatology*, 10(9). <http://www.embase.com/search/results?subaction=viewrecord&from=export&id=L51088555%5Cnhttp://www.biomedcentral.com/1471-5945/10/9%5Cnhttp://dx.doi.org/10.1186/1471-5945-10-9%5Cnhttp://sfx.library.uu.nl/utrecht?sid=EMBASE&issn=14715945&id=doi:10.1186%2F1471>
- Erickson, C., & Miller, S. J. (2010). Treatment options in melanoma in situ: Topical and radiation therapy, excision and Mohs surgery. *International Journal of Dermatology*, 49(5), 482–491. <https://doi.org/10.1111/j.1365-4632.2010.04423.x>
- Ericson, M. B., Wennberg, A. M., & Larkö, O. (2008). Review of photodynamic therapy in actinic keratosis and basal cell carcinoma. *Therapeutics and Clinical Risk Management*, 4(1), 1–9. <https://doi.org/10.2147/tcrm.s1769>
- Eriksson, T., & Tinghög, G. (2015). Societal cost of skin cancer in Sweden in 2011. *Acta Dermato-Venereologica*, 95(3), 347–348. <https://doi.org/10.2340/00015555-1938>
- Esteva, A., Kuprel, B., Novoa, R. A., Ko, J., Swetter, S. M., Blau, H. M., & Thrun, S. (2017). Dermatologist-level classification of skin cancer with deep neural networks. *Nature*, 542(7639), 115–118. <https://doi.org/10.1038/nature21056>

- Fargnoli, M. C., Altomare, G., Benati, E., Borgia, F., Broganelli, P., Carbone, A., Chimenti, S., Donato, S., Girolomoni, G., Micali, G., Moggio, E., Parodi, A., Piaserico, S., Pistone, G., Potenza, C., Puviani, M., Raucci, M., Vaccari, S., Veglio, S., ... Peris, K. (2017). Prevalence and risk factors of actinic keratosis in patients attending Italian dermatology clinics. *European Journal of Dermatology*, 27(6), 599–608. <https://doi.org/10.1684/ejd.2017.3126>
- Ferrara, F., Lacava, R., Barisani, A., Messori, S., Patrizi, A., Bardazzi, F., & Vaccari, S. (2019). Combined CO2 laser and photodynamic therapy enhances the efficacy of treatment of basal cell carcinomas. *JDDG - Journal of the German Society of Dermatology*, 17(12), 1251–1256. <https://doi.org/10.1111/ddg.14004>
- Fiechter, S., Skaria, A., Nievergelt, H., Anex, R., Borradori, L., & Parmentier, L. (2012). Facial basal cell carcinomas recurring after photodynamic therapy: A retrospective analysis of histological subtypes. *Dermatology*, 224(4), 346–351. <https://doi.org/10.1159/000339335>
- Figueras Nart, I., Cerio, R., Dirschka, T., Dréno, B., Lear, J. T., Pellacani, G., Peris, K., & Ruiz de Casas, A. (2018). Defining the actinic keratosis field: a literature review and discussion. *Journal of the European Academy of Dermatology and Venereology*, 32(4), 544–563. <https://doi.org/10.1111/jdv.14652>
- Fink, C., Blum, A., Buhl, T., Mitteldorf, C., Hofmann-Wellenhof, R., Deinlein, T., Stolz, W., Trennheuser, L., Cussigh, C., Deltgen, D., Winkler, J. K., Toberer, F., Enk, A., Rosenberger, A., & Haenssle, H. A. (2020). Diagnostic performance of a deep learning convolutional neural network in the differentiation of combined naevi and melanomas. *Journal of the European Academy of Dermatology and Venereology*, 34(6), 1355–1361. <https://doi.org/10.1111/jdv.16165>
- Fink, C., & Haenssle, H. A. (2017). Non-invasive tools for the diagnosis of cutaneous melanoma. *Skin Research and Technology*, 23(3), 261–271. <https://doi.org/10.1111/srt.12350>
- Fink, C., Jaeger, C., Jaeger, K., & Haenssle, H. A. (2017). Diagnostic performance of the MelaFind device in a real-life clinical setting. *JDDG - Journal of the German Society of Dermatology*, 15(4), 414–419. <https://doi.org/10.1111/ddg.13220>
- Fitzmaurice, S., & Eisen, D. B. (2016). Daylight photodynamic therapy: What is known and what is yet to be determined. *Dermatologic Surgery*, 42(3), 286–295. <https://doi.org/10.1097/DSS.0000000000000633>
- Fleming, C. J., Bryden, A., Evans, R. S., Dawe, S. H., & Ibbotson, S. H. (2004). A pilot study of treatment of lentigo maligna with 5% imiquimod cream. *British Journal of Dermatology*, 151(2), 485–488. <https://doi.org/10.1111/j.1365-2133.2004.05983.x>
- Flohil, S. C., Van Der Leest, R. J. T., Dowlatsahi, E. A., Hofman, A., De Vries, E., & Nijsten, T. (2013). Prevalence of actinic keratosis and its risk factors in the general population: The rotterdam study. *Journal of Investigative Dermatology*, 133(8), 1971–1978. <https://doi.org/10.1038/jid.2013.134>
- Florell, S. R., Boucher, K. M., Leachman, S. A., Azmi, F., Harris, R. M., Malone, J. C., Martignoni, G., Bowen, G. M., Gerwels, J. W., & Hood, A. F. (2003). Histopathologic recognition of involved margins of lentigo maligna excised by staged excision an interobserver comparison study. *Archives of Dermatology*, 139(5), 595–604. <https://doi.org/10.1001/archderm.139.5.595>
- Fogarty, G. B., Hong, A., Scolyer, R. A., Lin, E., Haydu, L., Guitera, P., & Thompson, J. (2014). Radiotherapy for lentigo maligna: A literature review and recommendations

- for treatment. *British Journal of Dermatology*, 170(1), 52–58. <https://doi.org/10.1111/bjd.12611>
- Franzen, L., & Windbergs, M. (2015). Applications of Raman spectroscopy in skin research - From skin physiology and diagnosis up to risk assessment and dermal drug delivery. *Advanced Drug Delivery Reviews*, 89, 91–104. <https://doi.org/10.1016/j.addr.2015.04.002>
- Fritsch, C., Homey, B., Stahl, W., Lehmann, P., Ruzicka, T., & Sies, H. (1998). Preferential Relative Porphyrin Enrichment in Solar Keratoses upon Topical Application of  $\delta$ -Aminolevulinic Acid Methylene Ester. *Photochemistry and Photobiology*, 68(2), 218. [https://doi.org/10.1562/0031-8655\(1998\)068<0218:prpeis>2.3.co;2](https://doi.org/10.1562/0031-8655(1998)068<0218:prpeis>2.3.co;2)
- Frost, C. A., & Green, A. C. (1994). Epidemiology of solar keratoses. In *British Journal of Dermatology* (Vol. 131, Issue 4, pp. 455–464). <https://doi.org/10.1111/j.1365-2133.1994.tb08544.x>
- Gambichler, T., Jaedicke, V., & Terras, S. (2011). Optical coherence tomography in dermatology: Technical and clinical aspects. In *Archives of Dermatological Research* (Vol. 303, Issue 7, pp. 457–473). *Arch Dermatol Res*. <https://doi.org/10.1007/s00403-011-1152-x>
- Gaudy-Marqueste, C., Madjlessi, N., Guillot, B., Avril, M. F., & Grob, J. J. (2009). Risk factors in elderly people for lentigo maligna compared with other melanomas: A double case-control study. *Archives of Dermatology*, 145(4), 418–423. <https://doi.org/10.1001/archdermatol.2009.1>
- Gaullier, J. M., Berg, K., Peng, Q., Anholt, H., Selbo, P. K., Ma, L. W., & Moan, J. (1997). Use of 5-aminolevulinic acid esters to improve photodynamic therapy on cells in culture. *Cancer Research*, 57(8), 1481–1486.
- Genouw, E., Verheire, B., Ongenaes, K., De Schepper, S., Creyten, D., Verhaeghe, E., & Boone, B. (2018). Laser-assisted photodynamic therapy for superficial basal cell carcinoma and Bowen's disease: a randomized inpatient comparison between a continuous and a fractional ablative CO2 laser mode. *Journal of the European Academy of Dermatology and Venereology*, 32(11), 1897–1905. <https://doi.org/10.1111/jdv.14989>
- Gerger, A., Koller, S., Kern, T., Massone, C., Steiger, K., Richtig, E., Kerl, H., & Smolle, J. (2005). Diagnostic applicability of in vivo confocal laser scanning microscopy in melanocytic skin tumors. In *Journal of Investigative Dermatology* (Vol. 124, Issue 3, pp. 493–498). Blackwell Publishing Inc. <https://doi.org/10.1111/j.0022-202X.2004.23569.x>
- Glud, M., Gniadecki, R., & Drzewiecki, K. T. (2009). Spectrophotometric intracutaneous analysis versus dermoscopy for the diagnosis of pigmented skin lesions: prospective, double-blind study in a secondary reference centre. *Melanoma Research*, 19(3), 176–179. <https://doi.org/10.1097/CMR.0b013e328322fe5f>
- Gniadecka, M., Philipsen, P. A., Sigurdsson, S., Wessel, S., Nielsen, O. F., Christensen, D. H., Hercogova, J., Rossen, K., Thomsen, H. K., Gniadecki, R., Hansen, L. K., & Wulf, H. C. (2004). Melanoma Diagnosis by Raman Spectroscopy and Neural Networks: Structure Alterations in Proteins and Lipids in Intact Cancer Tissue. *Journal of Investigative Dermatology*, 122(2), 443–449. <https://doi.org/10.1046/j.0022-202X.2004.22208.x>
- Gollnick, S. O., Evans, S. S., Baumann, H., Owczarczak, B., Maier, P., Vaughan, L., Wang, W. C., Unger, E., & Henderson, B. W. (2003). Role of cytokines in photodynamic therapy-induced local and systemic inflammation. *British Journal of Cancer*, 88(11), 1772–1779. <https://doi.org/10.1038/sj.bjc.6600864>

- Goon, P. K. C., Greenberg, D. C., Igali, L., & Levell, N. J. (2016). Squamous cell carcinoma of the skin has more than doubled over the last decade in the UK. *Acta Dermato-Venerologica*, *96*(6), 820–821. <https://doi.org/10.2340/00015555-2310>
- Green, A., & Battistutta, D. (1990). Incidence and determinants of skin cancer in a high-risk australian population. *International Journal of Cancer*, *46*(3), 356–361. <https://doi.org/10.1002/ijc.2910460303>
- Green, A., Williams, G., Neale, R., Hart, V., Leslie, D., Parsons, P., Marks, G. C., Gaffney, P., Battistutta, D., Frost, C., Lang, C., & Russell, A. (1999). Daily sunscreen application and betacarotene supplementation in prevention of basal-cell and squamous-cell carcinomas of the skin: A randomised controlled trial. *Lancet*, *354*(9180), 723–729. [https://doi.org/10.1016/S0140-6736\(98\)12168-2](https://doi.org/10.1016/S0140-6736(98)12168-2)
- Greveling, K., Wakkee, M., Nijsten, T., van den Bos, R. R., & Hollestein, L. M. (2016). Epidemiology of Lentigo Maligna and Lentigo Maligna Melanoma in the Netherlands, 1989–2013. *Journal of Investigative Dermatology*, *136*(10), 1955–1960. <https://doi.org/10.1016/j.jid.2016.06.014>
- Griffin, L. L., & Lear, J. T. (2016). Photodynamic therapy and non-melanoma skin cancer. *Cancers*, *8*(10). <https://doi.org/10.3390/cancers8100098>
- Guitera, P., Menzies, S. W., Argenziano, G., Longo, C., Losi, A., Drummond, M., Scolyer, R. A., & Pellacani, G. (2016). Dermoscopy and in vivo confocal microscopy are complementary techniques for diagnosis of difficult amelanotic and light-coloured skin lesions. *British Journal of Dermatology*, *175*(6), 1311–1319. <https://doi.org/10.1111/bjd.14749>
- Guitera, P., Pellacani, G., Crotty, K. A., Scolyer, R. A., Li, L. X. L., Bassoli, S., Vinceti, M., Rabinovitz, H., Longo, C., & Menzies, S. W. (2010). The impact of in vivo reflectance confocal microscopy on the diagnostic accuracy of lentigo maligna and equivocal pigmented and nonpigmented macules of the face. *Journal of Investigative Dermatology*, *130*(8), 2080–2091. <https://doi.org/10.1038/jid.2010.84>
- Gupta, A. K., & Paquet, M. (2013). Network meta-analysis of the outcome “participant complete clearance” in nonimmunosuppressed participants of eight interventions for actinic keratosis: A follow-up on a Cochrane review. *British Journal of Dermatology*, *169*(2), 250–259. <https://doi.org/10.1111/bjd.12343>
- Gupta, A. K., Paquet, M., Villanueva, E., & Brintnell, W. (2012). Interventions for actinic keratoses. *Cochrane Database of Systematic Reviews*. <https://doi.org/10.1002/14651858.cd004415.pub2>
- Gutkowitz-Krusin, D., Elbaum, M., Jacobs, A., Keem, S., Kopf, A. W., Kamino, H., Wang, S., Rubin, P., Rabinovitz, H., & Oliviero, M. (2000). Precision of automatic measurements of pigmented skin lesion parameters with a MelaFind™ multispectral digital dermoscope. *Melanoma Research*, *10*(6), 563–570. <https://doi.org/10.1097/00008390-200012000-00008>
- Haak, C. S., Farinelli, W. A., Tam, J., Doukas, A. G., Anderson, R. R., & Høedersdal, M. (2012). Fractional laser-assisted delivery of methyl aminolevulinate: Impact of laser channel depth and incubation time. *Lasers in Surgery and Medicine*, *44*(10), 787–795. <https://doi.org/10.1002/lsm.22102>
- Haak, C. S., Togsverd-Bo, K., Thaysen-Petersen, D., Wulf, H. C., Paasch, U., Anderson, R. R., & Høedersdal, M. (2015). Fractional laser-mediated photodynamic therapy of high-risk basal cell carcinomas - A randomized clinical trial. *British Journal of Dermatology*, *172*(1), 215–222. <https://doi.org/10.1111/bjd.13166>

- Hacioglu, S., Saricaoglu, H., Baskan, E. B., Uner, S. I., Aydogan, K., & Tunalı, S. (2013). The value of spectrophotometric intracutaneous analysis in the noninvasive diagnosis of nonmelanoma skin cancers. *Clinical and Experimental Dermatology*, 38(5), 464–469. <https://doi.org/10.1111/j.1365-2230.2012.04460.x>
- Hadley, G., Derry, S., & Moore, R. A. (2006). Imiquimod for actinic keratosis: Systematic review and meta-analysis. *Journal of Investigative Dermatology*, 126(6), 1251–1255. <https://doi.org/10.1038/sj.jid.5700264>
- Hædersdal, M., Erendsson, A. M., Paasch, U., & Anderson, R. R. (2016). Translational medicine in the field of ablative fractional laser (AFXL)-assisted drug delivery: A critical review from basics to current clinical status. *Journal of the American Academy of Dermatology*, 74(5), 981–1004. <https://doi.org/10.1016/j.jaad.2015.12.008>
- Hædersdal, M., Katsnelson, J., Sakamoto, F. H., Farinelli, W. A., Doukas, A. G., Tam, J., & Anderson, R. R. (2011). Enhanced uptake and photoactivation of topical methyl aminolevulinate after fractional CO<sub>2</sub> laser pretreatment. *Lasers in Surgery and Medicine*, 43(8), 804–813. <https://doi.org/10.1002/lsm.21096>
- Hædersdal, M., Sakamoto, F. H., Farinelli, W. A., Doukas, A. G., Tam, J., & Anderson, R. R. (2010). Fractional CO<sub>2</sub> laser-assisted drug delivery. *Lasers in Surgery and Medicine*, 42(2), 113–122. <https://doi.org/10.1002/lsm.20860>
- Hædersdal, M., Sakamoto, F. H., Farinelli, W. A., Doukas, A. G., Tam, J., & Anderson, R. R. (2014). Pretreatment with ablative fractional laser changes kinetics and biodistribution of topical 5-aminolevulinic acid (ALA) and methyl aminolevulinate (MAL). *Lasers in Surgery and Medicine*, 46(6), 462–469. <https://doi.org/10.1002/lsm.22259>
- Haenssle, H. A., Fink, C., Schneiderbauer, R., Toberer, F., Buhl, T., Blum, A., Kalloo, A., Ben Hadj Hassen, A., Thomas, L., Enk, A., Uhlmann, L., Alt, C., Arenbergerova, M., Bakos, R., Baltzer, A., Bertlich, I., Blum, A., Bokor-Billmann, T., Bowling, J., ... Zalaudek, I. (2018). Man against Machine: Diagnostic performance of a deep learning convolutional neural network for dermoscopic melanoma recognition in comparison to 58 dermatologists. *Annals of Oncology*, 29(8), 1836–1842. <https://doi.org/10.1093/annonc/mdy166>
- Halicek, M., Little, J. V., Wang, X., Chen, A. Y., & Fei, B. (2019). Optical biopsy of head and neck cancer using hyperspectral imaging and convolutional neural networks. *Journal of Biomedical Optics*, 24(03), 1. <https://doi.org/10.1117/1.jbo.24.3.036007>
- Halicek, M., Little, J. V., Wang, X., Patel, M. R., Griffith, C. C., Chen, A. Y., & Fei, B. (2018). *Tumor margin classification of head and neck cancer using hyperspectral imaging and convolutional neural networks*. 4. <https://doi.org/10.1117/12.2293167>
- Haniffa, M. A., Lloyd, J. J., & Lawrence, C. M. (2007). The use of a spectrophotometric intracutaneous analysis device in the real-time diagnosis of melanoma in the setting of a melanoma screening clinic. *British Journal of Dermatology*, 156(6), 1350–1352. <https://doi.org/10.1111/j.1365-2133.2007.07932.x>
- Harvey, I., Frankel, S., Marks, R., Shalom, D., & Nolan-Farrell, M. (1996). Non-melanoma skin cancer and solar keratoses. I. Methods and descriptive results of the South Wales skin cancer study. *British Journal of Cancer*, 74(8), 1302–1307. <https://doi.org/10.1038/bjc.1996.534>
- Hawker, G. A., Mian, S., Kendzerska, T., & French, M. (2011). Measures of adult pain: Visual Analog Scale for Pain (VAS Pain), Numeric Rating Scale for Pain (NRS Pain), McGill Pain Questionnaire (MPQ), Short-Form McGill Pain Questionnaire (SF-MPQ),

- Chronic Pain Grade Scale (CPGS), Short Form-36 Bodily Pain Scale (SF. *Arthritis Care and Research*, 63(SUPPL. 11), 240–252. <https://doi.org/10.1002/acr.20543>
- Hazan, C., Dusza, S. W., Delgado, R., Busam, K. J., Halpern, A. C., & Nehal, K. S. (2008). Staged excision for lentigo maligna and lentigo maligna melanoma: A retrospective analysis of 117 cases. *Journal of the American Academy of Dermatology*, 58(1), 142–148. <https://doi.org/10.1016/j.jaad.2007.09.023>
- Heaphy, M. R., & Ackerman, A. B. (2000). The nature of solar keratosis: A critical review in historical perspective. *Journal of the American Academy of Dermatology*, 43(1), 138–150. <https://doi.org/10.1067/mjd.2000.107497>
- Hedblad, M. A., & Mallbris, L. (2012). Grenz ray treatment of lentigo maligna and early lentigo maligna melanoma. *Journal of the American Academy of Dermatology*, 67(1), 60–68. <https://doi.org/10.1016/j.jaad.2011.06.029>
- Heppt, M. V., Leiter, U., Steeb, T., Amaral, T., Bauer, A., Becker, J. C., Breitbart, E., Breuninger, H., Diepgen, T., Dirschka, T., Eigentler, T., Flaig, M., Follmann, M., Fritz, K., Greinert, R., Gutzmer, R., Hillen, U., Ihrler, S., John, S. M., ... Garbe, C. (2020). *S3 guideline for actinic keratosis and cutaneous squamous cell carcinoma-short version, part 1: diagnosis, interventions for actinic keratoses, care structures and quality-of-care indicators*. <https://doi.org/10.1111/ddg.14048>
- Heppt, M. V., Steeb, T., Niesert, A. C., Zacher, M., Leiter, U., Garbe, C., & Berking, C. (2019). Local interventions for actinic keratosis in organ transplant recipients: a systematic review. *British Journal of Dermatology*, 180(1), 43–50. <https://doi.org/10.1111/bjd.17148>
- Hosking, A. M., Coakley, B. J., Chang, D., Talebi-Liasi, F., Lish, S., Lee, S. W., Zong, A. M., Moore, I., Browning, J., Jacques, S. L., Krueger, J. G., Kelly, K. M., Linden, K. G., & Gareau, D. S. (2019). Hyperspectral imaging in automated digital dermoscopy screening for melanoma. *Lasers in Surgery and Medicine*, 51(3), 214–222. <https://doi.org/10.1002/lsm.23055>
- Huerta-Brogeras, M., Olmos, O., Borbujo, J., Hernández-Núñez, A., Castaño, E., Romero-Maté, A., Martínez-Sánchez, D., & Martínez-Morán, C. (2012). Validation of dermoscopy as a real-time noninvasive diagnostic imaging technique for actinic keratosis. *Archives of Dermatology*, 148(10), 1159–1164. <https://doi.org/10.1001/archdermatol.2012.1060>
- Ibbotson, S. H., Stones, R., Bowling, J., Campbell, S., Kownacki, S., Sivaramakrishnan, M., Valentine, R., & Morton, C. A. (2017). A consensus on the use of daylight photodynamic therapy in the UK. *Journal of Dermatological Treatment*, 28(4), 360–367. <https://doi.org/10.1080/09546634.2016.1240863>
- Ibbotson, S. H., Wong, T. H., Morton, C. A., Collier, N. J., Haylett, A., McKenna, K. E., Mallipeddi, R., Moseley, H., Rhodes, L. E., Seukeran, D. C., Ward, K. A., Mohd Mustapa, M. F., & Exton, L. S. (2019). Adverse effects of topical photodynamic therapy: a consensus review and approach to management. *British Journal of Dermatology*, 180(4), 715–729. <https://doi.org/10.1111/bjd.17131>
- Inoue, K. (2017). 5-Aminolevulinic acid-mediated photodynamic therapy for bladder cancer. *International Journal of Urology*, 24(2), 97–101. <https://doi.org/10.1111/iju.13291>
- Jansen, M. H. E., Kessels, J. P. H. M., Nelemans, P. J., Kouloubis, N., Arits, A. H. M. M., Van Pelt, H. P. A., Quaedvlieg, P. J. F., Essers, B. A. B., Steijlen, P. M., Kelleners-Smeets, N. W. J., & Mosterd, K. (2019). Randomized trial of four treatment approaches for actinic keratosis. *New England Journal of Medicine*, 380(10), 935–946. <https://doi.org/10.1056/NEJMoa1811850>

- Juhász, M. L. W., & Marmur, E. S. (2015). Reviewing Challenges in the Diagnosis and Treatment of Lentigo Maligna and Lentigo-Maligna Melanoma. *Rare Cancers and Therapy*, 3(1–2), 133–145. <https://doi.org/10.1007/s40487-015-0012-9>
- Karam, A., Simon, M., Lemasson, G., & Misery, L. (2013). The use of photodynamic therapy in the treatment of lentigo maligna. *Pigment Cell and Melanoma Research*, 26(2), 275–277. <https://doi.org/10.1111/pcmr.12044>
- Karrer, S., Aschoff, R. A. G., Dominicus, R., Krähn-Senftleben, G., Gauglitz, G. G., Zarzour, A., Kerrouche, N., Chavda, R., & Szeimies, R. M. (2019). Methyl aminolevulinate daylight photodynamic therapy applied at home for non-hyperkeratotic actinic keratosis of the face or scalp: an open, interventional study conducted in Germany. *Journal of the European Academy of Dermatology and Venereology*, 33(4), 661–666. <https://doi.org/10.1111/jdv.15422>
- Kasprzak, J. M., & Xu, Y. G. (2015). Diagnosis and management of lentigo maligna: A review. *Drugs in Context*, 4, 1–16. <https://doi.org/10.7573/dic.212281>
- Kellner, C., Bauriedl, S., Hollstein, S., & Reinhold, U. (2015). Simulated-daylight photodynamic therapy with BF-200 aminolaevulinic acid for actinic keratosis: Assessment of the efficacy and tolerability in a retrospective study. *British Journal of Dermatology*, 172(4), 1146–1148. <https://doi.org/10.1111/bjd.13420>
- Kennedy, J. C., Pottier, R. H., & Pross, D. C. (1990). Photodynamic therapy with endogenous protoporphyrin IX: basic principles and present clinical experience. *Journal of Photochemistry and Photobiology. B, Biology*, 6(1–2), 143–148. [https://doi.org/10.1016/1011-1344\(90\)85083-9](https://doi.org/10.1016/1011-1344(90)85083-9)
- Kim, H. J., & Song, K. H. (2018). Ablative fractional laser–assisted photodynamic therapy provides superior long-term efficacy compared with standard methyl aminolevulinate photodynamic therapy for lower extremity Bowen disease. *Journal of the American Academy of Dermatology*, 79(5), 860–868. <https://doi.org/10.1016/j.jaad.2018.05.034>
- Kimyai-Asadi, A., Katz, T., Goldberg, L. H., Ayala, G. B., Wang, S. Q., Vujevich, J. J., & Jih, M. H. (2007). Margin involvement after the excision of melanoma in situ: The need for complete en face examination of the surgical margins. *Dermatologic Surgery*, 33(12), 1434–1441. <https://doi.org/10.1111/j.1524-4725.2007.33313.x>
- Klein, A., Karrer, S., Horner, C., Werner, A., Heinlin, J., Zeman, F., Koller, M., Landthaler, M., Szeimies, R. M., Gruber, M., Graf, B., Hansen, E., & Kerscher, C. (2015). Comparing cold-air analgesia, systemically administered analgesia and scalp nerve blocks for pain management during photodynamic therapy for actinic keratosis of the scalp presenting as field cancerization: A randomized controlled trial. *British Journal of Dermatology*, 173(1), 192–200. <https://doi.org/10.1111/bjd.13547>
- Ko, D. Y., Jeon, S. Y., Kim, K. H., & Song, K. H. (2014). Fractional erbium: YAG laser-assisted photodynamic therapy for facial actinic keratoses: a randomized, comparative, prospective study. *Journal of the European Academy of Dermatology and Venereology*, 28(11), 1529–1539. <https://doi.org/10.1111/jdv.12334>
- Ko, D. Y., Kim, K. H., & Song, K. H. (2014). A randomized trial comparing methyl aminolaevulinate photodynamic therapy with and without Er:YAG ablative fractional laser treatment in Asian patients with lower extremity Bowen disease: Results from a 12-month follow-up. *British Journal of Dermatology*, 170(1), 165–172. <https://doi.org/10.1111/bjd.12627>
- Kohl, E., Torezan, L., Landthaler, M., & Szeimies, R. M. (2010). Aesthetic effects of topical photodynamic therapy. *Journal of the European Academy of Dermatology and Venereology*, 24(11), 1261–1269. <https://doi.org/10.1111/j.1468-3083.2010.03625.x>



- Kraft, S., & Granter, S. R. (2014). Molecular pathology of skin neoplasms of the head and neck. *Archives of Pathology and Laboratory Medicine*, 138(6), 759–787. <https://doi.org/10.5858/arpa.2013-0157-RA>
- Krawtchenko, N., Roewert-Huber, J., Ulrich, M., Mann, I., Sterry, W., & Stockfleth, E. (2007). A randomised study of topical 5% imiquimod vs. topical 5-fluorouracil vs. cryosurgery in immunocompetent patients with actinic keratoses: A comparison of clinical and histological outcomes including 1-year follow-up. *British Journal of Dermatology*, 157(SUPPL. 2), 34–40. <https://doi.org/10.1111/j.1365-2133.2007.08271.x>
- Kunishige, J. H., Brodland, D. G., & Zitelli, J. A. (2012). Surgical margins for melanoma in situ. *Journal of the American Academy of Dermatology*, 66(3), 438–444. <https://doi.org/10.1016/j.jaad.2011.06.019>
- Kurwa, H. A., Yong-Gee, S. A., Seed, P. T., Markey, A. C., & Barlow, R. J. (1999). A randomized paired comparison of photodynamic therapy and topical 5- fluorouracil in the treatment of actinic keratoses. *Journal of the American Academy of Dermatology*, 41(3), 414–418. [https://doi.org/10.1016/S0190-9622\(99\)70114-3](https://doi.org/10.1016/S0190-9622(99)70114-3)
- Kvaskoff, M., Siskind, V., & Green, A. C. (2012). Risk factors for lentigo maligna melanoma compared with superficial spreading melanoma: A case-control study in Australia. *Archives of Dermatology*, 148(2), 164–170. <https://doi.org/10.1001/archdermatol.2011.291>
- Lacour, J. P., Ulrich, C., Gilaberte, Y., Von Felbert, V., Basset-Seguín, N., Dreno, B., Girard, C., Redondo, P., Serra-Guillen, C., Synnerstad, I., Tarstedt, M., Tsianakas, A., Venema, A. W., Kelleners-Smeets, N., Adamski, H., Perez-García, B., Gerritsen, M. J., Leclerc, S., Kerrouche, N., & Szeimies, R. M. (2015). Daylight photodynamic therapy with methyl aminolevulinic acid cream is effective and nearly painless in treating actinic keratoses: A randomised, investigator-blinded, controlled, phase III study throughout Europe. *Journal of the European Academy of Dermatology and Venereology*, 29(12), 2342–2348. <https://doi.org/10.1111/jdv.13228>
- Lallas, A., Giacomel, J., Argenziano, G., García-García, B., González-Fernández, D., Zalaudek, I., & Vázquez-López, F. (2014). Dermoscopy in general dermatology: Practical tips for the clinician. *British Journal of Dermatology*, 170(3), 514–526. <https://doi.org/10.1111/bjd.12685>
- Lallas, A., Tzellos, T., Kyrgidis, A., Apalla, Z., Zalaudek, I., Karatolias, A., Ferrara, G., Piana, S., Longo, C., Moscarella, E., Stratigos, A., & Argenziano, G. (2014). Accuracy of dermoscopic criteria for discriminating superficial from other subtypes of basal cell carcinoma. *Journal of the American Academy of Dermatology*, 70(2), 303–311. <https://doi.org/10.1016/j.jaad.2013.10.003>
- Lanoue, J., Do, T., & Goldenberg, G. (2015). Therapies for actinic keratosis with a focus on cosmetic outcomes. *Cutis*, 96(3).
- Lawrence, N., Cox, S. E., Cockerell, C. J., Freeman, R. G., & Cruz, P. D. (1995). A Comparison of the Efficacy and Safety of Jessner's Solution and 35% Trichloroacetic Acid vs 5% Fluorouracil in the Treatment of Widespread Facial Actinic Keratoses. *Archives of Dermatology*, 131(2), 176–181. <https://doi.org/10.1001/archderm.1995.01690140060009>
- Lebwohl, M. G., Rosen, T., & Stockfleth, E. (2010). The role of human papillomavirus in common skin conditions: current viewpoints and therapeutic options. *Cutis*, 86(5), suppl 1-11; quiz suppl 12. <http://www.ncbi.nlm.nih.gov/pubmed/21214125>

- Lebwohl, M. G., Shumack, S., Gold, L. S., Melgaard, A., Larsson, T., & Tyring, S. K. (2013). Long-term follow-up study of ingenol mebutate gel for the treatment of actinic keratoses. *JAMA Dermatology*, 149(6), 666–670. <https://doi.org/10.1001/jamadermatol.2013.2766>
- Lebwohl, M. G., Swanson, N., Anderson, L. L., Melgaard, A., Xu, Z., & Berman, B. (2012). Ingenol mebutate gel for actinic keratosis. *New England Journal of Medicine*, 366(11), 1010–1019. <https://doi.org/10.1056/NEJMoa1111170>
- Lee, J. H., Choi, J. W., & Kim, Y. S. (2011). Frequencies of BRAF and NRAS mutations are different in histological types and sites of origin of cutaneous melanoma: A meta-analysis. *British Journal of Dermatology*, 164(4), 776–784. <https://doi.org/10.1111/j.1365-2133.2010.10185.x>
- Leffell, D. J. (2000). The scientific basis of skin cancer. *Journal of the American Academy of Dermatology*, 42(1 Pt 2), 18–22. <https://doi.org/10.1067/mjd.2000.103340>
- Leon, R., Martinez-Vega, B., Fabelo, H., Ortega, S., Melian, V., Castaño, I., Carretero, G., Almeida, P., Garcia, A., Quevedo, E., Hernandez, J. A., Clavo, B., & M. Callico, G. (2020). Non-Invasive Skin Cancer Diagnosis Using Hyperspectral Imaging for In-Situ Clinical Support. *Journal of Clinical Medicine*, 9(6), 1662. <https://doi.org/10.3390/jcm9061662>
- Lerche, C. M., Heerfordt, I. M., Heydenreich, J., & Wulf, H. C. (2016). Alternatives to outdoor daylight illumination for photodynamic therapy—use of greenhouses and artificial light sources. *International Journal of Molecular Sciences*, 17(3). <https://doi.org/10.3390/ijms17030309>
- Lieber, C. A., Majumder, S. K., Ellis, D. L., Billheimer, D. D., & Mahadevan-Jansen, A. (2008). In vivo nonmelanoma skin cancer diagnosis using Raman microspectroscopy. *Lasers in Surgery and Medicine*, 40(7), 461–467. <https://doi.org/10.1002/lsm.20653>
- Lim, L., Nichols, B., Migden, M. R., Rajaram, N., Reichenberg, J. S., Markey, M. K., Ross, M. I., & Tunnell, J. W. (2014). Clinical study of noninvasive in vivo melanoma and nonmelanoma skin cancers using multimodal spectral diagnosis. *Journal of Biomedical Optics*, 19(11), 117003. <https://doi.org/10.1117/1.jbo.19.11.117003>
- Lippert, J., Šmucler, R., & Vlk, M. (2013). Fractional carbon dioxide laser improves nodular basal cell carcinoma treatment with photodynamic therapy with methyl 5-aminolevulinate. *Dermatologic Surgery*, 39(8), 1202–1208. <https://doi.org/10.1111/dsu.12242>
- Longo, C., Lallas, A., Kyrgidis, A., Rabinovitz, H., Moscarella, E., Ciardo, S., Zalaudek, I., Oliviero, M., Losi, A., Gonzalez, S., Guitera, P., Piana, S., Argenziano, G., & Pellacani, G. (2014). Classifying distinct basal cell carcinoma subtype by means of dermatoscopy and reflectance confocal microscopy. *Journal of the American Academy of Dermatology*, 71(4), 716-724.e1. <https://doi.org/10.1016/j.jaad.2014.04.067>
- Lu, G., & Fei, B. (2014). Medical hyperspectral imaging: a review. *Journal of Biomedical Optics*, 19(1), 010901. <https://doi.org/10.1117/1.jbo.19.1.010901>
- Lui, H., Zhao, J., McLean, D., & Zeng, H. (2012). Real-time raman spectroscopy for in vivo skin cancer diagnosis. *Cancer Research*, 72(10), 2491–2500. <https://doi.org/10.1158/0008-5472.CAN-11-4061>
- MacLellan, A. N., Price, E. L., Publicover-Brouwer, P., Matheson, K., Ly, T. Y., Pasternak, S., Walsh, N. M., Gallant, C. J., Oakley, A., Hull, P. R., & Langley, R. G. (2020). The Use of Non-Invasive Imaging Techniques in the Diagnosis of Melanoma: A Prospective Diagnostic Accuracy Study. *Journal of the American Academy of Dermatology*. <https://doi.org/10.1016/j.jaad.2020.04.019>

- Magro, C. M., Yang, S. E., Zippin, J. H., & Zembowicz, A. (2012). Expression of soluble adenylyl cyclase in lentigo maligna use of immunohistochemistry with anti-soluble adenylyl cyclase antibody (R21) in diagnosis of lentigo maligna and assessment of margins. *Archives of Pathology and Laboratory Medicine*, *136*(12), 1558–1564. <https://doi.org/10.5858/arpa.2011-0617-OA>
- Maier, T., Braun-Falco, M., Laubender, R. P., Ruzicka, T., & Berking, C. (2013). Actinic keratosis in the en-face and slice imaging mode of high-definition optical coherence tomography and comparison with histology. *British Journal of Dermatology*, *168*(1), 120–128. <https://doi.org/10.1111/j.1365-2133.2012.11202.x>
- Maisch, T., Santarelli, F., Schreml, S., Babilas, P., & Szeimies, R. M. (2010). Fluorescence induction of protoporphyrin IX by a new 5-aminolevulinic acid nanoemulsion used for photodynamic therapy in a full-thickness ex vivo skin model. *Experimental Dermatology*, *19*(8), 302–305. <https://doi.org/10.1111/j.1600-0625.2009.01001.x>
- Malvey, J., & Pellacani, G. (2017). Dermoscopy, confocal microscopy and other non-invasive tools for the diagnosis of non-melanoma skin cancers and other skin conditions. *Acta Dermato-Venerologica*, *97*, 22–30. <https://doi.org/10.2340/00015555-2720>
- Manstein, D., Herron, G. S., Sink, R. K., Tanner, H., & Anderson, R. R. (2004). Fractional photothermolysis: A new concept for cutaneous remodeling using microscopic patterns of thermal injury. *Lasers in Surgery and Medicine*, *34*(5), 426–438. <https://doi.org/10.1002/lsm.20048>
- March, J., Hand, M., & Grossman, D. (2015). Practical application of new technologies for melanoma diagnosis: Part I. Noninvasive approaches. *Journal of the American Academy of Dermatology*, *72*(6), 929–941. <https://doi.org/10.1016/j.jaad.2015.02.1138>
- Marks, R., Foley, P., Goodman, G., Hage, B. H., & Selwood, T. S. (1986). Spontaneous remission of solar keratoses: the case for conservative management. *British Journal of Dermatology*, *115*(6), 649–655. <https://doi.org/10.1111/j.1365-2133.1986.tb06644.x>
- Marks, R., Rennie, G., & Selwood, T. S. (1988). Malignant transformation of solar keratoses to squamous cell carcinoma. *The Lancet*, *331*(8589), 795–797. [https://doi.org/10.1016/S0140-6736\(88\)91658-3](https://doi.org/10.1016/S0140-6736(88)91658-3)
- Marmur, E. S., Schmults, C. D., & Goldberg, D. J. (2004). A Review of Laser and Photodynamic Therapy for the Treatment of Nonmelanoma Skin Cancer. *Dermatologic Surgery*, *30*(2 II), 264–271. <https://doi.org/10.1111/j.1524-4725.2004.30083.x>
- Marneffe, A., Suppa, M., Miyamoto, M., Del Marmol, V., & Boone, M. (2016). Validation of a diagnostic algorithm for the discrimination of actinic keratosis from normal skin and squamous cell carcinoma by means of high-definition optical coherence tomography. *Experimental Dermatology*, *25*(9), 684–687. <https://doi.org/10.1111/exd.13036>
- Martin, G. M., & Stockfleth, E. (2012). Diclofenac sodium 3% gel for the management of actinic keratosis: 10+ years of cumulative evidence of efficacy and safety. *Journal of Drugs in Dermatology: JDD*, *11*(5), 600–608.
- Martin, M. E., Wabuyele, M. B., Chen, K., Kasili, P., Panjehpour, M., Phan, M., Overholt, B., Cunningham, G., Wilson, D., Denovo, R. C., & Vo-Dinh, T. (2006). Development of an advanced Hyperspectral Imaging (HSI) system with applications for cancer detection. *Annals of Biomedical Engineering*, *34*(6), 1061–1068. <https://doi.org/10.1007/s10439-006-9121-9>

- Matts, P. J., Dykes, P. J., & Marks, R. (2007). The distribution of melanin in skin determined in vivo. *British Journal of Dermatology*, *156*(4), 620–628. <https://doi.org/10.1111/j.1365-2133.2006.07706.x>
- McGuire, L. K., Disa, J. J., Lee, E. H., Busam, K. J., & Nehal, K. S. (2012). Melanoma of the lentigo maligna subtype: Diagnostic challenges and current treatment paradigms. *Plastic and Reconstructive Surgery*, *129*(2), 288–299. <https://doi.org/10.1097/PRS.0b013e31823aeb72>
- McKenna, J. K., Florell, S. R., Goldman, G. D., & Bowen, G. M. (2006). Lentigo maligna/lentigo maligna melanoma: Current state of diagnosis and treatment. *Dermatologic Surgery*, *32*(4), 493–504. <https://doi.org/10.1111/j.1524-4725.2006.32102.x>
- McLeod, M., Choudhary, S., Giannakakis, G., & Nouri, K. (2011). Surgical treatments for lentigo maligna: A review. *Dermatologic Surgery*, *37*(9), 1210–1228. <https://doi.org/10.1111/j.1524-4725.2011.02042.x>
- Memon, A. A., Tomenson, J. A., Bothwell, J., & Friedmann, P. S. (2000). Prevalence of solar damage and actinic keratosis in a Merseyside population. *British Journal of Dermatology*, *142*(6), 1154–1159. <https://doi.org/10.1046/j.1365-2133.2000.03541.x>
- Menzies, S. W. (2002). Dermoscopy of pigmented basal cell carcinoma. *Clinics in Dermatology*, *20*(3), 268–269. [https://doi.org/10.1016/S0738-081X\(02\)00229-8](https://doi.org/10.1016/S0738-081X(02)00229-8)
- Menzies, S. W., Liyanarachchi, S., Coates, E., Smith, A., Cooke-Yarborough, C., Lo, S., Armstrong, B., Scolyer, R. A., & Guitera, P. (2020). Estimated risk of progression of lentigo maligna to lentigo maligna melanoma. *Melanoma Research*, *30*(2), 193–197. <https://doi.org/10.1097/CMR.0000000000000619>
- Mieloszyk, R. J., & Bhargava, P. (2018). Convolutional Neural Networks: The Possibilities are Almost Endless. *Current Problems in Diagnostic Radiology*, *47*(3), 129–130. <https://doi.org/10.1067/j.cpradiol.2018.01.008>
- Mirzoyev, S. A., Knudson, R. M., Reed, K. B., Hou, J. L., Lohse, C. M., Frohm, M. L., Brewer, J. D., Otley, C. C., & Roenigk, R. K. (2014). Incidence of lentigo maligna in Olmsted County, Minnesota, 1970 to 2007. *Journal of the American Academy of Dermatology*, *70*(3), 443–448. <https://doi.org/10.1016/j.jaad.2013.11.008>
- Moggio, E., Arisi, M., Zane, C., Calzavara-Pinton, I., & Calzavara-Pinton, P. G. (2016). A randomized split-face clinical trial analyzing daylight photodynamic therapy with methyl aminolaevulinate vs ingenol mebutate gel for the treatment of multiple actinic keratoses of the face and the scalp. *Photodiagnosis and Photodynamic Therapy*, *16*, 161–165. <https://doi.org/10.1016/j.pdpdt.2016.08.005>
- Moloney, F. J., & Collins, P. (2007). Randomized, double-blind, prospective study to compare topical 5-aminolaevulinic acid methylester with topical 5-aminolaevulinic acid photodynamic therapy for extensive scalp actinic keratosis. *The British Journal of Dermatology*, *157*(1), 87–91. <https://doi.org/10.1111/j.1365-2133.2007.07946.x>
- Moncrieff, M., Otton, S., Claridge, E., & Hall, P. (2002). Spectrophotometric intracutaneous analysis: A new technique for imaging pigmented skin lesions. *British Journal of Dermatology*, *146*(3), 448–457. <https://doi.org/10.1046/j.1365-2133.2002.04569.x>
- Monheit, G., Cognetta, A. B., Ferris, L., Rabinovitz, H., Gross, K., Martini, M., Grichnik, J. M., Mihm, M., Prieto, V. G., Googe, P., King, R., Toledano, A., Kabelev, N., Wojton, M., & Gutkowitz-Krusin, D. (2011). The performance of MelaFind: A prospective multicenter study. *Archives of Dermatology*, *147*(2), 188–194. <https://doi.org/10.1001/archdermatol.2010.302>

- Morton, C. A., Campbell, S., Gupta, G., Keohane, S., Lear, J., Zaki, I., Walton, S., Kerrouche, N., Thomas, G., Soto, P., & AKtion Investigators. (2006). Intraindividual, right-left comparison of topical methyl aminolaevulinate-photodynamic therapy and cryotherapy in subjects with actinic keratoses: a multicentre, randomized controlled study. *The British Journal of Dermatology*, 155(5), 1029–1036. <https://doi.org/10.1111/j.1365-2133.2006.07470.x>
- Morton, C. A., Szeimies, R. M., Sidoroff, A., & Braathen, L. R. (2013a). European guidelines for topical photodynamic therapy part 1: Treatment delivery and current indications - Actinic keratoses, Bowen's disease, basal cell carcinoma. *Journal of the European Academy of Dermatology and Venereology*, 27(5), 536–544. <https://doi.org/10.1111/jdv.12031>
- Morton, C. A., Szeimies, R. M., Sidoroff, A., & Braathen, L. R. (2013b). European guidelines for topical photodynamic therapy part 2: Emerging indications - Field cancerization, photorejuvenation and inflammatory/infective dermatoses. *Journal of the European Academy of Dermatology and Venereology*, 27(6), 672–679. <https://doi.org/10.1111/jdv.12026>
- Moy, R. L. (2000). Clinical presentation of actinic keratoses and squamous cell carcinoma. *Journal of the American Academy of Dermatology*, 42(1 SUPPL. 1). <https://doi.org/10.1067/mjd.2000.103343>
- Naldi, L., Chatenoud, L., Piccitto, R., Colombo, P., Placchesi, E. B., & La Vecchia, C. (2006). Prevalence of actinic keratoses and associated factors in a representative sample of the Italian adult population: Results from the prevalence of actinic keratoses Italian study, 2003-2004. *Archives of Dermatology*, 142(6), 722–726. <https://doi.org/10.1001/archderm.142.6.722>
- Neidecker, M. V., Davis-Ajami, M. L., Balkrishnan, R., & Feldman, S. R. (2009). Pharmacoeconomic considerations in treating actinic keratosis. In *PharmacoEconomics* (Vol. 27, Issue 6, pp. 451–464). <https://doi.org/10.2165/00019053-200927060-00002>
- Neittaanmäki-Perttu, N., Grönroos, M., Jeskanen, L., Pölönen, I., Ranki, A., Saksela, O., & Snellman, E. (2015). Delineating margins of lentigo maligna using a hyperspectral imaging system. *Acta Dermato-Venereologica*, 95(5), 549–552. <https://doi.org/10.2340/00015555-2010>
- Neittaanmäki-Perttu, N., Grönroos, M., Karppinen, T. T., Snellman, E., & Rissanen, P. (2016). Photodynamic therapy for actinic keratoses: A randomized prospective non-sponsored cost-effectiveness study of daylightmediated treatment compared with light-emitting diode treatment. *Acta Dermato-Venereologica*, 96(2), 241–244. <https://doi.org/10.2340/00015555-2205>
- Neittaanmäki-Perttu, N., Grönroos, M., Karppinen, T. T., Tani, T. T., & Snellman, E. (2016). Hexyl-5-aminolaevulinate 0.2% vs. methyl-5-aminolaevulinate 16% daylight photodynamic therapy for treatment of actinic keratoses: Results of a randomized double-blinded pilot trial. *British Journal of Dermatology*, 174(2), 427–429. <https://doi.org/10.1111/bjd.13924>
- Neittaanmäki-Perttu, N., Grönroos, M., Tani, T., Pölönen, I., Ranki, A., Saksela, O., & Snellman, E. (2013). Detecting field cancerization using a hyperspectral imaging system. *Lasers in Surgery and Medicine*, 45(7), 410–417. <https://doi.org/10.1002/lsm.22160>
- Neittaanmäki-Perttu, N., Grönroos, M., Tani, T., & Snellman, E. (2016). Long-term outcome of daylight photodynamic therapy with amino-5-laevulinate nanoemulsion

- vs. Methyl-5-aminolaevulinate for actinic keratoses. *Acta Dermato-Venerologica*, 96(5), 712–713. <https://doi.org/10.2340/00015555-2345>
- Neittaanmäki-Perttu, N., Karppinen, T. T., Grönroos, M., Tani, T. T., & Snellman, E. (2014). Daylight photodynamic therapy for actinic keratoses: A randomized double-blinded nonsponsored prospective study comparing 5-aminolaevulinic acid nanoemulsion (BF-200) with methyl-5-aminolaevulinate. *British Journal of Dermatology*, 171(5), 1172–1180. <https://doi.org/10.1111/bjd.13326>
- Neittaanmäki, N., Salmivuori, M., Pölönen, I., Jeskanen, L., Ranki, A., Saksela, O., Snellman, E., & Grönroos, M. (2017). Hyperspectral imaging in detecting dermal invasion in lentigo maligna melanoma. *British Journal of Dermatology*, 177(6), 1742–1744. <https://doi.org/10.1111/bjd.15267>
- Nissinen, L., Farshchian, M., Riihilä, P., & Kähäri, V. M. (2016). New perspectives on role of tumor microenvironment in progression of cutaneous squamous cell carcinoma. *Cell and Tissue Research*, 365(3), 691–702. <https://doi.org/10.1007/s00441-016-2457-z>
- Nori, S., Rius-Díaz, F., Cuevas, J., Goldgeier, M., Jaen, P., Torres, A., & González, S. (2004). Sensitivity and specificity of reflectance-mode confocal microscopy for in vivo diagnosis of basal cell carcinoma: A multicenter study. *Journal of the American Academy of Dermatology*, 51(6), 923–930. <https://doi.org/10.1016/j.jaad.2004.06.028>
- O’Gorman, S. M., Clowry, J., Manley, M., McCavana, J., Gray, L., Kavanagh, A., Lally, A., & Collins, P. (2016). Artificial white light vs daylight photodynamic therapy for actinic keratoses: A randomized clinical trial. *JAMA Dermatology*, 152(6), 638–644. <https://doi.org/10.1001/jamadermatol.2015.5436>
- Olsen, E. A., Lisa Abernethy, M., Kulp-Shorten, C., Callen, J. P., Glazer, S. D., Huntley, A., McCray, M., Monroe, A. B., Tschén, E., & Wolf, J. E. (1991). A double-blind, vehicle-controlled study evaluating masoprocol cream in the treatment of actinic keratoses on the head and neck. *Journal of the American Academy of Dermatology*, 24(5), 738–743. [https://doi.org/10.1016/0190-9622\(91\)70113-G](https://doi.org/10.1016/0190-9622(91)70113-G)
- Olsen, J., Holmes, J., & Jemec, G. B. E. (2018). Advances in optical coherence tomography in dermatology—a review. *Journal of Biomedical Optics*, 23(04), 1. <https://doi.org/10.1117/1.jbo.23.4.040901>
- Olsen, J., Themstrup, L., De Carvalho, N., Mogensen, M., Pellacani, G., & Jemec, G. B. E. (2016). Diagnostic accuracy of optical coherence tomography in actinic keratosis and basal cell carcinoma. *Photodiagnosis and Photodynamic Therapy*, 16, 44–49. <https://doi.org/10.1016/j.pdpdt.2016.08.004>
- Ozog, D. M., Rkein, A. M., Fabi, S. G., Gold, M. H., Goldman, M. P., Lowe, N. J., Martin, G. M., & Munavalli, G. S. (2016). Photodynamic Therapy: A Clinical Consensus Guide. *Dermatologic Surgery*, 42(7), 804–827. <https://doi.org/10.1097/DSS.0000000000000800>
- Panasyuk, S. V., Yang, S., Faller, D. V., Ngo, D., Lew, R. A., Freeman, J. E., & Rogers, A. E. (2007). Medical hyperspectral imaging to facilitate residual tumor identification during surgery. *Cancer Biology and Therapy*, 6(3), 439–446. <https://doi.org/10.4161/cbt.6.3.4018>
- Papanikolaou, M., & Lawrence, C. M. (2019). Long-term outcomes of imiquimod-treated lentigo maligna. *Clinical and Experimental Dermatology*, 44(6), 631–636. <https://doi.org/10.1111/ced.13896>

- Paraskevas, L. R., Halpern, A. C., & Marghoob, A. A. (2005). Utility of the Wood's light: Five cases from a pigmented lesion clinic. *British Journal of Dermatology*, *152*(5), 1039–1044. <https://doi.org/10.1111/j.1365-2133.2005.06346.x>
- Pariser, D., Loss, R., Jarratt, M., Abramovits, W., Spencer, J., Geronemus, R., Bailin, P., & Bruce, S. (2008). Topical methyl-aminolevulinate photodynamic therapy using red light-emitting diode light for treatment of multiple actinic keratoses: A randomized, double-blind, placebo-controlled study. *Journal of the American Academy of Dermatology*, *59*(4), 569–576. <https://doi.org/10.1016/j.jaad.2008.05.031>
- Pellacani, G., Guitera, P., Longo, C., Avramidis, M., Seidenari, S., & Menzies, S. (2007). The impact of in vivo reflectance confocal microscopy for the diagnostic accuracy of melanoma and equivocal melanocytic lesions. *Journal of Investigative Dermatology*, *127*(12), 2759–2765. <https://doi.org/10.1038/sj.jid.5700993>
- Petersen, B., Wiegell, S. R., & Wulf, H. C. (2014). Light protection of the skin after photodynamic therapy reduces inflammation: An unblinded randomized controlled study. *British Journal of Dermatology*, *171*(1), 175–178. <https://doi.org/10.1111/bjd.12882>
- Philipp-Dormston, W. G., Sanclemente, G., Torezan, L., Tretti Clementoni, M., Le Pillouer-Prost, A., Cartier, H., Szeimies, R. M., & Bjerring, P. (2016). Daylight photodynamic therapy with MAL cream for large-scale photodamaged skin based on the concept of “actinic field damage”: Recommendations of an international expert group. *Journal of the European Academy of Dermatology and Venerology*, *30*(1), 8–15. <https://doi.org/10.1111/jdv.13327>
- Philipsen, P. A., Knudsen, L., Gniadecka, M., Ravnbak, M. H., & Wulf, H. C. (2013). Diagnosis of malignant melanoma and basal cell carcinoma by in vivo NIR-FT Raman spectroscopy is independent of skin pigmentation. *Photochemical and Photobiological Sciences*, *12*(5), 770–776. <https://doi.org/10.1039/c3pp25344a>
- Piacquadro, D. J., Chen, D. M., Farber, H. F., Fowler, J. F., Glazer, S. D., Goodman, J. J., Hruza, L. L., Jeffes, E. W. B., Ling, M. R., Phillips, T. J., Rallis, T. M., Scher, R. K., Taylor, C. R., & Weinstein, G. D. (2004). Photodynamic Therapy With Aminolevulinic Acid Topical Solution and Visible Blue Light in the Treatment of Multiple Actinic Keratoses of the Face and Scalp: Investigator-Blinded, Phase 3, Multicenter Trials. *Archives of Dermatology*, *140*(1), 41–46. <https://doi.org/10.1001/archderm.140.1.41>
- Piccolo, D., Ferrari, A., Peris, K., Daidone, R., Ruggeri, B., & Chimenti, S. (2002). Dermoscopic diagnosis by a trained clinician vs. a clinician with minimal dermoscopy training vs. computer-aided diagnosis of 341 pigmented skin lesions: A comparative study. *British Journal of Dermatology*, *147*(3), 481–486. <https://doi.org/10.1046/j.1365-2133.2002.04978.x>
- Pölönen, I., Rahkonen, S., Annala, L., & Neittaanmäki, N. (2019). Convolutional neural networks in skin cancer detection using spatial and spectral domain. In B. Choi & H. Zeng (Eds.), *Photonics in Dermatology and Plastic Surgery 2019* (Vol. 10851, p. 10). SPIE. <https://doi.org/10.1117/12.2509871>
- Powell, A. M., Robson, A. M., Russell-Jones, R., & Barlow, R. J. (2009). Imiquimod and lentigo maligna: A search for prognostic features in a clinicopathological study with long-term follow-up. *British Journal of Dermatology*, *160*(5), 994–998. <https://doi.org/10.1111/j.1365-2133.2009.09032.x>

- Pralong, P., Bathelier, E., Dalle, S., Poulalhon, N., Debarbieux, S., & Thomas, L. (2012). Dermoscopy of lentigo maligna melanoma: Report of 125 cases. *British Journal of Dermatology*, *167*(2), 280–287. <https://doi.org/10.1111/j.1365-2133.2012.10932.x>
- Rajpara, S. M., Botello, A. P., Townend, J., & Ormerod, A. D. (2009). Systematic review of dermoscopy and digital dermoscopy/ artificial intelligence for the diagnosis of melanoma. *British Journal of Dermatology*, *161*(3), 591–604. <https://doi.org/10.1111/j.1365-2133.2009.09093.x>
- Read, T., Noonan, C., David, M., Wagels, M., Foote, M., Schaidler, H., Soyer, H. P., & Smithers, B. M. (2016). A systematic review of non-surgical treatments for lentigo maligna. *Journal of the European Academy of Dermatology and Venereology*, *30*(5), 748–753. <https://doi.org/10.1111/jdv.13252>
- Reed, J. A., & Shea, C. R. (2011). Lentigo maligna: Melanoma in situ on chronically sun-damaged skin. *Archives of Pathology and Laboratory Medicine*, *135*(7), 838–841. <https://doi.org/10.1043/2011-0051-RAIR.1>
- Reinhold, U. (2017). A review of BF-200 ALA for the photodynamic treatment of mild-to-moderate actinic keratosis. *Future Oncology*, *13*(27), 2413–2428. <https://doi.org/10.2217/fo-2017-0247>
- Reinhold, U., Dirschka, T., Ostendorf, R., Aschoff, R., Berking, C., Philipp-Dormston, W. G., Hahn, S., Lau, K., Jäger, A., Schmitz, B., Lübbert, H., & Szeimies, R. M. (2016). A randomized, double-blind, phase III, multicentre study to evaluate the safety and efficacy of BF-200 ALA (Ameluz®) vs. placebo in the field-directed treatment of mild-to-moderate actinic keratosis with photodynamic therapy (PDT) when using the BF-RhodoL. *British Journal of Dermatology*, *175*(4), 696–705. <https://doi.org/10.1111/bjd.14498>
- Rizvi, S. M. H., Veierød, M. B., Mørk, G., Helsing, P., & Gjersvik, P. (2019). Ablative fractional laser-assisted daylight photodynamic therapy for actinic keratoses of the scalp and forehead in organ transplant recipients: A pilot study. *Acta Dermato-Venerologica*, *99*(11), 1047–1048. <https://doi.org/10.2340/00015555-3274>
- Robertson, C. A., & Abrahamse, H. (2010). The in vitro PDT efficacy of a novel metallophthalocyanine (MPc) derivative and established 5-ALA photosensitizing dyes against human metastatic melanoma cells. *Lasers in Surgery and Medicine*, *42*(10), 926–936. <https://doi.org/10.1002/lsm.20980>
- Robinson, M., Primiero, C., Guitera, P., Hong, A., Scolyer, R. A., Stretch, J. R., Strutton, G., Thompson, J. F., & Peter Soyer, H. (2019). Evidence-Based Clinical Practice Guidelines for the Management of Patients with Lentigo Maligna. *Dermatology*, *410*(2), 111–116. <https://doi.org/10.1159/000502470>
- Rosen, R. H., Gupta, A. K., & Tyring, S. K. (2012). Dual mechanism of action of ingenol mebutate gel for topical treatment of actinic keratoses: Rapid lesion necrosis followed by lesion-specific immune response. *Journal of the American Academy of Dermatology*, *66*(3), 486–493. <https://doi.org/10.1016/j.jaad.2010.12.038>
- Rosen, T., & Lebwohl, M. G. (2013). Prevalence and awareness of actinic keratosis: Barriers and opportunities. *Journal of the American Academy of Dermatology*, *68*(1 SUPPL.1), S2. <https://doi.org/10.1016/j.jaad.2012.09.052>
- Rossi, R., Mori, M., & Lotti, T. (2007). Actinic keratosis. In *International Journal of Dermatology* (Vol. 46, Issue 9, pp. 895–904). <https://doi.org/10.1111/j.1365-4632.2007.03166.x>
- Röwert-Huber, J., Patel, M. J., Forschner, T., Ulrich, C., Eberle, J., Kerl, H., Sterry, W., & Stockfleth, E. (2007). Actinic keratosis is an early in situ squamous cell carcinoma: A proposal for reclassification (*British Journal of Dermatology* (2007) 156, SUPPL.,



- (S13-S17)). *British Journal of Dermatology*, 157(2), 431. <https://doi.org/10.1111/j.1365-2133.2007.08104.x>
- Rubel, D. M., Spelman, L., Murrell, D. F., See, J. A., Hewitt, D., Foley, P., Bosc, C., Kerob, D., Kerrouche, N., Wulf, H. C., & Shumack, S. (2014). Daylight photodynamic therapy with methyl aminolevulinate cream as a convenient, similarly effective, nearly painless alternative to conventional photodynamic therapy in actinic keratosis treatment: A randomized controlled trial. *British Journal of Dermatology*, 171(5), 1164–1171. <https://doi.org/10.1111/bjd.13138>
- Salasche, S. J. (2000). Epidemiology of actinic keratoses and squamous cell carcinoma. *Journal of the American Academy of Dermatology*, 42(1 SUPPL. 1). <https://doi.org/10.1067/mjd.2000.103342>
- Salmivuori, M., Grönroos, M., Tani, T., Pölönen, I., Räsänen, J., Annala, L., Snellman, E., & Neittaanmäki, N. (2020). Hexyl aminolevulinate, 5-aminolevulinic acid nanoemulsion, and methyl aminolevulinate in photodynamic therapy of non-aggressive basal cell carcinomas: A non-sponsored, randomized, prospective and double-blinded trial. *Journal of the European Academy of Dermatology and Venereology*, 0–3. <https://doi.org/10.1111/jdv.16357>
- Salmivuori, M., Neittaanmäki, N., Pölönen, I., Jeskanen, L., Snellman, E., & Grönroos, M. (2019a). Hyperspectral imaging system in the delineation of ill-defined basal cell carcinomas: a pilot study. *Journal of the European Academy of Dermatology and Venereology*, 33(1), 71–78. <https://doi.org/10.1111/jdv.15102>
- Salmivuori, M., Neittaanmäki, N., Pölönen, I., Jeskanen, L., Snellman, E., & Grönroos, M. (2019b). Hyperspectral imaging system in the delineation of ill-defined basal cell carcinomas: a pilot study. *Journal of the European Academy of Dermatology and Venereology*, 33(1), 71–78. <https://doi.org/10.1111/jdv.15102>
- Samrao, A., & Cockerell, C. J. (2013). Pharmacotherapeutic management of actinic keratosis: Focus on newer topical agents. *American Journal of Clinical Dermatology*, 14(4), 273–277. <https://doi.org/10.1007/s40257-013-0023-y>
- Sauder, D. N. (2003). Imiquimod: Modes of action. *British Journal of Dermatology, Supplement*, 149(66), 5–8. <https://doi.org/10.1046/j.0366-077x.2003.05628.x>
- Schaefer, I., Augustin, M., Spehr, C., Reusch, M., & Kornek, T. (2014). Prevalence and risk factors of actinic keratoses in Germany - Analysis of multisource data. *Journal of the European Academy of Dermatology and Venereology*, 28(3), 309–313. <https://doi.org/10.1111/jdv.12102>
- Schiffner, R., Schiffner-Rohe, J., Vogt, T., Landthaler, M., Wlotzke, U., Cagnetta, A. B., & Stolz, W. (2000). Improvement of early recognition of lentigo maligna using dermatoscopy. *Journal of the American Academy of Dermatology*, 42(1 I), 25–32. [https://doi.org/10.1016/S0190-9622\(00\)90005-7](https://doi.org/10.1016/S0190-9622(00)90005-7)
- Schleusener, J., Gluszczynska, P., Reble, C., Gersonde, I., Helfmann, J., Fluhr, J. W., Lademann, J., Röwert-Huber, J., Patzelt, A., & Meinke, M. C. (2015). In vivo study for the discrimination of cancerous and normal skin using fibre probe-based Raman spectroscopy. *Experimental Dermatology*, 24(10), 767–772. <https://doi.org/10.1111/exd.12768>
- Schmitz, L., Kahl, P., Majores, M., Bierhoff, E., Stockfleth, E., & Dirschka, T. (2016). Actinic keratosis: correlation between clinical and histological classification systems. *Journal of the European Academy of Dermatology and Venereology*, 30(8), 1303–1307. <https://doi.org/10.1111/jdv.13626>

- Schmitz, L., Novak, B., Hoeh, A. K., Luebbert, H., & Dirschka, T. (2016). Epidermal penetration and protoporphyrin IX formation of two different 5-aminolevulinic acid formulations in ex vivo human skin. *Photodiagnosis and Photodynamic Therapy*, *14*, 40–46. <https://doi.org/10.1016/j.pdpdt.2015.11.004>
- Schweitzer, V. G. (2001). Photofrin-Mediated Photodynamic Therapy for Treatment of Aggressive Head and Neck Nonmelanomatous Skin Tumors in Elderly Patients. *The Laryngoscope*, *111*(6), 1091–1098. <https://doi.org/10.1097/00005537-200106000-00030>
- See, J. A., Gebauer, K., Wu, J. K., Manoharan, S., Kerrouche, N., & Sullivan, J. (2017). High Patient Satisfaction with Daylight-Activated Methyl Aminolevulinate Cream in the Treatment of Multiple Actinic Keratoses: Results of an Observational Study in Australia. *Dermatology and Therapy*, *7*(4), 525–533. <https://doi.org/10.1007/s13555-017-0199-9>
- Serra-Guillén, C., Nagore, E., Bancalari, E., Kindem, S., Sanmartín, O., Llombart, B., Requena, C., Serra-Guillén, I., Calomarde, L., Diago, A., Bernia, E., & Guillén, C. (2018). A randomized intraindividual comparative study of methyl-5-aminolaevulinate vs. 5-aminolaevulinic acid nanoemulsion (BF-200 ALA) in photodynamic therapy for actinic keratosis of the face and scalp. *British Journal of Dermatology*, *179*(6), 1410–1411. <https://doi.org/10.1111/bjd.17014>
- Sgouros, D., Lallas, A., Julian, Y., Rigopoulos, D., Zalaudek, I., Longo, C., Moscarella, E., Simonetti, V., & Argenziano, G. (2014). Assessment of SIAscopy in the triage of suspicious skin tumours. *Skin Research and Technology*, *20*(4), 440–444. <https://doi.org/10.1111/srt.12138>
- Shahriari, N., Grant-Kels, J. M., Rabinovitz, H., Oliviero, M., & Scope, A. (2021). Reflectance confocal microscopy: Principles, basic terminology, clinical indications, limitations, and practical considerations. *Journal of the American Academy of Dermatology*, *84*(1), 1–14. <https://doi.org/10.1016/j.jaad.2020.05.153>
- Shain, A. H., & Bastian, B. C. (2016). From melanocytes to melanomas. *Nature Reviews Cancer*, *16*(6), 345–358. <https://doi.org/10.1038/nrc.2016.37>
- Shain, A. H., Yeh, I., Kovalyshyn, I., Sriharan, A., Talevich, E., Gagnon, A., Dummer, R., North, J., Pincus, L., Ruben, B., Rickaby, W., D'Arrigo, C., Robson, A., & Bastian, B. C. (2015). The Genetic Evolution of Melanoma from Precursor Lesions. *New England Journal of Medicine*, *373*(20), 1926–1936. <https://doi.org/10.1056/nejmoa1502583>
- Shrivastava, V., Bailin, P., Elliott, J., Bacnik, E., Gastman, B., Bergfeld, W., Billings, S. D., Piliang, M., Fernandez, A., Kovalyshyn, I., & Ko, J. S. (2019). Histopathologic correlation of high-risk MelaFind TM lesions: a 3-year experience from a high-risk pigmented lesion clinic. *International Journal of Dermatology*, *58*(5), 569–576. <https://doi.org/10.1111/ijd.14336>
- Siddiqi, A. M., Li, H., Faruque, F., Williams, W., Lai, K., Hughson, M., Bigler, S., Beach, J., & Johnson, W. (2008). Use of hyperspectral imaging to distinguish normal, precancerous, and cancerous cells. *Cancer*, *114*(1), 13–21. <https://doi.org/10.1002/cncr.23286>
- Siegel, J. A., Korgavkar, K., & Weinstock, M. A. (2017). Current perspective on actinic keratosis: a review. *British Journal of Dermatology*, *177*(2), 350–358. <https://doi.org/10.1111/bjd.14852>
- Silveira, F. L., Pacheco, M. T. T., Bodanese, B., Pasqualucci, C. A., Zângaro, R. A., & Silveira, L. (2015). Discrimination of non-melanoma skin lesions from non-tumor human skin

- tissues *in vivo* using Raman spectroscopy and multivariate statistics. *Lasers in Surgery and Medicine*, 47(1), 6–16. <https://doi.org/10.1002/lsm.22318>
- Sinikumpu, S. P., Huilaja, L., Jokelainen, J., Koironen, M., Auvinen, J., Hägg, P. M., Wikström, E., Timonen, M., & Tasanen, K. (2014). High prevalence of skin diseases and need for treatment in a middle-aged population. A Northern Finland Birth Cohort 1966 study. *PLoS ONE*, 9(6), 1–8. <https://doi.org/10.1371/journal.pone.0099533>
- Sinikumpu, S. P., Jokelainen, J., Haarala, A. K., Keränen, M. H., Keinänen-Kiukaanniemi, S., & Huilaja, L. (2020). The High Prevalence of Skin Diseases in Adults Aged 70 and Older. *Journal of the American Geriatrics Society*, 68(11), 2565–2571. <https://doi.org/10.1111/jgs.16706>
- Sotiriou, E., Evangelou, G., Papadavid, E., Apalla, Z., Vrani, F., Vakirlis, E., Panagiotou, M., Stefanidou, M., Pombou, T., Krasagakis, K., Rigopoulos, D., & Ioannides, D. (2018). Conventional vs. daylight photodynamic therapy for patients with actinic keratosis on face and scalp: 12-month follow-up results of a randomized, intra-individual comparative analysis. *Journal of the European Academy of Dermatology and Venereology*, 32(4), 595–600. <https://doi.org/10.1111/jdv.14613>
- Stadlmeier, E., Heitzer, E., Resel, M., Cerroni, L., Wolf, P., & Dandachi, N. (2014). The BRAF V600K mutation is more frequent than the BRAF V600E mutation in melanoma in situ of lentigo maligna type. *Journal of Investigative Dermatology*, 134(2), 548–550. <https://doi.org/10.1038/jid.2013.338>
- Steeb, T., Wessely, A., Harlaß, M., Heppt, F., Koch, E. A. T., Leiter, U., Garbe, C., Schöffski, O., Berking, C., & Heppt, M. V. (2020). A Systematic Review and Meta-Analysis of Interventions for Actinic Keratosis from Post-Marketing Surveillance Trials. *Journal of Clinical Medicine*, 9(7), 2253. <https://doi.org/10.3390/jcm9072253>
- Steeb, T., Wessely, A., Schmitz, L., Heppt, F., Kirchberger, M. C., Berking, C., & Heppt, M. V. (2021). Interventions for Actinic Keratosis in Nonscalp and Nonface Localizations: Results from a Systematic Review with Network Meta-Analysis. *Journal of Investigative Dermatology*, 141(2), 345–354.e8. <https://doi.org/10.1016/j.jid.2020.06.021>
- Stevenson, O., & Ahmed, I. (2005). *Prognosis and Treatment Options*. 6(3), 151–164.
- Stockfleth, E., Sterry, W., Carey-Yard, M., & Bichel, J. (2007). Multicentre, open-label study using imiquimod 5% cream in one or two 4-week courses of treatment for multiple actinic keratoses on the head. *British Journal of Dermatology*, 157(SUPPL. 2), 41–46. <https://doi.org/10.1111/j.1365-2133.2007.08272.x>
- Swanson, N., Smith, C. C., Kaur, M., & Goldenberg, G. (2014). Imiquimod 2.5% and 3.75% for the treatment of actinic keratoses: Two phase 3, multicenter, randomized, double-blind, placebo-controlled studies. *Journal of Drugs in Dermatology*, 13(2), 166–169.
- Swetter, S. M., Boldrick, J. C., Jung, S. Y., Egbert, B. M., & Harvell, J. D. (2005). Increasing incidence of lentigo maligna melanoma subtypes: Northern California and national trends 1990–2000. *Journal of Investigative Dermatology*, 125(4), 685–691. <https://doi.org/10.1111/j.0022-202X.2005.23852.x>
- Szeimies, R. M., Morton, C. A., Sidoroff, A., & Braathen, L. R. (2005). Photodynamic therapy for non-melanoma skin cancer. *Acta Dermato-Venerologica*, 85(6), 483–490. <https://doi.org/10.1080/00015550510044136>
- Szeimies, R. M., Radny, P., Sebastian, M., Borrosch, F., Dirschka, T., Krähn-Senftleben, G., Reich, K., Pabst, G., Voss, D., Foguet, M., Gahlmann, R., Lübbert, H., & Reinhold, U. (2010). Photodynamic therapy with BF-200 ALA for the treatment of actinic

- keratosis: Results of a prospective, randomized, double-blind, placebo-controlled phase III study. *British Journal of Dermatology*, 163(2), 386–394. <https://doi.org/10.1111/j.1365-2133.2010.09873.x>
- Terstappen, K., Larkö, O., & Wennberg, A. M. (2007). Pigmented basal cell carcinoma - Comparing the diagnostic methods of SIAscopy and dermoscopy. *Acta Dermato-Venerologica*, 87(3), 238–242. <https://doi.org/10.2340/00015555-0234>
- Terstappen, K., Suurküla, M., Hallberg, H., Ericson, M. B., & Wennberg, A.-M. (2013). Poor correlation between spectrophotometric intracutaneous analysis and histopathology in melanoma and nonmelanoma lesions. *Journal of Biomedical Optics*, 18(6), 061223. <https://doi.org/10.1117/1.jbo.18.6.061223>
- Thai, K. E., Fergin, P., Freeman, M., Vinciullo, C., Francis, D., Spelman, L., Murrell, D., Anderson, C., Weightman, W., Reid, C., Watson, A., & Foley, P. (2004). A prospective study of the use of cryosurgery for the treatment of actinic keratoses. *International Journal of Dermatology*, 43(9), 687–692. <https://doi.org/10.1111/j.1365-4632.2004.02056.x>
- Thunshelle, C., Yin, R., Chen, Q., & Hamblin, M. R. (2016). Current Advances in 5-Aminolevulinic Acid Mediated Photodynamic Therapy. *Current Dermatology Reports*, 5(3), 179–190. <https://doi.org/10.1007/s13671-016-0154-5>
- Tio, D., van der Woude, J., Prinsen, C. A. C., Jansma, E. P., Hoekzema, R., & van Montfrans, C. (2017). A systematic review on the role of imiquimod in lentigo maligna and lentigo maligna melanoma: need for standardization of treatment schedule and outcome measures. *Journal of the European Academy of Dermatology and Venereology*, 31(4), 616–624. <https://doi.org/10.1111/jdv.14085>
- Tio, D., Van Montfrans, C., Ruijter, C. G. H., Hoekzema, R., & Bekkenk, M. W. (2019). Effectiveness of 5% topical imiquimod for lentigo maligna treatment. *Acta Dermato-Venerologica*, 99(10), 884–888. <https://doi.org/10.2340/00015555-3241>
- Tkaczyk, E. R. (2017). Innovations and developments in dermatologic non-invasive optical imaging and potential clinical applications. *Acta Dermato-Venerologica*, 97, 5–13. <https://doi.org/10.2340/00015555-2717>
- Toender, A., Kjær, S. K., & Jensen, A. (2014). Increased incidence of melanoma in situ in Denmark from 1997 to 2011: Results from a Nationwide population-based study. *Melanoma Research*, 24(5), 488–495. <https://doi.org/10.1097/CMR.0000000000000092>
- Togsverd-Bo, K., Haak, C. S., Thaysen-Petersen, D., Wulf, H. C., Anderson, R. R., & Hædersdal, M. (2012). Intensified photodynamic therapy of actinic keratoses with fractional CO<sub>2</sub> laser: A randomized clinical trial. *British Journal of Dermatology*, 166(6), 1262–1269. <https://doi.org/10.1111/j.1365-2133.2012.10893.x>
- Togsverd-Bo, K., Lei, U., Erlendsson, A. M., Taudorf, E. H., Philipsen, P. A., Wulf, H. C., Skov, L., & Hædersdal, M. (2015). Combination of ablative fractional laser and daylight-mediated photodynamic therapy for actinic keratosis in organ transplant recipients - A randomized controlled trial. *British Journal of Dermatology*, 172(2), 467–474. <https://doi.org/10.1111/bjd.13222>
- Togsverd-Bo, K., Lerche, C. M., Poulsen, T., Wulf, H. C., & Hædersdal, M. (2010). Photodynamic therapy with topical methyl- and hexylaminolevulinate for prophylaxis and treatment of UV-induced SCC in hairless mice. *Experimental Dermatology*, 19(8), 166–172. <https://doi.org/10.1111/j.1600-0625.2009.01035.x>
- Tomatis, S., Carrara, M., Bono, A., Bartoli, C., Lualdi, M., Tragni, G., Colombo, A., & Marchesini, R. (2005). Automated melanoma detection with a novel multispectral

- imaging system: results of a prospective study. *MEDICINE AND BIOLOGY Phys. Med. Biol.*, *50*, 1675–1687. <https://doi.org/10.1088/0031-9155/50/8/004>
- Traianou, A., Ulrich, M., Apalla, Z., De Vries, E., Bakirtzi, K., Kalabalikis, D., Ferrandiz, L., Ruiz-De-Casas, A., Moreno-Ramirez, D., Sotiriadis, D., Ioannides, D., Aquilina, S., Apap, C., Micallef, R., Scerri, L., Pitkänen, S., Saksela, O., Altsitsiadis, E., Hinrichs, B., ... Trakatelli, M. (2012). Risk factors for actinic keratosis in eight European centres: A case-control study. *British Journal of Dermatology*, *167*(SUPPL. 2), 36–42. <https://doi.org/10.1111/j.1365-2133.2012.11085.x>
- Tschandl, P., Rinner, C., Apalla, Z., Argenziano, G., Codella, N., Halpern, A., Janda, M., Lallas, A., Longo, C., Malvehy, J., Paoli, J., Puig, S., Rosendahl, C., Soyer, H. P., Zalaudek, I., & Kittler, H. (2020). Human–computer collaboration for skin cancer recognition. *Nature Medicine*, *26*(8), 1229–1234. <https://doi.org/10.1038/s41591-020-0942-0>
- Tschandl, P., Rosendahl, C., Akay, B. N., Argenziano, G., Blum, A., Braun, R. P., Cabo, H., Gourhant, J. Y., Kreusch, J., Lallas, A., Lapins, J., Marghoob, A., Menzies, S., Neuber, N. M., Paoli, J., Rabinovitz, H. S., Rinner, C., Scope, A., Soyer, H. P., ... Kittler, H. (2019). Expert-Level Diagnosis of Nonpigmented Skin Cancer by Combined Convolutional Neural Networks. *JAMA Dermatology*, *155*(1), 58–65. <https://doi.org/10.1001/jamadermatol.2018.4378>
- Tschen, E. H., Wong, D. S., Pariser, D. M., Dunlap, F. E., Houlihan, A., Ferdon, M. B., Bruce, S., Jarratt, M. T., Loss, R. W., Weiss, J., Shavin, J. S., Barba, A., Zeide, D. A., & Brodell, R. T. (2006). Photodynamic therapy using aminolaevulinic acid for patients with nonhyperkeratotic actinic keratoses of the face and scalp: Phase IV multicentre clinical trial with 12-month follow up. *British Journal of Dermatology*, *155*(6), 1262–1269. <https://doi.org/10.1111/j.1365-2133.2006.07520.x>
- Tyrrell, J., Campbell, S., & Curnow, A. (2010). Protoporphyrin IX photobleaching during the light irradiation phase of standard dermatological methyl-aminolevulinate photodynamic therapy. *Photodiagnosis and Photodynamic Therapy*, *7*(4), 232–238. <https://doi.org/10.1016/j.pdpdt.2010.09.005>
- Tzellos, T., Kyrgidis, A., Mocellin, S., Chan, A. W., Pilati, P., & Apalla, Z. (2014). Interventions for melanoma in situ, including lentigo maligna. *Cochrane Database of Systematic Reviews*, *2014*(12). <https://doi.org/10.1002/14651858.CD010308.pub2>
- Ulrich, C., Jürgensen, J. S., Degen, A., Hackethal, M., Ulrich, M., Patel, M. J., Eberle, J., Terhorst, D., Sterry, W., & Stockfleth, E. (2009). Prevention of non-melanoma skin cancer in organ transplant patients by regular use of a sunscreen: A 24 months, prospective, case-control study. *British Journal of Dermatology*, *161*(SUPPL. 3), 78–84. <https://doi.org/10.1111/j.1365-2133.2009.09453.x>
- Ulrich, M., Maltusch, A., Röwert-Huber, J., González, S., Sterry, W., Stockfleth, E., & Astner, S. (2007). Actinic keratoses: Non-invasive diagnosis for field cancerisation. *British Journal of Dermatology*, *156*(SUPPL. 3), 13–17. <https://doi.org/10.1111/j.1365-2133.2007.07865.x>
- Ulrich, M., Reinhold, U., Falqués, M., Rodriguez Azeredo, R., & Stockfleth, E. (2018). Use of reflectance confocal microscopy to evaluate 5-fluorouracil 0.5%/salicylic acid 10% in the field-directed treatment of subclinical lesions of actinic keratosis: subanalysis of a Phase III, randomized, double-blind, vehicle-controlled trial. *Journal of the European Academy of Dermatology and Venereology*, *32*(3), 390–396. <https://doi.org/10.1111/jdv.14611>

- Ulrich, M., Stockfleth, E., Roewert-Huber, J., & Astner, S. (2007). Noninvasive diagnostic tools for nonmelanoma skin cancer. *British Journal of Dermatology*, *157*(SUPPL. 2), 56–58. <https://doi.org/10.1111/j.1365-2133.2007.08275.x>
- van Ruth, S., & Toonstra, J. (2008). Eponyms of Sir Jonathan Hutchinson. *International Journal of Dermatology*, *47*(7), 754–758. <https://doi.org/10.1111/j.1365-4632.2008.03696.x>
- Walter, F. M., Morris, H. C., Humphrys, E., Hall, P. N., Prevost, A. T., Burrows, N., Bradshaw, L., Wilson, E. C. F., Norris, P., Walls, J., Johnson, M., Kinmonth, A. L., & Emery, J. D. (2012). Effect of adding a diagnostic aid to best practice to manage suspicious pigmented lesions in primary care: Randomised controlled trial. *BMJ (Online)*, *345*(7866), 1–14. <https://doi.org/10.1136/bmj.e4110>
- Wassef, C., & Rao, B. K. (2013). Uses of non-invasive imaging in the diagnosis of skin cancer: An overview of the currently available modalities. *International Journal of Dermatology*, *52*(12), 1481–1489. <https://doi.org/10.1111/ijd.12159>
- Weinstock, M. A., Lee, K. C., Chren, M. M., & Marcolivio, K. (2009). Quality of life in the actinic neoplasia syndrome: The VA Topical Tretinoin Chemoprevention (VATTC) Trial. *Journal of the American Academy of Dermatology*, *61*(2), 207–215. <https://doi.org/10.1016/j.jaad.2009.02.022>
- Weinstock, M. A., & Sober, A. J. (1987). The risk of progression of lentigo maligna to lentigo maligna melanoma. *British Journal of Dermatology*, *116*(3), 303–310. <https://doi.org/10.1111/j.1365-2133.1987.tb05843.x>
- Weinstock, M. A., Thwin, S. S., Siegel, J. A., Marcolivio, K., Means, A. D., Leader, N. F., Shaw, F. M., Hogan, D., Eilers, D., Swetter, S. M., Chen, S. C., Jacob, S. E., Warshaw, E. M., Stricklin, G. P., Dellavalle, R. P., Sidhu-Malik, N., Konnikov, N., Werth, V. P., Keri, J. E., ... Huang, G. D. (2018). Chemoprevention of basal and squamous cell carcinoma with a single course of fluorouracil, 5%, cream: A randomized clinical trial. *JAMA Dermatology*, *154*(2), 167–174. <https://doi.org/10.1001/jamadermatol.2017.3631>
- Wells, R., Gutkowitz-Krusin, D., Veledar, E., Toledano, A., & Chen, S. C. (2012). Comparison of diagnostic and management sensitivity to melanoma between dermatologists and MelaFind: A pilot study. *Archives of Dermatology*, *148*(9), 1083–1084. <https://doi.org/10.1001/archdermatol.2012.946>
- Wenande, E., Phothong, W., Bay, C., Karmisholt, K. E., Hædersdal, M., & Togsverd-Bo, K. (2019). Efficacy and safety of daylight photodynamic therapy after tailored pretreatment with ablative fractional laser or microdermabrasion: a randomized, side-by-side, single-blind trial in patients with actinic keratosis and large-area field cancerization. *British Journal of Dermatology*, *180*(4), 756–764. <https://doi.org/10.1111/bjd.17096>
- Werner, R. N., Sammain, A., Erdmann, R., Hartmann, V., Stockfleth, E., & Nast, A. (2013). The natural history of actinic keratosis: A systematic review. *British Journal of Dermatology*, *169*(3), 502–518. <https://doi.org/10.1111/bjd.12420>
- Werner, R. N., Stockfleth, E., Connolly, S. M., Correia, O., Erdmann, R., Foley, P., Gupta, A. K., Jacobs, A., Kerl, H., Lim, H. W., Martin, G., Paquet, M., Pariser, D. M., Rosumeck, S., Röwert-Huber, H. J., Sahota, A., Sanguenza, O. P., Shumack, S., Sporbeck, B., ... Nast, A. (2015). Evidence- and consensus-based (S3) Guidelines for the Treatment of Actinic Keratosis - International League of Dermatological Societies in cooperation with the European Dermatology Forum - Short version. *Journal of the European Academy of Dermatology and Venereology*, *29*(11), 2069–2079. <https://doi.org/10.1111/jdv.13180>

- Wiegell, S. R., Fabricius, S., Gniadecka, M., Stender, I. M., Berne, B., Kroon, S., Andersen, B. L., Mørk, C., Sandberg, C., Ibler, K. S., Jemec, G. B. E., Brocks, K. M., Philipsen, P. A., Heydenreich, J., Hædersdal, M., & Wulf, H. C. (2012). Daylight-mediated photodynamic therapy of moderate to thick actinic keratoses of the face and scalp: A randomized multicentre study. *British Journal of Dermatology*, *166*(6), 1327–1332. <https://doi.org/10.1111/j.1365-2133.2012.10833.x>
- Wiegell, S. R., Fabricius, S., Stender, I. M., Berne, B., Kroon, S., Andersen, B. L., Mørk, C., Sandberg, C., Jemec, G. B. E., Mogensen, M., Brocks, K. M., Philipsen, P. A., Heydenreich, J., Hædersdal, M., & Wulf, H. C. (2011). A randomized, multicentre study of directed daylight exposure times of 11/2 vs. 21/2 h in daylight-mediated photodynamic therapy with methyl aminolaevulinate in patients with multiple thin actinic keratoses of the face and scalp. *British Journal of Dermatology*, *164*(5), 1083–1090. <https://doi.org/10.1111/j.1365-2133.2011.10209.x>
- Wiegell, S. R., Hædersdal, M., Eriksen, P., & Wulf, H. C. (2009). Photodynamic therapy of actinic keratoses with 8% and 16% methyl aminolaevulinate and home-based daylight exposure: a double-blinded randomized clinical trial. *British Journal of Dermatology*, *160*(6), 1308–1314. <https://doi.org/10.1111/j.1365-2133.2009.09119.x>
- Wiegell, S. R., Hædersdal, M., Philipsen, P. A., Eriksen, P., Enk, C. D., & Wulf, H. C. (2008). Continuous activation of PpIX by daylight is as effective as and less painful than conventional photodynamic therapy for actinic keratoses; a randomized, controlled, single-blinded study. *British Journal of Dermatology*, *158*(4), 740–746. <https://doi.org/10.1111/j.1365-2133.2008.08450.x>
- Wiegell, S. R., Hædersdal, M., & Wulf, H. C. (2009). Cold water and pauses in illumination reduces pain during photodynamic therapy: A randomized clinical study. *Acta Dermato-Venerologica*, *89*(2), 145–149. <https://doi.org/10.2340/00015555-0568>
- Wiegell, S. R., Petersen, B., & Wulf, H. C. (2014). Topical corticosteroid reduces inflammation without compromising the efficacy of photodynamic therapy for actinic keratoses: A randomized clinical trial. *British Journal of Dermatology*, *171*(6), 1487–1492. <https://doi.org/10.1111/bjd.13284>
- Wiegell, S. R., Stender, I. M., Na, R., & Wulf, H. C. (2003). Pain associated with photodynamic therapy using 5-aminolevulinic acid or 5-aminolevulinic acid methylester on tape-stripped normal skin. *Archives of Dermatology*, *139*(9), 1173–1177. <https://doi.org/10.1001/archderm.139.9.1173>
- Wiegell, S. R., & Wulf, H. C. (2006). Photodynamic therapy of acne vulgaris using methyl aminolaevulinate: A blinded, randomized, controlled trial. *British Journal of Dermatology*, *154*(5), 969–976. <https://doi.org/10.1111/j.1365-2133.2005.07107.x>
- Wiegell, S. R., Wulf, H. C., Szeimies, R. M., Basset-Seguín, N., Bissonnette, R., Gerritsen, M. J. P., Gilaberte, Y., Calzavara-Pinton, P., Morton, C. A., Sidoroff, A., & Braathen, L. R. (2012). Daylight photodynamic therapy for actinic keratosis: An international consensus: International Society for Photodynamic Therapy in Dermatology. *Journal of the European Academy of Dermatology and Venereology*, *26*(6), 673–679. <https://doi.org/10.1111/j.1468-3083.2011.04386.x>
- Winkler, J. K., Sies, K., Fink, C., Toberer, F., Enk, A., Deinlein, T., Hofmann-Wellenhof, R., Thomas, L., Lallas, A., Blum, A., Stolz, W., Abassi, M. S., Fuchs, T., Rosenberger, A., & Haenssle, H. A. (2020). Melanoma recognition by a deep learning convolutional neural network—Performance in different melanoma subtypes and localisations. *European Journal of Cancer*, *127*, 21–29. <https://doi.org/10.1016/j.ejca.2019.11.020>

- Wu, X. C., Eide, M. J., King, J., Saraiya, M., Huang, Y., Wiggins, C., Barnholtz-Sloan, J. S., Martin, N., Cokkinides, V., Miller, J., Patel, P., Ekwueme, D. U., & Kim, J. (2011). Racial and ethnic variations in incidence and survival of cutaneous melanoma in the United States, 1999-2006. *Journal of the American Academy of Dermatology*, *65*(5 SUPPL. 1), S26.e1-S26.e13. <https://doi.org/10.1016/j.jaad.2011.05.034>
- Xiong, Y. D., Ma, S., Li, X., Zhong, X., Duan, C., & Chen, Q. (2016). A meta-analysis of reflectance confocal microscopy for the diagnosis of malignant skin tumours. *Journal of the European Academy of Dermatology and Venerology*, *30*(8), 1295–1302. <https://doi.org/10.1111/jdv.13712>
- Xiong, Y. D., Mo, Y., Wen, Y.-Q., Cheng, M.-J., Huo, S.-T., Chen, X.-J., & Chen, Q. (2018). Optical coherence tomography for the diagnosis of malignant skin tumors: a meta-analysis. *Journal of Biomedical Optics*, *23*(02), 1. <https://doi.org/10.1117/1.jbo.23.2.020902>
- Youl, P. H., Youlden, D. R., & Baade, P. D. (2013). Changes in the site distribution of common melanoma subtypes in Queensland, Australia over time: Implications for public health campaigns. *British Journal of Dermatology*, *168*(1), 136–144. <https://doi.org/10.1111/j.1365-2133.2012.11064.x>
- Zalaudek, I., & Argenziano, G. (2015). Dermoscopy of actinic keratosis, intraepidermal carcinoma and squamous cell carcinoma. *Current Problems in Dermatology (Switzerland)*, *46*, 70–76. <https://doi.org/10.1159/000366539>
- Zalaudek, I., Kittler, H., Marghoob, A. A., Balato, A., Blum, A., Dalle, S., Ferrara, G., Fink-Puches, R., Giorgio, C., Hofmann-Wellenhoz, R., Malvehy, J., Moscarella, E., Puig, S., Scalvenzi, M., Thomas, L., & Argenziano, G. (2008). Time Required for a Complete Skin Examination With and Without Dermoscopy. *144*(4), 509–513.
- Zeitouni, N. C., Oseroff, A. R., & Shieh, S. (2003). Photodynamic therapy for nonmelanoma skin cancers: Current review and update. *Molecular Immunology*, *39*(17–18), 1133–1136. [https://doi.org/10.1016/S0161-5890\(03\)00083-X](https://doi.org/10.1016/S0161-5890(03)00083-X)



# PUBLICATIONS



# PUBLICATION

I

**5-aminolaevulinic acid nanoemulsion is more effective than  
methyl-5-aminolaevulinate in daylight photodynamic  
therapy for actinic keratosis: a nonsponsored randomized  
double-blind multicentre trial**



Räsänen JE, Neittaanmäki N, Ylitalo L, Hagman J, Rissanen P, Ylianttila L,  
Salmivuori M, Snellman E, Grönroos M.

*Br J Dermatol.* 2019 Aug;181(2):265-274.  
doi: 10.1111/bjd.17311

**Publication reprinted with the permission of the copyright holders.**



# 5-aminolaevulinic acid nanoemulsion is more effective than methyl-5-aminolaevulinate in daylight photodynamic therapy for actinic keratosis: a nonsponsored randomized double-blind multicentre trial

J.E. Räsänen <sup>1,2</sup> N. Neittaanmäki,<sup>3</sup> L. Ylitalo,<sup>2</sup> J. Hagman,<sup>4,5</sup> P. Rissanen,<sup>6</sup> L. Ylianttila,<sup>7</sup> M. Salmivuori <sup>1</sup>, E. Snellman<sup>2</sup> and M. Grönroos<sup>1</sup>

<sup>1</sup>Department of Dermatology, Joint Authority for Päijät-Häme Health and Wellbeing, Lahti, Finland

<sup>2</sup>Department of Dermatology, Faculty of Medicine and Life Sciences, Tampere University Hospital and University of Tampere, Tampere, Finland

<sup>3</sup>Departments of Pathology and Dermatology, Institutes of Biomedicine and Clinical Sciences, Sahlgrenska Academy, University of Gothenburg, Gothenburg, Sweden

<sup>4</sup>Department of Dermatology, Vaasa Central Hospital, Vaasa, Finland

<sup>5</sup>Department of Dermatology, Faculty of Medicine, University of Turku, Turku, Finland

<sup>6</sup>Faculty of Social Sciences (Health Sciences), University of Tampere, Tampere, Finland

<sup>7</sup>Radiation and Nuclear Safety Authority of Finland (STUK), Helsinki, Finland

## Summary

### Correspondence

Janne E. Räsänen.

E-mail: [janne.rasanen@sil.fimnet.fi](mailto:janne.rasanen@sil.fimnet.fi)

### Accepted for publication

4 October 2018

### Funding sources

This study has been supported by the Cancer Foundation of Finland, the Finnish Dermatological Society, the Foundation for Clinical Chemistry Research, the University of Tampere, and the Competitive Research Financing of Tampere University Hospital.

### Conflicts of interest

No medical companies participated in funding this trial. J.E.R. has received a travel grant from Galderma. N.N. has received travel grants and speaker honoraria from Galderma, Biofrontera and Desitin Pharma. The other authors have no conflicts of interest to declare.

DOI 10.1111/bjd.17311

**Background** Daylight photodynamic therapy (DL-PDT) with methyl-5-aminolaevulinate (MAL) is an effective treatment for mild and moderate actinic keratosis (AK).

**Objectives** To assess the clinical efficacy, tolerability and cost-effectiveness of 5-aminolaevulinic acid nanoemulsion (BF-200 ALA) compared with MAL in DL-PDT for grade I–II AKs.

**Methods** This nonsponsored, prospective randomized double-blind multicentre trial included 69 patients with 767 grade I–II AKs located symmetrically on the face or scalp. A single DL-PDT was given in a randomized split-face design. The primary outcome was clearance of the AKs at 12 months as assessed by a blinded observer. The secondary outcomes were pain, treatment reactions, cosmetic outcome and the cost-effectiveness of the therapy.

**Results** In the per-patient (half-face) analysis, clearance was better for the BF-200 ALA sides than for those treated with MAL ( $P = 0.008$ ). In total, BF-200 ALA cleared 299/375 AKs (79.7%) and MAL 288/392 (73.5%) ( $P = 0.041$ ). The treatment was practically painless with both photosensitizers, the mean pain visual analogue scale being 1.51 for BF-200 ALA and 1.35 for MAL ( $P = 0.061$ ). Twenty-six patients had a stronger skin reaction on the BF-200 ALA side, seven on the MAL side and 23 displayed no difference ( $P = 0.001$ ). The cosmetic outcome was excellent or good in > 90% of cases with both photosensitizers ( $P = 1.000$ ). The cost-effectiveness plane showed that the costs of DL-PDT were similar for both photosensitizers, but the effectiveness was slightly higher for BF-200 ALA.

**Conclusions** Our results indicate that BF-200 ALA is more effective than MAL in DL-PDT for grade I–II AKs. BF-200 ALA provides slightly better value for money than MAL.

### What's already known about this topic?

- Daylight photodynamic therapy (DL-PDT) with methylaminolaevulinate (MAL) is effective and practically painless for mild or moderate actinic keratosis (AK). Its long-term efficacy or cost-effectiveness is rarely reported.

### What does this study add?

- A single treatment with 5-aminolaevulinic acid nanoemulsion (BF-200 ALA) was shown in a 12-month follow-up to be more effective than MAL for use in DL-PDT given in a split-face design for grade I-II AKs. BF-200 ALA provides slightly better value for money than MAL.

Actinic keratosis (AK) is a chronic and increasingly prevalent disease in fair-skinned individuals with a history of chronic sun exposure.<sup>1,2</sup> Because field cancerization, i.e. chronically sun-damaged skin with recurrent AKs, increases the risk of nonmelanoma skin cancer,<sup>3</sup> early field-directed therapy is recommended for AKs.<sup>4,5</sup>

Photodynamic therapy (PDT), enabling treatment of large fields at one time, is effective for treating AKs and field cancerization,<sup>6–8</sup> but one drawback with conventional treatment (LED-PDT) is pain during illumination. Daylight photodynamic therapy (DL-PDT) is just as effective as LED-PDT for thin and moderate AKs and provides practically painless illumination while leading to high patient satisfaction.<sup>9–13</sup> Recent studies have shown the long-term efficacy of DL-PDT to be comparable with that of LED-PDT.<sup>14</sup>

Three photosensitizers have previously been studied for use in DL-PDT: methyl-5-aminolaevulinic acid (MAL), 5-aminolaevulinic acid nanoemulsion (BF-200 ALA) and low-concentration hexyl-5-aminolaevulinic acid.<sup>15–19</sup> In our earlier pilot study comparing MAL and BF-200 ALA when used in DL-PDT for grade I–III AKs, BF-200 ALA tended to show better efficacy.<sup>16,17</sup>

The aim of the present work was to verify the results of our pilot study in a larger multicentre setting by comparing the long-term 12-month efficacy and tolerability of BF-200 ALA and MAL in DL-PDT for mild or moderate AKs.

## Patients and methods

### Study design

This was a nonsponsored prospective multicentre trial comparing BF-200 ALA and MAL in a randomized, double-blind split-face setting (see [clinicaltrials.gov](http://clinicaltrials.gov) identifier number: NCT02464709). The protocol complied with the Declaration of Helsinki and was approved by the local ethics committee of Tampere University Hospital. Informed written consent was obtained from all participants.

### Photosensitizers

The photosensitizers used were BF-200 ALA gel 78 mg g<sup>-1</sup> (Ameluz<sup>®</sup>, Biofrontera AG, Leverkusen, Germany) and MAL cream 160 mg g<sup>-1</sup> (Metvix<sup>®</sup>, Galderma Nordic AB, Uppsala, Sweden).

### Participants and centres

The patients were enrolled by the investigators M.G., L.Y., J.H., M.S. and J.E.R. between June 2015 and September 2016 at three Finnish treatment centres: Päijät-Häme Central Hospital, Lahti (61°N), Tampere University Hospital, Tampere (61°N), and Vaasa Central Hospital, Vaasa (63°N). The trial enrolment ended when a predefined sample size had been achieved. The patients were aged over 18 years and had thin or moderately thick grade I–II AKs on the face or scalp. These AKs were required to be symmetrically located with at least three clear examples on each side of the face or scalp to form two symmetrical treatment fields. The exclusion criteria were: (i) thick grade III AKs, (ii) a diffuse field-cancerized area where the AK count could not be assessed, (iii) earlier treatment of the same area for AKs within the preceding 6 months, (iv) porphyria or photosensitivity, (v) allergy to either photosensitizer, (vi) pregnancy or breastfeeding, or (vii) impaired general condition which might hinder the required 2-h stay outdoors.

### Randomization

The validated web-based program used for randomization (Research Randomizer, <http://www.randomizer.org/>) generated the numbers 1 and 2 at random to assign the treatment sides (1 = BF-200 ALA right, MAL left; 2 = MAL right, BF-200 ALA left). N.N. conducted the randomization and concealed the results in numbered envelopes. The observer who conducted the follow-up visits (J.E.R.), was blinded, like the patients, with respect to the randomization.

### Clinical grading and lesion mapping

A detailed flowchart of the study is shown in Figure 1. The AKs were first outlined in two symmetrical and equal-sized treatment fields on both sides of the face or scalp (Fig. 2). The lesions falling within these fields were counted and assigned clinically to grade I or II according to Olsen *et al.*:<sup>20</sup> I, thin (slightly palpable AK, more easily felt than seen); II, moderate (moderately thick AK, easily felt). The AKs and treatment fields were marked on the skin, drawn on transparent plastic film and photographed.

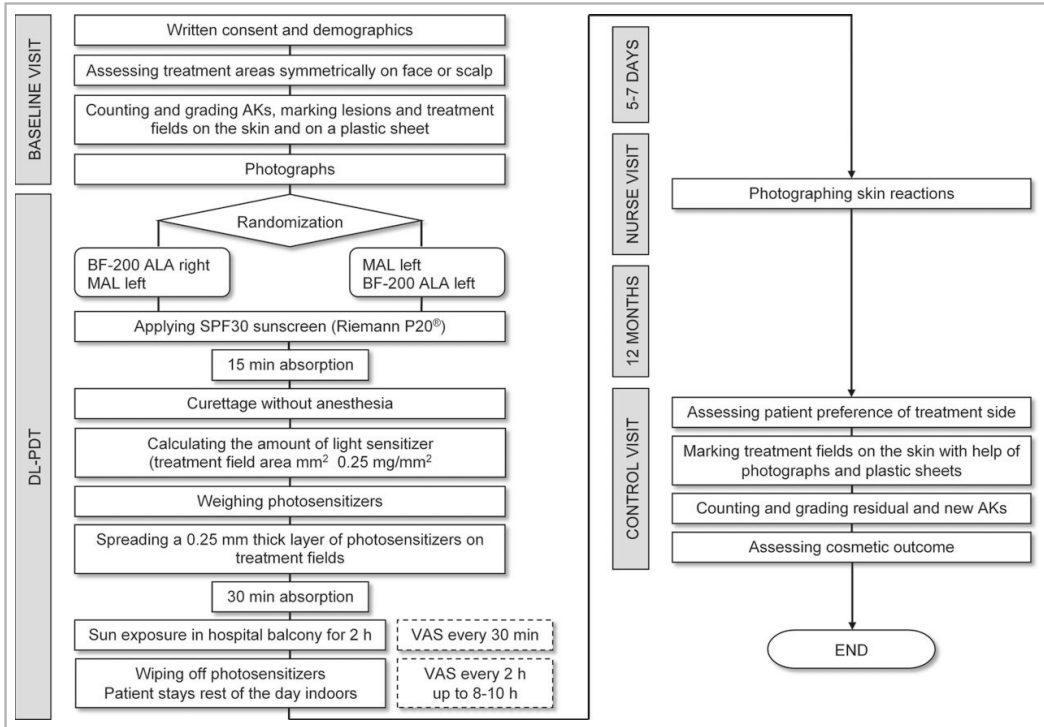


Fig 1. Flowchart of the protocol. AKs, actinic keratoses; BF-200 ALA, 5-aminolaevulinic acid nanoemulsion; MAL, methyl-5-aminolaevulinate; SPF, sun protection factor; DL-PDT, daylight photodynamic therapy; VAS, visual analogue scale.

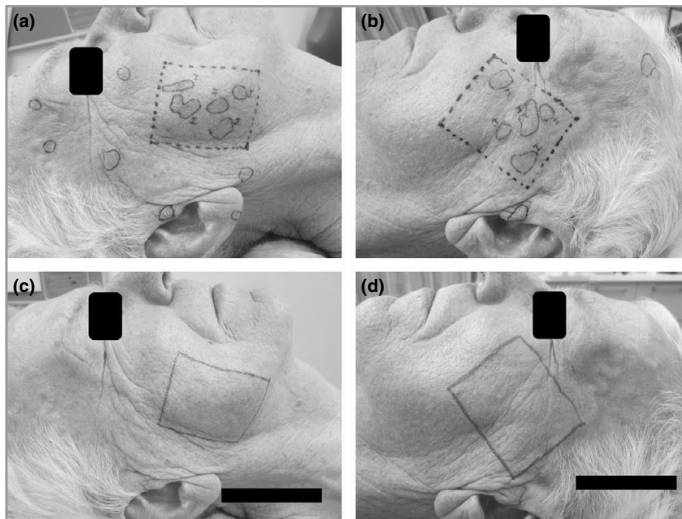


Fig 2. Photograph of a patient with symmetrical actinic keratosis on the cheek and a complete response of the treatment fields at 12 months: (a) the 5-aminolaevulinic acid nanoemulsion (BF-200 ALA) site at baseline, (b) the methyl-5-aminolaevulinate (MAL) site at baseline, (c) clinical response of the BF-200 ALA site at 12 months, (d) MAL clinical response at 12 months.

### Treatment procedure

The patients received a single DL-PDT treatment in this randomized split-face design using BF-200 ALA on one side and MAL on the other. The treatment procedures were conducted by the nonblinded investigators M.G., L.Y., J.H. and M.S.

A SPF30 sun protection cream (P20<sup>®</sup>, Riemann A/S, Hillerød, Denmark) was applied on all sun-exposed areas, including the treatment fields. After 15 min the treatment fields were superficially curettaged to remove the crusts. A 0.25-mm layer of BF-200 ALA gel or MAL cream was applied to each side of the face according to the randomization, the amount of photosensitizer being calculated from the formula (treatment area mm<sup>2</sup> \* 0.25 mg mm<sup>-2</sup>) and weighed on a balance to achieve a 0.25-mm layer. After an absorption time of 30 min the patients were guided to the hospital balcony or yard for a 2-h exposure to daylight. Afterwards, the photosensitizers were wiped off and patients were advised to stay indoors for the rest of the day.

### Weather and protoporphyrin IX-weighted light dose measurement

The weather and temperature were documented at the beginning and end of the daylight exposure. The cumulative protoporphyrin IX (PpIX)-weighted light dose was recorded at Päijät-Häme Central Hospital with a light dosimeter (X9-7, Gigahertz-Optik, Türkenfeld, Germany) equipped with a blue light hazard sensor (UV-3709-4, Gigahertz-Optik) to mimic the absorption spectrum of PpIX. The meter and sensor were calibrated for the PpIX-weighted light dose with a spectroradiometer (S2000, Ocean Optics, Seminole, FL, U.S.A.) by the Radiation and Nuclear Safety Authority of Finland (STUK).

### Efficacy assessment

The primary outcome was clinical clearance of the treated lesions as assessed at 12 months by a blinded observer (J.E.R.) who was not involved in the treatment procedure. With the aid of plastic sheets and clinical photographs the residual lesions in both treatment fields were counted and graded clinically as either cleared (disappearance of the lesion visually and on palpation) or of AK grades I–III according to Olsen *et al.*<sup>20</sup>

### Safety and tolerability assessment

The secondary outcomes of the study were (i) pain during daylight illumination, (ii) severity of the skin reaction 5–7 days after treatment, and (iii) the cosmetic result on both sides at 12 months.

During the daylight illumination the patients filled in visual analogue scales (VAS 0–10) depicting pain<sup>21</sup> separately for each treatment side at 30-min intervals and at 2-h intervals for up to 8–10 h after illumination. To evaluate the local skin reactions (erythema, crusting), a nurse photographed both sides on days 5–7 after the DL-PDT treatment. The blinded

observer (J.E.R.) assessed the severity of the skin reaction from photographs on a scale of 1–4 (1, negligible; 2, mild; 3, moderate; 4, severe). The cosmetic outcome was assessed separately for both sides at the 12-month follow-up visit by the same blinded observer (1, excellent; 2, good; 3, moderate; 4, poor), and the patient was asked which treatment he or she preferred (right side, left side or no preference).

### Sample size

The sample size was calculated for two outcome parameters separately. Firstly, based on the clinical response rate at 3 months in our earlier pilot study we assumed clinical clearance rates of 84.5% for BF-200 ALA and 74.1% for MAL.<sup>16</sup> Using an  $\alpha$  error of 0.05 and a power of 0.80, we calculated the desired sample size to be 256 AK lesions for each group, BF-200 ALA and MAL. Secondly, based on the total clearance of treatment fields at 12 months in the follow-up to the same pilot study,<sup>17</sup> we assumed an odds ratio for total clearance of 3.50 between the two treatments and a total clearance for the control group of 25%. Using an  $\alpha$  error of 0.05 and a power of 0.90 we arrived at a sample size of 69 subjects. Thus, we ended up with a minimum sample size of 69 patients (having a minimum of three AKs per treatment side).

### Statistical analysis

The statistical analyses were performed using IBM SPSS Statistics, Version 23.0 (IBM Corp., Armonk, NY, U.S.A.).

Differences in baseline lesion distribution, complete lesion clearance, partial response in clinical grading, count of new lesions and the differences in lesion clearance between the weather groups were tested for statistical significance using Fisher's exact test. Per-patient (half-face) differences in the baseline lesion count, lesion clearance, cosmetic outcome, local skin reaction severity and the VAS pain score were tested using Wilcoxon's signed-rank test. The existence of treatment effects on the lesion response due to weather conditions, temperature and the light dose was tested using the Kruskal–Wallis test. Individually, temperatures and light doses were tested using the Mann–Whitney test to ascertain whether they introduced an added variance component into the lesion clearance data. *P*-values < 0.05 were considered statically significant.

### Assessment of costs and cost-effectiveness

BF-200 ALA gel is approved for use in Finland, but is not currently imported. The gel used for the study was ordered separately for research purposes. Consequently, for the cost-effectiveness analysis (CEA) we used the prices obtained from the Swedish drug database (FASS, Farmaceutiska Specialiteter i Sverige, [www.fass.se](http://www.fass.se)). In practice, the prices for the two photosensitizer precursors were almost identical (Ameluz 201 € per 2-g tube and Metvix 205 € per 2-g tube). The other costs involved in the DL-PDT treatment were estimated to be similar



to those in our earlier cost-effectiveness study, other than that of the anaesthetic, which was not used in the present study.<sup>22</sup>

In the CEA, BF-200 ALA was regarded as the intervention and MAL as the control treatment. The total cost of treatment (C) was defined as the cost of the photosensitizer for each patient together with the mean societal and patients' costs for DL-PDT derived from our earlier study (Table 1).<sup>22</sup> The effectiveness (E) was defined as the field lesion clearance at 12 months for each patient's treatment field (ranging between 0 and 1). The CEA was performed to generate the incremental cost-effectiveness ratio (ICER) and uncertainty was assessed using 10 000 bootstrapping iterations. The results are presented in the form of a cost-effectiveness plane.

## Results

### Baseline characteristics

Altogether 73 patients were enrolled. Four were excluded from the analyses (one passed away due to unrelated causes, one had psoriasis plaques in the treatment fields, one had thick grade III AKs and one had only one AK in each treatment field).

All the remaining 69 patients, 43 men and 26 women, mean age 74.8 years (range 49–92), completed the study. Twelve had Fitzpatrick's skin phototype I, 41 phototype II and 16 phototype III. The patients had previous histories of skin cancers as follows: AK, *n* = 40 (58%); Bowen disease, *n* = 8 (11.6%); squamous cell carcinoma (SCC), *n* = 4 (5.8%); basal cell carcinoma, *n* = 25 (36.2%); melanoma in situ, *n* = 2 (2.9%); and malignant melanoma, *n* = 2 (2.9%). Previously, with a minimum 6-month wash-out period, 32 (46.4%) patients had received cryotherapy, eight (11.6%) DL-PDT, 10 (14.5%) LED-PDT, three (4.3%) imiquimod, three (4.3%) diclofenac gel and three (4.3%) surgery for the treatment fields. Fifty-one patients (74%) had not received PDT previously.

The baseline lesion characteristics are shown in Table 2. The distribution of AK grades between the sides was equal (*P* = 0.504). In the per-patient (half-face) analysis there was

no significant difference in the baseline lesion count for all lesions (*P* = 0.175), nor for grade I (*P* = 0.055) or grade II lesions separately (*P* = 0.935).

### Weather conditions and light dose

The daylight exposures were carried out between 9.00 h and 17.00 h, the weather being sunny for 45 patients (65.2%), partially cloudy for 16 (23.2%) and completely cloudy for eight (11.6%). DL-PDT was not conducted in rainy weather. The mean temperature was +20.4 °C (range 8.5–29 °C). The PpIX-weighted light dose was measured for 27 patients, giving a mean dose of 12.89 J cm<sup>-2</sup> (range 5.96–17.93).

### Primary outcome: 12-month clearance rates

The per-patient (half-face) analysis pointed to a significant difference in clinical lesion clearance between the BF-200 ALA and MAL groups. More lesions were cleared on the BF-200 ALA side than on the MAL side in 33 cases and more on the MAL side in 16, while no difference was found between the sides in 20 patients (*P* = 0.008). In the half-face analysis, no significant difference was seen in the clearance of grade I (*P* = 0.051) or grade II (*P* = 0.157) lesions when considered separately.

The complete clearance rates are shown in Table 3 and Figure 3. BF-200 ALA cleared significantly more AKs than did MAL, *P* = 0.041.

Complete field clearance at 12 months (the treatment field being completely clear of all AKs) was the same for both treatments: 19 of 69 (27.5%) in both groups (*P* = 1.000). Any residual lesions clearly located separately from the baseline lesions marked on the plastic sheet were classified as new lesions. Of the 50 fields in the BF-200 ALA group that were not completely cleared, 30 had only residual AKs, seven only new AKs and 13 both. In the MAL group 34 of the 50 fields had only residual AKs, three only new AKs and 13 both (*P* = 0.446). The characteristics of the residual lesions are shown in Table 3.

**Table 1** Cost items, unit costs and mean total costs of daylight photodynamic therapy (DL-PDT) using BF-200 ALA and MAL as photosensitizer precursors for the treatment of actinic keratosis (AK)

Cost item	Unit costs	Costs per patient, €, mean ± SD	
		BF-200 ALA	MAL
<b>Societal costs</b>			
Nurse's time with the patient	19 €/h	17.10	17.10
Doctor's time for the treatment	30.20 €/h	9.00	9.00
Treatment room rent	1.50 €/h	1.40	1.40
Photosensitizer cost BF-200 ALA	100.63 €/g	81.50 ± 43.30	–
Photosensitizer cost MAL	102.60 €/g	–	83.10 ± 44.10
Sunscreen	0.10 €/mL	1.60	1.60
<b>Patient's costs</b>			
Patients' (pensioner's) time used for the treatment	8.60 €/h	40.40	40.40
Patients' travel costs	0.45 €/h	25.00	25.00
Mean total costs		176.40 ± 43.50	178.00 ± 44.30

**Table 2** Patient characteristics and numbers of actinic keratoses (AK) at baseline

Characteristic	Total, n = 69	BF-200 ALA	MAL	P-value
Sex, n (%)				
Male	43 (62)			
Female	26 (38)			
Age, mean $\pm$ SD (range)	74.8 $\pm$ 7.1 (49–92)			
Treatment field area, cm <sup>2</sup> , mean $\pm$ SD (range)		32.6 $\pm$ 17.3 (4–104)	32.6 $\pm$ 17.3 (4–104)	
Amount of photosensitizers, mg, mean $\pm$ SD (range)		810 $\pm$ 430 (100–2600)	810 $\pm$ 430 (100–2600)	
Baseline AKs per patient, mean $\pm$ SD (range)				
All	11.1 $\pm$ 4.8 (4–32)	5.4 $\pm$ 2.5 (2–15)	5.7 $\pm$ 2.6 (2–17)	0.175
Grade I	8.6 $\pm$ 3.8	4.0 $\pm$ 2.3	4.5 $\pm$ 1.9	0.055
Grade II	3.9 $\pm$ 3.0	1.9 $\pm$ 1.5	1.9 $\pm$ 1.6	0.935
Number of baseline AKs, N				
All	767	375	392	0.504
Grade I	577	278	299	
Grade II	190	97	93	

BFA-200 ALA, 5-aminolaevulinic acid nanoemulsion; MAL, methyl-5-aminolaevulinic acid.

**Table 3** Actinic keratosis lesion counts and clinical lesion response rates

	Baseline Total lesions	12 months			Response rate			95% CI
		Total lesions	Residual	New	PR (%)	NR (%)	CR (%)	
<b>BF-200 ALA</b>								
Total	375	112	76	36			299 (79.7)	75.4–83.5
Grade I	278	87	55	32		46	232 (83.5)	78.6–87.4
Grade II	97	22	18	4	17	13	67 (69.1)	59.3–77.4
Grade III (residuals)	0	3	3	0				
<b>MAL</b>								
Total	392	134	104	30			288 (73.5)	68.9–77.6
Grade I	299	112	86	26		61	238 (79.6)	74.7–83.8
Grade II	93	21	17	4	31	12	50 (53.8)	43.7–63.5
Grade III (residuals)	0	1	1	0				
P-values	0.504						All, <b>0.041</b> Grade I, 0.241 Grade II, <b>0.037</b>	

CI, confidence interval; CR, complete response (lesion clearance); NR, no response; PR, partial response.

One patient developed a hyperkeratotic residual lesion which was excised 9 months after DL-PDT to exclude SCC. The histopathological diagnosis revealed AK of grade II and the lesion was regarded as a residual. None of the other 68 patients had lesions treated between the exposure visit and the 12-month follow-up.

### Secondary outcomes: safety and tolerability

Both treatments were well tolerated overall and almost painless. Pain scores, skin reactions (erythema, crusting) and cosmetic outcomes are shown in Table 4. Twenty-six patients had a stronger reaction on the BF-200 ALA side, seven on the MAL side and 23 displayed no difference,  $P = 0.001$ . The intensity of the skin reaction did not correlate with lesion clearance (BF-200 ALA  $P = 0.362$ , MAL  $P = 0.624$ ). The cosmetic outcomes were similar (Table 4). Twelve patients preferred BF-200 ALA, 12 MAL and 56 had no preference.

### Ancillary analyses: treatment month, weather and light dose vs. treatment efficacy

The weather conditions and light doses are shown in Table 4. For both photosensitizers the lesion clearance rate differed significantly between the weather groups. The temperatures differed significantly between the weather groups ( $P = 0.000$ ), but the light dose did not ( $P = 0.103$ ).

For MAL we found a significant treatment effect between lesion clearance (all lesions) and temperature ( $P = 0.025$ ), whereas for BF-200 ALA only a tendency was seen ( $P = 0.112$ ). No treatment effect between light dose and lesion clearance was found for either BF-200 ALA or MAL.

### Cost-effectiveness analysis

The imputed mean total costs per patient were 176.40 € for BF-200 ALA [95% confidence interval (CI) 165.90–186.90] and

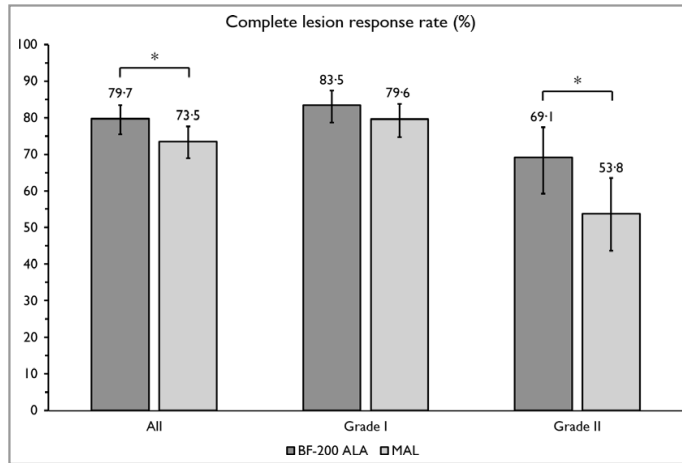


Fig 3. Clinical lesion response rates at 12 months. \*P-value < 0.05.

Table 4 Weather conditions for daylight photodynamic therapy (DL-PDT): light doses, temperatures and lesion clearance rates (%) in the weather groups. Pain during daylight exposure, severity of skin reaction and cosmetic outcome at 12 months

	n	Light dose (J cm <sup>-2</sup> )	Temperature (°C)	BF-200 ALA	MAL	P-value
Weather conditions		Mean ± SD	Mean ± SD	Clearance rate, %	clearance rate, %	
Sunny	45	13.3 ± 2.7	22.1 ± 4.0	83.5	77.5	
Half cloudy	16	13.0 ± 3.3	18.2 ± 4.7	73.1	69.1	
Completely cloudy	8	7.9 ± 2.2	15.3 ± 3.0	69.8	51.4	
P-value		0.103	<b>0.000</b>	<b>0.028</b>	<b>0.004</b>	
Pain VAS, mean ± SD				1.51 ± 1.61	1.35 ± 1.45	0.061
Severity of skin reaction				n (%)	n (%)	<b>0.001</b>
1, negligible				14 (25)	26 (46)	
2, mild				27 (48)	23 (41)	
3, moderate				13 (23)	6 (11)	
4, severe				2 (4)	1 (2)	
Cosmetic outcome at 12 months				n (%)	n (%)	1.000
1, excellent				38 (55)	35 (51)	
2, good				25 (36)	30 (43)	
3, moderate				6 (9)	4 (6)	
4, poor				0 (0)	0 (0)	

BFA-200 ALA, 5-aminolaevulinic acid nanoemulsion; MAL, methyl-5-aminolaevulinate; VAS, visual analogue scale.

178.00 € for MAL (95% CI 167.30–188.70), yielding an incremental cost saving of –1.60 € (Table 5). The mean field lesion clearances were 0.784 for BF-200 ALA (95% CI 0.728–0.839) and 0.701 for MAL (95% CI 0.628–0.774), thus resulting in an increase in the field lesion clearance of 0.083. The ICER demonstrated a monetary saving of –19.37 € per unit of effectiveness gained. The cost-effectiveness (CE) plane showed that the costs of DL-PDT for both photosensitizers were similar (in 58.7% of the simulated replica data MAL was more costly) but the effectiveness was slightly higher for BF-200 ALA (in 96.4% of the simulated data BF-200 ALA was more effective). Approximately 57% of the simulated replica data lie on the south-eastern part of the plane, indicating that BF-200 ALA provides a slightly better value for money than MAL (see Fig. 4).

## Discussion

We present here a comparison between two photosensitizers, BF-200 ALA and MAL, used in DL-PDT for grade I–II AKs. Our results confirm that BF-200 ALA is more effective than MAL in a long-term follow-up of 12 months.

Most earlier studies have focused on short-term efficacy (a follow-up of 3 months), with reported lesion clearance rates after a single treatment with MAL DL-PDT of 74–79% in various Nordic countries,<sup>9,15,16,18,23,24</sup> 70–83% in Central and Southern Europe<sup>12,14,25,26</sup> and 86–89% in Brazil and Australia.<sup>11,27</sup> Because AK is regarded as a chronic disease with a constant progression of spontaneous relapses,<sup>28</sup> the 12-month follow-up is a more reliable outcome, showing the need for re-treatments.

Table 5 Incremental cost-effectiveness ratio (ICER)

	Effectiveness (E)		Costs (C)		ICER € per field lesion clearance
	Field lesion clearance	Incremental effectiveness	Per patient, €	Incremental cost, €	
BF-200 ALA	0.784		176.40		
MAL	0.701	0.083	178.00	-1.6	-19.37

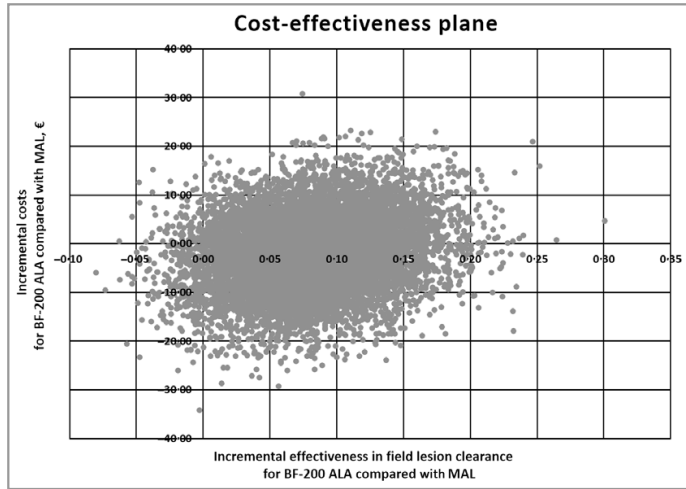


Fig 4. Incremental CE plane representing the incremental CE of DL-PDT using BF-200 ALA relative to DL-PDT using MAL for the treatment of actinic keratoses based on 10 000 simulated replica data items. Approximately 57% of the simulated replica data lie in the south-eastern part of the plane, indicating that BF-200 ALA provides slightly better value for money than MAL. BFA-200 ALA, 5-aminolaevulinic acid nanoemulsion; CE, cost-effectiveness; DL-PDT, daylight photodynamic therapy; MAL, methyl-5-aminolaevulinate.

There have been only a few assessments of the long-term efficacy of DL-PDT. In our earlier pilot studies the clinical lesion clearance rates after DL-PDT for grade I–III AKs at 12 months were 87% for BF-200 ALA and 62–66% for MAL, with an added remark that the grade I AKs had been treated once but grades II–III AKs twice.<sup>17,19</sup> In another recent study, the 12-month clearance rate for grade I–II AKs in MAL DL-PDT was 71.8% compared with 73.7% in MAL LED-PDT.<sup>14</sup> Our present lesion clearance rates at 12 months were 79.7% for BF-200 ALA and 73.5% for MAL, i.e. the clearance rate for BF-200 ALA was slightly lower than in our pilot study, which could be due to the fact that only a single DL-PDT treatment was given in this multicentre trial.

It is of clinical and economic importance to assess complete field clearance, although it has been argued that this is not as relevant an outcome indicator as the lesion clearance rate, as it is strongly biased by the area of the treatment field, the number of treatments, the follow-up time and the number of baseline lesions.<sup>29</sup> In the present study the field clearance was 27% for both photosensitizers, and in our earlier pilot study the complete field clearances at 12 months were 69% for BF-200 ALA and 23% for MAL.<sup>17</sup> This difference could be explained by the single treatment given in this trial, which may have

resulted in more residual lesions. Other studies have reported complete field clearances of 36–55% in MAL DL-PDT<sup>25,26</sup> and 75% in simulated DL-PDT with BF-200 ALA (two treatment sessions), at 3 months in both cases.<sup>30</sup> Due to the chronic course of AKs, clearance of the whole treatment field at 12 months is expected to be lower than at 3 months. Our results indicate that in most patients a single dose of DL-PDT may not suffice for the treatment of field cancerization or for preventing further AKs, which highlights the chronic nature of these lesions. The chronicity of AK is also apparent in our sample, with 58% of the patients having a previous history of treated AKs. Interestingly, our sample contained more male than female participants, which is in concordance with earlier reports.<sup>31</sup> However, there is no evidence that sex affects treatment efficacy.

LED-PDT has been shown to be more painful with BF-200 ALA than with MAL,<sup>32</sup> but the pain is significantly reduced in DL-PDT due to the low accumulation and continuous low-level activation of PpIX. This trend for reduced pain is shown in our present findings for both BF-200 ALA and MAL. VAS pain scores for DL-PDT have previously ranged between 0.7 and 2.1,<sup>11,12,15,16,23–26,33</sup> and our results are in accordance with this.

BF-200 ALA penetrates deeper into the epidermis and causes higher PpIX accumulation than MAL,<sup>34</sup> and accordingly the treatment reactions in our trial at 1 week (erythema, crusting) were stronger on the BF-200 ALA-treated sides than on the MAL sides. Significantly more moderate or severe skin reactions occurred on the BF-200 ALA sides (13 moderate, 2 severe) than on the MAL sides (6 moderate, 1 severe). The severity of the treatment reaction did not correlate with the treatment efficacy. The cosmetic outcome 12 months after DL-PDT was excellent or good in > 90% of cases in both treatments, which agrees with earlier DL-PDT studies.<sup>10–12,26</sup>

An adequate temperature, suitable weather and a sufficient light dose have been thought to be necessary for DL-PDT to achieve a successful outcome, but the protocol is still unclear. To overcome the variables of outdoor treatment, simulated daylight-PDT (sDL-PDT), with the advantages of a steady light dose and temperature, has been developed. In one retrospective study the use of BF-200 ALA in sDL-PDT led to a high lesion clearance rate of 92.8% at 3 months after two treatments.<sup>30</sup> Interestingly, we found that our treatment was more effective on sunny days and that there was a tendency for better clearance rates at higher light doses. Wiegell *et al.* have suggested that a sufficient PpIX-weighted light dose for use in DL-PDT would be either > 3.5 or > 8 J cm<sup>-2</sup>.<sup>9,15</sup> The average PpIX light dose in our study was 12.89 J cm<sup>-2</sup> (range 5.96–17.93) and in only two patients did the dose remain below 8 J cm<sup>-2</sup>. We failed to find any significant treatment effect between light dose and lesion clearance rate, nor could we identify a cut-off level below which the daylight dose might be less effective. One limitation was that light doses were measured at only one treatment centre (27 patients).

The CEA indicates that BF-200 ALA provides a slightly better value for money than MAL. Because the costs of the two photosensitizer precursors do not differ essentially and BF-200 ALA is slightly more effective than MAL, BF-200 ALA would be a more favourable choice in terms of cost-effectiveness. In our analysis the prices of the photosensitizer precursors were almost the same, but these prices, especially that of BF-200 ALA, vary among European countries, which may lead to even clearer differences in cost-effectiveness.

There were some limitations involved in our study. Firstly, even though the patient preference was assessed, the cosmetic outcome and the skin reaction were not reported from the patient's perspective separately. Secondly, the blinding of the patients with regard to the photosensitizer precursors was not absolute due to the different formulations (gel vs. cream). Thirdly, there were no untreated control patients in our study. Also, one limitation of the CEA was that quality-adjusted life years could not be incorporated due to the study design. The strengths of this study lie in its large sample size, the prospective split-face design with the patients serving as their own controls and the long-term follow-up of 12 months. Admittedly, only a single DL-PDT treatment was given, but high lesion clearance rates were achieved. However, it is evident that repeated treatments could lead to still higher field clearances.

In conclusion, the present results indicate that, as assessed in a long-term follow-up of 12 months, BF-200 ALA was more effective than MAL for use in DL-PDT for grade I–II AKs. BF-200 ALA showed significantly higher clearance rates in both the per-lesion and per-patient (half-face) analyses. The skin reaction a week after DL-PDT was more intense for BF-200 ALA, but there were no significant differences in pain scores, cosmetic outcome or patient preference. The use of BF-200 ALA may provide better value for money than MAL.

## Acknowledgments

We would like to thank the nurses Ulla Oesch-Lääveri at Päijät-Häme Central Hospital, Tiina Mäki at Tampere University Hospital and Isabella Norrgård at Vaasa Central Hospital, for their invaluable contributions to this study.

## References

- 1 Frost CA, Green AC. Epidemiology of solar keratoses. *Br J Dermatol* 1994; **131**:455–64.
- 2 Schaefer I, Augustin M, Spehr C *et al.* Prevalence and risk factors of actinic keratoses in Germany – analysis of multisource data. *J Eur Acad Dermatol Venereol* 2014; **28**:309–13.
- 3 Braakhuis BJ, Tabor MP, Kummer JA *et al.* A genetic explanation of Slaughter's concept of field cancerization: evidence and clinical implications. *Cancer Res* 2003; **63**:1727–30.
- 4 Werner RN, Stockfleth E, Connolly SM *et al.* Evidence- and consensus-based (S3) Guidelines for the Treatment of Actinic Keratosis – International League of Dermatological Societies in cooperation with the European Dermatology Forum – Short version. *J Eur Acad Dermatol Venereol* 2015; **29**:2069–79.
- 5 de Berker D, McGregor JM, Mohd Mustapa MF *et al.* British Association of Dermatologists' guidelines for the care of patients with actinic keratosis 2017. *Br J Dermatol* 2017; **176**:20–43.
- 6 Morton CA, Szeimies RM, Sidoroff A, Braathen LR. European Guidelines for Topical Photodynamic Therapy part 1: treatment delivery and current indications – actinic keratoses, Bowen's disease, basal cell carcinoma. *J Eur Acad Dermatol Venereol* 2013; **27**:536–44.
- 7 Morton CA, Szeimies RM, Sidoroff A, Braathen LR. European Guidelines for Topical Photodynamic Therapy part 2: emerging indications – field cancerization, photorejuvenation and inflammatory/infective dermatoses. *J Eur Acad Dermatol Venereol* 2013; **27**:672–9.
- 8 Braathen LR, Morton CA, Basset-Seguín N *et al.* Photodynamic therapy for skin field cancerization: an international consensus. *International Society for Photodynamic Therapy in Dermatology. J Eur Acad Dermatol Venereol* 2012; **26**:1063–6.
- 9 Wiegell SR, Fabricius S, Gniadecka M *et al.* Daylight-mediated photodynamic therapy of moderate to thick actinic keratoses of the face and scalp: a randomized multicentre study. *Br J Dermatol* 2012; **166**:1327–32.
- 10 Braathen LR. Daylight photodynamic therapy in private practice in Switzerland: gain without pain. *Acta Derm Venereol* 2012; **92**:652–3.
- 11 Rubel DM, Spelman L, Murrell DF *et al.* Daylight photodynamic therapy with methyl aminolevulinate cream as a convenient, similarly effective, nearly painless alternative to conventional photodynamic therapy in actinic keratosis treatment: a randomized controlled trial. *Br J Dermatol* 2014; **171**:1164–71.
- 12 Lacour JP, Ulrich C, Gilaberte Y *et al.* Daylight photodynamic therapy with methyl aminolevulinate cream is effective and nearly

- painless in treating actinic keratoses: a randomised, investigator-blinded, controlled, phase III study throughout Europe. *J Eur Acad Dermatol Venerol* 2015; **29**:2342–8.
- 13 See JA, Gebauer K, Wu JK *et al.* High patient satisfaction with daylight-activated methyl aminolevulinate cream in the treatment of multiple actinic keratoses: results of an observational study in Australia. *Dermatol Ther (Heidelb)* 2017; **7**:525–33.
- 14 Sotiriou E, Evangelou G, Papadavid E *et al.* Conventional vs. daylight photodynamic therapy for patients with actinic keratosis on face and scalp: 12-month follow-up results of a randomized, intra-individual comparative analysis. *J Eur Acad Dermatol Venerol* 2018; **32**:595–600.
- 15 Wiegell SR, Haedersdal M, Eriksen P, Wulf HC. Photodynamic therapy of actinic keratoses with 8% and 16% methyl aminolevulinate and home-based daylight exposure: a double-blinded randomized clinical trial. *Br J Dermatol* 2009; **160**:1308–14.
- 16 Neittaanmaki-Perttu N, Karppinen TT, Gronroos M *et al.* Daylight photodynamic therapy for actinic keratoses: a randomized double-blinded non-sponsored prospective study comparing 5-aminolevulinic acid nanoemulsion (BF-200) with methyl-5-aminolevulinate. *Br J Dermatol* 2014; **171**:1172–80.
- 17 Neittaanmaki-Perttu N, Gronroos M, Tani T, Snellman E. Long-term outcome of daylight photodynamic therapy with amino-5-laevulinate nanoemulsion vs. methyl-5-aminolevulinate for actinic keratoses. *Acta Derm Venerol* 2016; **96**:712–13.
- 18 Neittaanmaki-Perttu N, Gronroos M, Karppinen TT *et al.* Hexyl-5-aminolevulinate 0.2% vs. methyl-5-aminolevulinate 16% daylight photodynamic therapy for treatment of actinic keratoses: results of a randomized double-blinded pilot trial. *Br J Dermatol* 2016; **174**:427–9.
- 19 Neittaanmaki-Perttu N, Karppinen TT, Tani T *et al.* Long-term outcome of low-concentration hexyl-5-aminolevulinate daylight photodynamic therapy for treatment of actinic keratoses. *Acta Derm Venerol* 2017; **97**:120–1.
- 20 Olsen EA, Abernethy ML, Kulp-Shorten C *et al.* A double-blind, vehicle-controlled study evaluating masoprocol cream in the treatment of actinic keratoses on the head and neck. *J Am Acad Dermatol* 1991; **24**:738–43.
- 21 Hawker GA, Mian S, Kendzerska T, French M. Measures of adult pain: Visual Analog Scale for Pain (VAS Pain), Numeric Rating Scale for Pain (NRS Pain), McGill Pain Questionnaire (MPQ), Short-Form McGill Pain Questionnaire (SF-MPQ), Chronic Pain Grade Scale (CPGS), Short Form-36 Bodily Pain Scale (SF-36 BPS), and Measure of Intermittent and Constant Osteoarthritis Pain (ICOAP). *Arthritis Care Res (Hoboken)* 2011; **63** (Suppl. 11):S240–52.
- 22 Neittaanmaki-Perttu N, Gronroos M, Karppinen T *et al.* Photodynamic therapy for actinic keratoses: a randomized prospective non-sponsored cost-effectiveness study of daylight-mediated treatment compared with light-emitting diode treatment. *Acta Derm Venerol* 2016; **96**:241–4.
- 23 Wiegell SR, Haedersdal M, Philipsen PA *et al.* Continuous activation of PpIX by daylight is as effective as and less painful than conventional photodynamic therapy for actinic keratoses; a randomized, controlled, single-blinded study. *Br J Dermatol* 2008; **158**:740–6.
- 24 Wiegell SR, Fabricius S, Stender IM *et al.* A randomized, multicentre study of directed daylight exposure times of 1½ vs. 2½ h in daylight-mediated photodynamic therapy with methyl aminolevulinate in patients with multiple thin actinic keratoses of the face and scalp. *Br J Dermatol* 2011; **164**:1083–90.
- 25 Fai D, Romano I, Fai C *et al.* Daylight photodynamic therapy with methyl aminolevulinate in patients with actinic keratoses: a preliminary experience in Southern Italy. *G Ital Dermatol Venerol* 2016; **151**:154–9.
- 26 Moggio E, Arisi M, Zane C *et al.* A randomized split-face clinical trial analyzing daylight photodynamic therapy with methyl aminolevulinate vs ingenol mebutate gel for the treatment of multiple actinic keratoses of the face and the scalp. *Photodiagnosis Photodyn Ther* 2016; **16**:161–5.
- 27 Grinblat BM, Festa Neto C, Sanches JA Jr *et al.* Daylight photodynamic therapy for actinic keratoses in Sao Paulo, Brazil. *Photodermatol Photoimmunol Photomed* 2015; **31**:54–6.
- 28 Werner RN, Sammain A, Erdmann R *et al.* The natural history of actinic keratosis: a systematic review. *Br J Dermatol* 2013; **169**:502–18.
- 29 Szeimies RM, Atanasov P, Bissonnette R. Use of lesion response rate in actinic keratosis trials. *Dermatol Ther (Heidelb)* 2016; **6**:461–4.
- 30 Kellner C, Bauriedl S, Hollstein S, Reinhold U. Simulated-daylight photodynamic therapy with BF-200 aminolevulinic acid for actinic keratosis: assessment of the efficacy and tolerability in a retrospective study. *Br J Dermatol* 2015; **172**:1146–8.
- 31 Fitzmaurice S, Eisen DB. Daylight photodynamic therapy: what is known and what is yet to be determined. *Dermatol Surg* 2016; **42**:286–95.
- 32 Gholam P, Weberschock T, Denk K, Enk A. Treatment with 5-aminolevulinic acid methylester is less painful than treatment with 5-aminolevulinic acid nanoemulsion in topical photodynamic therapy for actinic keratosis. *Dermatology* 2011; **222**:358–62.
- 33 Fargnoli MC, Piccioni A, Neri L *et al.* Conventional vs. daylight methyl aminolevulinate photodynamic therapy for actinic keratosis of the face and scalp: an intra-patient, prospective, comparison study in Italy. *J Eur Acad Dermatol Venerol* 2015; **29**:1926–32.
- 34 Maisch T, Santarelli F, Schreml S *et al.* Fluorescence induction of protoporphyrin IX by a new 5-aminolevulinic acid nanoemulsion used for photodynamic therapy in a full-thickness *ex vivo* skin model. *Exp Dermatol* 2010; **19**:e302–5.

## Supporting Information

Additional Supporting Information may be found in the online version of this article at the publisher's website:

**Powerpoint S1** Journal Club Slide Set

# PUBLICATION

## II

### **Ablative fractional laser-assisted photodynamic therapy for lentigo maligna: a prospective pilot study**

Räsänen JE, Neittaanmäki N, Jeskanen L, Pölönen I, Snellman E, Grönroos M.

*J Eur Acad Dermatol Venereol.* 2020 Mar;34(3):510-517.  
doi: 10.1111/jdv.15925

**Publication reprinted with the permission of the copyright holders.**





## ORIGINAL ARTICLE

# Ablative fractional laser-assisted photodynamic therapy for lentigo maligna: a prospective pilot study

J.E. Räsänen,<sup>1,2,\*</sup>  N. Neittaanmäki,<sup>3</sup>  L. Jeskanen,<sup>4</sup> I. Pölönen,<sup>5</sup> E. Snellman,<sup>2</sup> M. Grönroos<sup>1</sup><sup>1</sup>Department of Dermatology, Päijät-Häme Social and Health Care Group, Lahti, Finland<sup>2</sup>Department of Dermatology, Faculty of Medicine and Medical Technology, Tampere University Hospital and Tampere University, Tampere, Finland<sup>3</sup>Department of Pathology and Dermatology, Institute of Biomedicine and Clinical Sciences, Sahlgrenska Academy, University of Gothenburg, Gothenburg, Sweden<sup>4</sup>Department of Pathology, University of Helsinki and HUSLAB, Helsinki, Finland<sup>5</sup>Department of Mathematical Information Technology, University of Jyväskylä, Jyväskylä, Finland

\*Correspondence: J. Räsänen. E-mail: janne.rasanen@sil.fimnet.fi

## Abstract

**Background** Lentigo maligna (LM) is an in situ form of melanoma carrying a risk of progression to invasive lentigo maligna melanoma (LMM). LM poses a clinical challenge, with subclinical extension and high recurrence rates after incomplete surgery. Alternative treatment methods have been investigated with varying results. Photodynamic therapy (PDT) with methylaminolaevulinic acid (MAL) has already proved promising in this respect.

**Objectives** To investigate the efficacy of ablative fractional laser (AFL)-assisted PDT with 5-aminolaevulinic acid nanoemulsion (BF-200 ALA) for treating LM.

**Methods** In this non-sponsored prospective pilot study, ten histologically verified LMs were treated with AFL-assisted PDT three times at 2-week intervals using a light dose of 90 J/cm<sup>2</sup> per treatment session. Local anaesthesia with ropivacaine was used. Four weeks after the last PDT treatment the lesions were treated surgically with a wide excision and sent for histopathological examination. The primary outcome was complete histopathological clearance of the LM from the surgical specimen. Patient-reported pain during illumination and the severity of the skin reaction after the PDT treatments were monitored as secondary outcomes.

**Results** The complete histopathological clearance rate was 7 out of 10 LMs (70%). The pain during illumination was tolerable, with the mean pain scores for the PDT sessions on a visual assessment scale ranging from 2.9 to 3.8. Some severe skin reactions occurred during the treatment period, however.

**Conclusions** Ablative fractional laser-assisted PDT showed moderate efficacy in terms of histological clearance. It could constitute an alternative treatment for LM but due to the side effects it should only be considered in inoperable cases.

Received: 17 April 2019; Accepted: 20 August 2019

## Conflicts of interest

The authors declare no conflicts of interest. The Revenio Group kindly loaned the HSC device for use in this study.

## Funding sources

This study has been supported by the Cancer Foundation of Finland and by the Tampere University Hospital.

## Introduction

Lentigo maligna (LM) is the most common subtype of melanoma in situ.<sup>1,2</sup> It occurs on the chronically sun-damaged skin of elderly patients, typically in the head and neck region.<sup>3,4</sup> If left untreated, it can progress to invasive lentigo maligna melanoma (LMM) with an estimated lifetime risk of 5–50%.<sup>5,6</sup> Due to the ageing population and high UV exposure, the incidence of

LM and LMM is steadily increasing in Europe, the USA and Australia.<sup>2,7–10</sup> LMM now encompasses 4–15% of all invasive melanomas.<sup>11</sup>

The gold standard treatment for LM is wide surgical excision with 5–10 mm peripheral margins.<sup>3</sup> Staged excision and Mohs micrographic surgery can be used to improve margin control and to strive for lower recurrence rates.<sup>12</sup> Due to the size and location of the LM and the age of the patient, surgery may sometimes be inappropriate or contraindicated, however.<sup>13</sup>

Clinicaltrials.gov Identifier number: NCT02685592

Alternative, non-surgical treatment modalities that have been investigated with varying results in terms of recurrence rates include cryotherapy, radiotherapy, Grenz ray therapy, topical imiquimod and photodynamic therapy (PDT).<sup>12,14,15</sup> Karam *et al.*<sup>15</sup> reported in a retrospective study that PDT with methylnolaevalinate (MAL) achieved complete clearance in 12/15 cases, although admittedly only parts of the lesions were examined histologically for possible recurrence.

Clinically, it can be difficult to distinguish between LM and LMM.<sup>11</sup> A novel imaging method employing a hyperspectral camera (HSC) can be used to delineate LM margins and detect dermal invasion.<sup>16,17</sup>

The aim of this prospective pilot study was to investigate whether ablative fractional laser (AFL)-assisted PDT with 5-aminolaevulinic acid nanoemulsion (BF-200 ALA) is effective for treating LM.

## Materials and methods

### Study design

The protocol for this non-sponsored prospective pilot study complied with the Declaration of Helsinki and was approved by the local ethics committee of Tampere University Hospital. Informed written consent was obtained from all the participants.

### Participants

Voluntary patients with a clinical suspicion of LM were enrolled from among those referred to the Department of Dermatology at Päijät-Häme Central Hospital, Lahti, Finland, between February 2016 and December 2017. Both male and female subjects aged over 18 years with a biopsy-proven LM located on the face, neck or upper body were included in the series. Exclusion criteria were as follows: (i) histologically verified invasive LMM, (ii) porphyria or photosensitivity, (iii) allergy to photosensitizer and (iv) pregnancy or breastfeeding.

### Treatment procedure

A flow chart of the study is presented in Fig. 1. During the first study visit, the suspected LM was examined clinically with a dermatoscope (Dermlite® DL3; 3Gen, San Juan Capistrano, CA, USA) and under Wood's light (Burton Div.-Cavitron Corp; Model 9312, Van Nuys, CA, USA), in order to help define the clinical borders.<sup>18</sup> These borders were then traced on a transparent plastic sheet and photographed. The lesions were also imaged with a HSC, prototype HSCP2 (Revenio Group, Vantaa, Finland), in order to reveal possible invasion and to provide a guide to the biopsy site.<sup>17</sup>

A 3-mm punch biopsy was taken from the darkest part of the lesion and/or from the most clearly emphasized area by HIS to confirm the histological diagnosis and to rule out invasion. The histopathological evaluations of the diagnostic samples were conducted by an experienced dermatopathologist (L.J.) who

received the samples without any background information other than the location of the lesion. Only patients with a biopsy-proven LM without any invasive component were included in the series from this point in the protocol onwards.

The histologically confirmed LMs were treated with PDT three times at 2-week intervals, employing the following procedure. First, a 5 mm margin was drawn around the lesion and the area was anaesthetized with a local anaesthetic (Ropivacaine Fresenius Kabi 7.5 mg/mL; Fresenius Kabi AS, Halden, Norway). The area was then pretreated with an ablative fractional CO<sub>2</sub> laser (DS-40UB Multixel; Daeshin Enterprise Co., Seoul, South Korea) to enhance the absorption of the photosensitizer precursor. The laser settings were as follows: Density level = 5, Depth level = 7 and Pulse duration = 700 ms, which correspond to a distance of 0.8 mm between the laser pores on the grid and a calculated pulse energy of 84 mJ per pore. After the pretreatment, a 1-mm-thick layer of photosensitizer precursor, 5-aminolaevulinic acid nanoemulsion gel, BF-200 ALA, 78 mg/g (Ameluz®; Biofrontera AG, Leverkusen, Germany) was applied to the skin over the whole treatment area, including the margins and occluded under a light impermeable cover for 3 h. Finally, the treatment area was illuminated with an Aktelite® CL128 lamp (Galderma Nordic AB, Uppsala, Sweden) at a light dose of 90 J/cm<sup>2</sup>.

Four weeks after the last PDT treatment, the lesions were excised surgically together with a 5 mm margin by the investigator M.G. and sent for routine histopathological examination. The lesion borders and margins were defined with the help of the pretreatment plastic sheets.

The specimens were fixed in 4% formalin, embedded in paraffin, sectioned using the traditional vertical bread-loaf technique and stained with haematoxylin-eosin (H&E). Immunohistochemistry (MART1/Melan A) was used as an aid to diagnosis where necessary.

### Efficacy assessment

The primary outcome was complete histopathological clearance of the LM from the surgical specimen. For this purpose, the excision specimens were evaluated by an experienced dermatopathologist (L.J.), who received the samples without any background information. The diagnosis was mainly based on routine staining with H&E, with additional immunohistochemical staining (MART-1/MelanA) if needed. The LM was considered to be histologically cleared if no sign or suspicion of atypical melanocytes could be seen, and uncured if the histological criteria for LM were still fulfilled or if there was any suspicion of atypical melanocyte proliferation.

### Safety and tolerability assessment

The declared secondary outcomes of the study were pain during the PDT illumination, the severity of the skin reaction 2 days after the first PDT treatment and the severity of delayed skin reactions after all the PDT sessions. The patients filled in visual

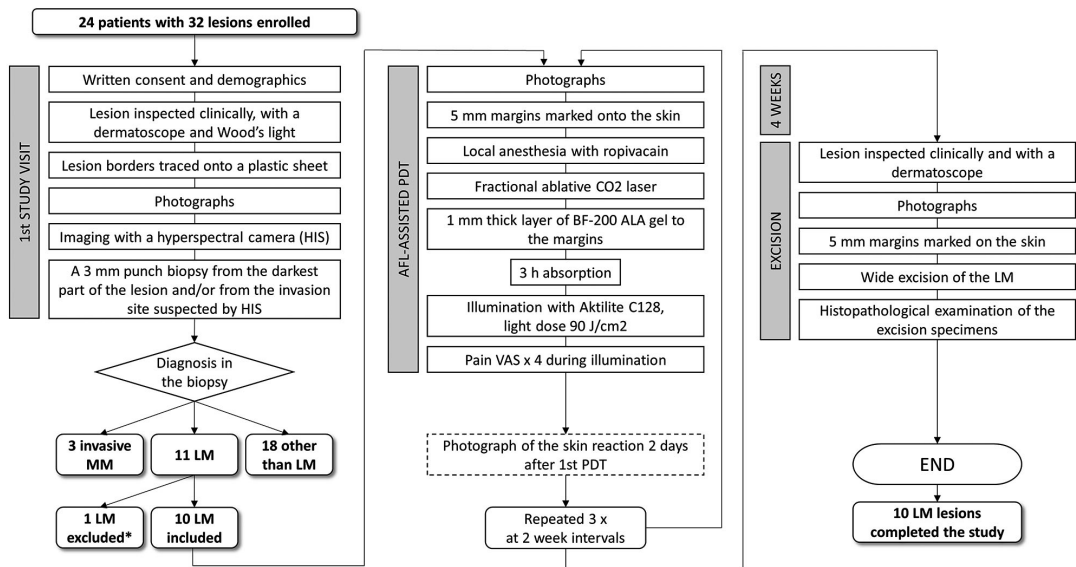


**Figure 1** Flow chart of the protocol. The histological diagnoses of the biopsied lesions were as follows: 11 LM, 2 LMM, 1 other MM, 1 lentigo, 2 seborrheic keratoses, 3 postinflammatory hyperpigmentation, six pigmented actinic keratosis, six dysplastic nevi. \*One lentigo maligna was excluded after biopsy because of difficulties in scheduling the PDT treatments according to the study protocol. LM, lentigo maligna; LMM, lentigo maligna melanoma; MM, malignant melanoma.

analogue scales for pain (VAS 0–10) (i) before the LED lamp illumination, (ii) 1 min after the start of the illumination, (iii) in the middle and (iv) at the end. To evaluate the local skin reactions (erythema, crusting, swelling), a nurse photographed the treatment area 2 days after the first PDT treatment and the investigator J.E.R. assessed the severity of the skin reaction from photographs on a scale of 1–4 (1 negligible; 2 mild; 3 moderate; 4 severe). Delayed inflammatory skin reactions were also evaluated during the second and third PDT treatments by J.E.R. or M.G., in addition to which the patients were asked to report any intense or unexpected skin reactions after any of the PDT sessions.

### Sample size

The exact optimal sample size could not be calculated for this pilot study due to a lack of previous research data. We were aiming at a sample size of 10–15 LM lesions.

## Results

### Baseline characteristics

Altogether, 24 patients with a total of 32 lesions were enrolled. Of these, 11 lesions were verified as LM and were included in the study. Three lesions were verified as invasive LMM, and 18

lesions as other pigmented lesions not fulfilling the criteria for LM and were thus excluded (Fig. 1). Furthermore, one LM was excluded after biopsy because of difficulties in scheduling the PDT treatments according to the study protocol. Thus, altogether 10 LMs in nine patients (one patient had two LMs) completed the study.

The patient demographics and the baseline characteristics of the LM lesions are presented in Table 1. None of the patients had received previous treatment (e.g. cryotherapy, surgery, PDT) in the skin areas where the LMs were located. The mean  $\pm$  SD (standard deviation) area of a LM lesion was  $98 \pm 58 \text{ mm}^2$ .

### Primary outcome: Histopathological clearance

Seven out of the ten lesions (70%) were histologically completely cleared from the wide excision specimens, whereas the histology of three lesions demonstrated a residual LM. Example photographs and histological images of one cured and one uncured LM are shown in Figs 2 and 3. Details of the clinical response, dermoscopy and histological clearance of the LM lesions are presented in Table 2. Of note, the numbering of the LM lesions (1–10) is uniform in Tables 1 and 2 so that the data can be compared between the tables. In two of the three uncured lesions, there was some visible and clinically detectable pigmentation left

**Table 1** Patient demographics and baseline characteristics of the lentigo malignas included in the series

Patient	Gender (M/F)	Age (years)	Skin photo-type	Previous skin cancers	LM lesion	Location	Lesion size (mm)	Lesion area (mm <sup>2</sup> )	Lesion histologically cleared (Y/N)
1	M	69	II	AK	1	Forehead	8 × 10	63	No
2	M	83	II	–	2	Cheek	14 × 21	231	No
3	M	62	II	BCC, SCC, DN × 2, MM × 2, LM × 2,	3	Forearm	10 × 17	134	Yes
4	M	71	I	AK	4	Upper back	12 × 13	123	Yes
5	M	75	II	–	5	Upper thorax	11 × 13	112	Yes
6	F	77	II	–	6	Forearm	9 × 12	84	No
7	M	77	II	AK, Mb Bowen, BCC	7	Cheek	10 × 14	110	Yes
8	F	71	II	BCC, LMM	8	Lower back	6 × 8	38	Yes
9	M	79	III	AK, keratoacanthoma	9†	Temple	8 × 8	50	Yes
9					10†	Neck	6 × 8	38	Yes

AK, actinic keratosis; BCC, basal cell carcinoma; DN, dysplastic nevus; LM, lentigo maligna; LMM, lentigo maligna melanoma; MM, malignant melanoma; SCC, squamous cell carcinoma.

†Patient 9 had two lentigo malignas.

after the treatments, so that a residual was suspected. Interestingly, one uncured lesion had no visible pigmentation to be seen, so that it was apparently clinically cleared. In the histologically

cleared lesions, there was either no visible pigmentation left (four lesions) or the pigmentation was almost invisible, with only a small area left (three lesions).

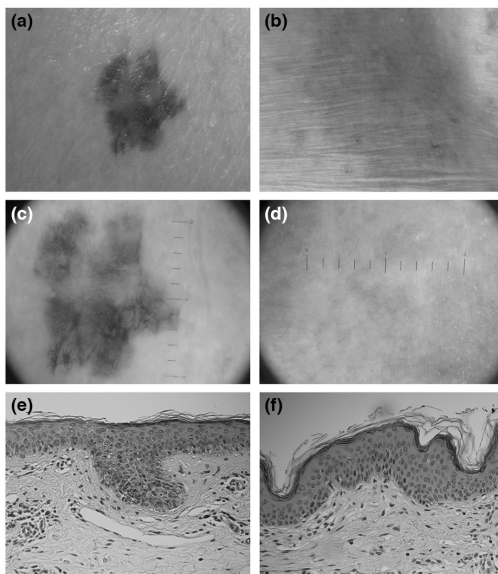


**Figure 2** Clinical, dermoscopic and histological images of a cured lentigo maligna (LM) before and after photodynamic therapy (PDT). (a) Photograph of a LM located on the chest before PDT, (b) photograph 4 weeks after the last PDT treatment, (c) dermoscopic image before PDT, (d) dermoscopic image after PDT shows no visible pigmentation, (e) histology before PDT shows confluent atypical melanocyte proliferation at the junction, (f) histology after PDT shows scar formation in the dermis with no sign of atypical melanocytes. Magnification 20×.

### Secondary outcomes: safety and tolerability

The pain VAS scores during the PDT illumination and the skin reactions 2 days after the first PDT are shown in Table 3. The maximal patient-reported pain was scored as moderate, and the highest VAS scores were reported during the second PDT session. The skin reaction was severe (swelling, pustules, intense erythema, crusting) in four LM lesions, moderate (marked erythema, crusting) in five and mild (mild erythema, scaling) in one. The delayed skin reaction 2 weeks after the first and second PDTs (assessed immediately before the second and third PDT treatments) was moderate in two patients, mild in five patients and negligible in two. Furthermore, some unexpected adverse effects occurred after the PDT treatment (Table 3). Two patients experienced moderate pain for several hours after the second PDT session, one patient had a very intense skin reaction and one displayed swelling of the skin of the eyelid and neck. Likewise, one patient experienced intense swelling, erythema and burning pain which led to a hospital visit on the day after the third PDT session. One patient suffered a continuous stinging pain in the excision area for 4 weeks after surgery, but it ceased after a second excision to increase the margins. Four weeks after the last PDT session (i.e. just before the excision) the following long-term adverse reactions of the treatment area were seen: postinflammatory erythema in five lesions, mild hypopigmentation in three lesions and mild hyperpigmentation in three lesions. None of the patients expressed visible scarring in the treatment area.

### Discussion

This pilot study is to our knowledge, the first prospective trial to investigate the efficacy of AFL-assisted PDT for treating LM. The

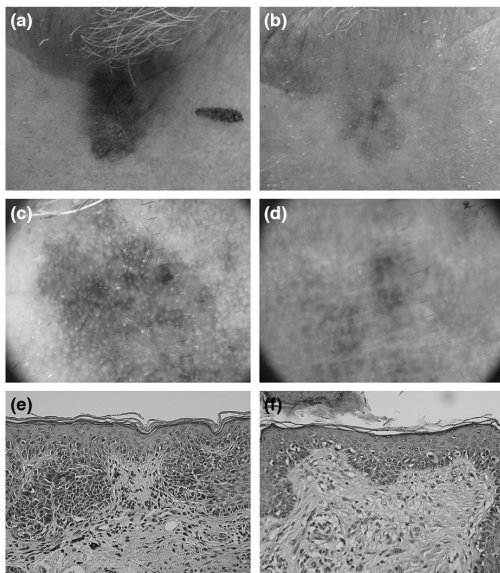


**Figure 3** Clinical, dermoscopic and histological images of a non-responding lentigo maligna (LM) before and after photodynamic therapy (PDT). (a) Photograph of a LM located on the cheek before PDT, (b) photograph of the residual LM 4 weeks after the last PDT treatment, (c) dermoscopic image before PDT, (d) dermoscopic image after PDT, showing a residual pigment network, erythema and white streaks, (e) histology before PDT, shows islands of atypical melanocytes with poor cohesion and atypical melanocyte proliferation at the junction, (f) histology after PDT, showing lentiginous proliferation of atypical melanocytes with variations in cell shape and size. Magnification 20 $\times$ .

histological clearance rate appeared to be moderate, seven out of ten LM lesions (70%) after three PDT sessions, but the treatment caused side effects and should only be considered in inoperable cases.

In an earlier retrospective study reported by Karam *et al.*<sup>15</sup> 15 LM lesions were treated with PDT, resulting in a cure rate of 12/15 (80%). Methylaminolaevulinate (MAL) was used as a photosensitizer, but the light dose and the number of PDT sessions varied among the patients (in the ranges 40–90 J/cm<sup>2</sup> and 3–9 sessions). It is worth noting, however, that the clearance of LMs was assessed by clinical follow-up after variable lengths of time (18–50 months), and by means of histological examinations of multiple biopsies rather than wide excisions, which may have resulted in missed histological residuals. In our present study, the lesions were excised completely after PDT for a full histopathological evaluation.

The gold standard treatment of LM is wide surgical excision which is also recommended by the current treatment consensus.

However, the surgery is not always easily applicable for example if the LM lesion is large and in aesthetically difficult location, or if anaesthesia is contraindicated, or if the patient simply refuses the surgery. In these cases, the alternative treatment options like AFL-assisted PDT could still be used. The follow-up for a possible recurrence of LM should be arranged in all non-surgical alternative therapies. It should be noted that clinical follow-up of LM alone after PDT involves a risk that a residual could be missed. This danger exists because, even though the treatment may destroy all the visible pigment, a histological examination can still reveal a residual LM. This was the case in one of the three residual cases found here. For this reason, a follow-up with histological verification is to be recommended even though the lesion may become clinically unpigmented and thus appear to be cured. We would suggest punch biopsies of the lesion in the follow-up visits taken from the previously visible centre of the lesion or any visible pigmentation.

It is not known what is a sufficient PDT light dose for treating melanocytic lesions. When treating non-melanocytic lesions, the photobleaching of PpIX is maximal in the initial phase of light illumination (more than 70% of PpIX is activated during the first 10 J/cm<sup>2</sup>) but the photobleaching continues slowly until the completion of the standard dose 37 J/cm<sup>2</sup>.<sup>19</sup> There is no earlier data available for the photobleaching of PpIX in melanocytic tumours but we assumed that it occurs in slower rate especially in the deeper situated melanocytes because melanin absorbs a portion of the red wavelength light. Karam *et al.*<sup>15</sup> used higher doses of 40–90 J/cm<sup>2</sup> (on average 60 J/cm<sup>2</sup>) than for the treatment of non-melanoma skin cancers (37 J/cm<sup>2</sup>), justifying this by the fact that melanin restricts the diffusion of red light into the deep layers of the epidermis. In the present pilot study, we used an experimental dose of 90 J/cm<sup>2</sup> to ensure that almost all PpIX is activated also in the deeper parts of the tumour during the slow gradual photobleaching after the rapid initial phase. This was partly because we did not want the efficacy of the PDT to be hindered due to unoptimal PDT protocol. The higher light dose lengthens the illumination time (approximately 18 min for 90 J/cm<sup>2</sup>) but causes no other disadvantage for the patient. Probably, a smaller light dose would also suffice, but to confirm this further investigations are warranted with measurement of the BF-200 ALA-induced fluorescence in LM lesions during illumination.

The mean patient-reported pain during PDT illumination remained low in our study, ranging from 2.9 to 3.8 on the VAS scale (0–10). The highest average pain was experienced during the second PDT session, and the maximum pain VAS value reported was 6.5. In the present instance, the lesional skin was injected with a local anaesthetic (ropivacaine) 3 h before illumination to reduce the pain to a more bearable level, taking into account the longer skin illumination time of approx. 18 min. For four out of the 10 patients, the first PDT treatment provoked a severe skin reaction 2 days after the session. The reaction subsided within 2 weeks, i.e. before the second PDT

**Table 2** Clinical response, dermoscopy and histological clearance of the lentigo malignas 4 weeks after the last photodynamic therapy

LM lesion	Clinical response	Dermoscopy	Histopathological findings in excision specimens	IHC used	Lesion histologically cleared (Y/N)
1	No visible pigment	White streaks, erythema	Atypical melanocyte proliferation/ lentigo maligna suspicion	–	No
2	Small pigmented area	Pigment network, erythema	Lentigo maligna	–	No
3	No visible pigment	White streaks, erythema	Scar and perivascular inflammation	–	Yes
4	No visible pigment	White streaks, erythema	Scar	–	Yes
5	Almost invisible pigmentation	Light diffuse pigmentation, erythema	Scar	–	Yes
6	Some pigmentation left, bleached	–	Lentigo maligna	–	No
7	Small pigmented area, mostly invisible	Small area of diffuse pigmentation, white streaks, erythema	Scar	–	Yes
8	Small pigmented dot in the middle	Small pigmented dot in the middle, erythema	Benign lentigo, fibrosis and inflammation	MART1, elastin	Yes
9†	No visible pigment	Erythema	Solar elastosis	MART1	Yes
10†	No visible pigment	Erythema	Scar and solar elastosis	MART1, Fontana	Yes

IHC, immunohistochemistry; LM, lentigo maligna.

†LM 9 and 10 belonged to the same patient.

**Table 3** Pain visual assessment scores (VAS) during the PDT illumination and the skin reaction 2 days after the 1st PDT session

LM lesion	Location	PDT 1 Max. pain (VAS 0–10)	PDT 2 Max. pain (VAS 0–10)	PDT 3 Max. pain (VAS 0–10)	Skin reaction 2 days after PDT 1 (0–4)	Notes
1	Forehead	1.8	4.4	2.2	4	After the excision a constant stinging pain occurred in the excised area. The pain ceased after a second excision for margin control
2	Cheek	0	0.1	1.2	2	A very intense skin reaction with erythema, swelling and burning pain after the 3rd PDT session
3	Forearm	0.9	5	2.3	4	–
4	Upper back	2.3	1.4	1.8	4	–
5	Upper thorax	5.4	6.5	3.7	3	Moderate pain continued for several hours after the 2nd PDT session
6	Forearm	4	4.4	1.6	3	Moderate pain continued for several hours after the 2nd PDT session
7	Cheek	2.2	1.4	1.5	3	Skin swelling of the eyelid and the neck after the 2nd PDT session
8	Lower back	4.4	4.7	5.5	4	A very intense skin reaction with violaceous erythema and abundant secretion after the 2nd PDT session
9†	Temple	5	5.1	4.3	2	–
10†	Neck	5	5.3	5.1	3	–
	<b>Mean ± SD</b>	<b>3.1 ± 1.9</b>	<b>3.8 ± 2.1</b>	<b>2.9 ± 1.6</b>	<b>3.3 ± 0.7</b>	

LM, lentigo maligna; PDT, photodynamic therapy, SD, standard deviation.

†LM 9 and 10 belonged to the same patient.

session. In two patients, an intense skin reaction also occurred after the second PDT session, and in one patient a very severe reaction was seen after the third PDT. The reactions were definitely more severe than those reported in PDT of non-melanocytic skin cancers.<sup>20,21</sup> We assume that the stronger reactions were caused by the pretreatment with AFL combined with the high

light dose of 90 J/cm<sup>2</sup> used. The increased amounts of inflammatory cells and cytokines in the lesional skin following the first PDT might explain why the most severe side effects were seen in relation to the second session.

The histopathological evaluation of the present excision specimens showed dermal scars in 5/10 lesions after PDT, which

could be due to the earlier biopsies or to the AFL pretreatment and not be actual reactions to the treatment. Before excision, no visible scarring could be seen in the treatment area for any of the ten LM lesions.

When treating LM non-surgically, one should note the growth of atypical melanocytes down the follicular units.<sup>22</sup> In a histopathological review of 100 patients, such follicular growth was seen in 95% of LMs, with a mean depth of 0.45 mm (range 0.1–1.1 mm).<sup>23</sup> For topical therapy to succeed, the topical agent such as the photosensitizer precursor should penetrate deep enough into the skin to reach all the atypical melanocytes, down to the deepest part. To ensure this and to enhance the efficacy of PDT, we considered it important to use ablative fractional CO<sub>2</sub>-laser pretreatment which increases the uptake and deep penetration of ALA and MAL into the skin.<sup>24</sup> AFL pretreatment has been shown earlier to enhance the clinical efficacy of PDT when treating non-melanoma skin cancer.<sup>25–27</sup> The photosensitizer distribution in the deeper layers of the skin does not depend on the depth of the laser pores in the dermis as long as the epidermis is penetrated.<sup>28</sup> The pulse energy of the CO<sub>2</sub>-laser used here, 84 mJ, corresponds to a channel in the skin that is approximately 200 µm deep (measured histologically from a skin biopsy of a healthy volunteer in Päijät-Häme Central Hospital, data not shown) which would be sufficient for full penetration of the epidermis, which is <100 µm thick except in the palms of the hands.<sup>29</sup>

The failure rate of AFL-assisted PDT, i.e. the number of histopathological LM residuals observed, was 3 out of 10 LM lesions (30%), whereas the reported recurrence rates for the standard surgical excision of LMs are in the range of 8–20% (mean 6.8% at 5 years), those for staged excision 0–7%, and those for Mohs micrographic surgery 0–2%.<sup>12,30</sup> In a recent review of non-surgical treatments available for LM, the recurrence rates were 0–31% (mean 11.5%) for radiotherapy, 4–50% (mean 24.5%) for imiquimod and 0–100% (mean 34.4%) for laser therapy, which are all inferior to those achieved with surgical methods.<sup>14</sup> The cure rate in our present pilot study is superior to that for laser therapy, in line with imiquimod, but inferior to radiotherapy. A high recurrence rate with any treatment modality may be derived from deep follicular extension, unsuspected invasion or subclinical extension of the LM.<sup>12</sup> Among our three non-responders, one LM was located on the cheek (Fig. 3) and the histopathological evaluation after PDT revealed LM with a 1 mm deep follicular extension, so that the accumulation of protoporphyrin in the deep part of the lesion may not have been sufficient, which could explain the failure of PDT in this case. Otherwise, no correlation between demographic data or lesion baseline characteristics and histological outcome could be found which is most likely due to small sample size.

The limitations of our study were as follows: the small number of cases, due to the piloting nature of the study; the duration

of adverse skin reactions was not recorded; and the use of the routine bread-loaf technique in the histological assessment of the lesions which could have caused us to miss some residual part of a lesion.<sup>31</sup> This must partly have been offset, however, by the fact that the lesions were completely excised with 5 mm margins after the treatment. A strength of this work lies in the fact that it is the first prospective study assessing the effect of AFL-assisted PDT in the treatment of LM, offering a basis for future larger studies.

In conclusion, the present results demonstrate that AFL-assisted PDT is an alternative effective option for treating LM. Histopathological assessment of the wide excision specimens showed that 7 out of the 10 lesions (70%) were histologically completely cleared after three AFL-assisted PDT sessions. The patient-reported pain during PDT illumination was moderate and tolerable, although a few severe skin reactions were observed after the PDT. AFL-assisted PDT could be considered as a treatment option for non-invasive LM in patients for whom surgery is contraindicated or as a second-line treatment for residual lesions. Further studies with larger samples are warranted to confirm these preliminary results.

## Acknowledgements

We would like to thank the nurse Ulla Oesch-Lääveri at Päijät-Häme Central Hospital for her dedication to this study, and Kari Saarinen, M.D., for his assistance in recruiting patients.

## References

- Hemminki K, Zhang H, Czene K. Incidence trends and familial risks in invasive and in situ cutaneous melanoma by sun-exposed body sites. *Int J Cancer* 2003; **104**: 764–771.
- Swetter SM, Boldrick JC, Jung SY *et al.* Increasing incidence of lentigo maligna melanoma subtypes: northern California and national trends 1990–2000. *J Invest Dermatol* 2005; **125**: 685–691.
- Bosbous MW, Dzwierzynski WW, Neuburg M. Lentigo maligna: diagnosis and treatment. *Clin Plast Surg* 2010; **37**: 35–46.
- Higgins HW 2nd, Lee KC, Galan A, Leffell DJ. Melanoma in situ: part I. Epidemiology, screening, and clinical features. *J Am Acad Dermatol* 2015; **73**: 181–190, quiz 191–2.
- Weinstock MA, Sober AJ. The risk of progression of lentigo maligna to lentigo maligna melanoma. *Br J Dermatol* 1987; **116**: 303–310.
- Stevenson O, Ahmed I. Lentigo maligna: prognosis and treatment options. *Am J Clin Dermatol* 2005; **6**: 151–164.
- Greveling K, Wakkee M, Nijsten T *et al.* Epidemiology of lentigo maligna and lentigo maligna melanoma in the Netherlands, 1989–2013. *J Invest Dermatol* 2016; **136**: 1955–1960.
- Toender A, Kjaer SK, Jensen A. Increased incidence of melanoma in situ in Denmark from 1997 to 2011: results from a nationwide population-based study. *Melanoma Res* 2014; **24**: 488–495.
- Mirzoyev SA, Knudson RM, Reed KB *et al.* Incidence of lentigo maligna in Olmsted County, Minnesota, 1970 to 2007. *J Am Acad Dermatol* 2014; **70**: 443–448.
- Youl PH, Youlden DR, Baade PD. Changes in the site distribution of common melanoma subtypes in Queensland, Australia over time: implications for public health campaigns. *Br J Dermatol* 2013; **168**: 136–144.
- McKenna JK, Florell SR, Goldman GD, Bowen GM. Lentigo maligna/lentigo maligna melanoma: current state of diagnosis and treatment. *Dermatol Surg* 2006; **32**: 493–504.

- 12 McGuire LK, Disa JJ, Lee EH et al. Melanoma of the lentigo maligna subtype: diagnostic challenges and current treatment paradigms. *Plast Reconstr Surg* 2012; **129**: 288e–299e.
- 13 Erickson C, Miller SJ. Treatment options in melanoma in situ: topical and radiation therapy, excision and Mohs surgery. *Int J Dermatol* 2010; **49**: 482–491.
- 14 Read T, Noonan C, David M et al. A systematic review of non-surgical treatments for lentigo maligna. *J Eur Acad Dermatol Venereol* 2016; **30**: 748–753.
- 15 Karam A, Simon M, Lemasson G, Misery L. The use of photodynamic therapy in the treatment of lentigo maligna. *Pigment Cell Melanoma Res* 2013; **26**: 275–277.
- 16 Neittaanmaki-Perttu N, Gronroos M, Jeskanen L et al. Delineating margins of lentigo maligna using a hyperspectral imaging system. *Acta Derm Venereol* 2015; **95**: 549–552.
- 17 Neittaanmaki N, Salmivuori M, Polonen I et al. Hyperspectral imaging in detecting dermal invasion in lentigo maligna melanoma. *Br J Dermatol* 2017; **177**: 1742–1744.
- 18 Kimyai-Asadi A, Katz T, Goldberg LH et al. Margin involvement after the excision of melanoma in situ: the need for complete en face examination of the surgical margins. *Dermatol Surg* 2007; **33**: 1434–1439. discussion 1439–41.
- 19 Tyrrell J, Campbell S, Curnow A. Protoporphyrin IX photobleaching during the light irradiation phase of standard dermatological methyl-aminolevulinate photodynamic therapy. *Photodiagnosis Photodyn Ther* 2010; **7**: 232–238.
- 20 Tschen EH, Wong DS, Pariser DM et al. Photodynamic therapy using aminolaevulinic acid for patients with nonhyperkeratotic actinic keratoses of the face and scalp: phase IV multicentre clinical trial with 12-month follow up. *Br J Dermatol* 2006; **155**: 1262–1269.
- 21 Wang I, Bendsoe N, Klinteberg CA et al. Photodynamic therapy vs. cryosurgery of basal cell carcinomas: results of a phase III clinical trial. *Br J Dermatol* 2001; **144**: 832–840.
- 22 Flotte TJ, Mihm MC Jr. Lentigo maligna and malignant melanoma in situ, lentigo maligna type. *Hum Pathol* 1999; **30**: 533–536.
- 23 Connolly KL, Giordano C, Dusza S et al. Follicular involvement is frequent in lentigo maligna: implications for treatment. *J Am Acad Dermatol* 2019; **80**: 532–537.
- 24 Haedersdal M, Sakamoto FH, Farinelli WA et al. Pretreatment with ablative fractional laser changes kinetics and biodistribution of topical 5-aminolevulinic acid (ALA) and methyl aminolevulinate (MAL). *Lasers Surg Med* 2014; **46**: 462–469.
- 25 Togsverd-Bo K, Haak CS, Thaysen-Petersen D et al. Intensified photodynamic therapy of actinic keratoses with fractional CO<sub>2</sub> laser: a randomized clinical trial. *Br J Dermatol* 2012; **166**: 1262–1269.
- 26 Ko DY, Kim KH, Song KH. A randomized trial comparing methyl aminolevulinate photodynamic therapy with and without Er:YAG ablative fractional laser treatment in Asian patients with lower extremity Bowen disease: results from a 12-month follow-up. *Br J Dermatol* 2014; **170**: 165–172.
- 27 Haak CS, Togsverd-Bo K, Thaysen-Petersen D et al. Fractional laser-mediated photodynamic therapy of high-risk basal cell carcinomas—a randomized clinical trial. *Br J Dermatol* 2015; **172**: 215–222.
- 28 Haak CS, Farinelli WA, Tam J et al. Fractional laser-assisted delivery of methyl aminolevulinate: impact of laser channel depth and incubation time. *Lasers Surg Med* 2012; **44**: 787–795.
- 29 Mogensen M, Morsy HA, Thrane L, Jemec GB. Morphology and epidermal thickness of normal skin imaged by optical coherence tomography. *Dermatology* 2008; **217**: 14–20.
- 30 Juhasz ML, Marmur ES. Reviewing challenges in the diagnosis and treatment of lentigo maligna and lentigo-maligna melanoma. *Rare Cancers Ther* 2015; **3**: 133–145.
- 31 Osborne JE, Hutchinson PE. A follow-up study to investigate the efficacy of initial treatment of lentigo maligna with surgical excision. *Br J Plast Surg* 2002; **55**: 611–615.



**PUBLICATION**  
**III**

**Hyperspectral imaging reveals spectral differences and can distinguish malignant melanoma from pigmented basal cell carcinomas: a pilot study**

Räsänen J, Salmivuori M, Pölönen I, Grönroos M, Neittaanmäki N.

*Acta Derm Venereol.* 2021 Feb 19;101(2):adv00405.

doi: 10.2340/00015555-3755

**Publication reprinted with the permission of the copyright holders.**



# Hyperspectral Imaging Reveals Spectral Differences and Can Distinguish Malignant Melanoma from Pigmented Basal Cell Carcinomas: A Pilot Study

Janne RÄSÄNEN<sup>1,2</sup>, Mari SALMIVUORI<sup>1-3</sup>, Ilkka PÖLÖNEN<sup>4</sup>, Mari GRÖNROOS<sup>1</sup> and Noora NEITTAANMÄKI<sup>5</sup>

<sup>1</sup>Department of Dermatology, Päijät-Häme Social and Health Care Group, Lahti, <sup>2</sup>Department of Dermatology, Tampere University Hospital and Tampere University, Faculty of Medicine and Medical Technology, Tampere, <sup>3</sup>Department of Dermatology and Allergology, University of Helsinki and Helsinki University Hospital, Helsinki, <sup>4</sup>Faculty of Information Technology, University of Jyväskylä, Jyväskylä, Finland and <sup>5</sup>Departments of Pathology and Dermatology, Institutes of Biomedicine and Clinical Sciences, Sahlgrenska Academy, University of Gothenburg, Gothenburg, Sweden

**Pigmented basal cell carcinomas can be difficult to distinguish from melanocytic tumours. Hyperspectral imaging is a non-invasive imaging technique that measures the reflectance spectra of skin *in vivo*. The aim of this prospective pilot study was to use a convolutional neural network classifier in hyperspectral images for differential diagnosis between pigmented basal cell carcinomas and melanoma. A total of 26 pigmented lesions (10 pigmented basal cell carcinomas, 12 melanomas *in situ*, 4 invasive melanomas) were imaged with hyperspectral imaging and excised for histopathological diagnosis. For 2-class classifier (melanocytic tumours vs pigmented basal cell carcinomas) using the majority of the pixels to predict the class of the whole lesion, the results showed a sensitivity of 100% (95% confidence interval 81–100%), specificity of 90% (95% confidence interval 60–98%) and positive predictive value of 94% (95% confidence interval 73–99%). These results indicate that a convolutional neural network classifier can differentiate melanocytic tumours from pigmented basal cell carcinomas in hyperspectral images. Further studies are warranted in order to confirm these preliminary results, using larger samples and multiple tumour types, including all types of melanocytic lesions.**

**Key words:** deep learning; neural network; basal cell carcinoma; malignant melanoma.

Accepted Jan 26, 2021; Epub ahead of print Feb 1, 2021

Acta Derm Venereol 2021; 101: adv00405.

**Corr:** Janne Räsänen, Department of Dermatology, Tampere University Hospital and Tampere University, Faculty of Medicine and Medical Technology, Riihipellonkatu 4 B 13, FIN-33530 Tampere, Finland. E-mail: janne.rasanen@sil.fimnet.fi

**B**asal cell carcinoma (BCC) is the most common skin cancer and the most frequently occurring form of all cancers among whites in the Western countries, with an estimated lifetime risk of  $\geq 30\%$  (1). The most common subtypes, nodular and superficial BCC, may occasionally contain melanin, referred to as “pigmented BCC”, which constitute  $\sim 7\%$  of all BCCs (2). Dermoscopy uses a magnifying lens and polarized light, to assess different structures and colours of a lesion. In dermoscopy the pigment in BCC can be seen as blue-grey ovoid nests

## SIGNIFICANCE

This is the first study to utilize hyperspectral images and a deep-learning convolutional neural network to acquire an automated diagnosis for melanocytic tumours and pigmented basal cell carcinomas. The results of this pilot study will serve as a basis for future research. The results indicate that, with a larger sample and training dataset, the convolutional neural network could accurately classify malignant melanocytic tumours from pigmented basal cell carcinomas. This finding may be used as the basis for development of future techniques in melanoma diagnostics, which also requires a hyperspectral camera to be commercially available to clinicians.

and globules, brown to blue-grey maple leaf-like structures, or small blue-grey dots (peppering) (2–4). Heavily pigmented BCCs may contain brown to black globules or dots, or blue-white veil-like structures, and are thus difficult to distinguish from melanocytic lesions (5). The pigmentation may cause confusion in diagnosing these lesions. Differential diagnoses for pigmented BCCs include melanoma *in situ* (MIS), invasive melanoma and benign pigmented lesions (2, 6). Usually, the clinical features suffice to establish the diagnosis of a pigmented BCC, but the diagnosis is not always clear-cut (Fig. 1). In uncertain cases diagnostic biopsy or excision is required.

Various non-invasive imaging modalities have been developed to aid in the diagnosis of BCC and to avoid unnecessary biopsies. These include reflectance confocal microscopy (RCM) and optical coherence tomography (OCT), as well as investigational methods still under development, such as Raman spectroscopy, high-resolution ultrasonography, and terahertz pulse imaging (4). Hyperspectral imaging (HSI) is a novel non-invasive imaging technique that measures the reflectance spectra of skin *in vivo* to identify different biological tissues (7, 8). We have previously shown that HSI can delineate the lesion borders of ill-defined BCCs and lentigo maligna (LM) more accurately than clinical examination, and can detect the invasive component in lentigo maligna melanoma (LMM) (9–11).

Convolutional neural networks (CNN) represent a form of artificial intelligence in decision-making and

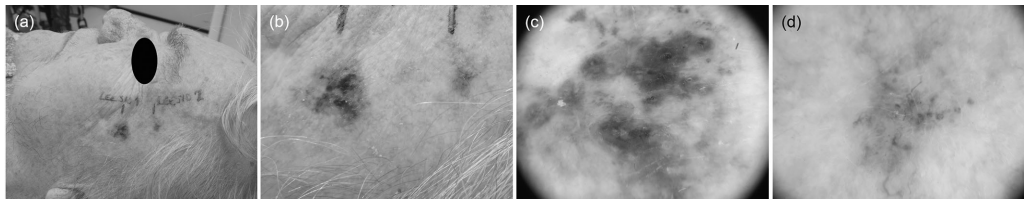


**Fig. 1. Photographs of a patient included in the study with both lentigo maligna melanoma (LMM) and pigmented basal cell carcinoma (BCC).** (a) Overview showing LMM (left) and BCC (right). (b) Close-up showing LMM (left) and BCC (right). (c) Dermoscopic image of the lesion on the left, histologically verified as LMM with Breslow depth 1.5 mm. (d) Dermoscopic image of the lesion on the right, histologically verified as a nodular pigmented BCC. The results of hyperspectral analyses are shown in Figs 2 and 3.

are a strongly emerging concept in dermatological diagnostics. CNNs can classify pigmented and non-pigmented skin tumours from clinical and dermoscopic images with an accuracy similar to that of dermatologists (12–14). In addition to 2-dimensional (2D) images, a CNN classifier has been utilized with hyperspectral images of *ex vivo* malignant tumours (15, 16).

The aim of this pilot study was to use a combination of 3-, 2- and 1-dimensional (3D, 2D and 1D) convolutional layers in a neural network classifier from hyperspectral images to distinguish between pigmented BCCs and malignant melanocytic tumours.

## MATERIALS AND METHODS

### Participant recruitment

The study protocol complied with the principles of the Declaration of Helsinki and was approved by the local ethics committee of Tampere University Hospital. All participants gave their written informed consent. Voluntary patients were recruited from among those referred for suspected skin malignancies to the Department of Dermatology at Päijät-Häme Central Hospital, Lahti, Finland, between May 2014 and November 2017. Inclusion criteria were clinically pigmented tumours, which were histologically confirmed as BCC, MIS, or invasive malignant melanoma (MM).

### Hyperspectral image acquisition and histopathological examination

All lesions were clinically examined with a dermatoscope (Dermlite DL3, 3Gen, San Juan Capistrano, CA, USA) and photographed. For subsequent orientation purposes, a small mark was drawn on the healthy skin beside the lesion, using a black marker pen. Hyperspectral images were taken *in vivo* with an HSI camera prototype (VTT FPI VIS-VNIR Spectral Camera, VTT Technical Research Centre of Finland, Espoo, Finland). Spectral separation of the imager is based on Fabry-Pérot interferometer (FPI), which enables fast scanning in the spectral domain. The imager measures diffuse reflectance on wavebands from visible to near infrared light (500–850 nm) for every pixel of the image. The full width of half maximum (FWHM) of each waveband varies from 10 to 30 nm. The imager rapidly captures 76 wavebands within a few seconds in a 120 mm<sup>2</sup> field of view with a spatial resolution of 640 pixels/mm<sup>2</sup> (pixel = 125 × 125 μm). The imaging depth of hyperspectral imaging depends on the wavelength (17). In the wavelength range used (450–850 nm) the imaging depth varies in the range 0.5–5.0 mm. Because the whole wavelength range is used in the analysis the mean imaging depth is approximately 2 mm. The concentration of melanin affects the imaging depth, but, because the whole

wavelength range is used, its effect on the mean imaging depth is minor (17). The outcome is a hyperspectral image: a 3D data cube containing a reflectance spectrum for each pixel of the 2D image. The HSI technique is described in more detail elsewhere (7, 10).

After imaging, the lesions were surgically excised and sent for routine histopathological examination. The tissue specimens were fixed in 4% formalin, embedded in paraffin, sectioned using the traditional vertical bread-loaf technique, and stained with haematoxylin and eosin (H&E).

### Data pre-processing and 3-dimensional convolutional neural network

Of the 76 wavebands, 66 were used for the analyses. Thus, HSI produced a raw data cube (size 240 × 320 × 66 pixels), which was calibrated to the radiance using Saari et al.'s method (18). A white reference target was captured for each data cube, and this was used to convert imaged radiance to reflectance  $R = I / I_0$ , where  $I$  is the imaged region of interest and  $I_0$  is the data cube from the white reference. To reduce the effect of vignetting and lighting irregularities, each imaged spectrum was subtracted by its average in the spectral domain (Fig. S1<sup>†</sup>).

A combination of 3D, 2D and 1D CNNs, operating separately and simultaneously in both spatial and spectral domains, was used to classify the lesions (19). For training the neural network, labelled data from captured hyperspectral images was used. For each image, a clinician (JER) manually annotated areas of histologically verified tumour, healthy skin and marker pen (Fig. S2<sup>†</sup>). From the annotated areas of each image approximately 1,000 datasets of 5 × 5-pixel neighbourhoods were selected for training purposes. The training set was sampled randomly from annotated points to contain a total of approximately 27,000 data-points from each class. For annotated points, data augmentation was used, such that each training cube was mirrored and flipped horizontally and vertically (20). These operations quadrupled the number of inputs in the training phase and resulted in a final training set of approximately 655,000 data-points.

Due to the limited number of lesions imaged ( $n = 26$ ), the hyperspectral images were divided into 2 parts in the vertical direction in the middle of the annotated lesion, so that one half served as a training image and the other half was used independently for classification. This ensured, firstly, that the training set did not contain data-points from the image currently being classified and, secondly, that the training set contained a sufficient variation of different lesion types (21–23).

For the implementation of CNN, the current study used Keras library, TensorFlow backend and Python 3.6. All calculations were performed on IBM PowerAI Platform, which includes 2 Nvidia

<sup>†</sup><https://www.medicaljournals.se/acta/content/abstract/10.2340/00015555-3755>

Tesla V100-SXM2 16 GB graphics processing units (GPUs). A more detailed description of our implementation of CNN in skin cancer detection is available elsewhere (18).

#### Sample size

Due to the pilot study set-up, it was not possible to calculate the accurate sample size needed. The study aimed at a sample size of 10–15 pigmented BCC and 10–15 melanocytic tumours.

## RESULTS

### Patient demographics and lesion characteristics

A total of 32 lesions fulfilling the inclusion criteria were imaged in Päijät-Häme Central Hospital, Lahti. Hyperspectral images of 6 lesions were excluded from the study because the HSI settings were not optimal at the time of imaging, leading to imaging artefacts (under-exposure or FPI switch inadvertently off). Hence, a total of 26 lesions from 24 patients were included in the study. Patient demographics and lesion characteristics are shown in **Table I**.

Fifteen patients were men and 9 women, mean age 73.1 (range 53–91) years. Thirteen had Fitzpatrick's skin phototype II, 8 phototype III, and, in 3 patients, the phototype was not reported. Fourteen patients had a previous history of skin cancer, as follows: AK ( $n=8$ ), Bowen's disease ( $n=4$ ), squamous cell carcinoma ( $n=3$ ), BCC ( $n=9$ ), and MIS or MM ( $n=4$ ). Five patients had

a history of other malignancy (2 prostate cancers, one tongue cancer, one lip cancer, and one hepatocellular and pancreatic carcinoma). Two of the patients were immunosuppressed: one patient was an organ-transplant receiver and used sirolimus for antirejection, and one patient used azathioprine for Crohn's disease.

The imaged lesions were located on the face ( $n=8$ ), neck ( $n=3$ ), torso ( $n=10$ ), upper extremity ( $n=4$ ) and lower extremity ( $n=1$ ). The mean  $\pm$  standard deviation (SD) diameter of the lesions was  $9.8 \pm 2.9$  mm (range 5.3–19 mm) and the mean  $\pm$  SD area was  $71.2 \pm 46.9$  mm<sup>2</sup> (range 11.0–247 mm<sup>2</sup>).

### Histopathological diagnoses

The histopathological diagnoses of the imaged lesions were as follows: 10 BCC (6 nodular, 2 superficial, 2 both superficial and nodular), 12 MIS (all lentigo maligna subtype), and 4 MM (3 lentigo maligna subtypes and 1 superficial spreading subtype, Breslow depths in the range 0.3–1.4 mm).

### Hyperspectral analysis

The hyperspectral analyses and lesion classification with CNN were conducted by a trained mathematician (IP). Due to limited sample size, all melanocytic tumours (MIS and MM) were first combined in single group for lesion classification. Each hyperspectral image was classified

**Table I. Patient demographics and baseline characteristics, histopathological diagnoses and the result of CNN classification for the lesions included in the study**

Lesion number	Age, years	Sex (F/M)	Lesion location	Size, mm	Histopathological diagnosis (=true label)	Predicted label by CNN (2 classes)	Predicted label by CNN (3 classes)
1	56	F	Eyelid	2 × 7	nBCC	Pigmented BCC	Pigmented BCC
2	82	F	Temple	11 × 12	LMM (Breslow 1.5)	Melanocytic	MM
3 <sup>a</sup>		a	Temple	5 × 6	nBCC	Pigmented BCC	Pigmented BCC
4	68	M	Upper back	8 × 8	LM	Melanocytic	MIS
5	69	M	Groin	8 × 10	n/sBCC	Melanocytic <sup>c</sup>	Pigmented BCC
6	69	M	Shoulder	15 × 21	MM (Breslow 1.4)	MM	MM
7	57	F	Breastbone	7 × 8	sBCC	Pigmented BCC	Pigmented BCC
8	73	M	Back	10 × 13	sBCC	Pigmented BCC	Pigmented BCC
9	81	F	Neck	6 × 13	n/sBCC	Pigmented BCC	Pigmented BCC
10	72	F	Nose	10 × 10	nBCC	Pigmented BCC	Pigmented BCC
11	53	F	Eyelid	4 × 12	nBCC	Pigmented BCC	Pigmented BCC
12	86	F	Upper back	7 × 12	nBCC	Pigmented BCC	Pigmented BCC
13	66	M	Shoulder	9 × 9	LM	Melanocytic	MIS
14	75	M	Shoulder	5 × 10	nBCC	Pigmented BCC	Pigmented BCC
15	91	M	Upper back	7 × 10	LM	Melanocytic	MIS
16	84	M	Chest	4 × 8	LMM (Breslow 0.3)	Melanocytic	MM
17	83	M	Chest	8 × 12	LMM (Breslow 0.4)	Melanocytic	MM
18	69	M	Forehead	8 × 10	LM	Melanocytic	MIS
19	80	M	Neck	8 × 12	LM	Melanocytic	MIS
20	62	M	Forearm	10 × 17	LM	Melanocytic	MIS
21	75	M	Chest	11 × 13	LM	Melanocytic	MIS
22	77	F	Forearm	9 × 12	LM	Melanocytic	MIS
23	77	M	Cheek	10 × 14	LM	Melanocytic	MIS
24	71	F	Lower back	6 × 8	LM	Melanocytic	MIS
25	79	M	Temple	8 × 8	LM	Melanocytic	MIS
26 <sup>b</sup>		b	Neck	6 × 8	LM	Melanocytic	MIS

The predicted label for the whole lesion was determined by the predicted class of the majority of pixels in the lesion area. The result of classification is presented for the study sample divided into 2 classes (pigmented basal cell carcinoma (BCC) and melanocytic tumours) and 3 classes (pigmented BCC, melanoma *in situ* (MIS) and malignant melanoma (MM)).

<sup>a</sup>Lesions 2 and 3 belonged to the same patient. <sup>b</sup>Lesions 25 and 26 belonged to the same patient. <sup>c</sup>Convolutional neural networks (CNN) classification erroneous. nBCC: nodular basal cell carcinoma; sBCC: superficial basal cell carcinoma; LMM: lentigo maligna melanoma.

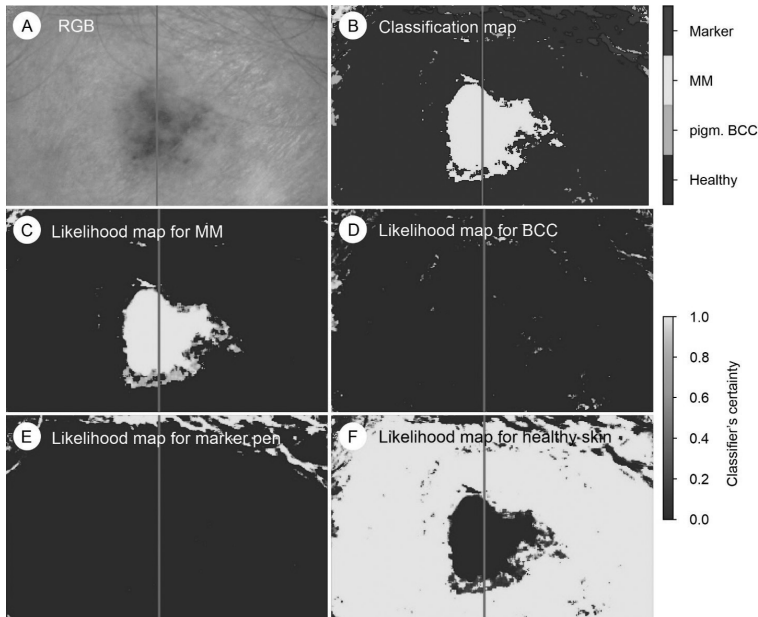


**Fig. 2. Classification and likelihood maps of a histologically confirmed invasive melanoma (lentigo maligna subtype, Breslow depth 1.5 mm).** The lesion was correctly classified as malignant melanoma (MM) by hyperspectral imaging using the majority of the pixels of the image taken by hyperspectral camera. (A) Red, green and blue (RGB) image taken by hyperspectral camera. (B) Classification map showing most of the pixels representing invasive malignant melanoma (MM). *Upper colour bar* depicts the 4 classes in image B. (C) Likelihood map for the localization of MM. (D) Likelihood map for the localization of pigmented basal cell carcinoma (BCC). Only some scattered artefactual pixels are shown outside the lesion area. (E) Likelihood map for the localization of marker pen. (F) Likelihood map for the localization of healthy skin. *Lower colour bar* represents the certainty of the classifier in each of the likelihood maps. *Red line* shows the division of the hyperspectral image into halves, one of which was used for the training of the classifier and the other for the classifying task.

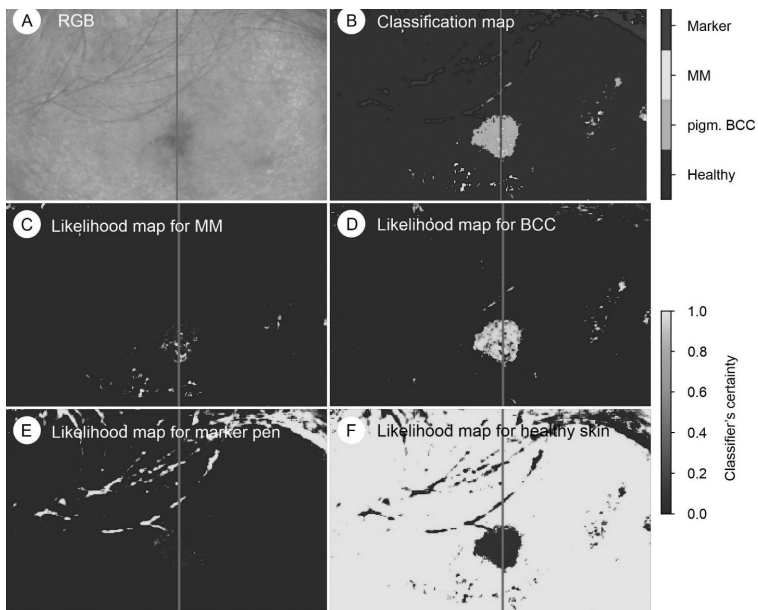


**Fig. 3. Classification and likelihood maps of a histologically confirmed pigmented basal cell carcinoma (BCC).** The lesion was correctly classified as BCC by hyperspectral imaging using the majority of the pixels classified as pigmented BCC. (A) Red, green and blue (RGB) image taken by hyperspectral camera. (B) Classification map showing most of the pixels classified as pigmented BCC. *Upper colour bar* depicts the 4 classes in image B. (C) Likelihood map for the localization of invasive melanoma (malignant melanoma; MM). (D) Likelihood map for the localization of pigmented basal cell carcinoma (BCC). (E) Likelihood map for the localization of marker pen. (F) Likelihood map for the localization of healthy skin. *Lower colour bar* represents the certainty of the classifier in each of the likelihood maps. *Red line* shows the division of the hyperspectral image into halves, one of which was used for the training of the classifier and the other for the classifying task.

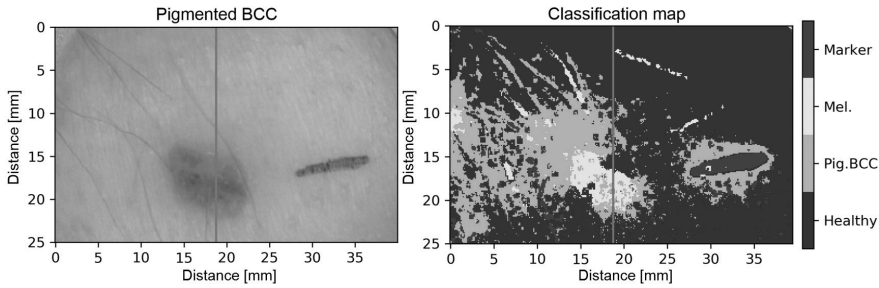


**Fig. 4. Classification map of a histologically confirmed pigmented basal cell carcinoma (BCC).** In this case the classifier falsely showed multiple pixels representing melanocytes in the lesional area. This may partly be explained by the fact that, histologically, there are some entrapped melanocytes in the area of pigmented BCC. Also, pigment macrophages may have been mistakenly identified as melanocytes. In this specific case the image quality was low, which also lead to misclassification of the pixels in the surrounding healthy skin.

pixel-wise by 3D CNN, which produced a classification map comprehending 4 classes (“pigmented basal cell carcinoma”, “melanocytic tumour”, “healthy skin” and “marker pen”) (Figs 2–4). The last layer of the classifier also created likelihood maps indicating how certain the CNN is about the classification. To obtain the classification for each pixel over each image, the maximum likelihood (the highest value of each pixel in likelihood maps) was used. Two different approaches were used for the analyses: (i) a majority of pixels classification; and (ii) a pixel-wise classification. The histopathological diagnoses of the excision specimens represented the true classification (true label) of the lesions.

In the majority of pixels classification, the classification maps were used to acquire an automated diagnosis for the imaged lesions, i.e. the whole lesion was predicted to belong to the same class as the majority of the pixels in the lesion area. In addition, the accuracy of CNN classification per individual pixel was computed in comparison with the manual annotations in the images (4 pixel classes, as discussed above). By using the pixel-wise classification the number of classified areas increased from 26 lesions to 164,144 classified pixels.

The confusion matrices for both lesion and pixel-wise classifications are shown in Fig. 5.

For the majority of pixel classification, sensitivity was 100% (16/16) (95% CI 81–100%), specificity 90% (9/10) (95% CI 60–98%) and PPV 94% (16/17) (95% CI 73–99%) in differentiating melanocytic tumours from pigmented BCCs. Only one true pigmented BCC was falsely predicted as a melanocytic tumour, and all melanocytic tumours were correctly predicted according to their true label. In pixel-wise classification the sensitivity for differentiating the class “melanocytic tumours” from the class “pigmented BCC” was 99.98% (95% CI 99.95–99.99%), specificity 93.2% (95% CI 92.6–93.7%) and PPV 97.8% (95% CI 97.6–98.0%).

This study also tested the accuracy of the CNN classifier, by dividing the sample into 3 groups: pigmented BCC ( $n=10$ ), MIS ( $n=12$ ) and MM ( $n=4$ ), and then used the classification maps to acquire an automated diagnosis for every lesion in a manner similar to that described above. Classifier accuracy by individual pixels was also computed (5 pixel classes). In the lesion classification using the majority of pixels, calculated sensitivity was 100% (4/4) (95% CI 51–100), specificity 100% (22/22)

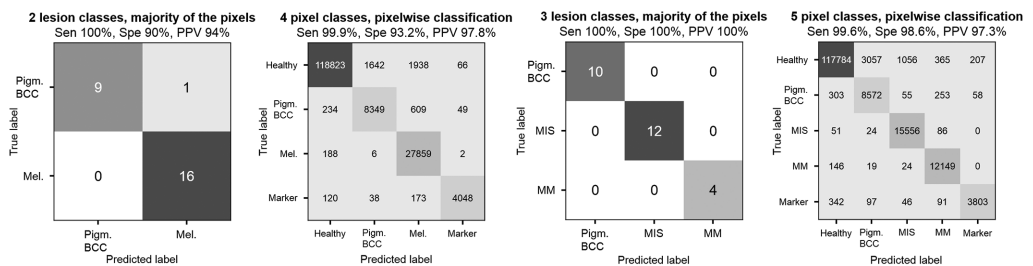


**Fig. 5. Confusion matrices for the convolutional neural network (CNN) classifier.** Left: lesion-based classification matrices for 2- and 3-class classification using the majority of the pixels to predict the label of whole lesion. Right: classification matrices per individual pixel compared with manual annotation in hyperspectral images (true label). In the case of 2 lesion classes the sample was divided into pigmented basal cell carcinomas (BCC) and malignant melanocytic tumours (Mel.). In the case of 3 lesion classes the sample was divided into pigmented BCCs, melanomas *in situ* (MIS) and malignant melanomas (MM). The statistical metrics were calculated for the class “Mel.” in case of 2 lesion classes and 4 pixel classes and for the class “MM” in case of 3 lesion classes and 5 pixel classes. Sen: sensitivity, Spe: specificity; PPV: positive predictive value.

(95% CI 85–100) and PPV 100% (4/4) (95% CI 51–100) in distinguishing MM from other lesions (MIS and pigmented BCC). In pixel-wise classification between tumour classes only, the statistical characteristics for class “MM” were as follows: sensitivity 99.6% (95% CI 99.5–99.7), specificity 98.6% (95% CI 98.5–98.8) and PPV 97.3% (95% CI 97.0–97.6). The confusion matrices for 3-class lesion classification and 5-class pixel-wise classification are shown in Fig. 4. The result of the CNN classification for all lesions in comparison with true histopathological diagnoses is shown in Table I. The difference in the spectra between different lesion types and healthy skin is shown in Fig. S3<sup>1</sup>.

## DISCUSSION

To the best of our knowledge, this pilot study is the first to utilize *in vivo* hyperspectral imaging (HSI) and a deep-learning CNN as a tumour classifier for skin tumours. The CNN lesion classifier using 2 different approaches (majority of pixels classifier and single pixel classifier) reached high sensitivity and specificity in distinguishing melanocytic tumours from pigmented BCCs.

HSI is a novel non-invasive optical imaging method that can be used to image tissues *in vivo* and *ex vivo* tissues rapidly in various medical applications. It produces a hyperspectral data cube in which different tissue types can be identified and visualized based on their specific reflectance spectra (8). Map-like images generated by HSI can be used to delineate malignant skin lesions preoperatively and to visualize invasive parts in large lesions to target biopsy sites (9–11).

Furthermore, HSI could be useful for dermatologists as a pre-surgical diagnostic aid for planning the surgical excision margins. HSI could be a helpful diagnostic tool even for inexperienced physicians, since it is user-independent and gives an automated most likely diagnosis.

No earlier reports on HSI combined with CNN for tumour classification were found in the literature. Among the available non-invasive diagnostic modalities, one reminiscent of the current method is MelaFind<sup>®</sup>, a multispectral imaging (MSI) system that acquires 10 wavebands in the range 430–950 nm, and uses automated algorithms based on linear classifiers for pattern recognition and differential diagnosis of pigmented lesions (24). MelaFind has demonstrated high sensitivity, of 82–98%, but only moderate specificity, of 8–52%, in recognizing melanomas (25–27). A limitation of MelaFind is that it may misclassify non-melanoma skin cancers, such as BCCs, because the technology is designed to assess overall structural disorganization of lesions, rather than atypical cellular features (28). Another non-invasive MSI technique is SIAscope (spectrophotometric intracutaneous analysis), which captures 8 narrowband spectral images in the range 400–1,000 nm to visualize the quantity and microscopic architecture of chromo-

phores (melanin, blood and collagen) in the lesion area (29). However, SIAscope does not improve diagnostic accuracy over dermoscopy in the diagnosis of pigmented BCC (30). Tomatis et al. (31) developed an artificial neural network (ANN) classifier for 1,391 pigmented lesions imaged with MSI, which was able to distinguish melanoma from other lesions with a sensitivity of 80% and specificity of 76%. In another study, Carrara et al. (32) developed an ANN classifier for MSI data to differentiate between reassuring lesions and those requiring excision, using a dataset of 1,966 excised and 1,940 non-excised and clinically non-suspicious lesions, resulting in sensitivity of 88% and specificity of 80%. For comparison, in meta-analyses, dermoscopy has achieved sensitivity and specificity of 88% and 86%, respectively, for the diagnosis of melanoma (33), 82.4% and 83.5% for the diagnosis of LM and LMM (34), and 81.9% and 81.8% for the diagnosis of superficial BCC (35). However, the diagnostic accuracy of dermoscopy is user-dependent and depends on the experience of the clinician. Recently, deep learning CNN have been utilized to facilitate and automate diagnostic classification in clinical and dermoscopic images, reaching diagnostic accuracies similar to those achieved by expert dermatologists, with the area under the curve (AUC) of the receiver operating curve (ROC) ranging from 0.74 to 0.96 (12–14).

The results of the current study indicate that HSI might be capable of spectral differentiation at the cellular level and of recognizing the tumour cell of origin (melanocyte vs keratinocyte). The CNN classification maps in pixel-wise resolution can be thought to represent aggregates of cells in the microscopic structure of the skin. The hyperspectral image analysis appears, in most cases, to recognize the different cell types in pigmented BCC and melanocytic tumours regardless of the presence of melanin pigment. Both tumour types have increased amounts of melanin in the dermis, often histologically visualized in macrophages. Thus, the results of the current study show that HSI does not only use pigment as a chromophore, but also recognizes other characteristics beyond the pigment. Further verification of this is required in studies at the cellular level. There were some cases with pixels misclassified as melanoma (Fig. 4) within the pigmented BCCs, which could be due to the fact that, histologically, there are some entrapped melanocytes in the areas of pigmented BCCs (36).

The current study used a combination of 3D, 2D and 1D CNN for automated pixel-wise tumour classification in hyperspectral images of the skin. 3D CNN was used because the standard 2D CNN used with clinical and dermoscopic photographs may not suffice to utilize spectral data, which is 3-dimensional in nature. This method produced classification maps of imaged lesions that predict the lesion's diagnosis pixel-wise (Figs 2 and 3). The classification map not only offers identification (the most likely diagnosis), but also delineation and map-like repre-



sentation of the lesion. Figs 2 and 3 show that there are a few misclassified pixels in the tumour area, but that, by far, most pixels are classified correctly, predicting the true histopathological diagnosis. In addition, at the periphery of the image in the area of healthy skin there are some rare misclassified pixels. Furthermore, the black hair has been classified as “marker pen”, since no separate class was created for hair. The few misclassified pixels could be explained by imaging errors, such as local increased noise or other perturbation in the hyperspectral image, or by inaccuracy in the CNN model. When classifying whole lesions using the majority of pixels method, the few misclassified pixels were averaged, leading to very high sensitivity and specificity for differential diagnosis of melanocytic tumours from BCCs. In the case of 3 tumour classes, the accuracy of the CNN classifier was also very high with all tumours classified correctly. The confusion matrices of individual pixel classification (Fig. 4) demonstrate the robustness of the CNN’s pixel-wise classification, but it should be noted that the pixel-wise accuracy is presented only in comparison with manually annotated pixel classes in images. The pixel-wise classification is fairly accurate in distinguishing tumour classes from each other, with high sensitivity and specificity for both 2-class and 3-class lesion classification. However, if all (4 or 5) pixel classes are observed, it can be seen that there is a portion of “healthy” annotated pixels that are assigned to tumour classes “pigmented BCC”, “melanocytic tumours”, “MIS” and “MM”, which are false positives in the whole imaged region and represent the inherent error in CNN classification. In this study setting, the majority of pixels method can be assumed to predict the diagnosis reliably, because we know *a priori* that no single BCC cells are situated inside a melanocytic tumour and vice versa. This is not necessarily the case when, for example, multiple melanocytic tumours are included in the classification task. In the development of the CNN classification method, this study strove for pixel-wise classification, because there are clinical situations in which a single skin lesion may include multiple tumour types (e.g. an invasive part of surrounding carcinoma *in situ*, or invasive melanoma arising in melanoma *in situ* or in pre-existing naevus). The CNN method used in the present study is novel and can be developed further. In addition, the classification of CNN improves with larger training datasets, which will require the collection of larger samples of different tumour types and from different locations on the body. With a larger training set the pixel-wise classification of CNN could be further improved to be more robust, thereby reducing the number of misclassified pixels.

#### Study limitations

This study has some limitations. Due to the pilot nature of the study, the sample size was small and halves of the

images were used for the CNN training phase. Ideally, the CNN training should be conducted with a dataset separate from that used for the classification task. However, the small sample size was compensated by the pixel-wise analysis, in which the pixels were analysed separately and could be counted as separate lesions. This increases the reliability of the findings. It should be noted that benign tumours clinically mimicking pigmented BCCs (benign lentigines, seborrhoeic keratosis, benign naevi) were not included, and further studies on this topic are warranted. The CNN classification method used is novel and requires further development work. An HSI camera prototype was used in this study, which could be developed further to be more robust in order to avoid imaging noise and artefacts. There is currently no commercially available HSI device for skin imaging.

#### Conclusion

This is the first study to utilize hyperspectral images and deep-learning CNN to achieve automated diagnosis for melanocytic tumours and pigmented BCCs. The results will therefore serve as a basis for future studies.

The results of this study suggest that, with a larger sample and training dataset, the CNN could accurately and pixel-wise distinguish between malignant melanocytic tumours and pigmented BCCs. To confirm these preliminary results, future studies with larger samples and multiple tumour types, including all types of melanocytic lesions, are warranted.

#### ACKNOWLEDGEMENTS

The patients in this paper provided written informed consent for publication of their case details.

The authors would like to thank Ulla Oesch-Lääveri, nurse at the Päijät-Häme Central Hospital, for her dedication to this study, and Heikki Saari from VTT Finnish Technical Centre of Finland and statistician Martin Gillsted for their help in the study.

This study was funded by the Cancer Foundation of Finland, by Tampere University Hospital and by the State Research Funding.

IP, MG and NN have a patent (US10478071B2) licensed. MG has received a consultation fee from Revenio Group. The other authors have no conflicts of interest to declare.

#### REFERENCES

1. Cameron MC, Lee E, Hibler BP, Barker CA, Mori S, Cordova M, et al. Basal cell carcinoma: Epidemiology; pathophysiology; clinical and histological subtypes; and disease associations. *J Am Acad Dermatol* 2019; 80: 303–317.
2. Menzies SW. Dermoscopy of pigmented basal cell carcinoma. *Clin Dermatol* 2002; 20: 268–269.
3. Wozniak-Rito A, Zalaudek I, Rudnicka L. Dermoscopy of basal cell carcinoma. *Clin Exp Dermatol* 2018; 43: 241–247.
4. Cameron MC, Lee E, Hibler BP, Giordano CN, Barker CA, Mori S, et al. Basal cell carcinoma: contemporary approaches to diagnosis, treatment, and prevention. *J Am Acad Dermatol* 2019; 80: 321–339.
5. Altamura D, Menzies SW, Argenziano G, Zalaudek I, Soyer HP, Sera F, et al. Dermoscopy of basal cell carcinoma:

- morphologic variability of global and local features and accuracy of diagnosis. *J Am Acad Dermatol* 2010; 62: 67–75.
6. Bosbous MW, Dzwierzynski WW, Neuburg M. Lentigo maligna: diagnosis and treatment. *Clin Plast Surg* 2010; 37: 35–46.
  7. Neittaanmaki-Perttu N, Gronroos M, Tani T, Polonen I, Ranki A, Saksela O, et al. Detecting field cancerization using a hyperspectral imaging system. *Lasers Surg Med* 2013; 45: 410–417.
  8. Lu G, Fei B. Medical hyperspectral imaging: a review. *J Biomed Opt* 2014; 19: 10901.
  9. Salmivuori M, Neittaanmaki N, Polonen I, Jeskanen L, Snellman E, Gronroos M. Hyperspectral imaging system in the delineation of III-defined basal cell carcinomas: a pilot study. *J Eur Acad Dermatol Venereol* 2019; 33: 71–78.
  10. Neittaanmaki-Perttu N, Gronroos M, Jeskanen L, Polonen I, Ranki A, Saksela O, et al. Delineating margins of lentigo maligna using a hyperspectral imaging system. *Acta Derm Venereol* 2015; 95: 549–552.
  11. Neittaanmaki N, Salmivuori M, Polonen I, Jeskanen L, Ranki A, Saksela O, et al. Hyperspectral imaging in detecting dermal invasion in lentigo maligna melanoma. *Br J Dermatol* 2017; 177: 1742–1744.
  12. Esteve A, Kuprel B, Novoa RA, Ko J, Swetter SM, Blau HM, et al. Dermatologist-level classification of skin cancer with deep neural networks. *Nature* 2017; 542: 115–118.
  13. Haenssle HA, Fink C, Schneiderbauer R, Toberer F, Buhl T, Blum A, et al. Man against machine: diagnostic performance of a deep learning convolutional neural network for dermoscopic melanoma recognition in comparison to 58 dermatologists. *Ann Oncol* 2018; 29: 1836–1842.
  14. Tschandl P, Rosendahl C, Akay BN, Argenziano G, Blum A, Braun RP, et al. Expert-level diagnosis of nonpigmented skin cancer by combined convolutional neural networks. *JAMA Dermatol* 2019; 155: 58–65.
  15. Halicek M, Little JV, Wang X, Patel M, Griffith CC, Chen AY, et al. Tumor margin classification of head and neck cancer using hyperspectral imaging and convolutional neural networks. *Proc SPIE Int Soc Opt Eng* 2018; 10576: 1057605.
  16. Halicek M, Little JV, Wang X, Patel M, Griffith CC, El-Deiry MW, et al. Optical biopsy of head and neck cancer using hyperspectral imaging and convolutional neural networks. *Proc SPIE Int Soc Opt Eng* 2018; 10469: 104690X.
  17. Barun, VV, Ivanov, AP, Volotovskaya, AV, Ulashchik, VS. Absorption spectra and light penetration depth of normal and pathologically altered human skin. *J Appl Spectrosc* 2007; 74: 430–439.
  18. Saari H, Polonen I, Salo H, Honkavaara E, Hakala T, Holmlund C, et al. Miniaturized hyperspectral imager calibration and UAV flight campaigns. *Sensors, Systems, and Next-Generation Satellites XVII* 2013; 8889: 888910.
  19. Polonen I, Rahkonen S, Annala L, Neittaanmaki N. Convolutional neural networks in skin cancer detection using spatial and spectral domain. *Photon Dermatol Plast Surg* 2019; 10851: 108510B.
  20. Goodfellow I, Bengio Y, Courville A, Bengio Y. *Deep learning*. Cambridge: MIT Press; 2016: p. 2.
  21. Audebert N, Le Saux B, Lefèvre S. Deep learning for classification of hyperspectral data: a comparative review. *IEEE Geosci Remote Sens Mag* 2009; 7: 159–173.
  22. Lunga D, Prasad S, Crawford MM, Ersoy O. Manifold-learning-based feature extraction for classification of hyperspectral data: a review of advances in manifold learning. *IEEE Signal Process Mag* 2013; 31: 55–66.
  23. Ghamisi P, Plaza J, Chen Y, Li J, Plaza, AJ. Advanced spectral classifiers for hyperspectral images: a review. *IEEE Geosci Remote Sens Mag* 2017; 5: 8–32.
  24. Elbaum M, Kopf AW, Rabinovitz HS, Langley RG, Kamino H, Mihm MC, Jr, et al. Automatic differentiation of melanoma from melanocytic nevi with multispectral digital dermoscopy: a feasibility study. *J Am Acad Dermatol* 2001; 44: 207–218.
  25. Wells R, Gutkowitz-Krusin D, Veledar E, Toledano A, Chen SC. Comparison of diagnostic and management sensitivity to melanoma between dermatologists and MelaFind: a pilot study. *Arch Dermatol* 2012; 148: 1083–1084.
  26. Monheit G, Cognetta AB, Ferris L, Rabinovitz H, Gross K, Martini M, et al. The performance of MelaFind: a prospective multicenter study. *Arch Dermatol* 2011; 147: 188–194.
  27. MacLellan AN, Price EL, Publicover-Brouwer P, Matheson K, Ly TY, Pasternak S, et al. The use of non-invasive imaging techniques in the diagnosis of melanoma: a prospective diagnostic accuracy study. *J Am Acad Dermatol* 2020 Apr 11 (Online ahead of print).
  28. March J, Hand M, Grossman D. Practical application of new technologies for melanoma diagnosis: Part I. Noninvasive approaches. *J Am Acad Dermatol* 2015; 72: 929–941, quiz 941–942.
  29. Moncrieff M, Cotton S, Claridge E, Hall P. Spectrophotometric intracutaneous analysis: a new technique for imaging pigmented skin lesions. *Br J Dermatol* 2002; 146: 448–457.
  30. Terstappen K, Larkö O, Wennberg AM. Pigmented basal cell carcinoma – comparing the diagnostic methods of SIAscopy and dermoscopy. *Acta Derm Venereol* 2007; 87: 238–242.
  31. Tomatis S, Carrara M, Bono A, Bartoli C, Lualdi M, Tragni G, et al. Automated melanoma detection with a novel multispectral imaging system: results of a prospective study. *Phys Med Biol* 2005; 50: 1675–1687.
  32. Carrara M, Bono A, Bartoli C, Colombo A, Lualdi M, Moglia D, et al. Multispectral imaging and artificial neural network: mimicking the management decision of the clinician facing pigmented skin lesions. *Phys Med Biol* 2007; 52: 2599–2613.
  33. Rajpara SM, Botello AP, Townend J, Ormerod AD. Systematic review of dermoscopy and digital dermoscopy/artificial intelligence for the diagnosis of melanoma. *Br J Dermatol* 2009; 161: 591–604.
  34. Carapeba MOL, Alves Pineze M, Nai GA. Is dermoscopy a good tool for the diagnosis of lentigo maligna and lentigo maligna melanoma? A meta-analysis. *Clin Cosmet Investig Dermatol* 2019; 12: 403–414.
  35. Lallas A, Tzellos T, Kyrgidis A, Apalla Z, Zalaudek I, Karatolias A, et al. Accuracy of dermoscopic criteria for discriminating superficial from other subtypes of basal cell carcinoma. *J Am Acad Dermatol* 2014; 70: 303–311.
  36. Brankov N, Prodanovic EM, Hurley MY. Pigmented basal cell carcinoma: increased melanin or increased melanocytes? *J Cutan Pathol* 2016; 43: 1139–1142.



